UNIVERSITAT DE BARCELONA

Blood barriers for oncolytic adenovirus efficacy: study of binding to erythrocytes via CAR and albumin-mediated evasion of neutralizing antibodies

Luis Alfonso Rojas Expósito

UNIVERSITAT DE BARCELONA
FACULTAT DE FARMÀCIA I CIÈNCIES DE L'ALIMENTACIÓ
DEPARTAMENT DE BIOQUÍMICA I BIOLOGIA MOLECULAR
PROGRAMA DE DOCTORAT EN BIOMEDICINA

BLOOD BARRIERS FOR ONCOLYTIC ADENOVIRUS EFFICACY: STUDY OF BINDING TO ERYTHROCYTES VIA CAR AND ALBUMIN-MEDIATED EVASION OF NEUTRALIZING ANTIBODIES

LUIS ALFONSO ROJAS EXPÓSITO
MARÇ 2017

UNIVERSITAT DE BARCELONA

FACULTAT DE FARMÀCIA I CIÈNCIES DE L'ALIMENTACIÓ

DEPARTAMENT DE BIOQUÍMICA I BIOLOGIA MOLECULAR

PROGRAMA DE DOCTORAT EN BIOMEDICINA

BLOOD BARRIERS FOR ONCOLYTIC ADENOVIRUS EFFICACY: STUDY OF BINDING TO ERYTHROCYTES VIA CAR AND ALBUMIN-MEDIATED EVASION OF NEUTRALIZING ANTIBODIES

LUIS ALFONSO ROJAS EXPÓSITO

2017

Memòria presentada per Luis Alfonso Rojas Expósito per optar al grau de Doctor per la Universitat de Barcelona

Dr. Ramon Alemany Bonastre	Dr. Francesc Viñals Canals	Luis Alfonso Rojas Expósito
Director	Tutor	Autor

AGRADECIMIENTOS

Durante esta tesis he iniciado más de diez proyectos, incluyendo el non-viral delivery de de genomas de adenovirus oncolíticos (mediante dendrímeros, liposomas, quitosanos, nanopartículas magnéticas y otras moléculas raras cuyo nombre no recuerdo), la inducción de expresión de heat-shock proteins en células de ratón para permitir la replicación del adenovirus humano, la inserción de mutaciones en el hexón mediante error-prone PCR para encontrar mutantes que se neutralicen menos en sangre, la modificación de las regiones hipervariables para reducir el secuestro por Kupffer, la inserción de una secuencia Kozak delante de la L4-100K para aumentar la replicación en células de ratón, la mutagénesis con 5-FU para aislar mutantes capaces de replicar en células murinas, la fusión de la PH20 a la Melitina mediante un linker de FAP para matar los fibroblastos del estroma, la hialuronidasa de la abeja como alternativa más potente a la PH20 humana, la inserción del motivo ABD en las regiones hipervariables (que casi descartamos también porque los virus no eran viables), o la interacción con eritrocitos humanos (alguno más me dejo). Mi afición por destruir los proyectos que Ramon me iba proponiendo hizo que mis compañeros de grupo me bautizaran como *Project killer* (muy majos ellos xD). Por suerte, tal y como me dijo Ramon que ocurriría, algún proyecto salió adelante y finalmente ha podido salir una tesis. A pesar de las múltiples frustraciones, haciendo balance general estoy muy contento de esta etapa y de lo mucho que he aprendido. Todo esto ha sido posible gracias a mucha gente, que en mayor o menor medida, me ha ayudado en este proceso.

En primer lloc haig d'agrair al Ramon, per transmetre'm paciència i perseverança. Per involucrar-te tant amb els teus becaris i tenir sempre bones idees per a projectes. Per ser un jefe tan proper, tan accessible i tenir sempre "cinc minuts" que després es convertien en dues hores. Per donar-nos sempre tanta llibertat, que crec que m'ha ajudat molt a créixer com a científic. Difícilment hauria pogut tenir un millor director de tesi i mentor.

Me gustaria agradecer también a Carmen San Martín y a Gabriela Condezo por toda la ayuda y todo el esfuerzo que invirtieron en poner a punto la detección de la albúmina mediante microscopia electrónica.

Tengo mucho que agradecer también a mis compañeros de grupo, los llamados "RATgitos". Empiezo por los que ya no están. Juanjo, gracias por enchufarme en el grupo ya que si no fuera por ti quizás no me hubieran cogido, ve hablando con tu jefe de Múnich (es broma xD). Gracias por mil consejos científicos y no científicos, por corregirme la tesis, y por

ser mucho más que un hermano y un grandísimo amigo. Sin duda eres un modelo a seguir. Raulito, tú fuiste mi verdadero maestro durante la tesis, estoy muy orgulloso de ser tu padawan. Alba, creo sin duda que tú has sido mi mayor apoyo durante toda la tesis, mil gracias por estar siempre ahí. Marta, quantes coses he après de tu! I quantes vegades m'has ajudat a l'estabulari i al lab! Sònia, els teus consells m'han ajudat moltíssim (sobretot als congressos!), ets una crack! Gracias también a Cris (la más fiel admiradora de mis chistes), Edu, Miguel, Hugo, Jordi y Daniela!

De los actuales RATgitos, ¡tengo que agradecer enormemente al equipo Maquinitas! Equipaso! Menudas risas han caído con los vicios, aunque fuerais un poco conos (Rafa 21 continues?). Rafa, seguramente hayas sido una de las personas más importantes en mi tesis. Gracias por tu amistad y por tu inestimable ayuda durante toda la tesis, porque aun siendo yo bético, siempre estabas dispuesto a ayudarme en cualquier experimento, sobretodo en el estabulario y con las real times (cuántos estándares me habrás dejado…). Sólo quiero decirte que ¡P*** SEVILLA, P*** SEVILLAAA! Beto, cuánto he aprendido de ciencia contigo…Eres un fenómeno y te admiro muchísimo. Marcel, mi más fiel compañero de chistes. Cuánto he disfrutado *trolleandote* (jódete). Vuestra amistad es una de las mejores cosas que me llevo de esta tesis. Ahmed, creo que nunca he conocido un tío tan alegre y con tanta bondad. ¡Ánimo que ya tienes ese paper y esa tesis! Jana i Martí (aka Mari o Matri), sou el futur del grup! Llàstima que sigueu lamentables al pàdel, però clar, no es pot tenir tot. Quiero agradecer también a Sílvia (gran admiradora también de mis chistes que nunca falla en el chat de Laboratorio), Loli, y a las chicas de VCN, Sara, Ana y Patri.

Tengo mucho que agradecer también a la gente del LRT1. Roser i Mariona, moltíssimes gràcies per ajudar-me sempre amb les immunos, tot i que us preguntava sempre les mateixes chorrades. Gràcies pel dia a dia, per fer sempre sa bereneta, i pel gran viatje a Menorca! (Mariona, Stroika sucks). Currito, ¡qué grande fue esa feria! Ahí conocimos a Peloma. Qué pena que no pude probar el rebujito. Gracias además por las múltiples barbacoas de gambones con Anthony B, y por las salidas a ver al Betis en campos de segunda (a destacar el diluvio en Palamós viendo el Llagostera din tei). Samuel, ¡AAAAAAAAAH!!! Cada vez que me acuerdo del dia de la Caipirinha 10X y de la fiesta de "chicos" en tu casa me parto de risa. ¡Enhorabuena por el reciente doctorado! Tampoco quiero alargarme demasiado pero hay más gente que ha sido importante y que merece una mención. ¡Eskerrik asko a Iratxe! Gracias también a Ali, Natalia, Elisenda, Joan (grans els oliverars, sorry per abonyegar-te les cassoles),

Jack, Nick, Nadia (por dejarme mil veces la poyata para montar real times), Eric, María, Gabi, Olga, etc.

A parte, me gustaría agradecer a ciertas personas por méritos o hazañas importantes que han realizado durante mi estancia en el laboratorio, a pesar de que algunos ya han sido mencionados:

Especial agradecimiento a Marcel e Iratxe por organizar el PhD day y permitirnos disfrutar de un día tan mágico, lleno de hadas y princesas Disney (xDDDDD).

Se merece también un agradecimiento a parte Rafa, por iniciar una tradición tan bonita como la ruta de bares camino a la cena de Navidad. Tradición que ya tiene multitud de seguidores y que espero que se mantenga muchos años. Agradecimiento también por supuesto a toda la gente del LRT1 y LRT2 que ha participado en esta caminata, que se hacía los dorsales, y pegaba ahí las etiquetas de los quintos.

Mención especial al Camallo Vallecano de Bellvitge. A la plantilla formada por Carles, Eric, Curro, Marcel, Beto, Rashid, Miguel, Jack, y Julián, al polémico periodista W.W. Roncero, y al presidente Al Zaher III (aunque tuvo muy pocos “valors” vendiendo el club).

Agradecer también a todos los participantes y co-organizadores de las porras de Eurocopas y Mundiales (excepto al corrupto de Beto xD). Aunque no estuve ni cerca de ganar ninguna (ríete Rafa), siempre eran semanas que daban mucha vidilla al laboratorio.

Finalmente tengo que agradecer a mi familia. A mis padres, porque si he podido llegar hasta aquí ha sido gracias a ellos. A mi hermano (que ya lo he mencionado antes) y Lucía, por todos los momentos y viajes compartidos: Coma-ruga, Cabo de Gata, Eslovenia y Croacia… Y por supuesto a Sonia. Poco puedo decirte que no sepas. Gracias por estar a mi lado en todo momento.

TABLE OF CONTENTS

LIST OF FIGURES

LIST OF TABLES

ABBREVIATIONS

%	Percentage
Å	Årmströng
°C	Centigrade degrees
Δ24	*delta*24 mutation, deletion of 24 bp in E1A protein
µF	microfarad
µg	microgram
µL	microliter
µm	micrometer
Ω	Ohm
AAALAC	Association for Assessment and Accreditation of Laboratory Animal Care
ABD	Albumin-Binding Domain
ABP	Albumin-Binding Peptide
Ad	Adenovirus
ADP	Adenovirus Death Protein
ALT	Alanine Transaminase
AST	Aspartate Transaminase
ATCC	American Type Cell Culture
BAC	Bacterial Artificial Chromosome
Bak	Bcl-2 homologous antagonist/killer
Bax	Bcl-2-associated X protein
BCA	Bicinchoninic Acid Assay
bp	base pairs
BSA	Bovine Serum Albumin
C4BP	Complement Binding Protein-4
$CaCl_2$	Calcium chloride
CAR	Coxsackievirus B and Adenovirus Receptor
CCE	Clarified Cell Extract
CD4 and 8	Cluster of differentiation 4 and 8
cDNA	complementary DNA
CE	Cell Extract
CFSE	Carboxyfluorescein succinimidyl ester
Cm	Chloramphenicol
cm	centimeter
CMV	Cytomegalovirus
CO_2	Carbon dioxide
CPE	Cytopathic effect
CR	Complement Receptors
CRAd	Conditionally Replicative Adenovirus
CsCl	Cesium chloride
CTL	Cytotoxic T Lymphocyte
CTLA-4	Cytotoxic T-Lymphocyte-Associated Protein 4
DAB	3,3'-Diaminobenzidine
DAPI	4',6-Diamidino-2-phenylindole dihydrochloride
DNA	Deoxyribonucleic acid
DC	Dendritic cell
ddH_2O	bi-distilled water
ddDNTP	2',3' dideoxynucleotides
DMEM	Dulbecco's Modified Eagle's Medium

DMSO	Dimethyl sulfoxide
DNA	Deoxyribonucleic Acid
dNTP	Nucleoside triphosphate
EDTA	Ethylenediaminetetraacetic acid
ELISA	Enzyme-Linked ImmunoSorbent Assay
ELISPOT	Enzyme-Linked Immunospot Assay
FACS	Fluorescence Activated Cell Sorting
FBS	Fetal Bovine Serum
FDA	Food and Drug Administration
FIX	Coagulation factor IX
FX	Coagulation factor X
g	acceleration of gravity
g	gram
GALV	Gibbon Ape Leukemia Virus
GM-CSF	Granulocyte Macrophage-Colony Stimulating Factor
h	hour
H_2O_2	Hydrogen peroxide
HA	Hyaluronic acid
HCl	Chloridric acid
HDAC	Histone deacetylases
HEK293	Human Embryonic Kidney 293
HEPES	4-(2-hydroxyethyl)-1-piperazineethanesulfonic acid
HIV	Human Immunodeficiency Virus
HRP	Horseradish peroxidase
HSA	Human Serum Albumin
HSG	Heparan-Sulphate-Glycosaminoglicans
HSV	Herpes Simplex Virus
HVR	Hypervariable Region
IC_{50}	Inhibitory Concentration 50
IFN	Interferon
Ig	Immunoglobulin
IL	Interleukin
IP	Intraperitoneal
IT	Intratumoral
ITR	Inverted Terminal Repeats
IU	International Units
IV	Intravenous
IVIS	*In Vivo* Imaging System
K	Kozak sequence
KH_2PO_4	Monopotassium phosphate
Kan	Kanamycin
kb	kilobase
KC	Kupffer Cell
KCl	Potassium chloride
L	Liter
LITR	Left Inverted Terminal Repeat
LRP	Lipoprotein Receptor-related Protein
LSEC	Liver Sinusoid Endothelial Cell
LU	Light Units
mA	Milliampere
mAb	monoclonal antibody

mg	milligram
MHC	Major Histocompatibility Complex
min	minute
mL	milliliter
MLP	Major Late Promoter
MLU	Major Late transcription Unit
mm	millimeter
mm^3	cubic millimeter
mM	millimolar
MOI	Multiplicity of Infection
mRNA	Messenger Ribonucleic Acid
MSA	Mouse Serum Albumin
MSC	Mesenchymal Stem Cell
MTT	3-(4,5-Dimethylthiazol-2-yl)-2,5-Diphenyltetrazolium Bromide
MVA	Modified Vaccinia Ankara
NAbs	Neutralizing antibodies
NaCl	Sodium chloride
NaH_2PO_4	Monosodium phosphate
Na_2HPO_4	Disodium phosphate
NaOH	Sodium hydroxide
NDV	Newcastle Disease Virus
NF-κβ	Nuclear factor Kappa-light-chain-enhancer of activated B cells
ng	nanogram
NK	Natural Killer
nm	nanometer
OCT	Optimum Cutting Temperature compound
OD	Optical Density
p	photons
pA	polyadenylation sequence
PAMP	Pathogen-Associated Molecular Pattern
PBS	Phosphate Buffered Saline
PCR	Polymerase Chain Reaction
PEG	Polyethylene Glycol
p.i.	Post-infection or post-injection
pg	picogram
PMA	Phorbol Myristate Acetate
pmol	picomol
PRR	Pattern Recognition Receptor
PS	Penicillin-Streptomycin
PSA	Prostate-Specific Antigen
Rb	Retinoblastoma
RGD	Arginine-glycine-aspartic acid
RITR	Right Inverted Terminal Repeat
RNA	Ribonucleic Acid
rpm	revolutions per minute
RPMI	Roswell Park Memorial Institute
RT	Room Temperature
RT-PCR	Real-Time PCR
SA	Splicing Acceptor
SD	Standard Deviation
SDS	Sodium dodecyl sulfate

SEM	Standard Error of the Mean
SFC	Spot forming colony
SPARC	Secreted Protein Acidic and Rich in Cysteine
Sr	Steradian
SR	Scavenger Receptor
Strep	Streptomycin
TAE	Tris-Acetate-EDTA
TAP	Transporter Associated to Antigen Processing
TE	Tris-EDTA
TGF-β	Transforming Growth Factor-β
TL	Track-Luc cassette (eGFP-Luciferase)
TLP	Tripartite Leader
TNF	Tumor Necrosis Factor
TLR	Toll-Like Receptor
TP	Terminal Protein
TRAIL	TNF-related apoptosis-inducing ligand
Tris	Tris(hydroxymethyl)aminomethane
TU	Transducing Unit
V	Volt or Volume
VA	Virus-Associated
vp	viral particle
VSV	Vesicular Stomatitis Virus
VV	Vaccinia Virus
WHO	World Health Organization
wt	wild type

Amino acids

F Phe, phenylalanine	**S** Ser, serine	**Y** Tyr, tyrosine	**K** Lys, lysine	**W** Trp tryptophan
L Leu, leucine	**P** Pro, proline	**H** his, histidine	**D** Asp, aspartic acid	**R** Arg, arginine
I Ile, isoleucine	**T** Thr, threonine	**Q** Gln, glutamine	**E** Glu, glutamic acid	**G** Gly, glycine
M Met, methionine	**A** Ala, alanine	**N** Asn, asparagine	**C** Cys, cysteine	**V** Val, valine

Nucleotides

A adenine **T** thymine **G** guanine **C** cytosine **U** uracil

RESUM

Els adenovirus oncolítics són agents terapèutics prometedors, degut a la seva capacitat d'infectar i eliminar selectivament les cèl·lules tumorals, sense afectar les cèl·lules normals. Tot i que la ruta preferida d'administració és la intravenosa per tal d'arribar a totes les metàstasis, la interacció del virus amb diversos components de la sang provoca la seva neutralització. Per tant, millorar l'arribada dels virus als tumors per via sistèmica és un aspecte clau per a l'èxit d'aquesta teràpia. En aquest treball s'ha estudiat la interacció de l'adenovirus serotip 5 amb els eritròcits humans a través del receptor CAR, la qual es va descriure que provocava el segrest i la inactivació del virus. Malgrat es va observar unió als eritròcits, aquesta no va reduir la transducció de cèl·lules tumorals *in vitro*. Degut a que els eritròcits murins no expressen CAR, es van transferir eritròcits humans a ratolins immunodeprimits per tal d'analitzar l'efecte de la interacció després de la injecció sistèmica. Tot i així, aquesta unió als eritròcits no va alterar la extravasació ni la transducció del fetge per part del virus, suggerint que la interacció és reversible i no neutralitzant.

Per altra banda, l'alta prevalença d'anticossos neutralitzants contra l'adenovirus 5 en la població humana representa un obstacle molt important per la injecció intravenosa d'aquest. Per protegir l'adenovirus contra els anticossos neutralitzants s'ha inserit un domini d'unió a albúmina (ABD) a la proteïna principal de la càpside viral, la proteïna hexó. Aquest domini s'uneix a l'albúmina sèrica, recobrint el virus amb aquesta després de l'administració sistèmica. Els virus modificats amb ABD són capaços d'unir-se tant a l'albúmina humana com a la murina, fet que els permet mantenir la infectivitat i la capacitat replicativa en presència d'anticossos neutralitzants. Els adenovirus no modificats són completament neutralitzats després de la administració sistèmica en ratolins pre-immunes, mentre que els virus modificats amb ABD mantenen la capacitat de transduïr els òrgans i controlar el creixement tumoral. Els resultats presentats en aquesta tesi recolzen l'ús d'aquesta estratègia per a tractar pacients amb adenovirus oncolítics per via sistèmica.

En resum, aquest treball està enfocat en millorar l'arribada dels adenovirus oncolítics als tumors després de l'administració intravenosa, una de les majors limitacions d'aquesta teràpia. Els resultats d'aquest treball demostren que mentre que la interacció amb eritròcits a través de CAR no inactiva el virus, els anticossos neutralitzants sí que representen un obstacle important per a l'eficàcia del tractament. En aquest sentit, la protecció de la càpside viral amb albúmina és una aproximació efectiva per a evadir-los. Aquesta estratègia té rellevància clínica en l'ús d'adenovirus per via sistèmica, no només en el camp de la viroteràpia sinó també en la teràpia gènica i en les vacunes basades en adenovirus.

SUMMARY

Cancer virotherapy with oncolytic adenoviruses represents a promising therapeutic approach due to the capacity of these viruses to infect and selectively kill tumor cells without damaging normal tissues. Although the intravenous is the preferred route of administration in order to reach disseminated metastasis, several interactions with blood components cause the neutralization of the virus. Thus, improving the delivery of such adenoviruses to tumors by systemic injection is crucial for the success of the therapy. In this work we have studied the interaction of the adenovirus serotype 5 (Ad5) with human erythrocytes through the receptor CAR, which was described to sequester and inactivate the virus. Although erythrocyte binding was observed, it did not reduce viral transduction of tumor cells *in vitro*. Since mouse erythrocytes do not express CAR, human erythrocytes were transferred into nude mice to analyze the impact of erythrocyte binding after systemic administration. However, adenovirus extravasation and transduction of liver and tumors was not reduced, suggesting that this binding is reversible and does not neutralize the virus.

On the other hand, the high prevalence of anti-Ad5 neutralizing antibodies (NAbs) is a major obstacle for the intravenous administration of adenoviruses. To protect adenovirus against NAbs we inserted an albumin-binding domain (ABD) in the main adenovirus capsid protein, the hexon. This domain binds serum albumin to shield the virus upon systemic administration. The ABD-modified adenoviruses bind human and mouse albumin, which allow them to maintain the infectivity and replication capacity in presence of NAbs. Non-modified adenoviruses are completely neutralized after systemic administration in pre-immune mice, whereas ABD-modified viruses preserve the ability to transduce target organs and induce oncolysis. The data presented in this thesis supports the use of this strategy to treat patients systemically with oncolytic adenoviruses.

In summary, this thesis focused on improving the intravenous delivery of oncolytic adenoviruses, which is one of the main limitations of this therapy. The results presented in this work demonstrate that while erythrocyte binding via CAR does not inactivate the virus, NAbs represent a major obstacle for efficacy. In this regard, albumin coating of the virus capsid represents an effective approach to evade pre-existing NAbs. This strategy has translational relevance in the use of adenovirus by systemic injection not only for cancer virotherapy, but also for gene therapy and vaccination.

INTRODUCTION

1. CANCER VIROTHERAPY

Cancer represents one of the leading causes of morbidity and mortality worldwide. According to the World Health Organization (WHO), cancer caused 8.8 million deaths in 2015, which corresponded to 16.6% of all human deaths. Cancer is a genetic disease in which somatic cells acquire several mutations that overcome cell division control mechanisms, resulting in uncontrolled proliferation and expansion. This abnormal proliferation leads to the formation of a primary tumor, which can invade surrounding tissues, and eventually spread by the lymphatic system to regional lymph nodes or by blood vessels to distant sites in a process known as metastasis. Conventional cancer treatments include surgery, chemotherapy, and radiation therapy, with successful therapeutic results in localized tumors and initial stages of the disease. Nevertheless, these therapies generally induce strong toxic side effects, and some tumors are refractory to them, especially at advanced stages. Thus, there is a great necessity to develop new treatments with higher specificity, lower toxicity profiles, and a different mechanism of action to act upon tumor cells resistant to conventional therapies.

During the last two decades, novel therapies targeting the immune system have proved to be encouraging in terms of overcoming the disadvantages of classical therapies. Tumors acquire different mechanisms during their progression to avoid recognition by the immune system. These immunotherapies, attempt to overcome these mechanisms and induce the immune system to destroy tumor cells. Strategies approved by FDA include non-specific therapies, such as cytokine therapies (interferon-alpha, IL-2, etc.) (Papaioannou et al., 2016), as well as antigen-specific therapies, such as cancer vaccines (activated autologous peripheral-blood mononuclear cells (PBMCs) for the recognition of Prostatic Acid Phosphatase (PAP) (Kantoff et al., 2010)), or checkpoint inhibitors (anti-CTLA4 antibody) (Pardoll, 2012). However, such therapies demonstrated limited efficacy in cancers from certain origins and in advanced stages, and the development of novel therapies with alternative anti-tumor mechanisms seems mandatory for improving the overall survival of patients.

Cancer virotherapy represents an innovative therapeutic modality with unique characteristics. Oncolytic viruses have the ability to selectively replicate in neoplastic cells without damaging normal tissues (Hedley et al., 2006; Russell et al., 2012). The viral progeny produced in the initial infection is released to the extracellular media where it can infect

neighboring cells, therefore amplifying the initially administered dose, ideally until the eradication of the tumor mass (**Figure 1**).

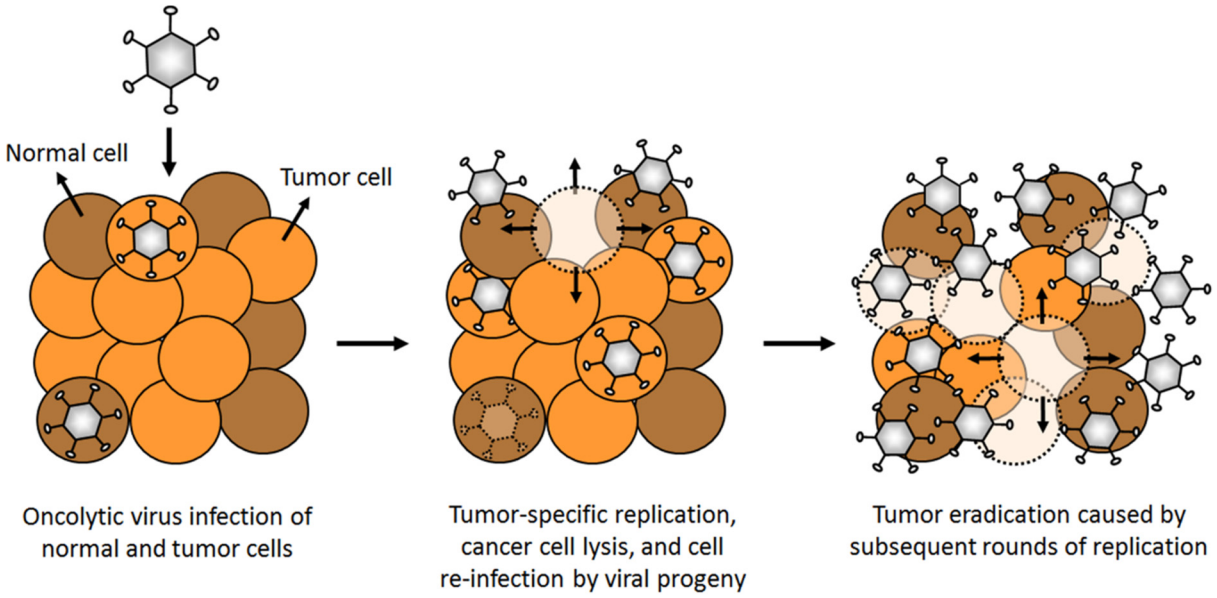

Figure 1. Principle of cancer virotherapy. The oncolytic virus infects preferably tumor cells and selectively replicates in them. If a normal cell is infected the replication cycle is aborted. Virus replication leads to cancer cell lysis and release of the viral progeny. The new generated viruses initiate new replicative cycles, disseminating throughout the tumor mass until its elimination.

In addition to the direct killing of cancer cells by virus replication, oncolytic viruses can also mediate the destruction of uninfected cancer cells by indirect mechanisms such as destruction of tumor blood vessels, bystander killing caused by the expression of therapeutic transgenes inserted in the oncolytic virus genome, or systemic antitumor immune responses triggered by viral tumor cell lysis (Russell et al., 2012; Ungerechts et al., 2016). In the last years, research and clinical translation has specifically focused on the latter, and on the combination of oncolytic viruses with immunotherapy approaches such as immune checkpoint inhibitors (Lichty et al., 2014; Rojas et al., 2015; Woller et al., 2014).

The concept of virotherapy emerged at the beginning of the 20th century after the observation of tumor regressions in patients who had suffered from virus infections or had been vaccinated (Pack, 1950). Dock and co-workers described in 1904 a leukemia case that regressed after an infection with influenza virus (Dock et al., 1904). Also, in 1912 DePace observed the remission of a cervix tumor after the administration of a rabies vaccine (De Pace, 1912). In 1950s and 1960s, the development of cell and tissue culture systems allowed *ex vivo*

virus propagation, and led to the evaluation in humans of different viruses that had been previously tested in rodents. However, the interest on the field was lost due to poor efficacy results and toxicity of some viruses. Virotherapy emerged back in the 1990s due to increasing knowledge in the molecular basis of cancer, virus biology, and the development of genetic engineering techniques, which permitted a more rational design of oncolytic viruses (Martuza et al., 1991). Thenceforth, several engineered oncolytic viruses from different families have been developed and tested in clinical trials including adenoviruses, HSVs (herpes simplex virus), coxsackieviruses, measles viruses, NDVs (Newcastle disease virus), parvoviruses, reovirus, VV (vaccinia virus), VSVs (vesicular stomatitis virus), etc. (Russell et al., 2012), demonstrating excellent tolerability profiles. Until now, evidences of antitumor activity after single-agent treatment in clinical trials have only been observed with two oncolytic viruses. The first one is talimogene laherparepvec (T-Vec, tradenamed Imlygic®, Amgen), an oncolytic HSV encoding the granulocyte macrophage-colony stimulating factor (GM-CSF). Intratumoral administrations of this virus resulted in complete regressions in 8 of 50 treated patients with metastatic melanoma in a phase II clinical trial (Senzer et al., 2009). More recently, a phase III clinical trial in patients with unresectable stage IIIB-IV melanoma showed an overall objective response rate of 26.4% including 10.8% of complete responses (Bartlett et al., 2013). Importantly, T-Vec was approved in 2015 for the treatment of melanoma, representing the first oncolytic virus approved by the US Food and Drug Administration (FDA) for cancer treatment. The second virus is a vaccinia virus (Wyeth strain) named pexastimogene devacirepvec or Pexa-Vec (also known as JX-594), which also expresses GM-CSF. Intratumoral administration of this virus induced objective responses in 3 out of 10 evaluable patients with unresectable hepatocellular carcinoma (Park et al., 2008). Also, a significant increase in survival from 6.7 to 14.1 months was achieved in a more recent phase I/II clinical trial in patients also suffering from hepatocellular carcinoma (Heo et al., 2013).

Generally speaking, although oncolytic viruses have shown to be safe and well tolerated in human patients, the antitumor efficacy still needs improvement. Furthermore, the majority of clinical studies with oncolytic viruses, and especially those where evidence of antitumor activity was observed, have used intratumoral injections. However, systemic delivery will be required for treatment of metastatic cancer and therefore represents a more desirable option. Intratumoral injections are not always feasible and are limited to those tumors physically accessible through clinical palpation or direct imaging. In contrast, the systemic injection allows the oncolytic virus to reach the multiple metastases in the case of disseminated tumors, and also results in a more uniform distribution of the virus within the tumor (Wein et al.,

2003). Unfortunately, clinical trials with intravenous injection of oncolytic viruses have shown in general worse outcomes. Oncolytic viruses encounter several barriers in the bloodstream such as liver or spleen sequestration, neutralization by serum factors, or difficulties in tumor extravasation, which prevent them from infecting tumors (see section 2.7.1). The most clinically advanced oncolytic viruses delivered by intravenous injection are the vaccinia virus Pexa-Vec (JX-594) and a wild-type reovirus serotype 3 (Dearing strain) named Reolysin®. A phase I clinical trial with Pexa-Vec demonstrated for the first time that the intravenously administered virus is able to infect and replicate in metastases located in different tissues, besides dose-dependent antitumor activity (Breitbach et al., 2011), which led to further clinical development. On the other hand, Reolysin® has been tested alone or in combination with chemotherapy via systemic injection, usually observing modest responses as monotherapy (Ungerechts et al., 2016). A phase I/II clinical trial by intravenous administration in combination with paclitaxel and carboplatin demonstrated a 70% of objectives responses (Karapanagiotou et al., 2012). Further results in phase II trials suggest a benefit when combining reovirus with chemotherapy (Villalona-Calero et al., 2016), and a phase III clinical trial demonstrated a significant improvement in overall survival compared to chemotherapy alone (Gong et al., 2016). Other oncolytic viruses tested by the intravenous route are the vaccinia virus GL-ONC1 for the treatment of solid tumors, the parvovirus H-1PV for glioblastoma, Newcastle disease viruses for glioblastoma (Russell et al., 2012), and several oncolytic adenoviruses (see section 2.6.).

In our group, we consider the intravenous administration route more relevant than the usually employed intratumoral route. Therefore, this thesis has focused on the systemic administration of oncolytic viruses, specifically of oncolytic adenoviruses.

2. ONCOLYTIC ADENOVIRUSES

Adenoviruses possess several features that make them attractive as oncolytic agents such as their low pathogenicity in immunocompetent patients, their potent lytic activity which results in the elimination of the infected cell, and the detailed knowledge of their structure and replication cycle which facilitates genetic modification to confer potency and selectivity. In addition, their high replicative capacity permits the obtention of high amounts and highly concentrated virus preparations (10^{12}-10^{13} vp/mL) for its use in the clinical setting (Cody and Douglas, 2009; Ungerechts et al., 2016).

2.1. ADENOVIRUS CLASSIFICATION

Adenoviruses are members of the family *Adenoviridae*, and their name derive from their isolation from human adenoid cells in 1953 (Rowe et al., 1953). Since then, more than 100 species have been characterized and currently 57 human serotypes have been described, originally based on their ability to be neutralized by specific animal antisera. These 57 human serotypes are divided in 7 subgroups (A-G, subgroup B is further divided into B1 and B2) based on their hemagglutination properties, oncogenic potential in rodents, DNA homology, and genomic organization (**Table 1**). Generally speaking there is a correlation (although imperfect) between subgroup and tissue tropism, as for instance groups B1, C, and E can cause respiratory infections, B2 infect the kidney and urinary tract, F cause gastroenteritis, and several group D serotypes are associated with conjunctivitis (Zhang and Bergelson, 2005). The human adenovirus serotype 5 (Ad5) (subgroup C) has been the most widely used in the fields of gene therapy, cancer virotherapy, and vaccination. Ad5 mainly infects epithelial cells from the respiratory tract, causing mild respiratory symptoms similar to a common cold. Ad5 is the serotype used in this thesis.

Table 1. Classification of human adenoviruses (adapted from (Hall et al., 2010))

Subgroup	Serotype	Receptor Usage	Associated disease
A	12, 18, 31	CAR	Gastroenteritis
B1	3, 7, 16, 21, 50	CD46, CD80, CD86	Respiratory disease
B2	11, 14, 34, 35, 55	CD46, CD80, CD86, Desmoglein-2	Urinary tract disease
C	1, 2, 5, 6, 57	CAR	Respiratory disease
D	8, 9, 10, 13, 15, 17, 19, 20, 22-30, 32, 33, 36-39, 42-49, 51, 53, 54, 56	CAR, Sialic acid, CD46	Keratoconjunctivitis
E	4	CAR	Respiratory disease, Conjunctivitis
F	40, 41	CAR	Gastroenteritis
G	52	Unknown	Gastroenteritis

2.2. ADENOVIRUS VIRION STRUCTURE

Adenoviruses are non-enveloped double-stranded DNA viruses, formed by an icosahedral capsid with 20 triangular faces and 60-90 nm of diameter. Each of the triangular faces is formed by 12 hexon trimers (polypeptide II), and complexes formed by the pentameric penton base (polypeptide III) and trimeric fiber (polypeptide IV) form the vertices. The fiber protein emerges from the 12 vertices as an antenna, and is structured in three domains: the N-terminal tail which attaches to the penton base, a central *shaft*, and a C-terminal globular *knob* domain. The fiber and the penton base interact with cellular receptors and determine virus tropism (Russell, 2009). In addition to these three main capsid proteins, other minority proteins such as protein pIIIa, pVI, pVIII, and pIX act as cement between hexons. The capsid protects the double-stranded viral DNA, which is associated to core proteins pV, pVII, Mu (pX), and terminal protein (TP) (**Figure 2**).

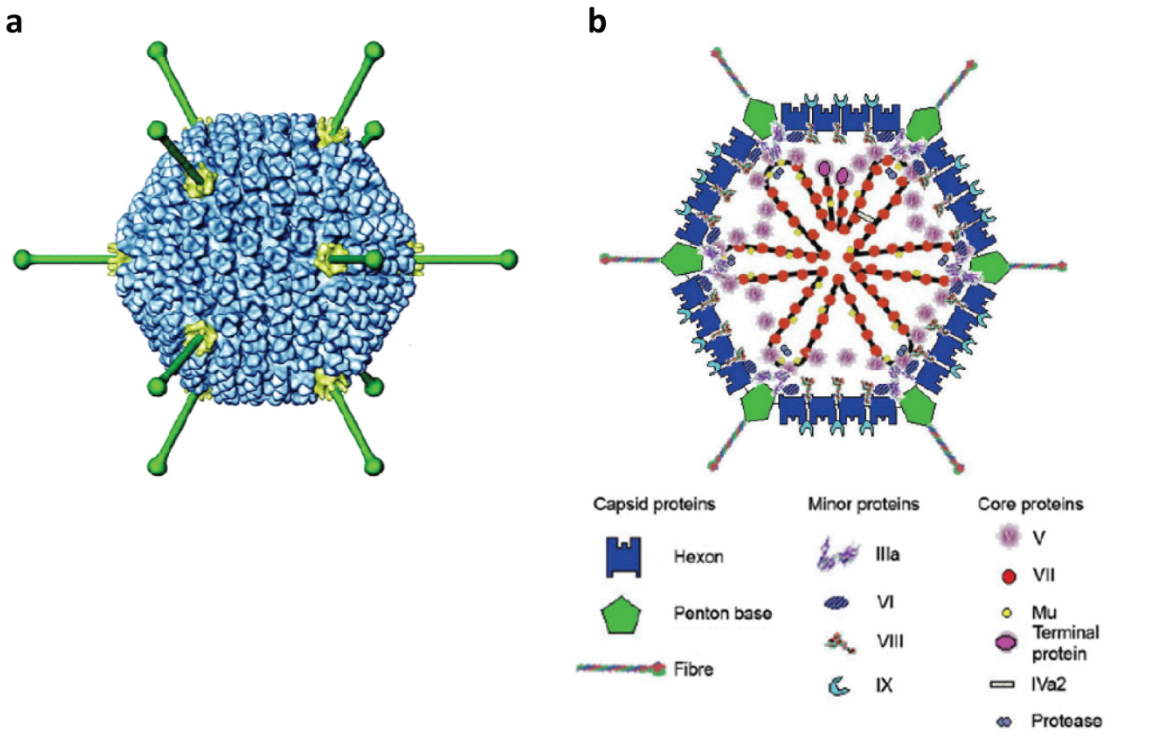

Figure 2. Adenovirus structure. (a) Virion structure at 17 Å resolution. The three main capsid proteins are depicted. The hexon protein (blue) is the most abundant capsid protein and forms the 20 triangles of the icosahedral capsid. At each vertex, the fiber protein (green) protrudes from the penton base (yellow) (from (Zhang and Bergelson, 2005). (b) Protein composition of adenovirus capsid. Capsid and minor protein locations are well defined whereas disposition of core proteins and virus DNA is conjectural (from (Russell, 2009)).

2.2.1. The hexon protein

The hexon is by far the most abundant structural protein of adenovirus capsid with 240 copies of its trimeric form, which form the 20 triangular faces of the icosahedral capsid. Sixty hexons associate with the penton base at the 12 apices and are named peripentonal hexons, whereas remaining hexons on the 20 faces of the icosahedron are designated “groups of nine” (GONs) (Russell, 2009). Comparison of hexons of different serotypes revealed the presence of highly conserved regions that play a very important role in capsid conformation, and 7 loops displayed at the surface of the molecule which are not conserved among serotypes named hypervariable regions (HVR) (Crawford-Miksza and Schnurr, 1996) (**Figure 3**). The conserved residues at the base confer the pseudo hexagonal shape of the trimeric form and interact with other capsid proteins, allowing the assembly of the virus capsid. Such structurally relevant regions rarely allow modifications as any instability in the hexon structure might compromise correct virion formation. On the other hand, HVRs do not play any structural role nor are implicated in binding other capsid proteins, and contain the antigenic determinants that characterize each serotype. The high flexibility and variability of these loops allow several modifications such as insertion of foreign sequences or interchange between serotypes without affecting the assembly of the capsid (Alba et al., 2009; Khare et al., 2011a; Roberts et al., 2006).

2.3. GENOME STRUCTURE

Ad5 genome is a 36 kb linear molecule of double-stranded DNA. At both ends of the genome there are the inverted terminal repeats (ITR), which contain the viral DNA replication origins. The packaging signal, located at 100 bp of the left ITR, is rich in adenine and thymine and plays an important role on genome encapsidation. Genetic information is organized in overlapping transcription units on both strands (**Figure 4**). Extensive splicing leads to the translation of over 50 proteins, from which 11 are structural virion proteins (Verma and Weitzman, 2005). Adenovirus genes are classified in three groups according to the time course of their expression during viral cycle: early (E1A, E1B, E2, E3, and E4), delayed (IX and IVa2), and the late transcription unit (MLU), whose expression is under the control of the major late promoter (MLP). The latter is processed into five mRNAs (L1-L5) which produce the structural proteins of the capsid. In addition, adenovirus genome also contains the viral-associated (VA) genes that codify for two non-coding RNAs.

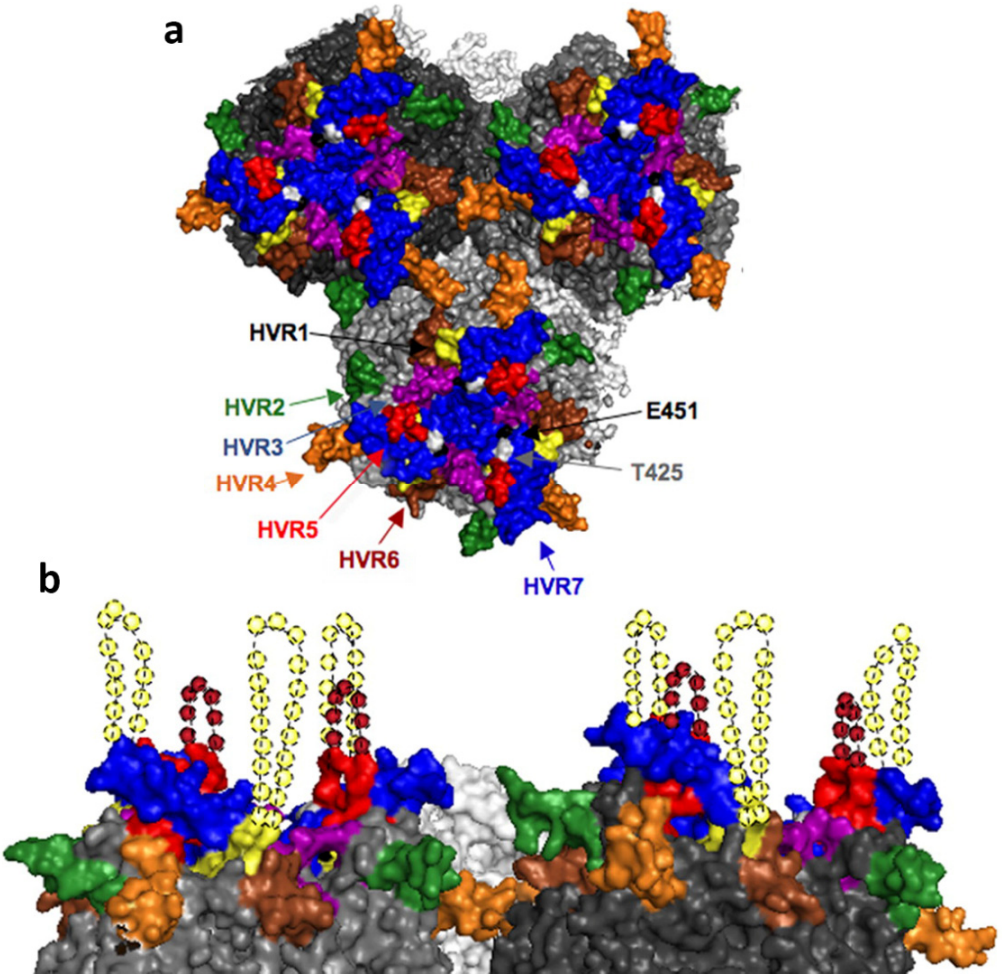

Figure 3. Model of Ad5 hexon trimer structure. (a) Top view, three hexon trimers are represented with structured HVR domain in color codes as follows: HVR1 yellow, HVR2 green, HVR3 purple, HVR4 orange, HVR5 red, HVR6 brown, HVR7 blue. (b) Side view, speculated location of the unstructured HVR1 and HVR5 loops in two adjacent hexon trimers (modified from (Khare et al., 2012)).

2.4. INFECTIOUS CYCLE

Adenoviruses are lytic viruses. The virus cycle can be divided in two phases: the early phase which comprises virus entry and internalization into host cell, endosome escape, transport to nucleus, transcription of early genes and genome replication; and the late phase which comprises transcription and translation of late genes, assembly of structural proteins to form the capsids, and genome encapsidation. The virus cycle finalizes with the lysis of the host cell and the release of the virus progeny to the extracellular media.

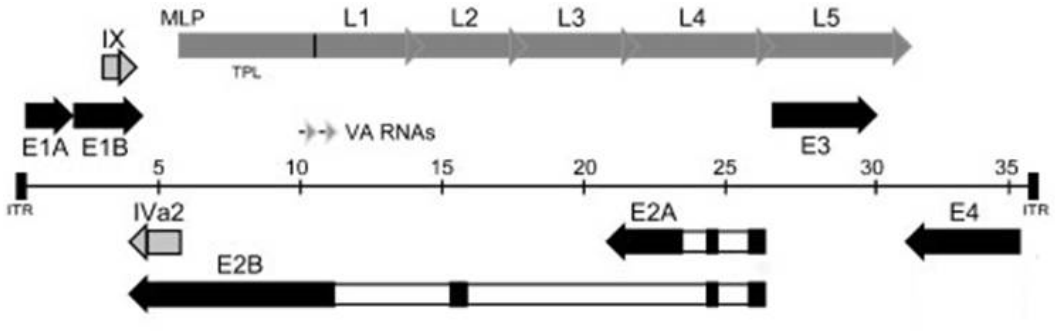

Figure 4. Adenovirus genome organization. The linear double-stranded DNA genome is depicted in the center as a thin line, with the inverted terminal repeats (ITR) at each end. DNA lengths are marked in kb. Transcription units are shown relative to their position and orientation in the genome. Early genes are indicated by black bars, intermediate and late genes are indicated by gray bars, and virus-associated (VA) RNAs are denoted by small arrows (modified from (Tauber and Dobner, 2001)).

2.4.1. Binding and entry

Initial interaction between Ad5 and host cell occurs through primary interaction between the fiber *knob* and the coxsackievirus and adenovirus receptor (CAR) on the cell surface. For the internalization of the virus, a second interaction is required between an RGD (Arg-Gly-Asp) motif located on the penton base and $\alpha_V\beta3$ and $\alpha_V\beta5$ integrins (Nemerow and Stewart, 1999). Alternatively, it was described that liver transduction after intravenous administration occur by a different mechanism due to virus interaction with blood factors, such as coagulation factor IX (FIX) and complement binding protein-4 (C4BP) which bind to fiber knob, or coagulation factor X (FX) which binds to the hypervariable regions (HVRs) of hexon. Both types of interactions act as a bridge between the virus and alternative cell receptors on hepatocytes such as HSGs (heparan sulphate-glycosaminoglicans) and lipoprotein receptor-related proteins (LRPs) (Kalyuzhniy et al., 2008; Shayakhmetov et al., 2005; Waddington et al., 2008). In addition, direct interaction between Ad5 and HSGs can also occur, and the $KKTK^{91\text{-}94}$ amino acidic sequence in the fiber *shaft* has been postulated as the HSG-binding motif (Zhang and Bergelson, 2005).

Binding of adenovirus particles to its cellular receptors triggers clathrin-dependent, receptor-mediated endocytosis (Coughlan et al., 2010). After the virus is internalized, endosome acidification promotes partial capsid disassembly and escape of virus particle to the cytoplasm before lysosome formation. Once in the cytoplasm, Ad5 hexon recruits the molecular motor protein cytoplasmic dynein in a pH-dependent manner, and the virus particle

is transported along the microtubules towards the nucleus. This function is critical for efficient infection, and the role of HVR1 on dynein recruitment was recently described (Scherer and Vallee, 2015). After reaching the nucleus, the capsid is completely disassembled and the viral DNA is translocated through the nuclear pore complex for subsequent transcription and replication (**Figure 5**).

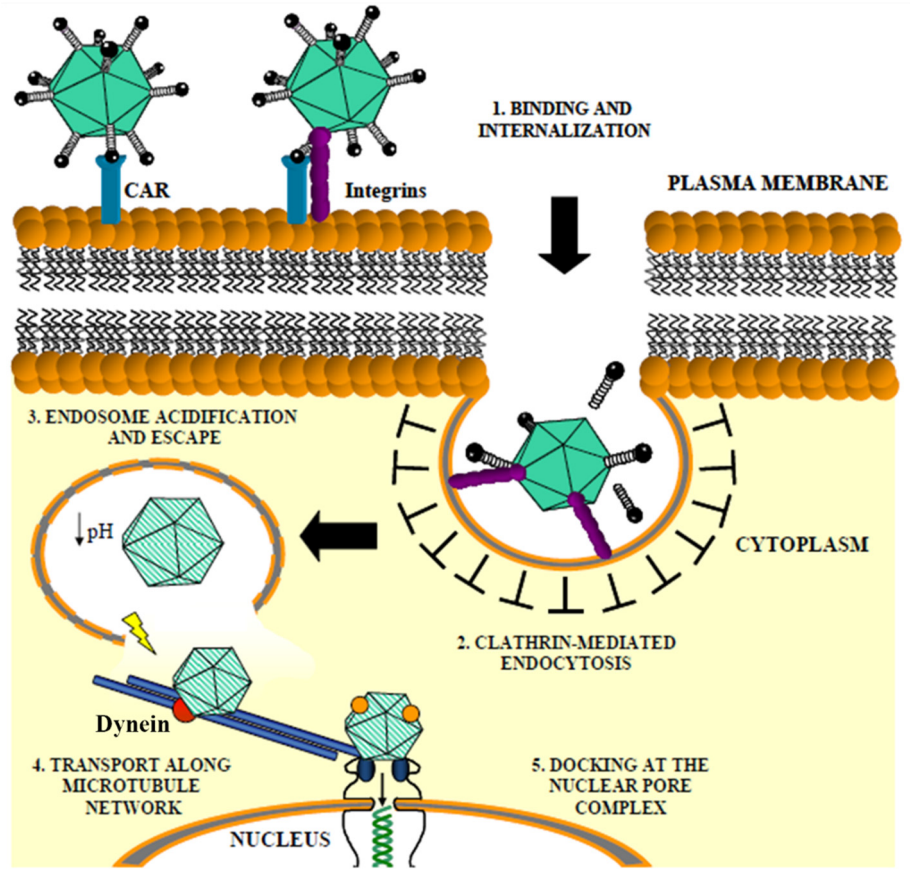

Figure 5. *In vitro* entry pathway of Ad5. Steps involved in the *in vitro* entry pathway of Ad5 are binding to CAR and integrins, internalization by clathrin-mediated endocytosis, endosome escape, dynein-mediated transport along microtubules, and DNA translocation into nucleus (modified from (Coughlan et al., 2010)).

2.4.2. Early gene expression and DNA replication

E1A is the first transcription unit expressed and its proteins perform several functions. E1A activates the cell cycle by interacting with Retinoblastoma protein (Rb), which is a tumor suppressor that inhibits the cell cycle via binding to E2F transcription factor. E1A products are able to sequester pRb and other members of its family such as p107 and p130, impeding E2F

sequestration by these proteins, and thus activating the cell cycle and allowing viral DNA replication (Parreno et al., 2001). In addition, E1A proteins activate the transcription of the rest of early transcription units (E1B, E2A, E2B, E3, and E4). The deregulation of the cell cycle caused by E1A results in the accumulation of the tumor suppressor p53, which induces apoptosis as a cell defense mechanism. To avoid apoptosis, viral protein E1B-55K directly binds p53 and induces its degradation, whereas E1B-19K binds to other proapoptotic proteins such as Bak and Bax. The genes in E2 region encode for the proteins required for the replication of the genome including DNA polymerase, preterminal protein, and the single-stranded DNA-binding protein. E3 proteins are responsible for inhibition of the immune response in order to avoid the destruction of the infected cell before completing the cycle. For instance, E3-19K sequesters MHC class I molecules in the endoplasmic reticulum, preventing its transport to the cell surface. Furthermore, it can also interfere in the loading of peptides onto MHC class I molecules by binding to the transporter associated to antigen processing (TAP). The E4 transcriptional unit is involved in viral replication, stability and transport of viral mRNA, and expression of late genes.

2.4.3. Late gene expression and viral assembly

Once DNA replication has been initiated, the transcriptional activity from the major late promoter (MLP) is intensified due to changes in genome structure and its activation mediated by viral protein IVa2. The MLP regulates the expression of genes from the major late transcription unit, which encodes for 15 to 20 different mRNAs derived from a single pre-mRNA by differential splicing and polyadenylation. Most late proteins are expressed from regions L1-L5, and correspond to structural proteins and proteins involved in virion assembly and genome packaging (Guimet and Hearing, 2016). Late mRNAs are accumulated in the cytoplasm and specifically translated in the late phase thanks to the tripartite leader sequence (TLP). All proteins are translated in the cytoplasm and subsequently transported to the nucleus. Hexon assembly begins in the cytoplasm and the trimers are then transported to the nucleus (McConnell and Imperiale, 2004). Once there, hexons associate with the penton base, the fiber, and minor proteins, and the DNA is incorporated guided by the encapsidation sequence and DNA-binding proteins. Capsids are accumulated in the nucleus, which becomes permeable and intermediate filaments are disaggregated, resulting in a cell round morphology characteristic of cytopathic effect (CPE). Although the mechanism is not well understood, expression of ADP (adenovirus death protein) favors the release of the virus progeny to the extracellular medium.

2.5. DESIGN OF TUMOR SELECTIVE ONCOLYTIC ADENOVIRUSES: ICOVIR15 AND ICOVIR15K

Contrary to other viruses such as reovirus, Newcastle disease virus (NDV), or vesicular stomatitis virus (VSV), adenovirus does not have a natural selectivity for tumor cells and therefore genetic manipulation is required to block replication in normal cells. Three main strategies have been applied to achieve tumor selectivity: deletion of viral genes that are complemented by tumor cells, control of the expression of essential viral genes by tumor-specific promoters (transcriptional or translational targeting), or modification of capsid proteins to confer specific or preferential infection of tumor cells (transductional targeting). ICOVIR15 (Rojas et al., 2010) and ICOVIR15K (Rojas et al., 2012) are two oncolytic adenoviruses designed in our group that combine the three approaches. These viruses are currently used in our group as platforms to incorporate and test novel modifications and improvements. A schematic representation of ICOVIR15 and ICOVIR15K genome with the modifications that make them tumor-selective is shown in **Figure 6**.

Adenoviruses require the host cell machinery for the replication of their genome. Therefore, mutations or deletions on viral genes involved in activating cell replication or in inhibiting apoptosis hinder virus replication in normal cells. In contrast, as cell replication is constantly activated in tumor cells and apoptosis pathways are usually inhibited, viruses bearing these deletions are able to replicate in cancer cells at normal ratios. In this regard, ICOVIR15 and ICOVIR15K contain the Δ24 mutation in E1A protein (Fueyo et al., 2000; Heise et al., 2000), which consists in the deletion of the E1A region responsible for binding and inactivating Rb. This function is necessary to induce S phase and thus replicate in normal cells (see section 2.4.2.), whereas it is not required in tumor cells which are in constant replication (**Figure 6b**).

As previously explained, E1A is essential for virus replication not only because it induces S phase in the host cell, but also because it activates the expression of the rest of adenovirus early genes. Therefore, viral replication can be restricted to tumor cells by controlling E1A expression with a tumor-specific promoter. Due to the deregulation of Rb pathway in almost all tumors, promoters that respond to E2F transcription factor are suitable to achieve restricted replication in a broad range of tumors. E1A regulation by E2F-1 promoter confers selectivity and high potency of transcription (Cascallo et al., 2007; Johnson et al., 2002; Rojas et al., 2009; Tsukuda et al., 2002). In such adenoviruses, E1A transcription is inhibited in normal cells due to binding of pRb-E2F-HDAC complexes to E2F-1 promoter. On the contrary, alteration of Rb pathway in tumor cells results in free E2F, which activates expression of E1A.

E1A activates the rest of viral genes including E4-6/7, which forms a complex with E2F and activates more efficiently the E2F-1 promoter and E2 promoter, resulting in a positive feedback loop. In contrast to the insertion of a whole exogenous promoter, ICOVIR15 and ICOVIR15K incorporate eight E2F responsive sites in the endogenous promoter of E1A (**Figure 6a**) (Rojas et al., 2010). In addition, a Sp-1 binding site was also included as both factors interact cooperatively to activate transcription (Karlseder et al., 1996). These additional boxes in the promoter enhance E1A expression in tumor cells compared to Adwt, resulting in increased oncolytic potency. Such modification only increases in 151 bp the adenovirus genome, allowing the insertion of foreign transgenes without affecting viral replication and oncolytic potency (Guedan et al., 2010, 2012; Rojas et al., 2010). Hence, these viruses present a double control of the viral cycle in quiescent cells, and in case that leaky expression of E1A occurs, the Δ24 deletion impedes the release of E2F from pRb.

The third approach used to limit adenovirus replication to the tumor tissue is the modification of capsid proteins to achieve preferential infection of tumor cells rather than normal cells. This strategy includes the ablation of the natural virus tropism (detargeting), and the redirection of virus infection to tumor-associated receptors (retargeting). Upon intravenous administration, adenovirus accumulates mostly in the liver causing toxicity and reducing the virus bioavailability. Therefore, liver detargeting has been an important subject in the field over the years. Abrogation of adenovirus interaction with coagulation factor X (FX) or mutation of the putative heparan sulfate glycosaminoglycan (HSG)-binding domain KKTK in the fiber *shaft* have demonstrated to reduce hepatic transduction (Alba et al., 2010; Smith et al., 2003; Waddington et al., 2008). However, these modifications also caused a reduced infection of tumors (Bayo-Puxan et al., 2006; Gimenez-Alejandre et al., 2008). With regard to tumor retargeting, adenoviruses exposing different ligands in different capsid locations such as fiber, hexon, penton base, or pIX have been described (Coughlan et al., 2010). Specifically, a widely used ligand to achieve tumor tropism is the RGD-4C motif (CDCRGDCFC) which targets RGD-binding integrins that are overexpressed in tumor cells (Cripe et al., 2001; Dmitriev et al., 1998; Grill et al., 2001; Nagel et al., 2003; Wesseling et al., 2001). The insertion of this ligand in the HI-loop of the fiber *knob* permits the use of integrins as primary receptors instead of CAR, which is not highly expressed in tumor cells (Bauerschmitz et al., 2002; Suzuki et al., 2001). This modification is included in ICOVIR15. In contrast, ICOVIR15K combines a liver detargeting and a tumor retargeting approach, consisting in the replacement of the KKTK domain in the fiber shaft with an RGD motif (**Figure 6c**). This strategy was described by our group demonstrating improved tumor-to-liver ratio *in vivo* in the context of a non-replicative

adenovirus (Bayo-Puxan et al., 2009). When inserted in an oncolytic platform, ICOVIR15K showed increased bioavailability after systemic administration and greater antitumor efficacy *in vivo* compared to ICOVIR15 (Rojas et al., 2012).

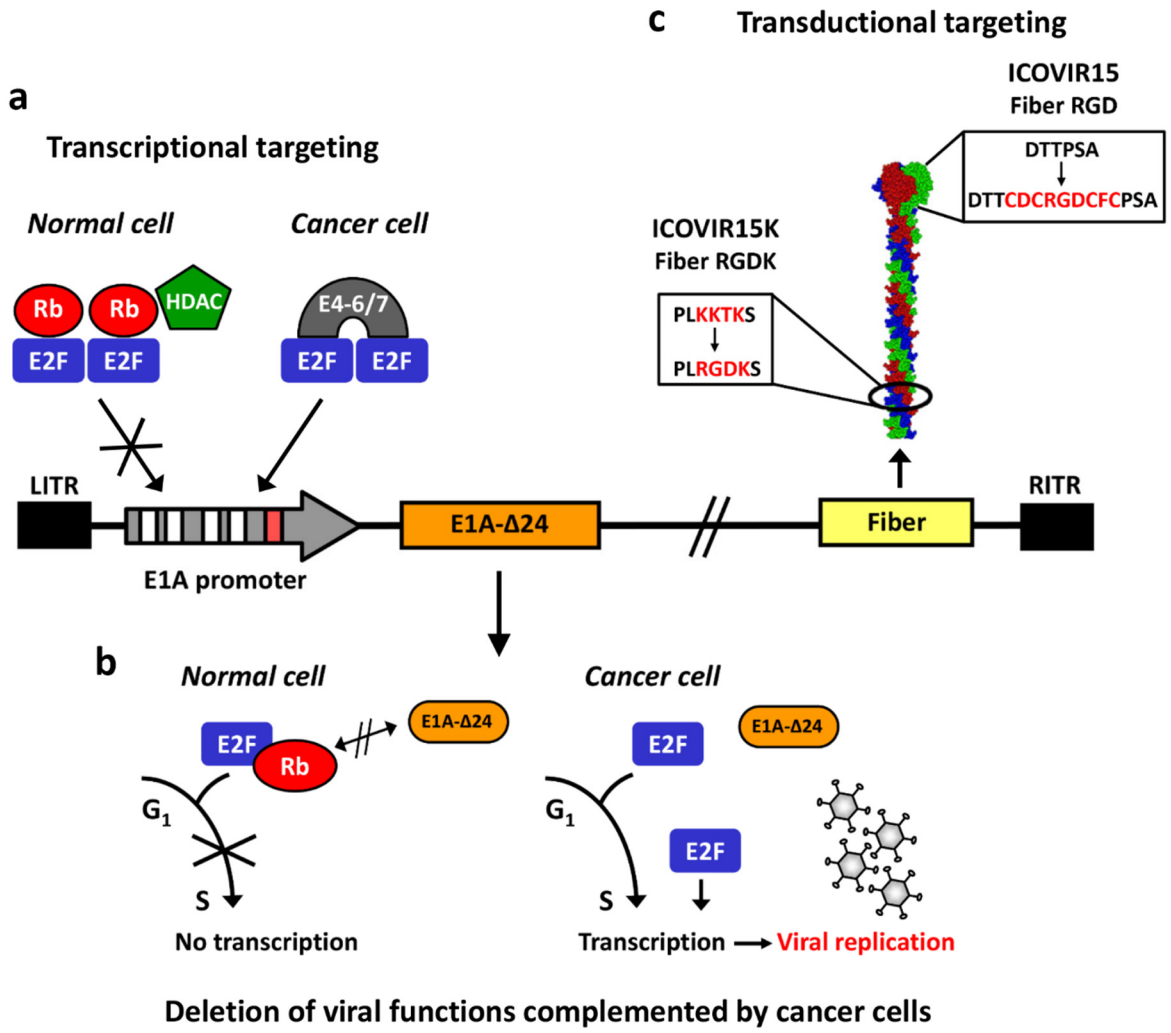

Figure 6. Schematic representation of the modifications in ICOVIR15 and ICOVIR15K genomes. Both oncolytic adenoviruses contain the modified E1A promoter with four E2F boxes (white squares) and one Sp1 box (red square), and the truncated E1A-Δ24 protein to confer selectivity for tumor cells. In ICOVIR15 the RGD motif is inserted in the HI-loop of the fiber *knob* (fiber RGD), whereas in ICOVIR15K is inserted in the fiber *shaft* replacing the KKTK domain.

2.6. CLINICAL EXPERIENCE WITH INTRAVENOUS INJECTION OF ONCOLYTIC ADENOVIRUSES

Few clinical trials have been performed by systemic injection of oncolytic adenoviruses. In fact, until 2010 only two candidates had been tested via intravenous route, ONYX-015 and

CG7870. *dl152* or ONYX-015, developed by Onyx pharmaceuticals, was the first engineered replication selective adenovirus to be used in humans. This virus harbors a deletion of the E1B-55K gene making it selective for p53-deficient tumors (Bischoff et al., 1996). Several trials were conducted by intravenous injection of ONYX-015 (some in combination with chemotherapy) in patients with colorectal tumors, hepatic tumors, and various disseminated solid tumors. The highest dose administered to a patient in dose-escalation studies was $2x10^{13}$ vp on day 1, followed by weekly doses of $2x10^{11}$ vp, resulting in an accumulated dose of $4.2x10^{13}$ vp (Nemunaitis et al., 2001). Albeit certain dose-dependent toxicity effects were observed (fever, vomits, nausea, or transitory transaminitis), maximum tolerated dose was not reached. Nevertheless, signs of antitumor efficacy were rarely detected and only some partial responses, stable diseases, or decrease of tumor markers were observed in some patients (Habib et al., 2002; Hamid et al., 2003; Nemunaitis et al., 2001; Reid et al., 2002). Despite this lack of efficacy, evidence of tumor transduction and virus replication was observed. However, in one study in which a patient died due to disease progression, tissue biopsies revealed that the majority of the virus was in the liver and the spleen, whereas virus presence in the tumor was significantly lower (Hamid et al., 2003). Notwithstanding the poor efficacy of ONYX-015, the Chinese company Sunway Biotech is commercializing a derivative of this virus named H101 for the intratumoral treatment of head and neck cancer in China. H101 contains an additional deletion of E3 genes, making it less potent and more immunogenic (Garber, 2006).

The next oncolytic adenovirus tested by systemic injection was CV787, renamed CG7870 after the acquisition of Calydon by Cell Genesys, and now developed by Cold Genesys. This virus expresses E1A under the control of probasin promoter, and E1B under the control of PSA promoter, making it selective for prostatic cancer (Yu et al., 1999). Similarly to ONYX-015, flu-like symptoms (fever, fatigue, nausea, vomiting, etc.) were reported in a phase I clinical trial, but dose-escalation had to be halted at $6x10^{12}$ vp due to more severe adverse effects (Small et al., 2006). A secondary peak in plasma of virus genomes suggested active viral replication. However, a drop on the tumor marker PSA in 3 out of 8 patients treated with the highest dose was the only reported response.

Currently, more oncolytic adenoviruses are being developed and administered systemically in clinical trials. ColoAd1 (Enadenotucirev) is an oncolytic adenovirus developed by Psioxus and generated by “directed evolution”. This process was performed by pooling an array of adenovirus serotypes (representing subgroups B-F), passaging the pools at high MOIs (multiplicity of infection) to promote recombination between serotypes, and then identifying

and selecting the most potent agents (Kuhn et al., 2008). The selected virus ColoAd1 is a chimeric Ad11 with a nearly complete E3 region deletion, a smaller deletion in E4 region, and a chimeric Ad3/Ad11p E2B region. Unlike Ad5, ColoAd1 demonstrated to retain its cancer killing activity in presence of fresh human blood (Di et al., 2014), making it an interesting candidate for systemic treatment. Several Phase I/II trials are currently testing ColoAd1 by intravenous administration in different types of cancer including ovarian cancer, colorectal cancer, or bladder cancer. Moreover, phase I clinical trials to test the safety and efficacy of two oncolytic adenoviruses developed by our group (ICOVIR5 and VCN01) by systemic injection are currently ongoing. ICOVIR5 is a derivative of AdΔ24RGD (Suzuki et al., 2001) which controls E1A expression by an insulated form of the E2F promoter (Cascallo et al., 2007) and has been clinically developed from the academia at ICO (Institut Català d'Oncologia). VCN01 (also known as ICOVIR17K) is a version of ICOVIR15K expressing the PH20 hyaluronidase (Rodriguez-Garcia et al., 2015), and has been developed clinically by VCN biosciences.

2.7. LIMITATIONS OF ONCOLYTIC ADENOVIRUSES

Cancer virotherapy with oncolytic adenoviruses presents several limitations, which account for this lack of efficacy in the clinic, especially after systemic administration. The bloodstream is a highly hostile environment for the virus and several interactions contribute to its neutralization and rapid clearance, preventing it from reaching tumors (**Figure 7**). It was reported that the adenovirus half-life after systemic administration was less than 2 minutes in mice (Alemany et al., 2000) and 10 minutes in humans (Reid et al., 2002). On top of this rapid clearance, the virus will face additional barriers in the tumor microenvironment such as limited intratumoral spread and the antiviral immune response

2.7.1. Systemic injection of adenoviruses

2.7.1.1. Adenovirus retention in the liver

Upon the intravenous administration, 90% of the injected dose is rapidly retained in the liver, causing hepatotoxicity and a significant reduction of the effective dose (Alemany et al., 2000). Such retention occurs due to the architecture of the liver sinusoids and interactions with different cell types, including hepatocytes, liver macrophages (Kupffer cells), and liver sinusoid endothelial cells (LSECs).

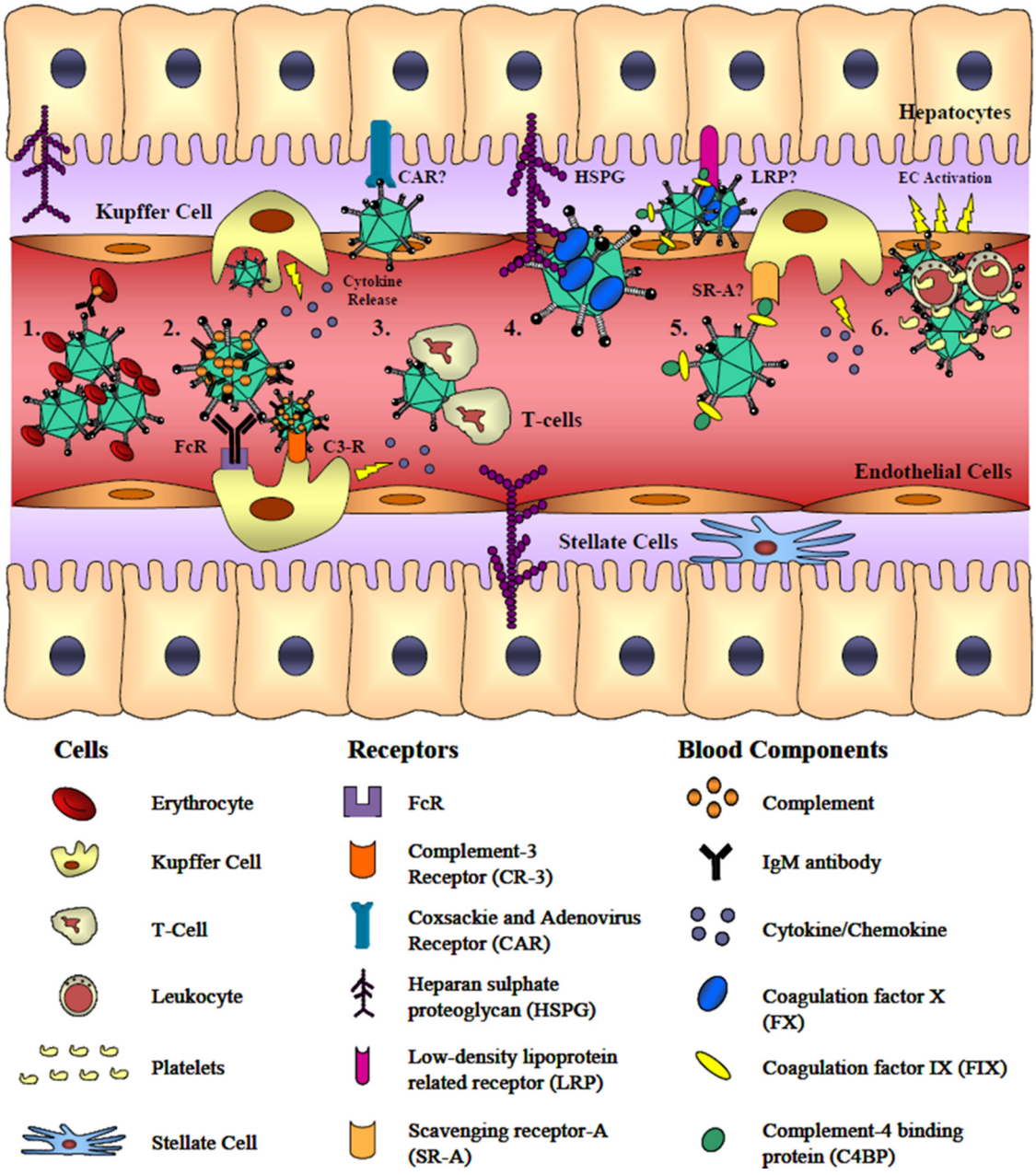

Figure 7. Ad5 interactions with blood components *in vivo*. 1. Ad5 binding to erythrocytes via CAR, or via CR1 through antibodies and complement traps the virus in the circulation. **2.** Ad5 opsonization by natural IgM and/or complement promotes Kupffer cell uptake via complement receptors or Fc receptors. **3.** Interaction with T-cells. **4.** FX binding to Ad5 hexon promotes hepatocyte transduction through HSPGs. **5.** Binding of FIX and C4BP to the fiber knob mediates hepatocyte transduction through HSPGs or LRP. **6.** Binding to platelets form aggregates which are cleared by scavenging macrophages (from (Coughlan et al., 2010)).

Liver reticuloendothelial system, formed by Kupffer cells and LSECs, highly contributes to adenovirus retention and elimination. Kupffer cells are specialized macrophages lining the walls of the sinusoids, and due to their location represent the first line of defense against

viruses. Adenovirus sequestration by Kupffer cells prevents transduction of hepatocytes, and results in necrosis of these cells, which plays a role in inflammation and triggers innate and adaptive immune responses to the virus (Liu and Muruve, 2003). The capability of adenovirus to transduce hepatocytes is not linearly dependent on the injected dose, as there is a threshold dose around 10^{11} vp/kg (Manickan et al., 2006) above which Kupffer cells are eliminated and hepatocytes are massively transduced (Tao et al., 2001). Scavenger receptors (SRs), which recognize hexon hypervariable regions (HVRs), are responsible for adenovirus uptake (Haisma et al., 2008; Xu et al., 2008). Specifically, HVR1, HVR2, HVR5, and HVR7, were proposed to be especially involved in Kupffer cell recognition (Khare et al., 2012). In addition to recognition by SRs, natural antibodies (IgMs) and complement proteins opsonize the virus and enhance Kupffer cell-mediated clearance through Fc receptors or complement receptors (Khare et al., 2013; Smith et al., 2008). Furthermore, LSECs are also a very important component of the liver reticuloendothelial system and along with Kupffer cells, contribute to eliminate the virus from circulation (Ganesan et al., 2011; Piccolo et al., 2013).

The viral dose able to escape Kupffer cells can then infect hepatocytes. Interaction with natural adenovirus receptors CAR and integrins does not play a relevant role in hepatocyte transduction after systemic administration. Instead, interaction with several blood proteins such as complement protein 3 (C3), complement protein 4 (C4), C4 binding protein (C4BP), coagulation factors VII (FVII), IX (FIX), but mainly coagulation factor X (FX), mediate hepatocyte transduction by binding to HSPGs and LRPs (Parker et al., 2006; Shayakhmetov et al., 2005). FX interacts with nanomolar affinity with the HVRs in the hexon, specifically with the loops of HVR3, HVR5, and HVR7 (Alba et al., 2009).

2.7.1.2. Adenovirus interaction with blood components

Another critical aspect in the intravenous administration of adenovirus is the interaction with different blood components, including cells and plasma proteins, which typically results in adenovirus neutralization and clearance from circulation.

Adenoviruses are able to interact with almost all blood cell populations, but in particular, interaction with erythrocytes has become a major focus of attention in the last years. Human but not mouse erythrocytes can sequester adenovirus particles directly via CAR, or indirectly via complement receptor 1 (CR1) after virus opsonization by antibodies and complement (Carlisle et al., 2009; Seiradake et al., 2009). Such interactions were reported to inactivate Ad5 by preventing extravasation and systemic infection. Therefore, the high concentration of

erythrocytes in blood would represent a severe barrier for systemic administration of oncolytic adenoviruses in humans. However, CAR-bound adenovirus particles cannot be internalized into erythrocytes due to the lack of integrins on their surface. Previous studies of adenovirus titration in whole blood reported no loss of adenovirus infectivity despite erythrocyte binding (Cichon et al., 2003). In addition, proof of adenovirus tumor transduction in humans after systemic administration has been reported before (Nemunaitis et al., 2001), and has also been detected in a recent clinical trial with ICOVIR5 (unpublished data). In light of these facts, in this thesis we question the neutralizing nature of the CAR-mediated interaction with human erythrocytes, and hypothesize a reversible binding with no impairment on adenovirus transduction.

Adenoviruses can also interact with platelets, resulting in a strong thrombocytopenia between 5 and 24 hours after vector administration, although the mechanism for this interaction (which was also proposed to be CAR-mediated) has been controversial (Gupalo et al., 2011). Furthermore, other cell types such as macrophages, monocytes, or neutrophils can also sequester opsonized adenovirus particles via Fc receptors and complement receptors (Cotter et al., 2005; Khare et al., 2013; Lyons et al., 2006).

Besides blood cells, adenovirus also interacts with a variety of plasma proteins. Among those, neutralizing antibodies (NAbs) represent one of the major limitations for systemic delivery. Ad5 is a very common pathogen and most of the human population has been exposed to the virus by natural infection. Although the levels of NAbs vary geographically, the general prevalence of anti-Ad5 NAbs is very high, reaching >90% in some locations (Barouch et al., 2011; Mast et al., 2010). Adenovirus capsid contains three proteins that are accessible to antibodies: hexon, penton, and fiber. Albeit each of these proteins can be the targeted by NAbs, the efficiency and the mechanism of neutralization differs considerably. Antibodies against penton can interfere with viral entry into cells, but their neutralizing capacity is relatively poor (Wohlfart et al., 1985). Anti-fiber NAbs can neutralize the virus by cross-linking virions into aggregates, and also by inhibiting binding or entry into cells (Wohlfart, 1988). However, antibodies against hexon are the ones that display the more potent neutralization activity (Bradley et al., 2012a; Roberts et al., 2006; Roy et al., 2005; Sumida et al., 2005). These antibodies are directed primarily against the solvent-exposed HVRs (Bradley et al., 2012b; Roberts et al., 2006). Unlike anti-fiber or anti-penton, anti-hexon NAbs do not cause aggregation nor block virus binding to cells, and can neutralize even if added after virion attachment to cells (Wohlfart, 1988). Thus, such antibodies exert their neutralizing action

after the virus has been internalized, either by impairing endosome escape or by blocking dynein-mediated transport along microtubules to the nucleus. Hence, the high prevalence of anti-Ad5 NAbs in humans represents a severe limitation not only for oncolytic adenoviruses, but also for other adenovirus-based therapeutic applications such as gene therapy vectors or vaccines. In addition, the NAbs newly generated after the first adenovirus injection will efficiently inactivate a second viral dose even in patients with no pre-existing immunity, impeding efficient vector re-administration.

In addition to direct neutralization, antibodies (both NAbs and natural IgMs) not only can neutralize the virus directly but can also trigger an innate immune response by complement activation, and by docking the virus particles to Fc receptors of macrophages, monocytes and neutrophils. This activation of the immune response is not only mediated by binding to antibodies, but also to direct binding of complement proteins and coagulation factors. In this regard, the role of FX has been controversial. Whereas a first study described that FX binding is a mechanism to activate innate immunity against adenovirus (Doronin et al., 2012), a more recent work claimed that FX shields Ad5 from attack by natural antibodies and complement (Xu et al., 2013). According to this report, Ad5 recruits FX as a defense mechanism against complement activation, and such protection is required for efficient intravenous delivery.

Due to the big challenge that represents the intravenous injection of adenovirus, this thesis was focused on adenovirus interactions on the bloodstream. First, we studied the interaction of Ad5 with human erythrocytes via CAR. Second, we developed a strategy to avoid neutralization by antibodies. Nevertheless, oncolytic adenoviruses also face other barriers which also need addressing.

2.7.2. Intratumoral spread of oncolytic adenoviruses

Propagation of the oncolytic effect within tumors as a consequence of virus replication is one of the great advantages of virotherapy compared to conventional therapies. Intratumoral spread is essential in order to generate a significant antitumor effect from an initial low dose. The difficulty to obtain complete tumor regressions even in animal models indicates an inefficient virus distribution. Tumors are not only formed by tumor cells but also by the tumor stroma, including extracellular matrix composed by collagen, hyaluronic acid, elastin, and proteoglycans, and non-tumor cells such as fibroblasts. Oncolytic adenoviruses can neither cross the barriers imposed by extracellular matrix nor replicate in non-dividing cells, representing therefore important limitations for intratumoral spread. Our group has

previously published the expression of hyaluronidase from an oncolytic adenovirus which degrades hyaluronic acid and significantly improves intratumoral distribution and antitumor activity (Guedan et al., 2010; Rodriguez-Garcia et al., 2015). In addition, specific elimination of tumor fibroblasts is also being addressed in our group by expression of several molecules from the oncolytic adenovirus (unpublished data).

2.7.3. Immune responses

The intravenous administration of adenoviruses leads to a strong activation of the innate immune system. Innate immune cells such as macrophages or dendritic cells (DCs) capture the virus and recognize pathogen-associated molecular patters (PAMPs) through pattern recognition receptors (PRRs), such as Toll-like receptors (TLRs). For instance, TLR9 recognizes non-methylated CpG islands in the adenovirus genome. Such interactions trigger the expression of inflammatory cytokines and chemokines such as IL-6, TNF-α, MIP-2, MIP-1α, and type I interferons (IFNs) (Hartman et al., 2008), which recruit neutrophils and NK cells to the site of infection, as well as monocytes and T cells. Furthermore, DCs travel to draining lymph nodes where they engage adaptive and memory immune responses which eliminate the infected cells (Alemany and Cascallo, 2009).

The role of the immune system in cancer virotherapy has been controversial. A more classic point of view is “virocentrism”, which considers the immune system as an enemy for oncolytic viruses. According to virocentrics, immunosuppression is a beneficial strategy as it would allow a more efficient replication of the virus and it would avoid its elimination by the immune system. Data from clinical trials in which better responses were observed in immunosuppressed patients support this hypothesis (Kelly and Russell, 2007). On the other hand, and partly due to the increasing success of cancer immunotherapy, “immunocentrics” consider the immune system as an ally for the eradication of tumors. The immunogenicity of the oncolytic viruses might revert the immunosuppressive environment of tumors, and generate specific antitumor immune responses able to eliminate the tumors (Alemany and Cascallo, 2009). Of note, the most clinically advanced oncolytic viruses that have demonstrated efficient antitumor responses (T-vec, and Pexa-vec) express the immunostimulatory molecule GM-CSF (granulocyte-macrophage colony-stimulating factor). In any case, the high immunogenicity of the virus results in a dominant response against the virus rather than against the tumor, which is always detrimental for the efficacy of the therapy.

2.8. STRATEGIES TO EVADE NEUTRALIZING ANTIBODIES

As previously explained, anti-adenovirus neutralizing antibodies (NAbs) represent a major hurdle not only for oncolytic adenoviruses, but also for other adenovirus-based clinical applications such as vaccination or gene therapy. Therefore, researchers have invested great efforts in designing strategies to avoid pre-existing antibodies. Among those, the most commonly used strategies include the use of alternative serotypes or non-human adenoviruses, genetic modifications of capsid proteins to generate pseudotyped or chimeric vectors, and chemical modifications of the capsid.

2.8.1. Use of rare human serotypes or non-human adenoviruses

Anti-Ad5 humoral immunity may be circumvented by using less common serotypes that have low natural seroprevalence in the general human population, leading to transgene expression or to a transgene immune response in vaccine applications in the presence of anti-Ad5 NAbs (Zaiss et al., 2009). However, other properties besides the seroprevalence should be considered when selecting a vector, such as tissue tropism, oncolytic activity, immunogenicity, or toxicity. Utilization of other than species C adenoviruses can be appealing in virotherapy due to their use of alternative receptors, since CAR has been shown to be down-regulated in tumor cells (Li et al., 1999; Wunder et al., 2012). Adenovirus subgroup D, which has the largest diversity of viruses, has the advantage of showing reduced hepatotropism due to their low affinity for FX (Waddington et al., 2008). In a study where several alternative serotypes were analyzed for their ability to spread in the tumor mass, Ad serotype 9 from subgroup D demonstrated better spreading ability in both CAR negative and positive cancer cells, suggesting its use for cancer applications (Uchino et al., 2014). Another study compared the replication efficacy and oncolytic potency of several species B, C, D, and F viruses in B cell cancer cell lines and primary B cell cancers (Chen et al., 2011). Among those, species D adenoviruses mediated the most robust killing, and Ad26 and Ad45 significantly reduced tumor growth after intratumoral administration in lymphoma xenografts. Subgroup B adenoviruses have also been vectorized due to their tropism profile and low seroprevalence in humans. These include serotypes 3, 11, 35, and 50 (Alonso-Padilla et al., 2016), among which Ad3 has been tested in humans as an oncolytic virus (Hemminki et al., 2012). In addition, a chimeric oncolytic adenovirus based on serotypes 3 and 11p from subgroup B (ColoAd1) was generated by “directed evolution”, showing improved potency and selectivity (Kuhn et al., 2008) (see section 2.6.). Other serotypes such as Ad35, Ad26, and Ad48 were shown to be more immunogenic than Ad5 in rhesus monkeys (Teigler et al., 2012), a desirable trait for their

use as vaccine vectors. However, such high immunogenicity might not be desirable for other applications such as gene therapy vectors, whereas it is less clear for oncolytic adenoviruses. Some studies have demonstrated unexpected toxicities of some serotypes such as Ad11, Ad3, and Ad4, at virus titers usually employed for administration of Ad5 (Stone et al., 2007). Of note, the majority of the studies with alternative serotypes have explored them as vaccine vectors, and their applicability as oncolytic agents needs further development.

Nevertheless, most humans have NAbs against a range of adenovirus serotypes (Vogels et al., 2003) and in addition, specific T-cells against one serotype might crossreact against related serotypes (Zaiss et al., 2009). An alternative strategy to avoid such crossreactivity is the use of non-human adenoviruses. Vectors based on simian (Colloca et al., 2012; Tatsis et al., 2006), ovine (Hofmann et al., 1999), bovine (Reddy et al., 1999), porcine (Tuboly and Nagy, 2001), and canine adenoviruses (Perreau and Kremer, 2006) have been tested. The canine adenovirus serotype 2 (CAV-2) has been developed in our group as an oncolytic agent to treat canine patients (Laborda et al., 2014). Nonetheless, the use of non-human adenoviruses to treat human tumors is not feasible due to the species-specificity of adenoviruses, and thus they have been developed especially as gene therapy and vaccine vectors.

2.8.2. Genetic modifications of adenovirus capsid proteins

An alternative approach to changing the entire vector to a different serotype is to genetically modify the vector major capsid components or switching them for those of less seroprevalent or immunogenic serotypes. Fiber modifications or substitutions alone are not enough to circumvent pre-existing immunity (Bradley et al., 2012a; Gall et al., 1996; Zaiss et al., 2009), since the bulk of antibody response to adenoviruses is directed against the hexon protein (Roberts et al., 2006; Sumida et al., 2005). However, hexon exchange strategies can easily impact folding and assembly of virus particles, resulting in poor functional titers or complete failure to rescue viable recombinants. In this regard, hexon swaps between closely related serotypes are better accepted than between distantly related serotypes (Byrnes, 2016). Replacement of Ad5 hexon gene with the hexon from Ad2 (both species C) resulted only in partial evasion of anti-Ad5 serum, probably due to crossreactivity of the NAbs (Gall et al., 1998). In contrast, Ad5 hexon replacement with hexons from Ad3, Ad6, or Ad12 successfully evaded neutralization in mice immunized with Ad5 (Roy et al., 1998; Wu et al., 2002; Youil et al., 2002).

Neutralizing antibodies against Ad5 are mainly directed against the seven hypervariable regions (HVRs) of hexon and thus, the exchange Ad5 HVRs for those of non-prevalent serotypes has also been explored, in contrast to the exchange of the whole hexon protein. An Ad5 vaccine vector bearing the HVRs from rare Ad48 efficiently evaded NAbs, and generated CD8+ T cell responses against the expressed simian immunodeficiency virus (SIV) Gag in Ad5 immunized mice and rhesus monkeys (Roberts et al., 2006). Similarly, replacement of HVRs with those of the low prevalent Ad43 in an Ad5-based malaria vaccine, resulted in robust T cell responses against the parasite antigen in mice with high levels of Ad5 NAbs (Bruder et al., 2012). Despite being subdominant, antifiber Nabs can also contribute to neutralization, and the combination of hexon HVRs exchange for those of Ad48 together with the exchange of the fiber knob with that of the chimpanzee adenovirus AdC68, resulted in an even more efficient neutralization escape (Bradley et al., 2012a).

It is highly likely that these approaches (both the use of alternative serotypes and the generation of chimeric/pseudotyped vectors) will not prevent the development of humoral and cellular immune responses after the first administration of the vector. For this reason and in order to allow efficient multiple dosing, the sequential administration of antigenically distinct vectors has also been proposed. Heterologous prime-boosts regimens in the field of vaccination have been tested combining different serotypes such as Ad5, Ad11, and Ad35 (Lemckert et al., 2005), Ad35 and Ad49 (Thorner et al., 2006), or Ad26 and Ad35 (Zahn et al., 2012) among others, including even the combination of adenovirus and other types of virus vectors such as Modified Vaccinia Ankara (MVA) (Draper et al., 2010). In the field of oncolytic viruses, a protocol of sequential administrations of oncolytic adenovirus and Newcastle disease virus (NDV) showed a significant benefit in antitumor effect compared to each virus as a monotherapy, in the immunocompetent Syrian hamster model (Nistal-Villan et al., 2015). Nevertheless, an important consideration about these strategies is the necessity to develop more than one clinical candidate.

2.8.3. Chemical modifications of adenovirus capsid

Another approach to reduce virus neutralization is to “mask” viral epitopes by attaching chemical polymers or lipid molecules to adenovirus capsid proteins. Polyethylene glycol (PEG) has been the most used polymer for this purpose, although other polymers such as N-[2-hydroxyl]methacrylamide (HPMA) have also been used (Croyle et al., 2001; Fisher and Seymour, 2010; Green et al., 2004; O’Riordan et al., 1999; Wortmann et al., 2008). Proteins on the exterior of Ad surface have abundant free amines, thus PEGylation of Ad capsid can be

achieved via amine-mediated covalent bonding, resulting in labeling of all three major capsid proteins (Choi et al., 2012). Chemical shielding not only can protect the vector from NAbs but can also reduce Kupffer cell uptake (due to interferences in the interaction with scavenger receptors (SRs) (Haisma et al., 2009)), hepatotropism (due to evasion of FX binding), and extend serum half-life. In addition, this mechanism of protection also reduces innate immune responses against the virus as evidenced by reduction in plasma levels of IL-6 after intravenous injection (Jung et al., 2007), and in antibody-depenent complement activation (Tian et al., 2009). However, it has been reported that PEGylation can significantly reduce the transduction efficiency of adenovirus vectors, due to steric interference of the polymer chains with attachment to cell receptors (Eto et al., 2005). This issue can be partially overcome by subsequent addition of tumor-binding ligands to the distal end of PEG, such as RGD (Eto et al., 2005), the MAb Herceptin (Kim et al., 2011), or fibrobast growth factor receptor (FGFR) ligands (Green et al., 2008). Nevertheless, PEG is also immunogenic and can itself induce antibody responses that neutralize the PEGylated Ad vector, hampering the efficiency of multiple administrations (Byrnes, 2016; Shimizu et al., 2012). In addition to chemical polymers, some studies have also demonstrated that adenovirus vectors can also be shielded from antibodies by liposomes (Steel et al., 2004; Uusi-Kerttula et al., 2015; Yotnda et al., 2002). However, unlike genetic modifications, polymers and liposomes are not heritable and therefore, progeny virions will lack the shielding modification.

As previously explained, the majority of these strategies have been applied to adenovirus vectors either for gene therapy or for vaccination, and can present certain limitations in oncolytic adenoviruses. Thus, the design of oncolytic adenoviruses able to circumvent NAbs remains relatively unexplored. In this thesis, we have developed a novel strategy to circumvent anti-Ad NAbs after the systemic administraiton, by using endogenous serum albumin to mask viral epitopes and shield the adenovirus capsid.

3. ALBUMIN AS A DRUG CARRIER

3.1. GENERAL CHARACTERISTICS OF ALBUMIN

Human serum albumin (HSA) (585 aa, MW 66.5 kDa) is by far the most abundant protein in blood plasma, with a concentration of 35-50 mg/mL. Structurally, it is a heart-shaped α-helical protein composed of three homologous domains (I, II, III), each further subdivided in

two sub-domains (A and B) formed by 4 and 6 α-helices, respectively (Larsen et al., 2016) (**Figure 8**). Albumin is synthesized predominantly in the liver and is rapidly secreted to circulation at a rate of 10-15 g/day. The binding properties and functions of HSA are manifold. To name a few, it is involved in the regulation of both pH and osmotic pressure in the vascular system, it acts as a transport vehicle for fatty acids, hormones, metal ions (copper, nickel, calcium, or zinc), and therapeutic drugs (penicillins, benzodiazepines, sulfonamides, etc.), and it can also act as an amino acid source to nourish peripheral tissues (Kratz, 2008).

3.2. ALBUMIN PROPERTIES AS A DRUG CARRIER

In the last years, albumin has emerged as a versatile protein carrier for drug targeting and for improving the pharmacokinetic profile of drugs, including therapeutic proteins, peptides, and small molecules. Albumin has several traits that make it an ideal candidate as a drug carrier. Some desirable properties are its high solubility, stability, and biodegradability, along with its lack of toxicity and immunogenicity. In addition, its extremely long plasma half-life and its accumulation in malignant and inflamed tissues are especially relevant for this purpose.

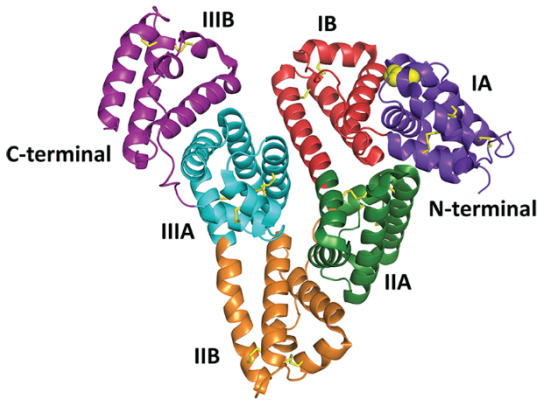

Figure 8. Crystal structure of human serum albumin. The tertiary structure of human serum albumin is represented. The domains and sub-domains are shown in purple (IA), red (IB), green (IIA), orange (IIB), blue (IIIA), and violet (IIIB) (modified from (Larsen et al., 2016)).

3.2.1. Albumin plasma half-life

Albumin has a particularly long circulatory half-life of 19 days in humans. This is in part due to its size, which is above the renal clearance threshold, and to its specific interaction and recycling by the neonatal Fc receptor (FcRn) (Peters Jr, 1995). With the exception of IgGs, no

other soluble serum protein is known to exhibit such a long half-life. Interestingly, the long half-life of IgGs (23 days) is also due to FcRn-mediated recycling (Lencer and Blumberg, 2005). FcRn is an MHC class I-related receptor involved in transplacental transport of maternal IgGs to the fetus and in antigen presentation (Roopenian and Akilesh, 2007). In addition, FcRn also extends the serum half-life of albumin and IgG molecules. Specifically, albumin is pinocytosed along with other serum proteins by many types of cells, and it is transported by endocytic vesicles which contain FcRn. FcRn shows no affinity for albumin at neutral pH, but binds to it with high affinity at low pH (Chaudhury et al., 2003). When endosomes are acidified, binding to FcRn rescues albumin from degradation, diverting it from the lysosomal pathway. Albumin is then transported back to the extracellular space where it is released at physiologic pH, thereby prolonging its half-life (**Figure 9**).

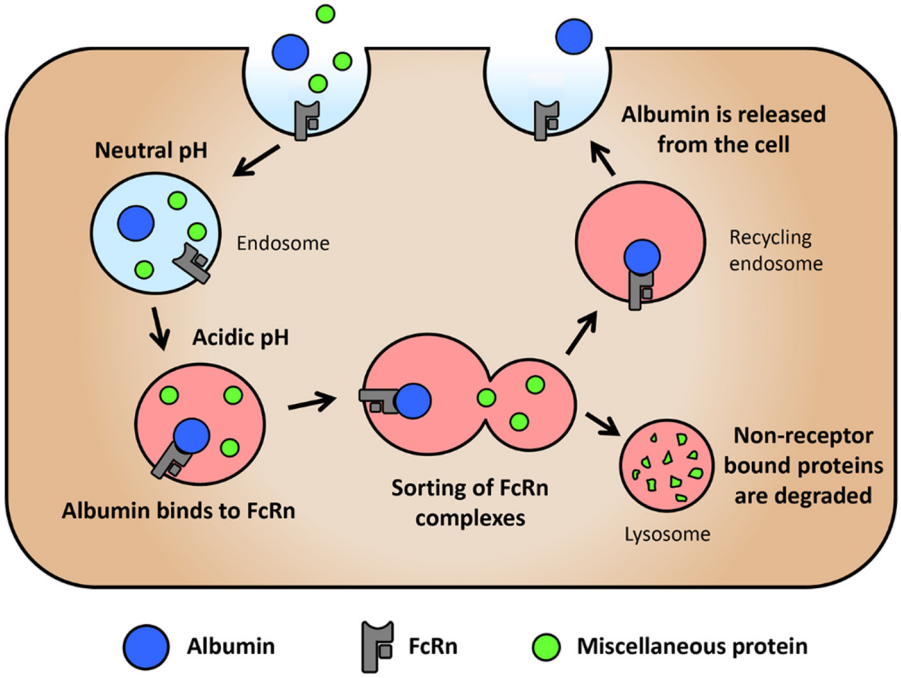

Figure 9. Albumin recycling by FcRn. Extracellular albumin is pinocytosed along with other serum proteins at neutral pH (blue shading). Upon endosome acidification (red shading), albumin binds with high affinity to FcRn. Non-FcRn bound proteins are sorted to the lysosome for degradation whereas vesicles containing albumin-FcRn complexes are recycled back to the cell membrane and upon exposure to the extracellular neutral pH, albumin is released back to circulation.

Many therapeutic molecules are smaller than the renal filtration threshold, resulting in their rapid clearance from the bloodstream, which severely limits their therapeutic effect (Sleep et al., 2013). In this regard, binding to albumin either covalently or non-covalently, has

demonstrated to be a useful strategy to significantly increase the plasma half-life of such drugs, from minutes to hours or from hours to days. Examples of drugs using the albumin-binding strategy for half-life extension, either already approved or in clinical or pre-clinical stages, will be detailed below (section 3.3.).

3.2.2. Albumin accumulation in solid tumors

The fact that albumin is accumulated in solid tumors makes it very attractive as a carrier for anticancer drugs. Three main factors are responsible for the accumulation of this plasma protein in tumors. One factor is the enhanced permeability and retention of macromolecules in relation to passive tumor targeting (EPR effect) (Maeda et al., 2000). The EPR effect is the property by which high-molecular-weight molecules tend to accumulate in tumor tissue much more than in normal tissue. This effect occurs due to the abnormal vasculature of tumors, usually conformed by poorly aligned endothelial cells with wide fenestrations. Such leaky and defective tumor blood vessels are highly permeable for macromolecules, while in the vasculature of healthy tissue only small molecules can cross the endothelial barrier. The high intratumoral concentration of macromolecules such as albumin is not only explained by this enhanced permeability, but also by a high retention. Whereas low-molecular-weight substances can return to circulating blood by diffusion, the lack of a proper lymphatic drainage in tumors (due to an impaired or absent lymphatic system) cause the accumulation of macromolecules (Kratz, 2014).

In addition to the EPR effect, a specific albumin transport pathway based on the interplay of two albumin-binding proteins (gp60 and SPARC), also contributes to the absorption and accumulation of albumin in the tumor interstitium. Circulating albumin binds to gp60, located on the endothelial cell surface, inducing vesicle formation and transcytosis, which transports albumin through the endothelial cell into the subendothelial space (Schnitzer, 1992). Upon entering the tumor interstitium, a second albumin-binding protein, SPARC (Secreted Protein Acidic and Rich in Cysteine), binds to albumin with high affinity and traps it in the tumor interstitium (**Figure 10**).

Finally, it has also been described that the proliferating tumor mass actively sequesters and digests albumin to cover its high demand for amino acids and metal ions, generally resulting in hypoalbuminemia, a characteristic feature of patients with advanced solid tumors.

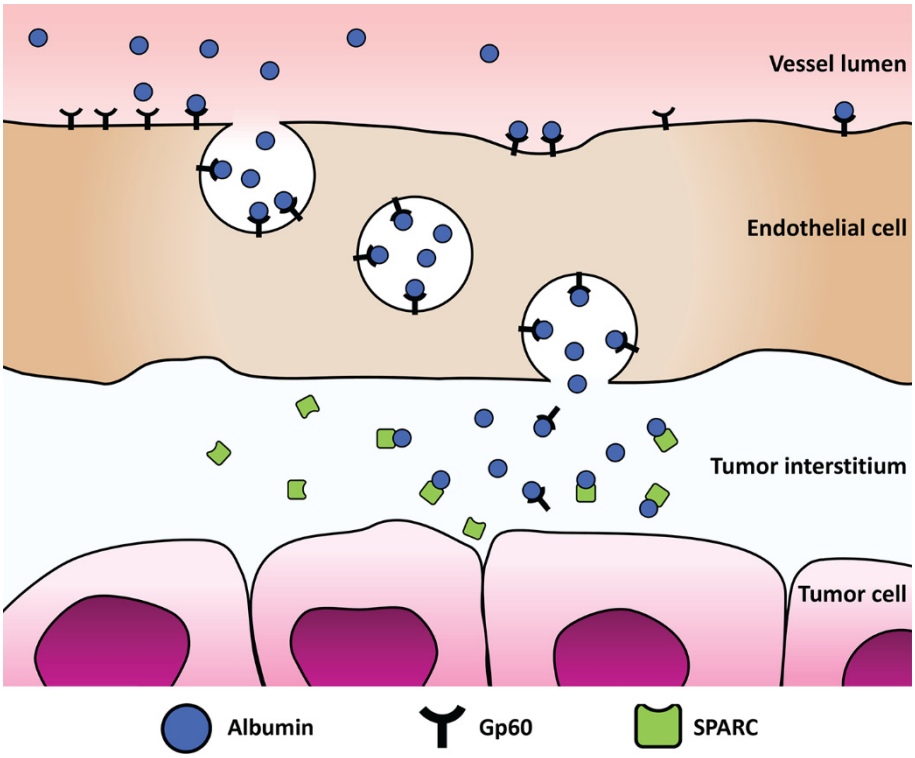

Figure 10. Gp60 and SPARC are responsible for albumin accumulation in tumors. Circulating albumin is uptaken by endothelial cells through the gp60-mediated transcytosis pathway and is retained in the tumor interstitium by subsequent binding to SPARC.

3.3. STRATEGIES TO ACHIEVE ALBUMIN BINDING

The use of albumin as a carrier protein for treating various diseases (primarily cancer, rheumatoid arthritis, diabetes, and hepatitis) has resulted in several marketed products and numerous clinical trials. Such products have been developed with different strategies to achieve albumin binding, including covalent binding and non-covalent binding methods.

3.3.1. Albumin fusions

A possible strategy to combine protein-based drugs with albumin is the genetic fusion to the N- or C-terminal of albumin, or even to both ends. The gene of the protein of interest is connected to the albumin gene and the fusion protein is obtained upon expression in a suitable host (usually yeast). The resulting fusion protein combines the therapeutic activity of the partner with the long half-life of albumin. Of note, the proper folding of albumin should not be altered by the linker or the fused protein, in order to maintain its functionality and long half-life (Larsen et al., 2016). In the last decade, a large number of different proteins have

been genetically fused to albumin, including peptides, cytokines, coagulation factors, hormones, etc.

Albiglitude (tradenames Eperzan® and Tanzeum®) is a glucagon-like peptide-1 agonist (GLP-1 agonist) developed by Human Genome Sciences and marketed by GlaxoSmithKline for the treatment of type II diabetes. It consists of two human GLP-1 repeats fused to the N-terminus of recombinant human albumin (Bush et al., 2009). Data from clinical trials demonstrated a significant increase in the plasma half-life of approximately 5 days, compared to 1-2 minutes of endogenous GLP-1. In 2014, Albiglitude was approved for treatment of type II diabetes. Other albumin-fused drugs in advanced clinical stages are FIX (rIX-FP) for the treatment of hemophilia B (Santagostino et al., 2012), IFNα-2b (Albuferon®) for the treatment of hepatitis C (Rustgi, 2009), or the bispecific fusion MM-111, consisting of an albumin molecule fused at both N- and C- terminus with a scFv (single-chain variable fragment antibody) directed against HER-2 and HER-3 for the treatment of HER-2 positive tumors (McDonagh et al., 2012).

3.3.2. Chemical conjugation

A second approach is chemical conjugation of the drug to albumin, usually to either lysines, tyrosines, or the free SH-group in the cys34. This strategy usually requires a release mechanism from albumin, which can be achieved, for instance, with a cleavable linker. Kratz *et al.* developed Aldoxorubicin, a maleimide-modified doxorubicin which covalently conjugates with cys34 of albumin upon intravenous administration. Aldoxorubicin accumulates in tumors where the acidic environment cleaves the acid sensitive linker, releasing doxorubicin to exert its action. Preclinical and advanced clinical studies indicated reduced adverse effects and improved tumor accumulation and efficacy than native doxorubicin (Chawla et al., 2015; Graeser et al., 2010; Unger et al., 2007). The chemical conjugation strategy has also been successfully applied to increase the plasma half-life of methotrexate (MTX-HSA) for cancer treatment (Bolling et al., 2006), and of a peptide with anti-HIV activity (Xie et al., 2010), among others.

3.3.3. Nanoparticle albumin-bound technology (nab technology)

American Bioscience Inc. developed an albumin-based technology useful for encapsulating lipophilic drugs into nanoparticles. The principle is based on mixing the drug with serum albumin in an aqueous solvent and submitting it to high pressure through a jet, to form drug

albumin nanoparticles ranging 100-200 nm (Kratz, 2008). This technology was used to encapsulate the chemotherapeutic agent paclitaxel, generating Abraxane® (nab-paclitaxel). This novel formulation of paclitaxel avoids the use of the solvent Cremophor EL, associated with severe side effects. In addition of being less toxic than its free drug counterpart, Abraxane® also exhibits higher antitumor activity compared to free paclitaxel (Desai et al., 2006). Along with the EPR effect, the gp60 and SPARC-mediated albumin retention mechanism were proposed as responsible for the enhanced tumor accumulation of Abraxane®. In fact, clinical data revealed a significant benefit in overall survival in patients with high SPARC levels treated with the combination of Abraxane® and gemcitabine (Desai et al., 2009; Von Hoff et al., 2011). In 2005 it was approved for the treatment of metastatic breast cancer, representing the first albumin-based drug delivery system to be approved in oncology. In 2010, it was acquired by Celgene Corporation to be further tested for other types of cancer. In 2012 it was approved for the first-line treatment of locally advanced or metastatic non-small cell lung carcinoma (NSLC) in combination with carboplatin, and in 2013 for the treatment of pancreatic cancer in combination with gemcitabine (Kratz, 2014). The high albumin-mediated tumor accumulation of this delivery system makes it very attractive to test other chemotherapeutic agents. Celgene has a portfolio of nab-technology based drugs currently in clinical development such as nab-docetaxel (ABI-008) for prostate cancer treatment, or nab-rapamycin (ABI-009) for colon and breast tumors (Neil, 2007).

3.3.4. Incorporation of endogenous albumin ligands

Albumin acts as a transporter for a broad variety of molecules such as fatty acids and therefore contains several fatty acid binding sites. Attachment of a fatty acid to the desired drug is a feasible way to achieve non-covalent binding to albumin. This has been applied by NovoNordisk in the development of Levemir® (insulin detemir) and Victoza® (Liraglutide) for the treatment of diabetes. Levemir® is a myristic acid modified insulin analog, whereas Victoza® is a glucagon-like peptide-1 agonist (GLP-1) modified with a palmitic acid. Upon injection, the fatty acid moiety binds to albumin and slowly dissociates over time, improving the bioavailability and distribution. Such modifications resulted in a remarkable increase in half-life from 4-6 min to 5-7 h for insulin, and from 2 min to 11-15 h for GLP-1 analog (Sleep et al., 2013). Successful results in clinical trials (Dornhorst et al., 2007; Pratley et al., 2010) led to the approval of Levemir® in 2004 for the treatment of type 1 and 2 diabetes, and of Victoza® in 2009-2010 for type 2 diabetes.

3.3.5. Albumin-binding domains (ABDs) or peptides (ABPs)

Very similarly to this last strategy, non-covalent reversible binding to albumin can also be accomplished through protein modules with the capacity to interact with albumin. In this case and due to their protein origin, they are often genetically fused to the therapeutic protein. These can include wild-type proteins with an intrinsic affinity for albumin or molecules artificially engineered to bind to albumin.

Proteins with albumin-binding activity have been identified in certain bacteria, such as the streptococcal protein G. Protein G of Streptococcus is a cell surface receptor containing tandem repeats of serum albumin-binding domains (ABDs). Specifically, domain 3 (hereinafter named ABD) has been extensively studied and characterized. ABD is composed of 46 amino acids (5-6 kDa) which form a left-handed three α-helix bundle (Kraulis et al., 1996). Structural data of an ABD homolog in complex with human serum albumin (HSA), revealed that helix two and three of ABD interacts with domain II of HSA, not interfering with the FcRn binding site located in domain III (**Figure 11**). The ABD on its own maintains the albumin-binding functionality and is highly stable, not requiring disulfide bonds or metal ions. The affinity for human albumin has been determined to be in the range of 1-4 nM (Kontermann, 2009). The species specificity of the domain has been studied showing high affinity not only for human but also for mouse, rat, hamster, and baboon albumin, whereas low or no affinity for cow, rabbit, pig, dog, or sheep albumin (among others) (Falkenberg et al., 1992; Nygren et al., 1990). This binding to albumin of several species is highly relevant as it facilitates its use in pre-clinical and clinical models.

A large number of pre-clinical studies have demonstrated the applicability of fusion to the ABD to improve the plasma half-lives of therapeutic proteins, especially of small antibody molecules and variants. A HER-2 binding Fab (Fragment antigen-binding) derived from the clinically approved mAb Trastuzumab (Herceptin®) was fused to ABD, resulting in a half-life in mice of 20.9 h compared to 2.1 h of the Fab fragment alone (Schlapschy et al., 2007). Similarly, the same strategy was applied to a bispecific single-chain diabody (scDb CEA-CD3) developed for the retargeting of cytotoxic T cells to CEA-expressing tumor cells (**Figure 12**), obtaining an enhanced half-life from 5.6 to 27.6 h in mice. Importantly, this prolonged half-life led to a strongly increased accumulation of the scDb-ABD in CEA-positive tumors in animal models (Stork et al., 2007). Furthermore, the tumor accumulation of the scDb-ABD fusion was also higher than that of a PEGylated scDb derivative which displayed a similar enhanced half-life, indicating a specific contribution of albumin in tumor penetration (Stork et al., 2009). Some

studies have confirmed that the drug-ABD/albumin interaction survives the FcRn-mediated recycling process, and that ABD seems to follow the same kinetics and distribution as serum albumin itself (Andersen et al., 2011; Kontermann, 2011; Stork et al., 2009). More recent pre-clinical studies have described an enhancement in the plasma half-life and in the antitumor effect of TRAIL (tumor necrosis factor-related apoptosis inducing ligand) and anti-HER2 immunotoxins by fusion to ABD (Guo et al., 2016; Li et al., 2016). The company Affibody has developed Albumod™, a technology for half-life extension based on the ABD, which offers for outlicensing.

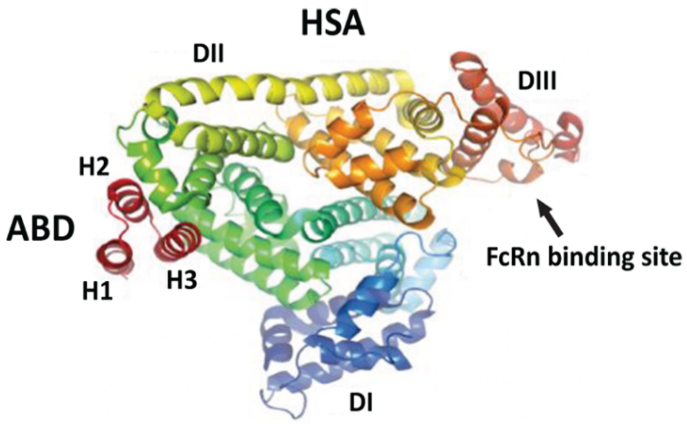

Figure 11. Interaction of a bacterial albumin-binding domain with human serum albumin. Crystal structure of the complex formed by the albumin-binding domain of protein PAB of *Finegoldia magna* (homolog to ABD3 of streptococcal protein G) and HSA. α-helices 2 and 3 (H2 and H3) of the albumin-binding domains recognize a site located in domain II (DII) of HSA, which does not overlap with the binding site of the neonatal Fc-receptor (FcRn) located in domain III (DIII) (modified from (Nilvebrant and Hober, 2013)).

Alternatively to bacterial ABDs, some molecules have been specifically engineered to bind to albumin, including domain antibodies or peptides. Albumin-binding peptides (ABPs) have been isolated from random peptide libraries by phage display. Such peptides have the advantage of being smaller, but on the other hand display lower affinities for albumin. For example, an 18 amino acid ABP (SA21) obtained from a peptide phage library had an affinity ranging 266-467 nM for albumin of different species (Dennis et al., 2002). Still, fusion to an anticoagulant anti-tissue factor Fab significantly increased its plasma half-life 37-fold to 32.4 h in rabbits and 26-fold to 10.4 h in mice, representing the 25-43% of the albumin half-life in these models, and maintained its anticoagulant activity.

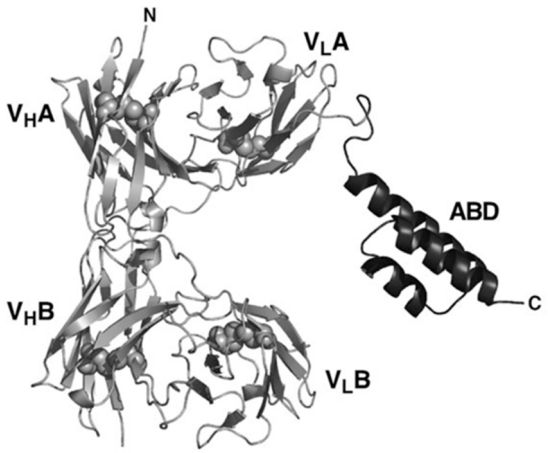

Figure 12. Model structure of the fusion of the ABD3 from streptococcal protein G (ABD) to the C-terminal end of a single chain diabody (scDb) (from (Stork et al., 2007)).

In the last years, the use of albumin as a carrier protein has emerged as a hot field, and several approaches and technologies have been developed to attach albumin to drugs. Among all these strategies, in this thesis we used the albumin-binding domain of streptococcal protein G (ABD) and albumin-binding peptides (ABPs) to promote adenovirus binding to albumin. Such modifications were tested in our standard oncolytic platforms ICOVIR15, and ICOVIR15K to protect them from neutralizing antibodies (NAbs) after the systemic administration.

OBJECTIVES

One of the main limitations in the efficacy of adenoviral therapies is the neutralization of the virus in the bloodstream after the systemic administration. Contrary to previous reports, human erythrocytes have been described to bind and inactivate Ad5 via CAR. In addition, the high prevalence of anti-Ad5 neutralizing antibodies (NAbs) in the human population represents a significant hurdle for adenovirus-based gene therapy vectors, oncolytics, and vaccines.

The general objective of this thesis was to study the interaction of Ad5 with two blood components: human erythrocytes and NAbs, and due to the significant problem the latter represent, develop an oncolytic adenovirus able to evade NAbs upon systemic administration by using serum albumin as a shield. This thesis was carried out in the context of two independent projects, reflected in two different chapters. Several specific objectives were planned:

Chapter 1:

- To study the CAR-mediated interaction between Ad5 and human erythrocytes, and determine its impact on adenovirus bioactivity *in vitro* and *in vivo*.

Chapter 2:

- To insert albumin-binding moieties on adenovirus capsid, and confirm their functionality by demonstrating the ability of the viruses to bind albumin.

- To characterize the effect of albumin binding *in* vitro in the absence of NAbs, and its impact *in vivo* on the blood persistence, toxicity, organ transduction, and antitumor efficacy of the adenovirus after intravenous administration in mice without NAbs.

- To assess if albumin binding can protect adenovirus from anti-Ad5 NAbs *in vitro,* and analyze the ability of the virus to transduce target organs and reduce tumor growth in pre-immune mouse models after the systemic administration.

- To test the ability of albumin-binding adenoviruses to evade NAbs generated *de novo* against their own capsid and therefore, the feasibility of virus readministration.

- To study the combination of the albumin-binding insertion with other adenovirus modifications such as the replacement of fiber shaft HSG-binding motif with RGD.

MATERIALS AND METHODS

1. HANDLING OF BACTERIA

In order to obtain enough amounts of plasmid DNA to be easily manipulated, its amplification in bacteria was required. For this purpose, the plasmid should contain a replication origin that allows its replication on the desired strain and an antibiotic-resistance gene to select the bacteria and avoid contaminations. In this work, the *Escherichia coli* strain SW102 has been used with this purpose and to perform homologous recombination.

1.1. PLASMIDIC DNA EXTRACTION FROM BACTERIAL CULTURES

Plasmid DNA was obtained from saturated *E.coli* cultures grown in LB with antibiotic according to protocols based on an alkaline lysis with SDS. DNA was prepared at small and large scale.

1.1.1. Small scale DNA preparations

DNA minipreparations were performed following an adapted protocol described by Birnboim and Doly (Birnboim and Doly, 1979). A colony grown in an LB-antibiotic dish was inoculated in 3 mL of LB+antibiotic and incubated overnight at 32ºC. A 2 mL aliquot of the grown culture was centrifuged at 13000 rpm for 1 minute. The cell pellet was resuspended in 200 µL of pre-cooled solution 1 (25 mM Tris-HCl pH 8, 10 mM EDTA, 50 mM glucose, 0.1 mg/mL RNAse). 200 µL of freshly prepared solution 2 (SDS 1%, NaOH 0.2 M) were added and the mixture was blended by inversion. 200 µL of pre-cooled solution 3 (3 M potassium acetate, 11.5% acetic acid) were added and the mixture was blended again by inversion until a white precipitate appeared. The mixture was incubated 5 minutes on ice and centrifuged 15 minutes at 13000 rpm. The clear supernatant was collected without taking the white pellet (corresponding to cellular DNA, proteins, and SDS) and 2 volumes of ethanol were added. The mixture was incubated 15 minutes at room temperature (RT) and the plasmid DNA was precipitated by centrifugation for 10 minutes at 13000 rpm. The supernatant was discarded and the DNA pellet was washed with 70% ethanol by centrifugation at 13000 rpm 5 minutes. The supernatant was discarded again, the pellet was dried and finally, plasmid DNA was resuspended in 50 µL of TE (10 mM Tris-HCl, 1 mM EDTA).

1.1.2. Large scale DNA preparations

DNA maxipreparations allow the obtention of large amounts of high purity plasmid DNA (≥100 µg). Maxipreparations were prepared from 200 mL of saturated bacteria culture using

the commercial kit "PureLinkTM HiPure Plasmid Filter Purification Kits" (Invitrogen, Waltham, MA, USA), following manufacturer's instructions.

1.2. HOMOLOGOUS RECOMBINATION IN BACTERIA

Homologous recombinations performed in this work have been conducted in bacteria using the high efficiency system developed by Richard Stanton (Stanton et al., 2008), who kindly gave us the plasmid pAdZ5-CV5-E3+ in SW102 strain of *E.coli*. This plasmid contains the adenovirus type 5 genome (E1-) as a bacterial artificial chromosome (BAC), with a chloramphenicol (Cm)-resistance gene. This system works using phage λ genes Redγβα under the control of a temperature-sensitive promoter, which is repressed at 32°C and activated when bacteria are grown at 42°C. The positive-negative selection cassette rpsL-Neo was used to identify recombinant clones. Plasmid pAdZ5-CV5-E3+ was modified in order to obtain pAdZICOVIR15, pAdZICOVIR15K, pAdZGL, and pAdZGLRGD plasmids, which were used to introduce the modifications described in this thesis.

Modifications were performed in two steps. In the first step or positive selection, the rpsL-Neo cassette was inserted in the target region to modify. For that, a DNA fragment containing the rpsL-Neo flanked by homology regions (40 bp) with the recombination sites was generated by PCR and used to transform the bacteria. After this first recombination step and due to the incorporation of the rpsL-Neo, recombinant clones become Kanamycin (Kan) resistant and Streptomycin (Strep) sensitive (SW102 strain is naturally resistant to Strep), and are selected in Kanamycin LB plates. In the second step or negative selection, the rpsL-Neo is substituted by the desired modification. In this case, a DNA fragment containing the modification flanked by the same homology regions is also generated by PCR and used to transform the bacteria. In this case and due to the loss of the rpsL-Neo, recombinant clones become again Kan sensitive and Strep resistant and are selected in Streptomycin LB plates.

The procedure that has been followed to perform recombinations is described next. First of all, glycerinates of the bacteria that contain the plasmid to be modified were scratched with a sterile pipette tip, inoculated in 5 mL of LB media including Cm + Strep antibiotics (12.5 µg/mL, and 1 mg/mL, respectively), and incubated overnight at 32°C and constant agitation. Then, 25 mL of LB Cm + Strep were inoculated with 0.5 mL of the previous culture and incubated 32°C with agitation until it reached an OD measure of 0.5-0.6 at 600 nm. At this moment, culture was divided in two Falcon tubes with equal volumes. The expression of the Red recombinase genes was induced in one of the falcon tubes by incubating it for 15 minutes

at 42°C, and then cultures were incubated on ice 15 minutes more. From that moment, manipulation was done at 4°C in order to ensure good transformation efficiency. Both cultures (induced and non-induced) were centrifuged 5 min at 4000 g at 4°C and supernatant was discarded. Bacteria pellet was resuspended in 11 mL of cold ddH_2O water and centrifugation was repeated. Three total washing steps were performed and in the last one, the pellet was resuspended in the remaining water (≤300 µL). Afterwards, 50 µL aliquots of bacteria (both, from the induced and non-induced cultures) were transformed by electroporation with 100-200 ng of DNA (the fragment which contains rpsL-neo). Electroporation was performed with the electroporator machine Electro Cell ManipulatorTM ECM 630 at the following conditions: 50 µF, 1500 V and 125 Ω. Pulses lower than 5 milliseconds were considered correct. Bacteria were recovered in 1 mL of LB without antibiotics and incubated 70 minutes at 32°C. Finally, they were plated into LB plates containing Cm and Kan (12.5 µg/mL, and 15 µg/mL, respectively) and incubated overnight at 32°C. 24 hours later, colonies should be grown and the ratio between the colonies in the induced culture (recombinant) and the non-induced one (control) were compared in order to assess recombination efficiency. Colonies were picked, minipreparations of DNA were performed and restriction patterns of different clones were checked. Finally, the correct clone was frozen as a glycerinate.

A similar procedure was followed for the second phase, in which the clones obtained in the previous step were inoculated in 5 mL of LB Cm+Kan and cultured overnight at 32°C. The next day, expression of recombinase genes was induced, and the bacteria were made competent for its transformation by electroporation in the same way described previously. Again, 100-200 ng of DNA containing the desired modification were transformed. After the recovery incubation 100 µL of a 1/25 dilution of the culture were plated in LB agar Cm+Strep and plates were incubated overnight at 32°C. 24 hours later, colonies were picked, minipreparations of DNA were performed and clones were checked by the analysis of restriction pattern and/or sequencing of the recombinant region.

2. CELL CULTURE

2.1. HEK293

Human Embryonic Kidney 293 (HEK293) cells derive from human primary embryonic kidney cells. This cell line has been transformed with a fragment of the Ad5 genome including

the E1A gene (Graham et al., 1977). 293 cells are highly permissive for the generation and replication of adenoviruses and are easily transfectable by the calcium phosphate method. HEK293 are packaging cells and have been used for the generation and amplification of non-replicative E1-deleted adenoviral vectors, and for the generation and functional titration of oncolytic adenoviruses.

2.2. TUMOR CELL LINES

The different tumor cell lines used in this thesis are summarized in the following table:

Table 2. Tumor cell lines used in this work

Cell line	Tumor type	Origin species
A549	Lung adenocarcinoma	Human
Sk-mel28	Melanoma	Human
NP-9	Pancreatic	Human
NP-18	Pancreatic	Human
A431	Epidermoid carcinoma	Human
B16	Melanoma	Mouse
B16-CAR	Melanoma	Mouse

A549 cell line has been used to amplify the different oncolytic adenoviruses due to its high efficiency to produce virus. NP-9 and NP-18 pancreatic tumor cells line were established by the Servei de Digestiu de l'Hospital de la Santa Creu i Sant Pau from Barcelona and provided by the Laboratori d'Investigació Gastrointestinal from the same Hospital (Villanueva et al., 1998). B16 murine cell line was obtained from Dr. Pablo Sarobe (CIMA, Pamplona). B16CAR murine cell line was obtained from Dr. Philippe Erbs (Transgene, France). The rest of the cell lines were obtained from the American Type Cell Culture (ATCC, Manassas, VA, USA). All cell lines were maintained in Dulbecco's modified Eagle's medium (DMEM) supplemented with 5% fetal bovine serum (FBS, Invitrogen Carlsbad, CA, USA) (previously inactivated by heating at 56°C for 30 minutes) and penicillin-streptomycin (PS, Gibco-BRL, Barcelona, Spain) (100 U/mL and 100 μg/mL, respectively), at 37°C and 5% CO_2. B16CAR were maintained with 0.5 mg/mL hygromycin (Invivogene, San Diego, CA).

2.3. CELL COUNTING

To determine cell numbers, manual or automatic methods were performed using trypan blue dying exclusion test. Adherent cells were detached by Trypsin-EDTA 0.05% (GIBCO RBL) incubation and were resuspended in fresh medium supplemented with FBS. For the manual counting, a dilution in which 10 to 100 cells could be counted in each quadrant of the Neubauer chamber was made. Viable cells in each quadrant were counted and the mean was calculated. The number of cells per mL was calculated according to the following formula:

$$\text{Cells/mL} = \text{Mean number of viable cells per quadrant} \times \text{Dilution factor} \times 10^4$$

The automatic counting was performed with a cell counter TC20TM (Bio-Rad, Hercules, CA, USA) according to the manufacturer's instructions.

2.4. CELL FREEZING AND CRYOPRESERVATION

Cells were counted as described above and resuspended in cold freezing medium (90% FBS 10% DMSO) at a final concentration of 5-10x10^6 cells/mL depending on the cell line. Cell suspension was distributed in cryotubes at 1 mL/tube and placed in a container filled with 2-propanol for its freezing at -80°C during 24 hours. The cryotubes were then stored in a liquid nitrogen tank. For cell thawing, cells were rapidly moved from the liquid nitrogen to a water bath at 37°C. Cells were then diluted in pre-warmed medium and transferred to a 15 mL Falcon tube. Soft centrifugation at 1000 g was carried out for 5 minutes, and the pellet of cells was resuspended in fresh medium and plated at high confluence to optimize the recovery.

2.5. MYCOPLASMA TEST

All cell lines were routinely tested for mycoplasma contamination by PCR using the following oligonucleotides:

Table 3. Oligonucleotides used for detection of mycoplasma contamination

Oligonucleotide	Sequence
MICO-1	5'-GGCGAATGGGTGAGTAACACG-3'
MICO-2	5'-CGGATAACGCTTGCGACTATG-3'

As a template for the PCR, medium from cells that had been in overconfluence in absence of antibiotics for at least 5 days was used. If the result was positive, cells were discarded.

2.6. PURIFICATION OF HUMAN ERYTHROCYTES

Human blood samples were obtained by venipuncture into Lithium-heparinized tubes (Greiner Bio-One, Monroe, NC, USA) with donor consent and approval by the IDIBELL's Ethics Committee. After centrifugation at 2000 g for 10 min at room temperature, the plasma and leukocyte layer were removed by aspiration. Erythrocytes were resuspended in 3 volumes of PBS and centrifuged again with the same settings. This washout step was repeated 4 times. Washed erythrocytes were counted in the Neubauer chamber and resuspended in PBS at the indicated concentrations.

3. RECOMBINANT ADENOVIRUSES

All adenoviruses employed in this thesis derive from the human adenovirus serotype 5 (Ad5). First generation vectors as well as oncolytic adenoviruses were used. Wild-type human adenovirus 5 (Adwt) was obtained from ATCC. ICOVIR15, and ICOVIR15K have been previously described (Rojas et al., 2010, 2012). AdGL is an E1-deleted first generation vector expressing the EGFP-Luciferase fusion protein cassette from pEGFPLuc (Clontech, Mountain View, CA, USA). AdGLRGD is the same adenovirus vector harboring the RGD (Arg-Gly-Asp) domain in the HI-loop of the fiber. Both adenovirus vectors had been generated in our group before this thesis (unpublished data).

3.1. CONSTRUCTION OF RECOMBINANT ADENOVIRUSES

The details of the construction of the recombinant adenoviruses generated in this work are described below. The oligonucleotide primers used and their sequence are summarized in **Table 4**.

ICOVIR15-H1-ABD

To insert the ABD in the HVR1 of the hexon, the first step was the amplification of the rpsL-neo cassette by PCR from pJetRpsLneo, a plasmid containing the rpsL-Neo positive-negative selection markers cloned into pJet1.2/blunt (GenScript, Wheelock House, Hong Kong). The specific oligonucleotides used were HVR1rpsLF and HVR1rpsLR. The rpsL-Neo cassette was

then inserted in the HVR1 of pAdZICOVIR15 plasmid, which contains the genome of ICOVIR15 in the pAdZ backbone. The DNA fragment containing the ABD was generated by PCR using the following overlapping oligonucleotides: ABDH1F, ABDR1, ABDF2, ABDR2, ABDF3, ABDR3, and ABDH1R. The generated fragment was used to replace the rpsL-Neo cassette in the HVR1.

ICOVIR15-H5-ABD

In this case, the rpsL-Neo was amplified with the oligonucleotides HVR5rpsLF and HVR5rpsLR and inserted in pAdZICOVIR15 plasmid. The ABD was amplified from the genome of ICOVIR15-H1-ABD using oligonucleotides ABDH5F and ABDH5R, and this DNA fragment was used to replace the rpsL-Neo in the HVR5.

AdGL-H1-ABD

The same DNA fragments used to construct ICOVIR15-H1-ABD were used to recombine in pAdZGL plasmid, which contains the genome of AdGL in the pAdZ backbone.

AdGLRGD-H1-ABD

The same DNA fragments used to construct ICOVIR15-H1-ABD were used to recombine in pAdZGLRGD plasmid, which contains the genome of AdGLRGD in the pAdZ backbone.

AdGLRGD-H5-ABD

The same DNA fragments used to construct ICOVIR15-H5-ABD were used to recombine in pAdZGLRGD plasmid.

ICOVIR15K-H1-ABD

The same DNA fragments used to construct ICOVIR15-H1-ABD were used to recombine in pAdZICOVIR15K plasmid, which contains the genome of ICOVIR15K in the pAdZ backbone.

ICOVIR15-Luc

The luciferase gene was amplified by PCR from pVK503TrackLuc, a plasmid containing the genome of an E1-deleted adenovirus with the GFP and luciferase genes cloned in the E1 region, using the oligonucleotides 3AlucF and 3AlucR. The DNA fragment generated in this PCR contains the splicing acceptor 3VDE (from the adenovirus protein IIIa), a Kozak sequence to enhance the translation efficiency, the luciferase gene, and a polyA sequence. To insert the

transgene after the fiber and under the control of the major late promoter (MLP), this DNA fragment was used to replace the rpsL-Neo cassette of pAdZICOVIR15-fi-rpsL-Neo, located after the fiber of oncolytic adenovirus ICOVIR15.

Table 4. Primers used for the construction of recombinant adenovirus genomes

Primer	Sequence (5'→3')
HVR1rpsLF	GCCCTGGCTCCCAAGGGTGCCCCAAATCCTTGCGAATGGGGCCTGGTGATGATGGC
HVR1rpsLR	GTAATATTTATACCAGAATAAGGCGCCTGCCCAAATACGTGAGTTCAGAAGAACTCGTCTCAAGAAG
ABDH1F	CCCAAGGGTGCCCCAAATCCTTGCGAATGGGATGAAGCTGCTACTGCTCTTGAAATAAACCTAGAAGAAG AGGACGGCAGCGGATCCCTG
ABDR1	CCCGGTTCGCAAGCACCTTAGCCTCGGCCAGGGATCCGCTGCCCCATTC
ABDF2	GCTTGCGAACCGGGAACTAGACAAATACGGTGTTTCTGATTATTACAAG
ABDR2	CGACGGTTTTGGCATTGTTAATCAAATTCTTGTAATAATCAGAAACACCG
ABDF3	ATGCCAAAACCGTCGAGGGCGTAAAGGCTCTGATCGACGAAATACTTGCG
ABDR3	ATACGTGAGTGCTACCAGACCCGGGTAGGGCCGCAAGTATTTCGTCGATC
ABDH1R	CAGAATAAGGCGCCTGCCCAAATACGTGAGTTTTTTGCTGCTCAGCTTGCTCGTCTACTTCGTCTTCGTTGT CATCGCTACCAGACCCGGG
HVR5rpsLF	GAAAGCTAGAAAGTCAAGTGGAAATGCAATTTTTCTCAACTGGCCTGGTGATGATGGC
HVR5rpsLR	CTTCTTGACGAGTTCTTCTGACCTAAAGTGGTATTGTACAGTGAAGATGTAGATATAGAAAC
ABDH5F	GCTAGAAAGTCAAGTGGAAATGCAATTTTTCTCAACTACTGAGGCAGCCGCAGGCAGCGGATCC
ABDH5R	CTATATCTACATCTTCACTGTACAATACCACTTTAGGAGTCAAGTTATCACCATTGCCGCTACCAGACCC
3AlucF	CAATTGGTACTAAGCGGTGATGTTTCTGATCAGCCACCATGGAAGACGCCAAAAACAT
3AlucR	GACTTGAAATTTTCTGCAATTGAAAAATAAAGTTTATTACACGGCGATCTTTCCGC

3.2. GENERATION OF RECOMBINANT ADENOVIRUSES BY CALCIUM PHOSPHATE TRANSFECTION

Once the desired modifications have been incorporated into the viral genome, this recombinant viral DNA needs to be introduced into packaging cells to generate the adenovirus. For this purpose, HEK293 cells were transfected with the plasmid containing the viral genome by the calcium phosphate-based method. For the transfection with pAdZ plasmids, previous linearization of the viral genome is not required since these plasmids incorporate a self-excising system. Once the plasmid enters the cell, the endonuclease I-SceI is expressed and releases the viral genome. This system increases the efficiency of the transfection, as circular DNA is transfected more efficiently than linear DNA. After the

transfection, the viral cycle begins, and after several rounds of replication (about 7 days post-transfection), foci of cytopathic effect are clearly seen.

For transfection, monolayers of HEK293 cells seeded in 6-well plates at a confluence of 60-80% were used. For each plasmid to be transfected the following mixture was prepared in a 1.5 mL tube:

- 19.5 µL of CaCl2 2 M
- 3 µg of DNA
- ddH_2O up to a final volume of 162 µL

This solution was mixed up softly for 10 seconds, and another 1.5 mL tube containing 162 µL of HBS 2X (NaCl 274 mM, HEPES 50 mM, and NaH_2PO_4 1.5 mM in H_2O, pH adjusted to 6.95-7.05 with NaOH) was prepared. The solution containing the DNA was added drop by drop to the tube containing the HBS while air was being bubbled with a pipette. The mixture was incubated for 1 minute at RT and added to the cells while shaking softly the plate to allow a homogenous distribution. 2 hours later calcium phosphate precipitates became visible and at 16 hours post-transfection the medium was removed and exchanged by fresh medium.

When the foci of cytopathic effect were visible, cells were collected together with the supernatant (cell extract, CE) and underwent 3 rounds of freeze (-80°C) and thaw (37°C) to completely release the viral particles from the cells. This way, we obtain the first viral lysate (cell extract passage 0, CEp0).

3.3. CLONE ISOLATION BY PLAQUE PURIFICATION ASSAY

In order to have a homogenous stock of each generated recombinant adenovirus, clone isolation by plaque purification assay was performed with the CEp0. For first generation vectors, the assay was performed in HEK293 cells as they provide E1A protein allowing the replication of E1-deleted adenoviruses. For oncolytic adenoviruses, this assay was performed in A549 cells in order to avoid the possible recombination between the modified E1 region of the adenovirus and the wild-type E1 region of HEK293 cells. Once isolated, the clones were characterized and those that were correct were amplified for its subsequent use in *in vitro* and *in vivo* assays. The plaque formation assay is based on the infection of cell monolayers with a bank of serial dilutions made from the CEp0 of the different adenoviruses. The infected cells are covered with an agarose matrix that allows nutrient and gas exchange with the medium but does not allow the diffusion of the viral progeny. This way, the viral particles released from

the cells are only able to infect neighboring cells leading to the formation of viral plaques after several rounds of replication.

First, serial dilutions ranging from 10^{-1} to 10^{-7} were prepared from the CEp0 in DMEM 5% FBS. Each well of the 6-well plate, which contains monolayers of A549 cells at an 80% of confluence, was infected with 100 µL of each viral dilution during 4 hours at 37°C. Cells were covered with 3 mL of a 1:1 solution of DMEM 5% FBS and 1% agarose previously prepared at 56°C. Once solidified, 2 mL of fresh medium was added over the agarose matrix. The plates were incubated at 37°C until plaques appeared at day 5-8 post infection. At that moment, the medium was carefully removed and the plaques were picked through the agarose matrix using a pipette tip. The aspirated agarose/medium was resuspended in 500 µL of DMEM 5% FBS.

3.4. AMPLIFICATION AND PURIFICATION OF ADENOVIRUSES

Amplification and purification allows the obtainment of sufficient amounts of adenovirus and in the appropriated formulation to be used for *in vitro* and *in vivo* assays. The amplification of the adenovirus is based on the propagation of the virus through culture plates of larger sizes at each passage and in bigger amounts. The purification of the adenovirus is based on its separation from the cell debris by ultracentrifugation steps in cesium chloride. Both processes are described in the following sections.

3.4.1. Amplification of adenoviruses

Amplification of non-replicative vectors was carried out in HEK293 cells as E1A protein is indispensable for adenovirus replication, whereas amplification of oncolytic adenoviruses was performed in A549 cells to avoid recombinations in the E1 region.

The starting material for the amplification of the adenoviruses was the plaque obtained from the plaque isolation assay. 250 µL of the medium containing the isolated clone were used to infect a well from a 6-well plate of the corresponding cells. When the cytopathic effect (CPE) was completed, the cells were harvested together with the supernatant (CE) and submitted to 3 rounds of freeze and thaw to release the viral particles from the cells. With the CE obtained from the 6-well plate (CEp1), 2 plates of 10 cm were infected. Again, when CPE was complete (around 72 hours post-infection) the CE was collected (CEp2). One of these plates was used to obtain viral DNA by Hirt's method (detailed in following sections) and the second one was used to infect 2 plates of 15 cm and continue with the amplification process. The CE from one of these 15 cm plates contains the sufficient amount of virus to perform *in vitro*

studies, and was kept at -80°C for this use. In order to purify the virus for in vivo usage, the CE from the other plate was used to infect 20 more 15 cm plates. For this final amplification step, the CE was collected when the CPE was evident in 90-100% of the cells but they were not completely detached from the plate, since the purification is carried out with cell pellets and the virus present in the supernatant will be lost. At that moment, the cells and the supernatant were collected in 50 mL Falcon tubes and centrifuged 5 minutes at 1000 g. The supernatant was discarded (except for 40 mL that were kept at -80°C to be used in the purification process) and the cells from each tube were resuspended and joined into one Falcon tube in an approximate volume of 10 mL. This CE was kept at -80°C until the moment of purification.

3.4.2. Purification of adenoviruses

The purification of the adenoviruses is performed in order to have a viral stock with the appropriate formulation and concentration to be administered in mice by systemic injection. The method used in this work for the purification of adenoviruses is based on cesium chloride (CsCl) density gradients combined with ultracentrifugation to separate viral particles from the rest of the CE components (cell debris, empty viral capsids, etc.) and to concentrate them. The buffer-exchange was performed by dialysis.

In order to release the viral particles from the cells, the pellet obtained in the last amplification step was submitted to 3 freeze/thaw cycles. The viral extract was centrifuged 5 minutes at 1000 g and the supernatant containing the virus (clarified cell extract, CCE) was collected. The pellet was resuspended in 10 mL of the supernatant kept from the amplification process and centrifuged again at the same conditions. This step was repeated 3 times until a volume of 42 mL of CCE was obtained. This CCE was then loaded onto the CsCl gradients. The CsCl gradients were prepared in ultracentrifugation tubes (Beckman Coulter, Brea, CA, USA) using 2 solutions at different concentrations. CsCl solutions B and C were prepared from the stock solution A (1.5 g/mL). The gradients were carefully prepared adding 2.5 mL of solution C (1.25 g/mL) dropwise onto 2.5 mL of solution B (1.35 g/mL). Finally, 7 mL of the CCE were carefully loaded onto each tube containing the gradients. Then the tubes were ultracentrifuged 2 hours at 10°C and 35000 rpm (SW40 Ti rotor, Beckman). At these conditions, viral particles are separated from cell debris and appeared as 2 bluish-white bands at the interface between 1.25 and 1.35 g/mL layers. The upper band corresponds to empty viral capsids and was removed by suction. Then, the band of interest was carefully collected and placed on ice in a 50 mL Falcon tube. For further purification, a second centrifugation step using a continuous CsCl gradient was necessary. The solution containing the virus was brought

up to 24 mL with the CsCl solution at 1.35 g/mL and distributed into 2 ultracentrifuge tubes. The second centrifugation was carried out overnight at the same conditions. After this centrifugation, the solution above the white band was discarded by suction and the band corresponding to the virus was collected in the smallest volume possible (in order to keep the virus highly concentrated) and introduced into a dialysis membrane. Three steps of 2 hours dialysis at 4°C were carried out against 1 L of Tris buffer (Tris-HCl 20 mM, NaCl 2 mM, and glycerol 2.5%). After the last dialysis, the virus was separated in aliquots and stored at -80ºC.

3.5. TITRATION OF ADENOVIRUSES

3.5.1. Determination of physical particles by spectrophotometry

This method is used to quantify the viral particles (vp) from a purified adenovirus stock without discrimination between infective or defective particles, and is based on the determination of the absorbance of viral DNA at a wavelength of 260 nm.

Three different dilutions (1/5, 1/10, and 1/20) of the purified viral stock were prepared in lysis buffer (Tris 10 mM, EDTA 1 mM, 0.1% SDS, pH 8.0) and incubated for 5-10 minutes at 56°C. Then, the OD was measured at 260 nm and 280 nm with a spectrophotometer. The final concentration of the virus was calculated with the following formula, taking into account that the extinction coefficient of adenoviruses is 1.1×10^{12} per OD unit:

$$vp/mL = OD_{260\ nm} \times \text{sample dilution} \times 1.1 \times 10^{12}$$

The ratio between the absorbance at 260 nm and 280 nm gives an idea of the integrity of the purified sample, and should be around 1.4.

3.5.2. Determination of physical particles by real-time PCR

This technique was used to detect and quantify adenovirus genomes in PBS samples with or without human erythrocytes, serum samples, and tissue extracts. The PCR was carried out using the oligonucleotide primers and probe detailed in **Table 5**, which identify the hexon region.

Table 5. Primers and probe used to quantify adenovirus genomes by real-time PCR

Primer	Sequence
Ad18852	5'- CTTCGATGATGCCGCAGTG-3'
Ad18918R	5'-GGGCTCAGGTACTCCGAGG -3'
TaqMan probe	5'-FAM-TTACATGCACATCTCGGGCCAGGAC-TAMRA-3'

A standard curve was prepared by diluting a known number of adenovirus genome copies in the adequate diluent for each type of sample. For each sample and standard curve point, the following mixture was prepared in 384-well plates:

- 4 µL of DNA sample [25 ng/µL]
- 0.36 µL of Ad18852 [10 µM]
- 0.36 µL of Ad18912R [10 µM]
- 0.1 µL of TaqMan probe [10 µM]
- 5 µL Premix ExTaq 2x
- 0.18 µL of ddH_2O

The following amplification protocol was followed:

- Denaturation 95 ºC for 10 min
- 40 cycles:
    - 95 ºC for 15 s
    - 60 ºC for 1 min

Genome copies were calculated using LightCycler® v4.05 software (Roche, Basel, Switzerland).

3.5.3. Determination of functional particles by anti-hexon staining

This method is based on the detection of positive cells for the immunostaining of the viral protein hexon in monolayers of HEK293 cells infected with serial dilutions of the virus. This technique allows the determination of functional infective viral particles (Transducing Units, TU) in purified stocks as well as in cell extract samples.

Serial 1/10 dilutions of the viral stock were prepared per triplicate in 96-well plates in a total volume of 100 µL per well of DMEM 5% FBS. Then, 50 µL of a cell suspension at a

concentration of $2x10^6$ cells/mL was added to the wells. After 36 hours incubation at 37°C, the medium was removed by suction and the cells were dried for 5 minutes at RT. To fix and permeabilize the cells, 100 µL/well of cold methanol were added and incubated 10 minutes at -20°C. The methanol was removed and the wells were washed twice with PBS++ containing 1% BSA. Next, the cells were incubated with a primary antibody against the hexon protein obtained from the hybridoma 2Hx-2 (ATCC), diluted 1/5 during 1 hour at 37°C. Afterwards, cells were washed three times and incubated with an anti-mouse secondary antibody conjugated with the fluorochrom Alexa-488 (Invitrogen) diluted 1/500 for 1 hour. Finally, the cells were washed thrice and the viral titer was determined by the counting of stained cells using an inverted fluorescence microscope. To calculate the number of transducing units per mL the following formula was used:

$$\text{TU/mL} = \frac{\text{Mean of positive cells}}{100\ \mu\text{L}} \times \text{Dilution factor} \times 1000\ \mu\text{L}$$

3.5.4. Quantification of viral protein by Bradford assay

A standard curve was performed with known concentrations of BSA in 96-well plates. BSA was serially diluted in ddH_2O in order to have 0, 1, 2, 3, 4, 5, and 6 µg of protein in a final volume of 160 µL. Purified adenovirus samples were diluted in ddH_2O depending on the physical titer previously obtained (dilutions ranging from 1/5 to 1/100) in a volume of 160 µL (always handling the samples on ice). 40 µL of Bradford reagent were added to the wells and mixed carefully without making bubbles. After 5 minutes, absorbance at 595 nm was read and protein concentration was determined taking into account the absorbance of the BSA standard curve.

3.6. CHARACTERIZATION OF RECOMBINANT ADENOVIRUSES

3.6.1. Methods for purification of viral DNA

In this work, viral DNA has been obtained from two different sources: infected cells or purified virus stocks. The methods used in each case are detailed below.

3.6.1.1. Purification of viral DNA from infected cells

This method has been used for the analysis and validation of the clones obtained in the plaque formation assay.

The cell extract of infected cells was harvested and centrifuged 5 minutes at 1000 g. The supernatant was discarded and the cell pellet resuspended in 1 mL of PBS. The cell suspension was pelleted again by centrifugation and resuspended in 350 µL of ddH_20. 350 µL of Hirt's solution 2X (10 mM Tris pH 8.0, 20 mM EDTA, 1.2% SDS, and 200 µg/mL of proteinase K) were added to the cell suspension and the sample was mixed and incubated for 1 hour at 56°C. 200 µL of NaCl 5 M were added dropwise while vortexing, and the mixture was incubated at 4°C for 8-16 hours until a white precipitate (corresponding to the cellular DNA) appeared. In order to eliminate this cellular DNA, the suspension was centrifuged for 30 minutes at 15000 g and 4°C and the clear supernatant containing the viral DNA was collected. Incubation with RNAse at a final concentration of 100 µg/µL was carried out for 1 hour at 37°C. Then, a phenol:chloroform DNA extraction was performed and the DNA was precipitated with ethanol containing 2% of sodium acetate. Finally, the pellet corresponding to the viral DNA was resuspended in 50 µL of TE pH 8.0.

3.6.1.2. Purification of viral DNA from purified virus stocks

This method has been used to verify the identity of each generated virus purified stock. Usually, the starting material has been a 50 µL aliquot of purified virus, containing approximately $2x10^{10}$ vp, corresponding to 1 µg of viral DNA.

The following was added to this aliquot and incubated 2 hours at 56ºC:

- 16 µL of EDTA pH 8.0 [0.5 M]
- 20 µL SDS 10%
- 8 µL proteinase K [10 mg/mL]
- TE pH 8.0 up to 400 µL

After the incubation, a phenol:chloroform DNA extraction was performed and the DNA was precipitated with ethanol containing 2% of sodium acetate. Finally, the pellet corresponding to the viral DNA was resuspended in 50 µL of TE pH 8.0.

3.6.2. Digestion of viral DNA with restriction enzymes

As starting material for the digestion of viral DNA with restriction enzymes, 500 ng of DNA were used. To this amount of DNA, 1 unit of the enzyme, the appropriate buffer to each enzyme (provided by the manufacturer at 10X), and ddH_2O up to the desired final volume were added. The mixture was incubated normally for 2 hours in a water-bath at 37°C and then the samples were resolved in a 1% agarose electrophoresis gel prepared in Tris-Acetate-EDTA (TAE) buffer, together with a molecular weight marker.

3.6.3. Viral DNA sequencing

Sequencing of viral DNA was performed using 200 ng of DNA, 2 µL of the sequencing mix 3.1 (Applied Biosystems, Foster City, CA, USA) containing dNTPs and ddNTPs marked with different fluorochroms, 2 µL of 5X sequencing buffer, 3.2 pmols of the corresponding oligonucleotide, and ddH_2O up to 10 µL. The conditions of the sequencing reaction were 24 cycles consisting on: 30 seconds at 96°C, 15 seconds at 50°C, and 2 minutes at 60°C. The sequencing reactions were analyzed with an automatic sequencer at the "Laboratori de Recerca Translacional 2" of the "Institut Català d'Oncologia" (ICO).

4. *IN VITRO* ASSAYS WITH RECOMBINANT ADENOVIRUSES

4.1. BINDING ASSAYS TO HUMAN ERYTHROCYTES

All *in vitro* studies in this thesis were performed in triplicate. AdGL was incubated with freshly isolated and washed human erythrocytes at the indicated concentrations for 30 min at 37 ºC with constant agitation. For the CAR blocking assay, a preincubation of human erythrocytes with anti-CAR antibody from RmcB hybridoma (1/5 dilution, ATCC) was performed for 1 h at 4 ºC before incubation with AdGL. After the incubation, samples were centrifuged at 8000 rpm for 10 min at room temperature, the supernatant was separated and brought up to 1 mL of PBS, and the erythrocyte pellet was resuspended in 1 mL of PBS. Supernatant and pellet samples were digested with proteinase K and SDS to release the viral DNA as follows:

- 5 µL of sample
- 2 µL of proteinase K buffer 2X

- 2 µL of proteinase K
- 0.5 µL of SDS 4%
- 10.5 µL of ddH_2O

Mixtures were incubated 45 min at 54 ºC and 10 min at 90 ºC. After the digestion, samples were diluted 1/20 in ddH_2O and adenovirus genome quantification was performed by real-time PCR. Two different standard curves were prepared for the supernatant samples and for the erythrocyte fraction samples. $1.8x10^8$ vp were diluted in 1 ml of PBS (supernatant samples) or in 1 ml of PBS with $5x10^9$ erythrocytes (erythrocyte fraction samples). Subsequent 1/2 dilutions were performed in PBS or in PBS containing erythrocytes. These standard curve samples were treated equally as the test samples regarding the digestion with proteinase K and SDS, and subsequent dilution in ddH_2O.

4.2. DETECTION OF ALBUMIN BINDING BY ELISA

Detection of binding to human serum albumin (HSA) and mouse serum albumin (MSA) was performed following an ELISA protocol adapted from Konig and Skerra (Konig and Skerra, 1998). Incubations were performed 1 h at room temperature followed by three washing steps with 200 µL of PBS containing 0.1% Tween20, which was also the buffer used to dilute viruses and antibodies. The 96-well plate was coated with 200 µL of BSA, HSA, or MSA (Sigma, St. Louis, MO) at 2 mg/mL diluted in PBS. Alternatively, wells were coated with human or mouse serum previously diluted 1/25 in PBS. Remaining binding sites on the plastic surface were blocked with 2 mg/mL of BSA diluted in PBS containing 0.5% Tween20. 25 ng of viral protein of the purified viruses were added in a volume of 50 µL. For the dose-dependent binding 0, 0.25, 2.5, or 25 ng of viral protein were used. Viral protein concentration of the purified virus samples was quantified using Bio Rad Protein assay as described in section 3.5.4. Detection of viruses in wells coated with purified albumins or human serum was performed with anti-hexon antibody from 2Hx-2 hybridoma supernatant (50 µL per well at a dilution of 1/5, ATCC) and a polyclonal goat anti-mouse conjugated with horseradish peroxidase (50 µL per well at a dilution of 1/2000, Life Technologies, Carlsbad, CA, USA). Detection of viruses in wells coated with mouse serum was performed with anti-Ad5 Ab6982 (50 µL per well at a dilution of 1/500, Abcam, Cambridge, UK) and a polyclonal goat anti-rabbit conjugated with horseradish peroxidase (50 µL per well at a dilution of 1/2000, Life Technologies). Wells were stained adding 100 µL per well of freshly mixed 3,3',5,5'-Tetramethylbenzidine (Thermo Fisher, Waltham, MA, USA) peroxidase substrate solution and incubated 15 min with shaking. The

reaction was stopped adding 100 µL of sulfuric acid 2N and the absorbance was measured at 450 nm.

4.3. DETECTION OF ALBUMIN BINDING BY IMMUNOELECTRON MICROSCOPY

Purified samples of ICOVIR15 and ICOVIR15-ABD were adsorbed for 2 min onto glow-discharged, collodion/carbon coated nickel grids. Unspecific binding was blocked by floating grids on a drop of TBG (30 mM Tris-HCl pH 8, 150 mM NaCl, 0.1% BSA and 1% gelatin) for 10 min. Grids were then incubated for 30 min with a 1:1 dilution of stock of HSA in TBG (2 mg/mL in 20 mM Tris-HCl pH 7.8, 150 mM NaCl), washed in TBG (3x3 min), and incubated for 15 min on a drop of mouse anti-HSA (Sigma) diluted 1:500 in TBG. After 4 x 2 min rinses with 0.1% gelatin in PBS (137 mM NaCl, 2.7 mM KCl, 10 mM Na_2HPO_4, 1.8 mM KH_2PO_4 pH 7.4) and 5 min incubation in TBG, grids were incubated for 15 min in goat anti-mouse IgG-gold conjugate (EM.GAF10, British Biocell International, Cardiff, UK) diluted 1:40 in TBG. Finally, grids were washed in 0.1% gelatin in PBS (5x2 min), milliQ water (3x2 min), and stained with 2% uranyl acetate (30 sec). Grids were examined in a JEOL 1230 electron microscope.

4.4. DETECTION OF ALBUMIN BINDING BY CRYO-ELECTRON MICROSCOPY

4.4.1. Cryo-electron microscopy

75 µL of ICOVIR15-ABD ($8x10^{11}$ vp/mL in 20 mM Tris pH7.8, NaCl 25mM, 2.5% glycerol) were mixed with 0.75 µL of stock HSA and incubated for 30 min at room temperature to obtain an ICOVIR-ABD-HSA complex for cryo-EM imaging. Glycerol and free HSA were removed, and the virus concentrated, by adding 2.3 volumes of 20 mM Tris pH7.8, NaCl 25mM and spinning at 4°C in a 100,000 MWCO Amicon Ultra centrifugal filter (Millipore, Billerica, MA, USA). Final virus concentration was $2.4x10^{12}$ vp/mL. Samples were applied to glow discharged Quantifoil R2/4 300 mesh Cu/Rh grids, vitrified in liquid ethane using a Leica CPC plunger, mounted in a Gatan 626 cryostage and examined in a FEI Tecnai G2 FEG microscope operating at 200 kV. Low dose cryo-EM images were acquired using a 4 K x 4 K Eagle CCD camera, with a magnification of x50,000 and a defocus range of 0.5-4 µm, with a nominal sampling rate of 2.16 Å/px in the sample.

4.4.2. Three-dimensional reconstruction and difference mapping

Image processing and three-dimensional reconstruction were performed using the software package Xmipp (de la Rosa-Trevin et al., 2013). The contrast transfer function (CTF)

parameters of 177 micrographs were determined using CTFFIND4 (Rohou and Grigorieff, 2015). An initial set of 1181 particles manually selected was extracted into 516x516 pixel boxes, with one pixel corresponding to 2.16 Å in the sample, normalized, and reduced to 256x256 box size (4.35 Å/px) for computational efficiency. Orientation search and 3D reconstruction were carried out using projection matching in Xmipp. The initial model for the first refinement iteration was a map calculated from the high resolution cryo-EM model of human adenovirus type 5 (HAdV-C5) (Liu et al., 2010) using the program pdb2mrc (Ludtke et al., 1999) and low-pass filtered to 60 Å resolution. A total of 1121 particles were included in the final 3D map at 19.6 Å resolution, estimated by Fourier shell correlation with the threshold set at 0.5. Icosahedral symmetry was imposed throughout refinement. A difference map showing the HVR1, ABD and HSA density was calculated by subtracting the HAdV-C5 model from the ICOVIR15-ABD-HSA map after filtering both to the same resolution (19.6 Å), normalizing, and refining the scale of the experimental map. Scale refinement, subtraction and figure creation were carried out with UCSF Chimera (Pettersen et al., 2004).

4.5. VIRAL PRODUCTION ASSAYS

To perform viral production assays, a known number of cells were seeded into 24-well plates in order to have an 80% of confluence at the moment of the infection. Cells were infected per triplicate at an MOI to allow for 80 to 100% of infection. A549 were infected at 800 vp/cell, and HEK293 cells at 100 vp/cell. 4 hours later, infection media was removed, cells were washed 3 times with PBS and incubated with fresh medium. At indicated time points (4, 24, 48, and 72 hours post infection), cells and medium (CE) were harvested and subjected to 3 rounds of freeze-thaw lysis. After the lysis, cell extracts were centrifuged 5 min at 5000 g to separate cell debris and viral titers were determined according to the anti-hexon staining method described in section 3.5.3.

4.6. VIRAL INFECTIVITY ASSAYS

Viral infectivity assays were performed by infecting different cell lines with the non-replicative vectors expressing the GFP-Luciferase fusion protein. Transduction efficiency of the different capsids was determined by measuring the luciferase activity of the cell lysates 24 hours after infection for HEK293 cells, and 36-48 hours after infection for tumor cell lines. Medium was removed and cells were lysed adding 50 µL of Reporter Lysis Buffer 1X (Promega, Madison, WI, USA) and frozen-thawed once. Lysates were centrifuged at 4000 rpm for 5 minutes at 4ºC and the luciferase enzyme activity of the supernatant was measured mixing 8

µL of sample with 20 µL of Luciferase Assay Reagent (Promega) in a luminometer (Berthold Junior, Berthold GmbH&Co, KG, Germany).

4.6.1. Infectivity in the presence of HSA

SK-mel28 (10,000 cells/well), NP-9 (15,000 cells/well), A549, B16, or B16-CAR (30,000 cells/well) were seeded in 96-well plates. The following day, cells were infected in normal medium or in human serum albumin-containing medium (HSA 1mg/mL, Sigma) with the MOIs indicated in each figure caption in the Results section. Alternatively, A549 cells were also infected in medium containing 0, 0.01, 0.1, 1, and 10 mg/mL of HSA to test the effect of albumin concentration. At 36 hours post-infection luciferase activity was measured as described above.

4.6.2. Infectivity in the presence of HSA and FX

30,000 A431 cells per well were seeded in 96-well plates. The day after, cells were washed with PBS, and incubated with FBS-free medium in the presence and absence of HSA (1 mg/mL) and in the presence and absence of FX (12.25 µg/mL, Assaypro, St. Charles, MO, USA). Cells were infected with 1000 vp/cell. 8 hours after the infection cells were washed with PBS and incubated with fresh DMEM 10% FBS. 24 hours after the infection luciferase activity was measured as described above.

4.6.3. Infectivity in the presence of human erythrocytes

700,000 A549 cells per well were seeded in 24-well plates the day before the assay. $1.8x10^8$ vp of AdGL were incubated with $5x10^9$ freshly isolated and washed human erythrocytes in 1 mL of PBS, or in 1 mL of PBS without erythrocytes for 30 min at 37 ºC with constant agitation. After the incubation, samples were centrifuged at 8000 rpm for 10 min at room temperature, the supernatant was discarded and the erythrocyte pellet was resuspended in 1 mL of PBS. 30 µL of the resuspended erythrocyte pellet were used to infect A549 cells. Erythrocytes alone in A549 cells and erythrocytes with AdGL in the absence of A549 cells were used as negative controls. 48 hours after the infection luciferase activity was measured as described above.

4.7. CYTOTOXICITY ASSAYS

Cytotoxicity analysis *in vitro* is based on the evaluation of the cell viability after the exposure of tumor cells to the different adenoviruses. Such analysis was performed by the

quantification of total protein content by the bicinchoninic acid assay (BCA, Pierce Biotechnology, Rockford, IL, USA). This assay combines the reduction of Cu^{2+} to Cu^{1+} by proteins in an alkaline medium with the highly sensitive and selective colorimetric detection of the cuprous cation (Cu^{1+}) by bicinchoninic acid. The reaction of two molecules of BCA with one Cu^{1+} results in an intense purple-colored product that exhibits a strong linear absorbance at 540 nm with increasing protein concentrations.

Cytotoxicity assays were performed by seeding 30,000 A549 per well in a 96-well plate. Cells were infected in normal medium or in HSA-containing medium (50 ng/µL or 1mg/mL) with serial dilutions of the viruses with the MOIs indicated in the figures in the Results section. At day 5-7 post-infection plates were washed with PBS and incubated with 200 µL of BCA reagent during 30 minutes at 37ºC. Absorbance was quantified at 540 nm and the MOI required to produce 50% of growth inhibition (IC_{50} value) was determined from dose-response curves by standard nonlinear regression (GraphPad Prism 5; GraphPad Inc., La Jolla, CA).

4.8. ANTIBODY-MEDIATED NEUTRALIZATION ASSAYS

4.8.1. Determination of anti-Ad5 NAbs titer in serum samples

This method is based on the transduction analysis of a reporter adenoviral vector after the incubation with serial dilutions of a serum sample. The transduction efficiency increases as the serum is diluted and the percentage of neutralization is calculated in each dilution.

Starting from an initial 1/10 dilution, serial 1/2 dilutions of the serum sample were prepared per triplicate in 96-well plates in a total volume of 50 µL per well of DMEM 5% FBS containing $5x10^5$ TU/mL of the indicated virus. The plate was incubated 1 hour at room temperature to allow the binding of neutralizing antibodies to the virus. Then, 50 µL of a cell suspension of HEK293 at a concentration of $2x10^6$ cells/mL was added to the wells, corresponding to an MOI of 0.25 TU/cell. A positive control of virus and cells without serum, and a negative control of only cells were also included to calculate the percentage of neutralization. After 24 hours incubation at 37°C, the luciferase activity of the samples was measured as described above. To calculate the percentage of neutralization of each serum dilution the following formula was used:

$$\%\ \text{neutralization} = \left(1 - \frac{\text{LU sample} - \text{LU negative control}}{\text{LU positive control} - \text{LU negative control}}\right) \times 100$$

The titer of the serum corresponds to the dilution in which the percentage of neutralization is closest to the 50% value.

4.8.2. Transduction in presence of NAbs

This method was used to test the ability of adenoviruses to transduce target cells in presence of neutralizing antibodies. It is a variation of the NAbs tittering method described above. The assay was performed using the anti-Ad5 neutralizing antibody Ab6982, mouse serum, or human serum. Serial dilutions of the neutralizing agent were performed in 96-well plates as indicated, in a total volume of 50 µL per well of DMEM 5% FBS containing the different reporter vectors or oncolytic adenoviruses, and containing or not HSA (1 mg/mL). After 1 hour incubation at room temperature, 50 µL of a cell suspension was added to the wells (100,000 HEK293, and 30,000 A549 or Sk-mel28 cells per well) to obtain the desired multiplicity of infection (10 vp/cell for HEK293 and A549, and 40 vp/cell for Sk-mel28). A positive control of virus without neutralizing agent and a negative control of only cells were also included to calculate the percentage of neutralization. After 24 hours incubation at 37°C, the luciferase activity of the samples was measured. If oncolytic adenoviruses were used, the plate was developed by anti-hexon staining method 36 hours after the infection. The percentage of neutralization is calculated as described above but the data is represented in percentage of transduction:

$$\% \text{ transduction} = 100 - \% \text{ neutralization}$$

Alternatively, the effect of HSA concentration on neutralization escape was also analyzed. A single 1/36 dilution of Ab6982 was performed in medium containing the different reporter vectors, and containing 0, 0.01, 0.1, 1, or 10 mg/mL of HSA. The transduction of the vectors in these conditions in A549 cells was performed as described above.

4.8.3. Cytotoxicity in presence of NAbs

This method was used to test the ability of adenoviruses to kill cancer cells in presence of neutralizing antibodies. The principle is the same as the transduction assay in presence of NAbs. Serial dilutions of the neutralizing agent were performed in medium containing the different oncolytic adenoviruses. After 1 hour incubation at room temperature, cells were added to the wells to obtain the desired multiplicity of infection. At day 5-7 post-infection cell viability was quantified using the BCA reagent as described in section 4.7.

5. *IN VIVO* ASSAYS WITH RECOMBINANT ADENOVIRUSES

5.1. ANIMALS AND CONDITIONS

All the animal studies were performed at the IDIBELL facility (AAALAC unit 1155) and approved by the IDIBELL's Ethical Committee for Animal Experimentation.

In this work, female immunocompetent Balb/C mice were used for the toxicity studies, female immunodeficient Athymic nu/nu mice were used for the blood persistence analysis, biodistribution, and antitumor activity experiments; and female immunocompetent C57BL/6 mice were used for the immunization, blood persistence, biodistribution, and ELISPOT experiments. In all cases, 6-8 week-old mice with a body weight between 20 and 30 g were used.

Animals were housed at a temperature between 22 and 24°C under an artificial circadian 12 hour light/12 hour dark cycle, and received *ad libitum* standard diet and water. The number of animals used in each study is indicated in the figure captions.

5.2. SUBCUTANEOUS IMPLANTATIONS OF TUMOR CELLS AND MONITORING

Tumor cells were maintained in 15 cm plates at standard *in vitro* conditions. At the moment of implantation, cells were trypsinized, resuspended with DMEM 5% FBS, centrifuged during 5 minutes at 1000 g, washed with PBS, and counted. Finally, they were resuspended in an appropriate volume of PBS to obtain the desired cell concentration. The number of cells per tumor varied depending on the cell line and ranged from $3x10^6$ to $1x10^7$ cells/tumor, implanted in a volume of 200 µL. Mice were anesthetized with isoflurane before the implantation of the tumors and shaved in the case of immunocompetent C57BL/6 mice. The subcutaneous injections were carried out with 29 G hypodermic needles. After tumor implantation, the appearance of the tumors was monitored by palpation, and when they had a measurable volume, tumors were measured with a caliper. Tumor volume was calculated according to the following equation:

$$V\ (mm^3) = \frac{\pi}{6} \times L \times W^2$$

where W and L are the width and the length of the tumor, respectively.

When tumors reached a volume of 100-200 mm^3, animals were randomized into experimental groups and were treated as corresponded.

5.3. ADMINISTRATIONS

Solutions for the administration *in vivo* were prepared by diluting purified washed human erythrocytes, purified viral stocks, or mouse serum in PBS. For the systemic administration, a maximum volume of 200 µL was injected with hypodermic 29 G needles via tail vein. When adenovirus and erythrocytes were co-injected, they were incubated for 30 min at 37 ºC before the injection. For the intraperitoneal administration, hypodermic 29 G needles were also employed. Viruses were injected in a volume of 200 µL and the volume of mouse serum administered depended on the serum titer and is indicated in each experiment in the results section. The injected doses of adenovirus or erythrocytes are also detailed in each experiment.

5.4. SAMPLE COLLECTION

The obtention of blood samples and organs for their analysis was carried out after killing the mice by asphyxiation in a CO_2 chamber. Alternatively, small blood samples were also taken by a small cut on the tail without killing the mice.

5.4.1. Blood or serum for erythrocyte or virus detection

Blood samples were collected after a small cut in the mouse tail at the indicated time points after the systemic administration. For the detection of human erythrocytes, blood samples were collected in EDTA-coated capillary tubes to avoid clotting. Erythrocyte detection was performed by flow cytometry analysis as described below in section 5.5. For the detection of adenovirus particles, blood samples were collected in capillary tubes without anticoagulant and allowed to clot. The serum was separated by centrifugation 5 minutes at 6500 g. Virus genomes were quantified by real-time PCR as described in section 3.5.2., and adenovirus transducing units were quantified by anti-hexon staining method described in section 3.5.3.

5.4.2. Serum for biochemical analysis or NAbs titration

Blood samples were obtained by cardiac puncture with a hypodermic 25 G needle. For the biochemical analysis, tubes containing heparin (BD Microtainer, PSTTM LH tubes) were used and the samples were centrifuged 5 min at 6500 g to obtain the serum, which was analyzed by the “Servei de Bioquímica Clínica Veterinària de la Facultat de Veterinària de la Universitat

Autònoma de Barcelona". For NAbs tittering, serum samples were heat-inactivated at 56ºC for 30 min. Determination of NAbs titer was performed as described in section 4.8.1.

5.4.3. Organ collection

Organs were collected using surgical instruments and washed with saline solution. Organs were directly imaged with an *in vivo* bioluminescent imaging machine (IVIS), or divided into pieces and fixed in formaldehyde 4% for 16 hours for paraffin inclusion, or directly frozen for DNA extraction. Spleens for ELISPOT analysis were harvested in 15 mL conical Falcon tubes containing 5 mL of RPMI medium supplemented with 10% FBS and 1% PS for subsequent isolation of splenocytes.

5.5. DETECTION OF HUMAN ERYTHROCYTES IN MOUSE BLOOD

Freshly isolated and washed human erythrocytes were incubated with carboxyfluorescein succinimidyl ester (CFSE) at a final concentration of 10 µM for 5 min and protected from light. After the incubation, PBS + 5% FBS was added up to a volume of 50 mL, and erythrocytes were centrifuged for 7 min at 2000 g. This washing step was performed three times. After the last centrifugation, erythrocytes were counted and brought to a concentration of $4x10^9$ cells/mL in PBS. A total of $8x10^8$ CFSE-labeled erythrocytes in 200 µL of PBS were intravenously injected in nude mice. Blood samples were collected from the tail vein at the indicated time points as described in section 5.4.1. A Gallios™ (Beckman Coulter) cytometer was used for the detection of CSFE-labeled human erythrocytes. 100,000 events were analyzed for each sample and FlowJo v7.6.5 (Tree Star, Inc.) software was used for the analysis of the data.

5.6. BIODISTRIBUTION ANALYSIS OF ADENOVIRUSES

The accumulation and transduction of adenoviruses in the organs was analyzed by two methods as described below:

5.6.1. Analysis of luciferase activity in organs

The transduction in the different organs was determined by measuring the luciferase activity after the systemic administration of the non-replicative reporter vectors, or the replicative luciferase-expressing adenovirus ICOVIR15-Luc.

Three days after vector administration mice received an intraperitoneal injection of 250 µL of D-Luciferin (15mg/mL; Biosynth, Staad, Switzerland). 10 minutes after Luciferin injection

mice were killed and the organs were harvested for imaging. The IVIS Lumina XR (Caliper Life Sciences, Hopkinton, MA, USA) machine was employed. Livers were usually exposed for 10 seconds whereas the rest of the organs were exposed for 1 minute. The Living Image v4.0 software was used to quantify the emission of light.

To track the replication *in vivo* of the reporter adenovirus ICOVIR15-Luc the IVIS imaging system was also used. Mice were injected with D-Luciferin 10 minutes after the injection. After 10 minutes, mice were anesthetized with isoflurane by inhalation using an anesthetic machine. A 2% dose was used with a constant oxygen flux of 2.5 L/s. Images were taken with 30s-1min of exposure.

5.6.2. Quantification of virus genomes in tissue extracts

Frozen tumors were ground to a fine powder in liquid nitrogen using a pestle and a mortar, and DNA was purified using the QIAmp DNA MiniKit (QIAGEN, Valencia, CA, USA) according to manufacturer's instructions. The obtained DNA was quantified by measuring the absorbance at 260 nm in a nanodrop spectrophotometer (NanoDrop technologies) from 1.5 µL of the DNA solution. All DNA samples were diluted to a concentration of 25 ng/µL with ddH_2O. Viral genome quantification was performed by real-time PCR as previously described in section 3.5.2.

5.7. QUANTIFICATION OF CTL-SPECIFIC IMMUNE RESPONSES BY ELISPOT

5.7.1. Isolation of splenocytes

The whole process was carried out in sterile conditions. A cell strainer (40-100 µm) was placed in a 6 cm plate and the spleens were mechanically disrupted with the flat portion of a syringe plunger until no fragments remained. The cell strainer was washed several times with RPMI 10% FBS 1% PS medium, and the cell suspension was transferred to a clean 15 mL Falcon tube. Cells were centrifuged at 500 g for 10 minutes and the supernatant was removed. In order to lyse the red blood cells, the pellet was resuspended in 2 mL of ACK lysis buffer (NH_4Cl 150 mM, $KHCO_3$ 10 mM, EDTA 1 mM, pH 7.2). The suspension was incubated at RT for 3 min, the tube was filled with fresh medium, and centrifuged again at 500 g for 10 min. The supernatant was removed and the cell pellet was resuspended in PBS. Two more washes were performed with PBS to discard any tissue debris. Finally, the cells were counted with the automatic cell counter TC20TM and brought to a concentration of $2.5x10^6$ cells/mL.

5.7.2. ELISPOT

CTL-specific responses were evaluated by anti-IFN-γ Enzyme-linked immunospot assay (ELISPOT). This method is based on the measurement of the frequency of cytokine-secreting cells at a single-cell level, in response to the stimulation with a specific antigen by employing the sandwich enzyme-linked immunosorbent assay (ELISA) technique.

All steps until the development of the plates were performed under sterile conditions. 96-well polyvinylidene fluoride membrane ELISPOT plates (Multiscreen plates, Millipore) were treated with 15 µL of 35% ethanol per well for 1 minute. Then, 5 washes with ddH_2O were performed and plates were incubated overnight at 4°C with a murine IFN-γ-specific capture antibody (clone AN-18, BD 551309, San Jose, CA, USA) at 4 µg/mL diluted in PBS at a final volume of 100 µL/well. The day after, the antibody was discarded and plates were washed 5 times with PBS and blocked with 200 µL/well of supplemented RPMI medium for 2 h at RT. During this incubation, the splenocytes were isolated as explained above and 100 µL of a $2.5x10^6$ cells/mL cell suspension were added to each well ($2.5x10^5$ cells/well). The peptide used for the stimulation of the splenocytes was $E1b_{192}$ (VNIRNCCYI) and was synthesized by GenScript USA Inc. (Piscataway, NJ, USA) at 95% purity and re-suspended following the manufacturer's instructions. Stimulation with the peptide was performed at a final concentration of 1 µM. Phorbol-myristate-acetate (PMA at 15 ng/mL) plus ionomycin (250 ng/mL) were used as positive control of stimulation and medium only as negative control, at 100 µL/well. Plates were incubated with the splenocytes for at least 18 hours at 37°C and 5% CO_2. From that moment, sterility was not required. Cells and medium were removed and the plates were washed 5 times with PBS. Then, the biotinylated anti-IFNγ secondary antibody (clone RA-6A2, BD 55156, San Jose, CA) was added at a concentration of 1 µg/mL in PBS 0.5% FBS at a final volume of 100 µL/well and incubated for 2 hours at RT. Next, the antibody was removed and the plates were washed 5 times with PBS. The streptavidin-ALP (ExtrAvidin Ref E2636-2ML Sigma E2636) was then added diluted 1/2500 in PBS 0.5% FBS (100 µL/well) and incubated for 1 hour at RT. 5 washes with PBS were performed and finally 50 µL/well of the substrate BCIP/NBT solution (Ref B1911-100ML, Sigma) were added. Plates were developed for 15-30 minutes until spots emerged and the plate was washed with tap water to stop the reaction. Plates were left to dry overnight and spots were counted using the AID ELISPOT reader classic (ELR07 de AID GmbH, Straßberg, Germany).

6. HISTOLOGY

6.1. PARAFFIN INCLUSION

Fixation of tissues in formaldehyde was followed by washing them with a saline solution in order to eliminate the fixative agent. Next, tissues underwent a battery of alcohols of crescent graduation in order to dehydrate them to allow the penetration of paraffin. Tissues were submerged for 1 hour in ethanol 70%, for 2 hours in ethanol 96%, and then in new 96% ethanol overnight. Next day, tissues went through a battery consisting of 3 absolute ethanol (1.5 hours each) and then were submerged into xylol for 1.5 hours more. Finally, they were submerged into liquid paraffin at 65°C overnight and the next day they were included in blocks.

6.2. IMMUNOHISTOCHEMISTRY IN PARAFFINIZED SECTIONS

Paraffin-embedded blocks were cut into 4-µm thick sections with a microtome and deposited into poly-L-lysine treated slides. Sections were deparaffinized by subjecting them to a battery of 4 xylols (10 minutes each), 3 absolute ethanol, 3 96% ethanols, 1 70% ethanol, and 1 50% ethanol (5 minutes each). The sections were rehydrated by submerging them in ddH_2O. Antigens masked during routine fixation were retrieved by submerging the slides in sodium citrate solution (pH 6.0) and heating during 12 minutes. Slides were washed for 5 minutes in ddH_2O. Next, endogenous peroxidase activity was blocked by three washes with 6% H_2O_2 (1 x 5 minutes, 2 x 10 minutes), and tissue sections were permeabilized for 10 minutes in PBS 0.1% Triton X-100. Sections were blocked in order to reduce unspecific binding with Normal Goat serum diluted 20% in PBS for 1 hour at RT. All incubations were performed in a humidity chamber. Primary antibody incubation was performed using an anti-Ad2/5 E1A antibody (SC-430, Santa Cruz, Dallas, TX, USA) diluted 1/200 in PBS 5% goat serum overnight at 4ºC. After washing thrice with PBS 0.1% Triton X-100 (1 x 5 minutes, 2 x 10 minutes), sections were incubated for 1 hour at RT with anti-mouse Envision+-System-HRP (Dako Laboratories, Glostrup, Denmark). Slides were washed again with PBS 0.1% Triton X-100 and developed by covering the sections with the chromogenic substrate DAB+ (Envision Kit, Dako CYtomation K3468) for 10 minutes. The reaction was stopped by rinsing the slides with tap water. Finally, the sections were counterstained with hematoxylin, dehydrated again (1 ethanol 7%, 3 ethanol 96%, 3 absolute ethanol, and 4 xylols; 5 minutes per ethanol, 10 minutes per xylol) and mounted in DPX (VWR International).

7. STATISTICAL ANALYSIS

Graphs and statistic tests were performed with GraphPad Prism software v6.02. Two-tailed unpaired Student's *t*-test was used to evaluate the statistical significance between groups. A log-rank Mantel-Cox test was used to determine statistically significant differences between survival curves. The statistic significance was defined at a *p* value lower than 0.05.

RESULTS

1. ANALYSIS OF THE CAR-MEDIATED INTERACTION BETWEEN ADENOVIRUS TYPE 5 AND HUMAN ERYTHROCYTES AND ITS EFFECT ON VIRUS BIOACTIVITY

Carlisle et al. (Carlisle et al., 2009) and Seiradake et al. (Seiradake et al., 2009) described that unlike mouse erythrocytes, human erythrocytes express the primary type 5 adenovirus (Ad5) receptor, the coxsackie and adenovirus receptor (CAR). The binding of Ad5 to human erythrocytes via CAR was described to be a neutralizing interaction, sequestering the virus and preventing systemic infection. However, the absence of integrins on erythrocyte membrane precludes internalization of the bound Ad5. In addition, human erythrocytes also present complement receptor 1 (CR1), which binds Ad5 in the presence of antibodies and complement (Carlisle et al., 2009). These findings generated great skepticism in the capability of CAR-binding adenoviruses to reach specific organs or tumors upon systemic administration in humans. Although we acknowledge that the CR1-mediated pathway might inactivate Ad5, we hypothesized that the interaction of Ad5 with CAR in human erythrocytes could be reversible, and upon long-time incubation periods, the virus could be available for infection. In this first chapter, we studied how this CAR-mediated interaction affected the ability of the virus to infect cells and transduce target organs. The results of this chapter are gathered in the manuscript "Adenovirus coxsackie and adenovirus receptor-mediated binding to human erythrocytes does not preclude systemic transduction" enclosed in the annex section.

1.1. *IN VITRO* CAPACITY OF HUMAN ERTRHOCYTES TO BIND ADENOVIRUS TYPE 5

AdGL is an Ad5-derived non-replicative luciferase-expressing vector (described in Materials and methods section 3) and was used throughout this chapter. Ad5 binding to human erythrocytes was first evaluated *in vitro* using different Ad:erythrocyte ratios. After incubation of erythrocytes and AdGL, the supernatant and the erythrocyte pellet were separated by centrifugation, and the Ad5 genomes in each fraction were detected by real-time PCR (**Figure 13**). The theoretical distribution of Ad5 particles in each fraction assuming no erythrocyte binding (considering the relative volume of the fractions in each condition) was used to calculate the fold-clearance in the supernatant. In the first condition we incubated $1x10^9$ vp of AdGL with $1x10^7$ erythrocytes in 1ml of PBS (100 Ad particles per erythrocyte). After centrifugation, the supernatant represented the 99% of the total volume, whereas the cell pellet the 1%. Most of the Ad particles were found in the supernatant (98.5% in the supernatant vs 1.5% in the erythrocyte fraction), indicating that in these conditions erythrocytes were not able to efficiently pull-down the viral particles. A second condition was

analyzed in which $2x10^8$ vp of AdGL were incubated with $5x10^9$ erythrocytes in 1 mL of PBS (0.04 Ad particles per erythrocyte). These are clinically relevant conditions (for 5 L of blood it would correspond to an intravenous dose of $1x10^{12}$ viral particles) and as such have been analyzed previously (Carlisle et al., 2009). Owing to the high erythrocyte concentration, the cell pellet occupied the 40% of the total volume. In this case, an 88% of the viral input was in the erythrocyte fraction, and only a 12% was found in the supernatant, confirming the published results (Carlisle et al., 2009). This corresponds to an 8-fold clearance of the adenovirus content in the supernatant or liquid fraction, indicating that there was an efficient pulldown of Ad particles to the erythrocyte pellet. As only approximately a 10% of the Ad input was found free, we next reduced the Ad dose by a further 10% to check if all the viral particles could be bound to erythrocytes in such conditions. Accordingly, $1.8x10^8$ vp of AdGL were incubated with $5x10^9$ erythrocytes in 1ml of PBS (0.036 Ad particles per erythrocyte). Indeed, the 99.6% of the viral input was recovered in the erythrocyte fraction, corresponding to a 95-fold clearance of the adenovirus content in the liquid fraction. These data indicate that erythrocytes bind and pull down Ad5 particles. Nonetheless, taking into account the MOIs (multiplicity of infection) used, the erythrocyte capacity to bind adenovirus via CAR is limited since approximately 28 erythrocytes are needed to efficiently pull down one Ad5 particle. These results match with previous studies that show relatively low levels of CAR on human erythrocytes (Seiradake et al., 2009). However, using physiological erythrocyte concentrations and a clinically relevant adenovirus dose (e.g. $1x10^{12}$ vp per patient), 88% of the viral input dose would bind to erythrocytes.

1.2. COMPETITIVE INHIBITION OF CAR TO BLOCK ADENOVIRUS BINDING

To prove that the interaction is CAR-mediated and not simply a nonspecific binding, we used an anti-CAR antibody to block the interaction. AdGL and human erythrocytes pre-incubated or not with anti-CAR antibody were incubated at an Ad:erythrocyte ratio of 0.04 as described above. In the absence of anti-CAR antibody, only a 4.2% of the viral input was found free, and considering that the supernatant represented the 55% of the total volume, this represents a 13-fold clearance of the viral content in this fraction (**Figure 14**). In contrast, when human erythrocytes were pre-incubated with anti-CAR, the 33% of the viral dose was found free in the supernatant fraction, representing only a 1.6-fold clearance. Although the blocking of CAR was not complete, the Ad5 binding to human erythrocytes was remarkably reduced by the anti-CAR antibody, indicating that CAR is responsible for the pulldown of the virus.

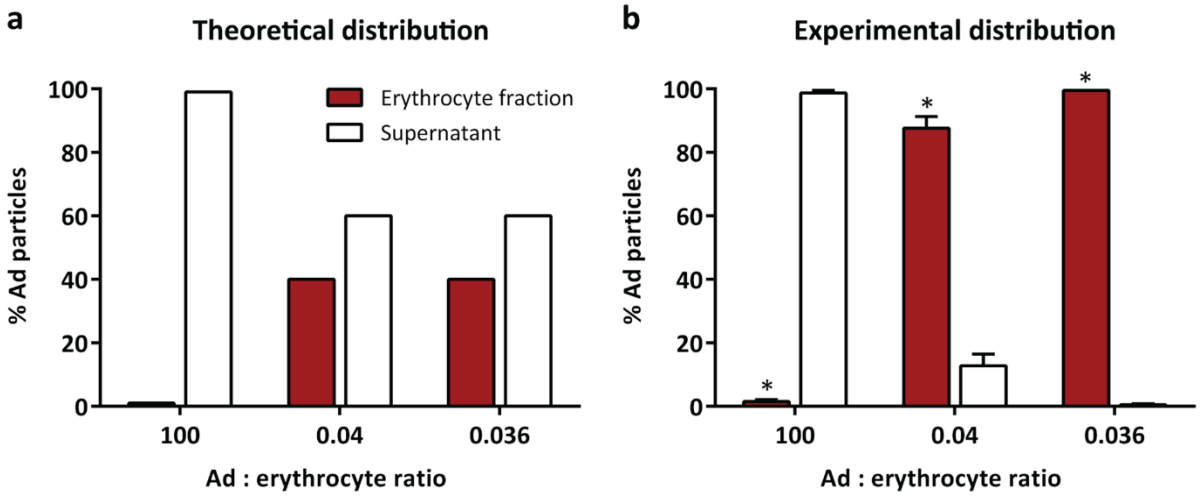

Figure 13. Detection of Ad5 binding to human erythrocytes. Human erythrocytes were incubated with AdGL at the indicated proportions of virus particle per erythrocyte for 30 min at 37 ºC. Samples were centrifuged to separate the liquid and cell fractions, and Ad5 detection was performed by quantitative real-time PCR. (a) Theoretical distribution of Ad5 in each fraction assuming no erythrocyte binding, and considering the relative volume of each fraction. (b) Experimental distribution obtained in each condition. Data are represented as % of Ad particles recovered in each fraction. Mean values + SD are shown. *, significant ($p<0.05$) by two-tailed unpaired Student's t-test compared with Supernatant.

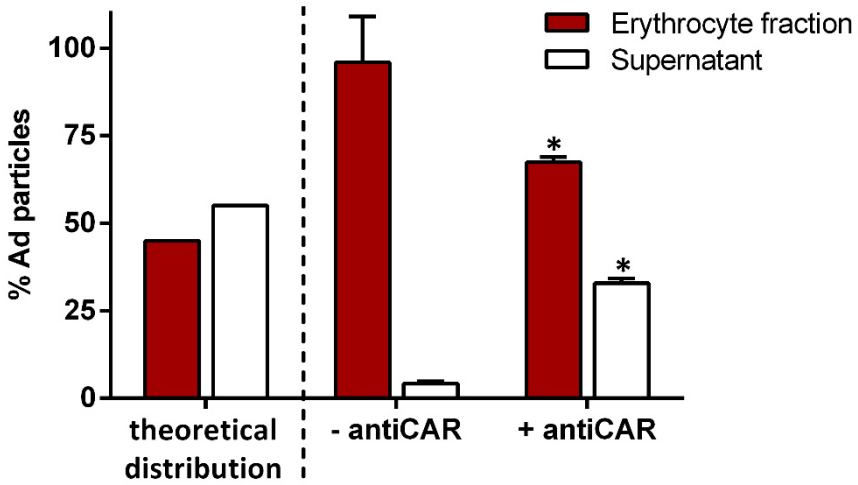

Figure 14. CAR-blocking assay to inhibit Ad5 binding to erythrocytes. Human erythrocytes were preincubated or not with anti-CAR antibody (RmcB) and then incubated with AdGL. After centrifugation, Ad5 detection in the liquid and cell fractions was performed by quantitative real-time PCR. The theoretical distribution of Ad5 in each fraction assuming no erythrocyte binding, and considering the relative volume of each fraction is shown in the left side of the graph. Data are represented as % of Ad particles recovered in each fraction. Mean values + SD are shown. *, significant ($p<0.05$) by two-tailed unpaired Student's t-test compared with the absence of anti-CAR.

1.3. *IN VITRO* TRANSDUCTION OF ADENOVIRUS IN PRESENCE OF HUMAN ERYTHROCYTES

To analyze whether erythrocyte binding inactivated Ad5 *in vitro*, we analyzed the infectivity of AdGL in A549 cells in the presence or absence of human erythrocytes. To achieve complete binding, the Ad:erythrocyte ratio used was 0.036. After incubation, the erythrocyte pellet was separated and used to infect A549 cells. The erythrocyte-bound Ad5 was kept in contact with the tumor cells for 48 h before luciferase expression was measured. Erythrocytes alone with A549 cells as well as erythrocytes with AdGL in the absence of A549 cells were included as negative conditions. Contrary to what was observed in previous studies (Carlisle et al., 2009), AdGL displayed the same levels of transduction regardless of the presence of human erythrocytes (**Figure 15**), indicating that although Ad5 efficiently binds erythrocytes via CAR, this binding is reversible and in the long term it does not inhibit the infection of tumor cells. The discrepancies between our results and the previously published work will be commented in the discussion chapter.

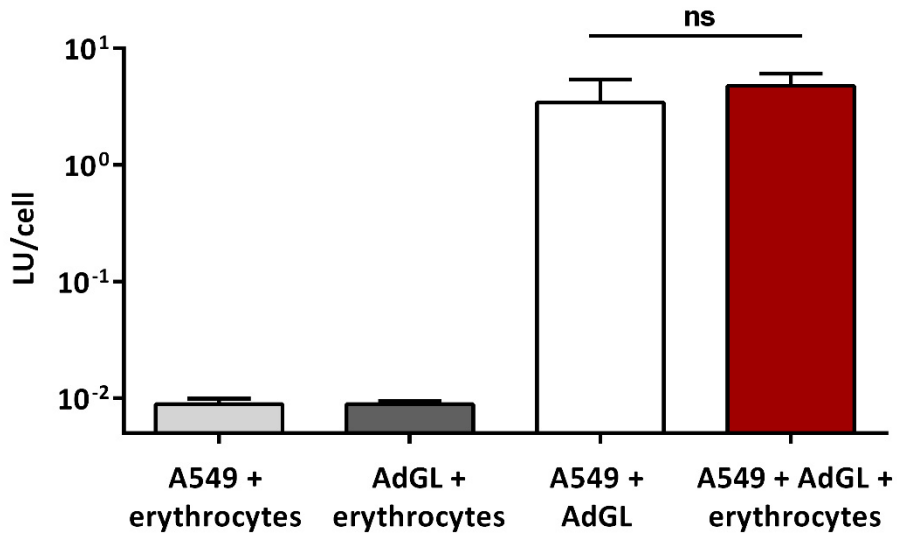

Figure 15. Ad5 transduction of tumor cells in the absence or presence of human erythrocytes. AdGL was incubated with or without human erythrocytes (0.036 vp per cell), and after centrifugation, the cell fraction was used to infect A549 cells. At 48 h after infection, cell transduction was analyzed by luciferase expression. Erythrocytes alone in A549 cells and erythrocytes with AdGL in the absence of A549 cells were used as negative controls. Mean + SD. ns, nonsignificant ($p<0.05$) by two-tailed unpaired Student's t-test.

1.4. BLOOD PERSISTENCE OF HUMAN ERYTRHOCYTES AFTER INTRAVENOUS ADMINISTRATION IN NUDE MICE

Not having observed an inhibition of Ad5 infectivity due to erythrocyte binding *in vitro*, we next wanted to address the influence of human erythrocytes on the systemic transduction of Ad5. This was tested in mice transplanted with human erythrocytes and therefore, we first wanted to analyze the blood persistence of human erythrocytes in the recipient mice after the intravenous administration. $8x10^8$ human erythrocytes were labelled with CFSE (carboxyfluorescein succinimidyl ester) and intravenously injected in nude mice. Blood samples were collected from the tail vein at the indicated time points to detect the CFSE-labeled human erythrocytes by flow cytometry. As shown in **Figure 16**, human erythrocytes are rapidly cleared from mouse circulation, as more than the 50% of the injected dose is eliminated 7 minutes after the transference. However, this erythrocyte clearance was relatively slow when compared to our historical data of Ad5 clearance in nude mice (Gimenez-Alejandre et al., 2008). As the erythrocytes stay much longer than adenovirus particles in circulation, we believe this model should be sensitive to measure the effect of human erythrocytes in the systemic transduction of Ad5.

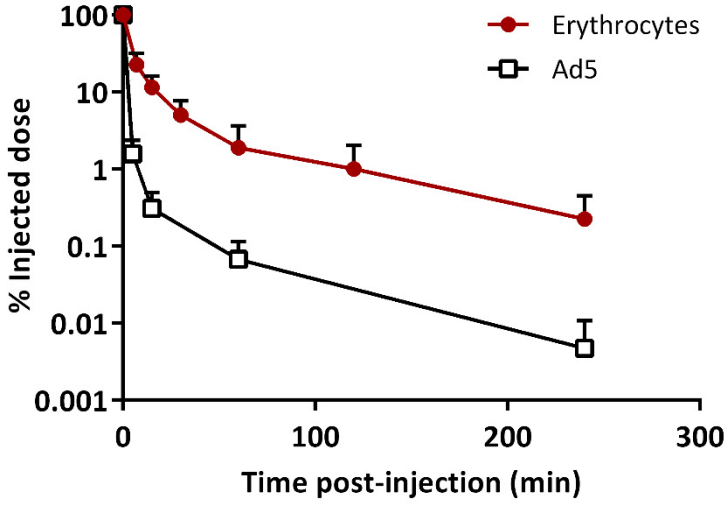

Figure 16. Blood persistence of human erythrocytes after intravenous injection in nude mice. Nude mice were intravenously injected with $8x10^8$ CFSE-labeled human erythrocytes. At the indicated time points, blood samples were collected and human erythrocytes were detected by flow cytometry (n = 3 mice). Results are plotted including our previous data of Ad5 persistence in nude mice (Gimenez-Alejandre et al., 2008). Mean + SEM is shown.

1.5. SYSTEMIC TRANSDUCTION IN THE PRESENCE AND ABSENCE OF HUMAN ERYTHROCYTES

Nude mice bearing A549 xenograft tumors were intravenously injected with $5x10^{10}$ vp of AdGL alone or previously incubated with $8x10^{8}$ human erythrocytes. This MOI of 62.5 Ad particles per erythrocyte was used to have enough adenovirus to bypass Kupffer cells, a barrier not present in previous *in vitro* experiments. At 3 days after virus administration, mice were killed and livers and tumors were harvested for *in vivo* bioluminescent imaging (IVIS) and Ad genome detection by real-time PCR. Luciferase expression analysis showed no significant differences in liver and tumor transduction between AdGL alone and AdGL + erythrocytes (**Figure 17a**). The adenovirus vector was able to transduce efficiently the liver and, to a lesser extent, the tumors regardless of previous incubation with human erythrocytes. Accordingly, no significant differences were found in the presence of adenovirus genomes in liver and tumors in both conditions (**Figure 17b**), corroborating that human erythrocytes did not prevent extravasation or organ transduction. These results are also contrary to the previously published work where the systemic infection and the presence of Ad genomes were significantly reduced due to erythrocyte binding (Carlisle et al., 2009). These differences will also be discussed further in the discussion chapter.

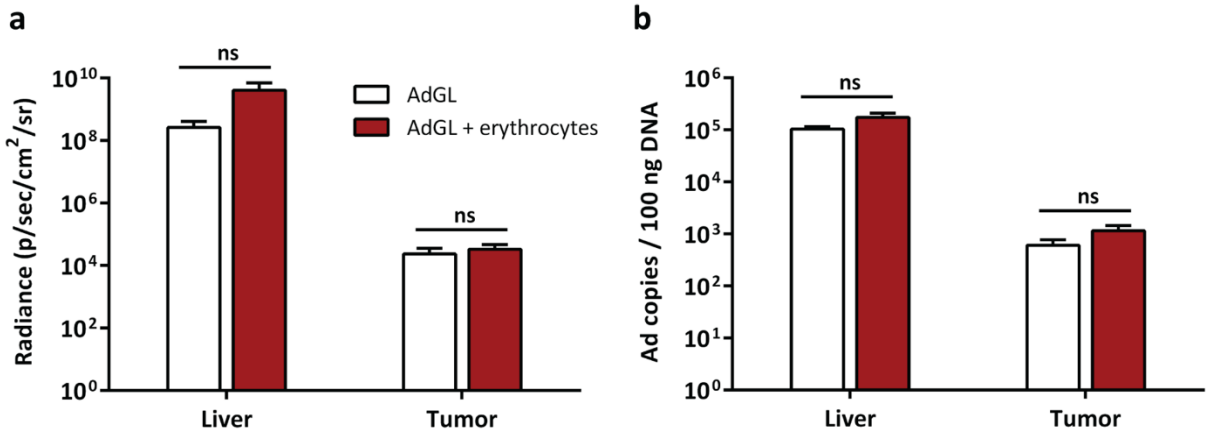

Figure 17. Ad5 biodistribution in the presence or absence of human erythrocytes. Nude mice bearing subcutaneous A549 tumors were injected intravenously with $5x10^{10}$ vp of AdGL previously incubated with or without $8x10^{8}$ human erythrocytes. (a) After 3 days, liver and tumors were collected and luciferase activity was analyzed by bioluminescence imaging. (b) Organs were frozen for subsequent Ad5 genome detection by real-time PCR. Livers n = 5 and tumors n = 8-10. Mean values + SEM are depicted. ns, nonsignificant ($p<0.05$) by two-tailed unpaired Students t-test.

Altogether, our results suggest that human erythrocytes bind Ad5 via CAR, but the viral particle is not internalized and is eventually released to infect other CAR-expressing cells. We therefore believe that human erythrocytes do not represent a major obstacle for systemic delivery of adenoviruses and consider that efforts should be focused on barriers such as liver sequestration and neutralizing antibodies.

2. GENERATION OF AN ALBUMIN-BINDING ADENOVIRUS TO EVADE NEUTRALIZATION BY ANTIBODIES

The results of this chapter generated the manuscript “Albumin-binding adenoviruses circumvent pre-existing neutralizing antibodies upon systemic delivery” and the patent “Adenovirus comprising an albumin-binding moiety” (PCT/EP2015/059593), both enclosed in the annex section.

2.1. INSERTION OF ALBUMIN-BINDING MOIETIES IN ADENOVIRUS CAPSID

Although albumin binding has been generally used as a method to increase the plasma half-life of drugs, in this work we aimed to use it as a mechanism to protect the adenovirus against antibody-mediated neutralization. The modifications designed to achieve albumin binding were incorporated into the oncolytic adenovirus ICOVIR15 (Rojas et al., 2010) and into the non-replicative reporter vector AdGLRGD (described in Materials and methods section 3). The non-replicative vectors were used to determine the biodistribution of the novel modifications, and the oncolytic adenoviruses for assessing the advantages in antitumor activity.

Among the different strategies to achieve albumin binding, we used the genetic insertion of small peptide motifs that display high affinity for albumin. Three different albumin-binding moieties were tested: the albumin-binding domain 3 (ABD) from the protein G of Streptococcus, and two albumin-binding peptides named SA21 and RB5. The amino acid sequence of these motifs is shown in **Figure 18**. The ABD is the most widely used strategy and has been successfully fused to protein-based drugs, achieving remarkable half-life extensions (Andersen et al., 2011; Guo et al., 2016; Li et al., 2016; Schlapschy et al., 2007; Stork et al., 2007). ABD binds human and mouse albumin but not bovine albumin, a convenient species-specificity in case binding impairs virus replication. However, the insertion of foreign

sequences in adenovirus capsid has its limitations. The length of the domain (46 aa) and its strong secondary structure (3 α-helix) might compromise the viability of the virus. SA-21 and RB-5 are peptides developed by phage display to selectively bind albumin from multiple species with high affinity (Dennis et al., 2002). The advantage over the ABD is their short length (18 and 20 aa respectively) and the fact that they are unstructured. While Dennis *et al*. studied the SA-21 peptide in depth, the effects of RB-5 fusion were not reported. However, this peptide was also selected for this work due to its inability to bind BSA.

ABD (46 aa): LAEAKVLANRELDKYGVSDYYKNLINNAKTVEGVKALIDEILAALP

SA21 (18 aa): RLIEDICLPRWGCLWEDD

RB5 (20 aa): QWHMEDICLPQWGCLWGDVL

Figure 18. Amino acid sequence and length of the albumin-binding motifs tested in this work.

We hypothesized that in order to prevent binding of NAbs, the virus capsid needs to be efficiently coated with albumin. In order to maximize the number of albumin molecules bound to the virus, the hexon protein was chosen to insert these motifs, as it is the main and most abundant protein of the capsid. The hypervariable regions (HVRs) were selected as the insertion point because the albumin-binding motifs need to be exposed to the surface. In addition, these HVRs are the main target of anti-Ad5 NAbs. Two different locations were tested, one in the HVR1 and the other in the HVR5, substituting the wild-type loops as indicated in **Figure 19**. To confer flexibility, the motifs were flanked by two flexible GSGS linkers.

HVR1 loop: 132-CEWDEAATALEINLEEEDDDNEDEVDEQAEQQKTHVF-170

HVR5 loop: 267-STTEAAAGNGDNLTPK-284

Figure 19. Substitution of the hypervariable region loops by the albumin-binding motifs. The amino acid sequence of the HVR1 and HVR5 of Ad5 hexon protein is shown. The residues that were replaced by the albumin-binding motifs are shown in red.

Plasmids containing the genomes of the modified adenoviruses were generated by homologous recombination in bacteria and then transfected into HEK293 cells for virus generation. However, the transfection of these plasmids did not generate any virus and after

five independent transfections, it was concluded that the adenoviruses harboring these modifications were not viable. A second insertion strategy was tested in which the domains with the GSGS linkers were inserted in the middle of the loops without deleting any residue from the wt HVRs. The insertion point in the HVR1 was after the D150 aa and in the HVR5 after the A274 aa (**Figure 20**). These new constructions were transfected but only the plasmids that contained the ABD insertion generated viable viruses. After five more unsuccessful attempts of generating the viruses containing the SA21 and RB5 insertions, these peptides were discarded and the project was continued only with the ABD. The modified oncolytic adenoviruses were named ICOVIR15-H1-ABD and ICOVIR15-H5-ABD, and the non-replicative modified vectors AdGLRGD-H1-ABD and AdGLRGD-H5-ABD. A schematic representation of their genome is shown in **Figure 20**.

2.2. COMPARATIVE STUDY OF ABD INSERTION IN HVR1 AND IN HVR5

Once the viruses were generated, amplified, and purified, a comparative study was performed to characterize the effects of the ABD insertion in the two different locations. The capacity to bind albumin, the viral production, the infectivity, and the ability to evade NAbs were compared.

2.2.1. Albumin-binding capacity of ABD-modified adenoviruses

The first feature to analyze was the functionality of the ABD in both locations of the viral capsid. Detection of binding to human (HSA), mouse (MSA), and bovine serum albumin (BSA) was performed by ELISA using commercially available purified albumins. ICOVIR15-H1-ABD and ICOVIR15-H5-ABD showed positive binding in HSA- and MSA-coated wells (**Figure 21**). However, a significantly higher signal was obtained with ICOVIR15-H1-ABD than with ICOVIR15-H5-ABD in both HSA and MSA. This could mean that although the domain is functional in both viruses, the affinity for albumin of the ABD is higher when inserted in the HVR1. In agreement with the binding pattern of ABD to albumin of different species (Falkenberg et al., 1992; Nygren et al., 1990), none of the ABD-modified adenoviruses bound to BSA. As expected, the parental virus ICOVIR15 did not bind to any albumin.

2.2.2. Viral production assay

To analyze if the insertion of the ABD has some detrimental effect on the viral production yield, the cell extracts of HEK293 infected with AdGLRGD, AdGLRGD-H1-ABD, or AdGLRGD-H5-ABD were tittered at different time points post-infection (0, 24, 48, and 72 hours). Whereas

no differences were observed between AdGLRGD and AdGLRGD-H5-ABD at any time-point, the AdGLRGD-H1-ABD suffered a slight loss of total production yield compared with both vectors at 48 and 72 hours post-infection (**Figure 22**). The production loss was 3-fold at 48 h and 5.5-fold at 72 h compared to AdGLRGD, and 2-fold at 48 h and 3.5-fold at 72 h compared to AdGLRGD-H5-ABD. This indicates that while the ABD insertion in the HVR5 does not alter the viral production yields, the same insertion in the HVR1 causes a certain loss on the productivity of the virus.

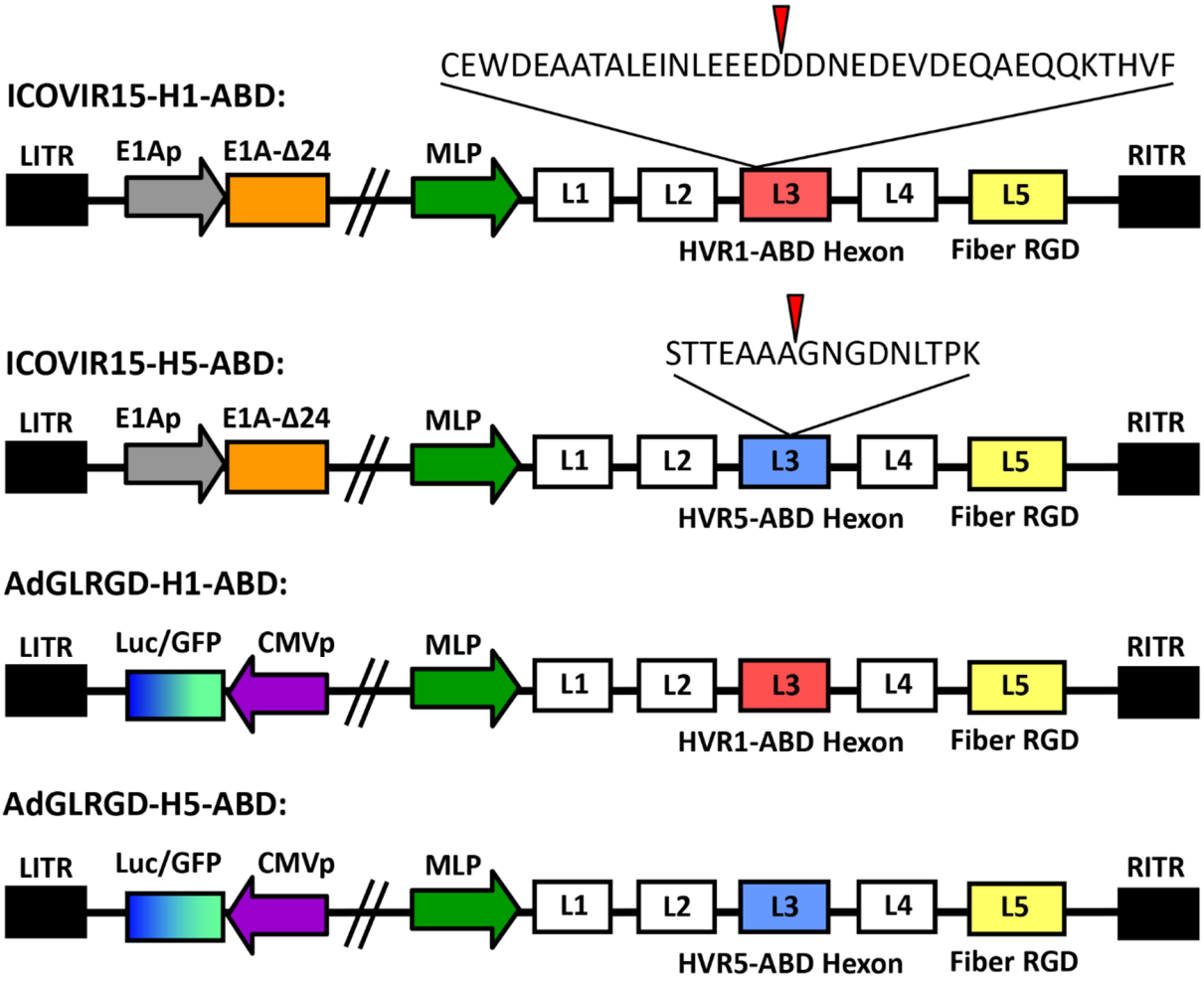

Figure 20. Albumin-binding adenoviruses generated in this study. Schematic representation of the genomes of the different adenoviruses harboring the ABD insertion. The main genetic modifications of each virus are indicated. ICOVIR15 oncolytic backbone contains the modified E1A promoter (including four E2F boxes and one Sp1 box) and the truncated E1A-Δ24 protein to confer selectivity for tumor cells, and the RGD motif inserted in the HI-loop of the fiber knob to enhance infection of tumor cells. AdGLRGD is an E1-deleted vector expressing a GFP-luciferase fusion protein under the control of a CMV promoter, and also contains the RGD motif in the HI-loop of the fiber knob. The ABD was inserted in the hexon HVR1 generating ICOVIR15-H1-ABD and AdGLRGD-H1-ABD, or in the HVR5 generating ICOVIR15-H5-ABD and AdGLRGD-H5-ABD. The insertion point of the ABD in the HVR1 and HVR5 loops are indicated with a red arrow.

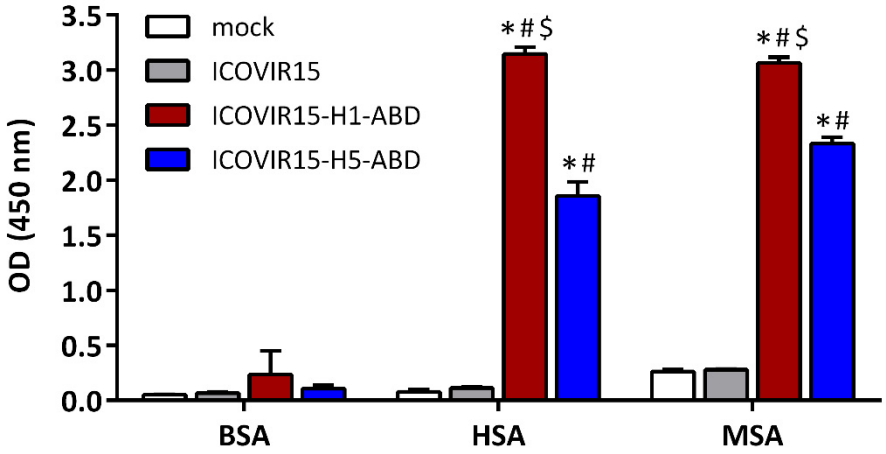

Figure 21. Analysis of albumin binding by ICOVIR15-H1-ABD and ICOVIR15-H5-ABD. ELISA plates were coated with purified bovine (BSA), human (HSA), or mouse serum albumin (MSA). Binding of ICOVIR15, ICOVIR15-H1-ABD, or ICOVIR15-H5-ABD to albumin-coated wells was detected with anti-hexon antibody and peroxidase-labeled secondary antibody by colorimetric analysis. A mock group with no virus was included as negative control. Mean + SD is plotted. *, significant ($p<0.05$) by two-tailed unpaired Student's t-test compared with mock. #, significant ($p<0.05$) by two-tailed unpaired Student's t-test compared with ICOVIR15. $, significant ($p<0.05$) by two-tailed unpaired Student's t-test compared with ICOVIR15-H5-ABD.

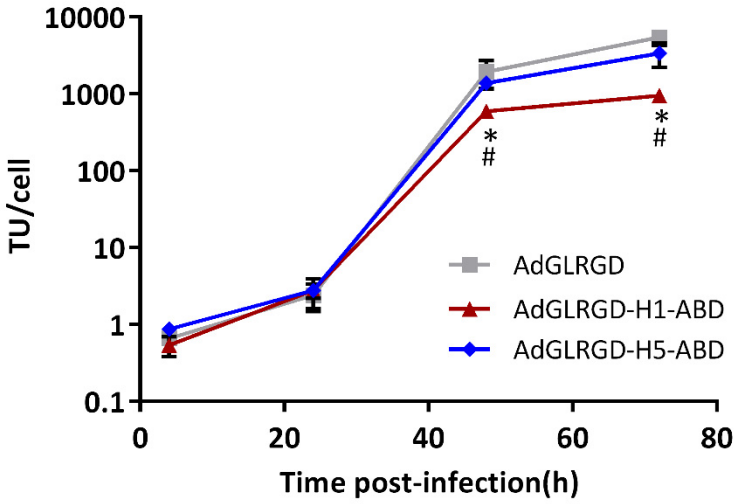

Figure 22. Viral production of the ABD-modified vectors in HEK293 cells. Cell monolayers were infected at 100 vp/cell to achieve a 100% of infection. At the indicated time points (4, 24, 48, and 72 hours post-infection), cell extracts were collected and virus production was determined using an anti-hexon staining method. Mean ± SD is represented. *, significant ($p<0.05$) by two-tailed unpaired Student's t-test compared with AdGLRGD. #, significant ($p<0.05$) by two-tailed unpaired Student's t-test compared with AdGLRGD-H5-ABD.

2.2.3. Infectivity in tumor cell lines in presence or absence of HSA

To study not only the effect of the ABD insertion but also the effect of albumin binding in the infectivity of the viruses, the transduction of the reporter vectors was analyzed in presence and absence of albumin in a panel of tumor cell lines. The physiological concentration of HSA (50 mg/ml) is so high that it was unfeasible to use it for *in vitro* studies. For this reason, a more cost-effective concentration of 1 mg/ml was used in most experiments unless indicated otherwise. In the absence of albumin the three vectors showed similar levels of transduction, indicating that the ABD insertion *per se* does not interfere in the infectivity of the viruses (**Figure 23**). In general terms, addition of albumin caused a reduction in the transduction ability of all vectors. However, whereas the non-modified AdGLRGD only suffered a 2-fold loss of transduction in most of the cell lines tested, the ABD-modified adenoviruses were more notably affected. Moreover, the loss of infectivity of AdGLRGD-H1-ABD due to albumin binding seemed to be higher than that of AdGLRGD-H5-ABD (20-fold vs 13-fold in A549, 10-fold vs 8-fold in Sk-mel28, 10-fold vs 5-fold in NP-9, 6-fold vs 4-fold in B16, and 3-fold vs 2.5-fold in B16-CAR respectively). If albumin binding to the virus capsid interferes in the transduction of the viruses, the lower affinity for albumin of the HVR5-ABD construction observed in **Figure 21** could explain these differences.

2.2.4. Infectivity in presence or absence of FX and HSA

Our group previously demonstrated that the interaction between Ad5 and coagulation factor X (FX) not only plays a key role in the transduction of hepatocytes, but also in the transduction of tumor cells (Gimenez-Alejandre et al., 2008). Since FX binds to the adenovirus hexon HVRs, the binding of FX to the ABD-modified adenoviruses was analyzed in the presence of albumin. The study by Gimenez-Alejandre *et al.* demonstrated that FX increases the infectivity to tumor cells *in vitro* and therefore, this was taken as a sign of FX binding. The infectivity of AdGLRGD, AdGLRGD-H1-ABD, and AdGLRGD-H5-ABD was determined in the presence and absence of FX (at the physiological concentration of 12.25 µg/ml) combined with the presence and absence of HSA (1 mg/ml). A431 cells were used in this study as they are resistant to Ad5 infection (they express low levels of CAR and integrins) and hence, the effect of FX on transduction is more noticeable. Indeed, addition of FX significantly enhanced the transduction of all viruses in the absence of albumin (14-fold, 6.5-fold, and 8-fold for AdGLRGD, AdGLRGD-H1-ABD, and AdGLRGD-H5-ABD respectively) (**Figure 24**). Surprisingly, the transduction of AdGLRGD was enhanced in the presence of albumin and absence of FX (albeit lower than with FX only), contrary to what was observed in the other tumor cell lines

analyzed in section 2.2.4. On the contrary, the ABD-modified adenoviruses suffered again a reduction in transduction due to HSA presence, and this reduction was again higher for the HVR1-ABD virus (17-fold vs 10-fold). In the condition where both FX and HSA were present, the transduction of the non-modified virus increased again to the same levels as with FX only. Interestingly, in this condition the ABD-modified vectors behaved in completely opposed manners. Whereas the transduction levels of AdGLRGD-H1-ABD remained as low as with only HSA, the transduction of AdGLRGD-H5-ABD was enhanced to almost the same levels as with FX only. This suggests that when both FX and HSA are present, the HVR1-modified virus is mainly coated with HSA, whereas the virus with the ABD in the HVR5 is mainly coated with FX. This result supports the hypothesis of the lower affinity for albumin of AdGLRGD-H5-ABD.

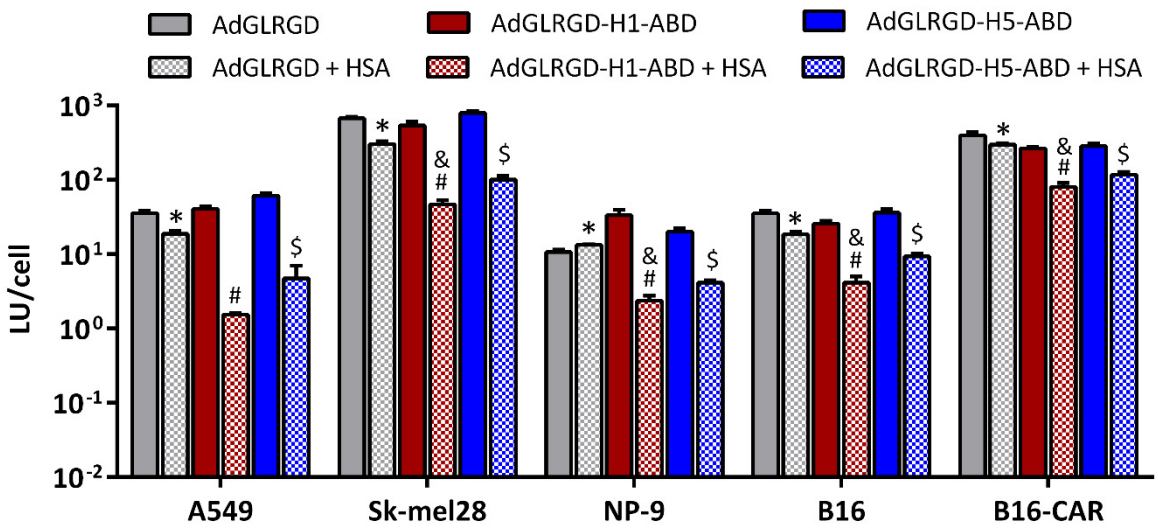

Figure 23. Infectivity of the ABD-modified vectors in tumor cells in the presence or absence HSA. A panel of tumor cell lines was infected with the luciferase-expressing vectors (100 vp/cell for A549, 400 vp/cell for B16-CAR, 600 vp/cell for SK-mel28 and NP-9, and 1200 vp/cell for B16) in the presence or absence of HSA. At 36 hours post-infection, cell transduction was analyzed by luciferase expression. Mean + SD is shown. *, significant ($p<0.05$) by two-tailed unpaired Student's t-test compared with AdGLRGD. #, significant ($p<0.05$) by two-tailed unpaired Student's t-test compared with AdGLRGD-H1-ABD. $, significant ($p<0.05$) by two-tailed unpaired Student's t-test compared with AdGLRGD-H5-ABD. &, significant ($p<0.05$) by two-tailed unpaired Student's t-test compared with AdGLRGD-H5-ABD + HSA.

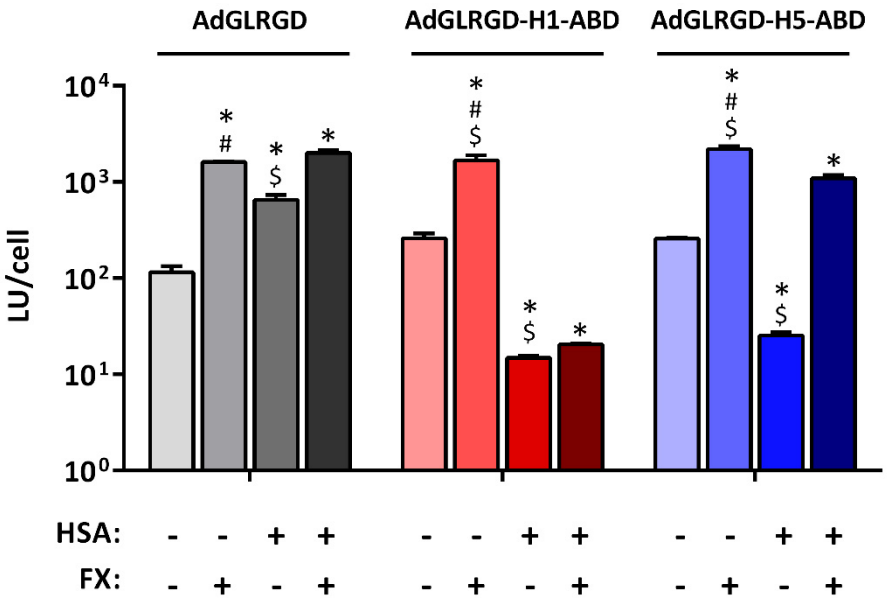

Figure 24. Infectivity of the ABD-modified adenoviruses in the presence or absence of FX and HSA. A431 cells were infected with 1000 vp/cell of the luciferase-expressing vectors in normal medium, in medium containing either FX (12.25 µg/ml) or HSA (1 mg/ml), or in medium containing both FX and HSA. At 24 hours post-infection cell transduction was analyzed by luciferase expression. Mean values + SD are shown. *, significant ($p<0.05$) by two-tailed unpaired Student's t-test compared with -HSA -FX. #, significant ($p<0.05$) by two-tailed unpaired Student's t-test compared with +HSA -FX. $, significant ($p<0.05$) by two-tailed unpaired Student's t-test compared with +HSA +FX.

2.2.5. Infectivity in presence of neutralizing antibodies

Having demonstrated the ability of the ABD-modified adenoviruses to bind albumin, we then evaluated if this albumin coating could protect the viruses from NAbs *in vitro*. For these studies, the commercial antibody Ab6982 was used. This is a polyclonal neutralizing antibody against Ad5, which targets several capsid proteins including hexon, fiber, and penton. AdGLRGD, AdGLRGD-H1-ABD, or AdGLRGD-H5-ABD in absence or presence of HSA were incubated with serial dilutions of Ab6982, and then used to infect 293 and Sk-mel28 cells. The transduction efficiency in each dilution was calculated as percentage of transduction compared to a control without Ab6982, which was taken as the 100% infection value for each vector. Very similar results were obtained in both cell lines (**Figure 25**). Ab6982 neutralizes the viruses in a dose-dependent manner, and high transduction values are only achieved when the antibody is highly diluted. Addition of albumin did not alter the transduction of the non-modified AdGLRGD, which was efficiently neutralized in both conditions. On the contrary, when albumin was present the transduction of AdGLRGD-H1-ABD was remarkably enhanced,

reaching high percentages of transduction at low antibody dilutions. However, this albumin-mediated protection was not observed with AdGLRGD-H5-ABD. Only a minor advantage can be seen in presence of albumin at certain points with high antibody dilutions, but this gain is minimal compared to the HVR1-modified vector. These findings indicate that albumin is able to protect the virus against neutralization when the ABD is located in the HVR1 but not in the HVR5. These results indicate that owing to the low affinity of albumin to the ABD in the HVR5, albumin is displaced from the viral capsid by other molecules such as FX or NAbs. Even though the loss of production and infectivity is higher with the HVR1-ABD construction, the protection provided by albumin in the presence of NAbs was considered of great importance. For this reason, the construction HVR5-ABD was discarded and the project was continued only with the viruses with the ABD insertion in the HVR1. Henceforth, the modified viruses will be named ICOVIR15-ABD (for the oncolytic version) and AdGLRGD-ABD (for the non-replicative vector).

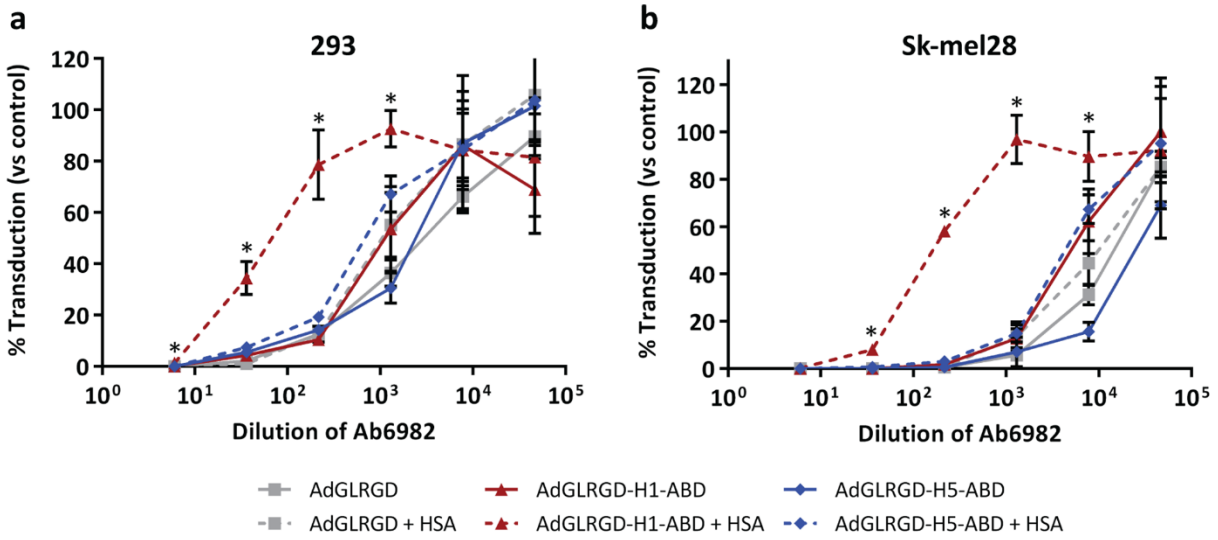

Figure 25. Comparative *in vitro* transduction of ABD-modified vectors in presence of Ab6982. Adenovirus vectors, in the presence or absence of HSA, were incubated with serial dilutions of the polyclonal neutralizing antibody Ab6982. After 1 hour incubation, the viruses were used to infect (a) HEK293 cells or (b) Sk-mel28 cells at 10 vp/cell or 40 vp/cell respectively. Luciferase expression was analyzed 24 hours after the infection. A control without Ab6982 was included to obtain the 100 % infection value. Results are represented as % transduction versus the 100 % infection control. Mean values ± SD are depicted. *, significant ($p<0.05$) by two-tailed unpaired Student's t-test compared with all groups.

2.3. CHARACTERIZATION OF THE ABD INSERTION IN THE ABSENCE OF NEUTRALIZING ANTIBODIES

After a first comparison of the two insertion sites, a deeper study of the HVR1-ABD construction is now presented. This first section studies the impact of the ABD insertion on the adenovirus, without considering the detrimental effects of the NAbs on the bioactivity of the virus. *In vitro* experiments were performed without NAbs, and *in vivo* studies were performed using immunodeficient mice or naïve immunocompetent mice.

2.3.1. Albumin binding study of the ABD-modified adenovirus

2.3.1.1. Binding to purified albumin and albumin present in serum

Albeit the binding to HSA and MSA has already been demonstrated, a more thorough study was performed only with the HVR1-ABD construction. The binding to purified HSA and BSA was analyzed again by ELISA in a dose-dependent manner using different amounts of virus (**Figure 26**). Positive signal was obtained when adding ICOVIR15-ABD to HSA-coated wells and the intensity of the signal increased with the amount of virus used. When BSA was used instead of HSA, no signal was observed regardless of the amount of virus added. The parental virus ICOVIR15 did not bind to HSA or BSA, confirming the previously obtained results.

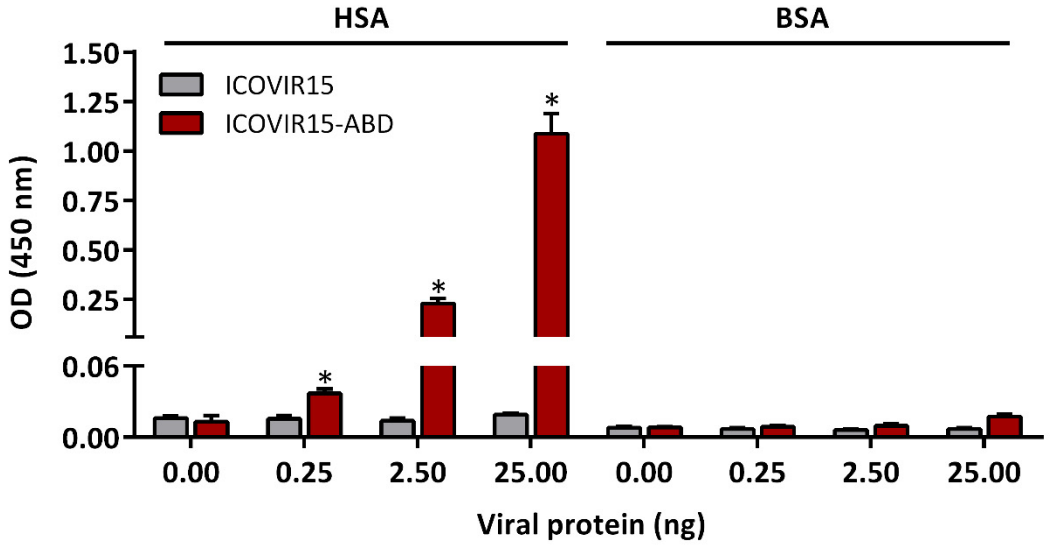

Figure 26. Analysis of ICOVIR15-ABD binding to purified HSA and BSA. ELISA plates were coated with purified BSA, or HSA. Binding of ICOVIR15 or ICOVIR15-ABD was tested using three different amounts of total viral protein (0.25, 2.5, and 25 ng). Adenovirus binding to albumin-coated wells was detected after incubation with anti-hexon antibody and peroxidase-labeled secondary antibody by colorimetric analysis. Mean + SD is plotted. *, significant ($p<0.05$) by two-tailed unpaired Student's t-test compared with ICOVIR15.

To obtain more insight on the ability of the virus to bind albumin *in vivo*, we investigated if ICOVIR15-ABD could also bind to the albumin present in serum. This study was also performed by ELISA, coating the wells with diluted human or mouse serum. As shown in **Figure 27**, ICOVIR15-ABD was able to bind to albumin in both human and mouse serum in a dose-dependent manner, contrary to the non-modified virus which did not show any binding.

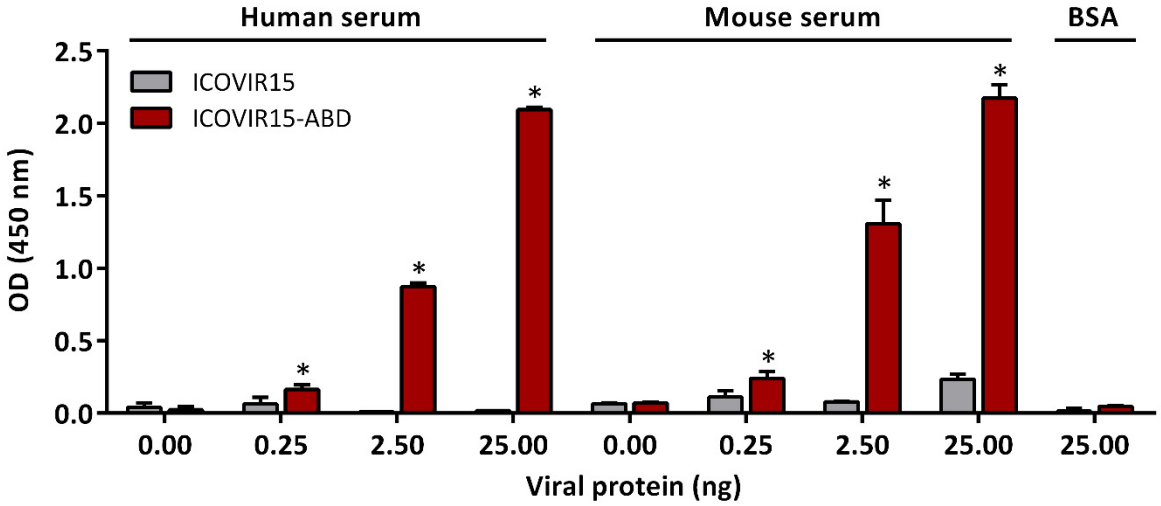

Figure 27. Analysis of ICOVIR15-ABD binding to albumin present in human and mouse serum. ELISA plates were coated with human or mouse serum previously diluted 25-fold. Adenovirus binding was tested using three different amounts of total viral protein (0.25, 2.5, and 25 ng). Adenovirus detection was performed using an anti-hexon antibody and peroxidase-labeled secondary antibody by colorimetric analysis. BSA-coated wells were used as negative control. Mean + SD is plotted. *, significant ($p<0.05$) by two-tailed unpaired Student's t-test compared with ICOVIR15.

2.3.1.2. Analysis of albumin binding by electron microscopy techniques

In collaboration with Carmen San Martin from the *Centro Nacional de Biotecnologia* (CNB-CSIC) in Madrid, we further studied the interaction between the viral capsid and albumin using electron microscopy techniques. First, we analyzed the binding of ICOVIR15-ABD to HSA by immunoelectron microscopy. After incubating the viruses with albumin, HSA was stained using a gold-labeled secondary antibody, which can be directly visualized using transmission electron microscopy (TEM). Analysis of ICOVIR15-ABD revealed specific HSA staining, as black dots corresponding to the gold-labeled antibody can be observed surrounding the viral capsids (**Figure 28**). In contrast, no specific staining was observed in ICOVIR15 capsids as expected.

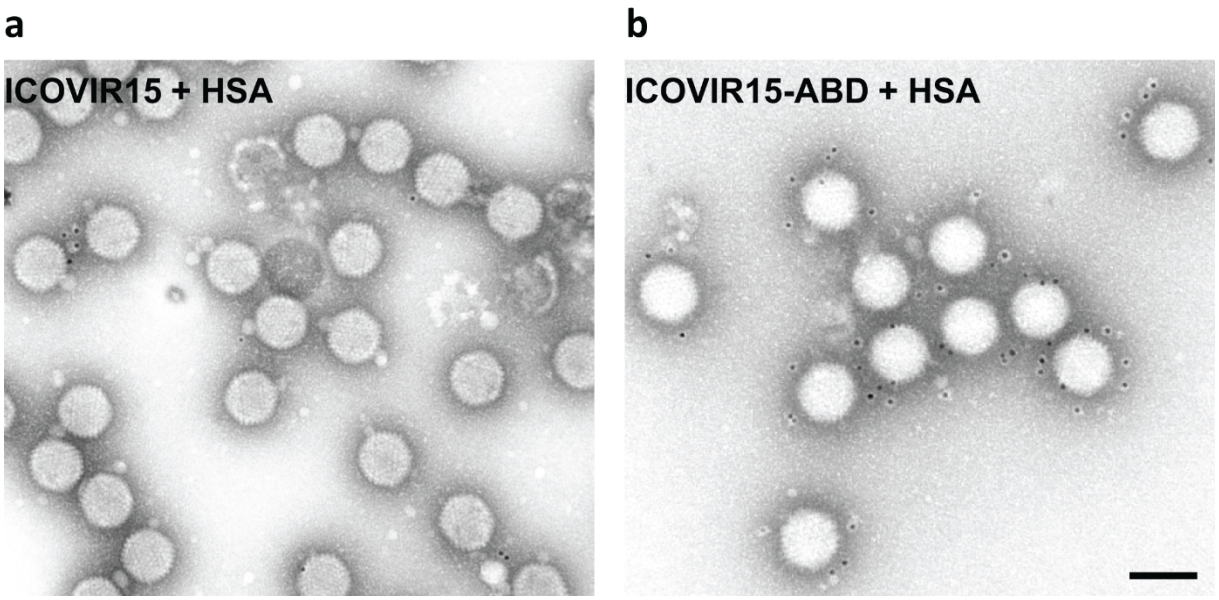

Figure 28. Detection of albumin binding by immunoelectron microscopy. (a) ICOVIR15 or (b) ICOVIR15-ABD were incubated with HSA, and then labeled with anti-HSA antibody and 10 nm gold particle-conjugated secondary antibody. Black dots indicate positive HSA staining. Scale bar, 100 nm.

Second, the interaction between HSA and the capsid was studied using cryo-electron microscopy. A map showing the HVR1, ABD and putative HSA was generated by three dimensional reconstruction. A view from outside the capsid shows additional electron densities in the vicinity of the HVR1 of all hexons, compatible with bound albumin (**Figure 29a**). A much closer side view shows the fitting of an albumin molecule into the extra density between two hexon trimers (**Figure 29b**). A model of the interaction between the hexon trimer and HSA was generated by fitting their crystallographic structures into the maps generated by cryo-electron microscopy (**Figure 29c**).

2.3.2. *In vitro* characterization of oncolytic properties

Once demonstrated the ability of the ABD-modified adenovirus to bind albumin from both human and mouse origin, we analyzed the oncolytic properties of ICOVIR15-ABD in terms of viral production and cytotoxicity to cancer cells *in vitro*.

2.3.2.1. Viral production of ICOVIR15-ABD

To confirm the results obtained with the non-replicative vectors in the comparative study of the ABD location (section 2.2.2.), the production of ICOVIR15-ABD was analyzed again in 293 cells but also in A549 cells at 24, 48, and 72 hours post-infection, in a single-round

replication experiment. The results of the oncolytic virus corroborate those obtained with the vectors. In 293 cells, ICOVIR15-ABD suffers a loss of production of 3.5-fold and 6-fold at 48 h and 72 h post-infection respectively, compared to the control virus ICOVIR15 (**Figure 30a**). In A549 cells the production yields of ICOVIR15-ABD were also lower than those of ICOVIR15, although only 2-3 times lower in all time points (**Figure 30b**). Since these studies were performed in the absence of albumin, it is likely that the insertion of the domain is what is causing the reduction in the production yields of the virus.

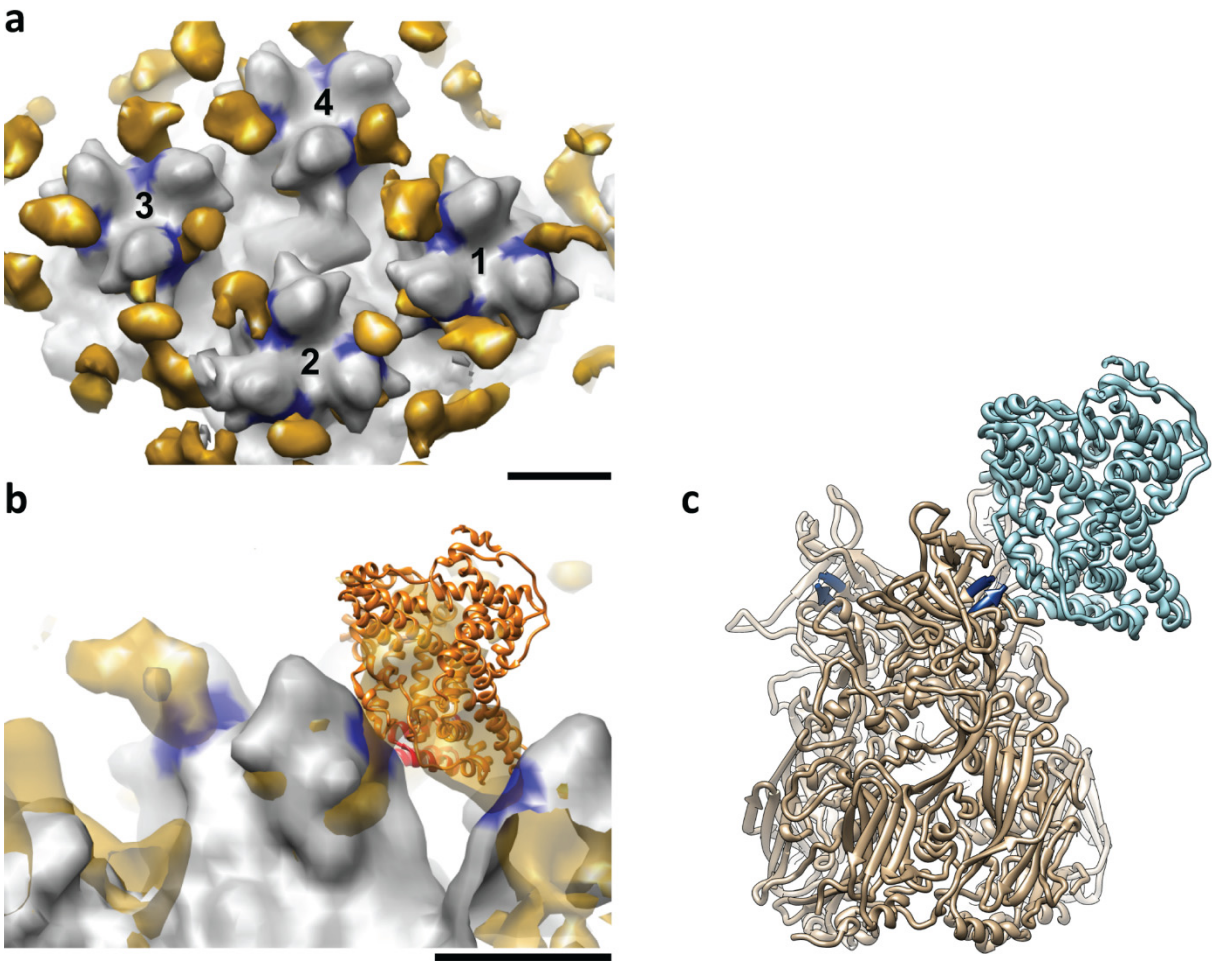

Figure 29. Cryo-electron microscopy difference map showing the location of bound HSA in the ICOVIR15-ABD capsid. (a) View from outside the capsid. The four hexon trimers in the capsid asymmetric unit (numbered 1-4) are shown in gray. In each hexon, the location of the HVR1 residues is indicated in blue. The difference density between Ad5 and the ICOVIR15-ABD-HSA complex, shown in gold, is present near the HVR1 location in all hexons. (b) Side view. Close up detail showing the crystallographic structure of a bacterial albumin-binding domain (red ribbon) and bound HSA (orange ribbon), fitted to the difference intensity located between two hexon trimers. Scale bars, 50 Å. (c) Crystallographic structures of hexon (brown) and bound HSA (blue) were fitted to the cryo-electron microscopy maps from (b).

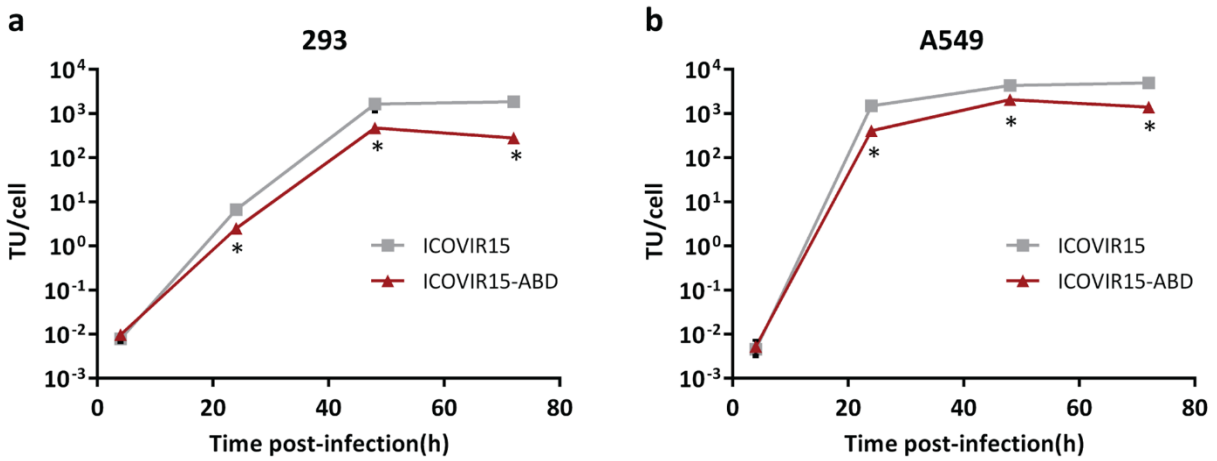

Figure 30. Viral production of ICOVIR15-ABD. (a) HEK293 cells or (b) A549 cells were infected with 100 vp/cell and 800 vp/cell, respectively, to achieve a 100 % of infection. At the indicated time points, cell extracts were harvested and titrated using an anti-hexon staining method. Mean ± SD is represented. *, significant ($p<0.05$) by two-tailed unpaired Student's t-test compared with ICOVIR15.

2.3.2.2. Cytotoxicity in the presence and absence of HSA

In vitro cytotoxicity was evaluated as an index of virus replication potency and ability to propagate within multiple rounds of replication. The impact of albumin binding in the replication of the virus was also analyzed. A549 cells were infected in normal medium or in HSA-containing medium with a broad range of MOIs and, 5-7 days later the percentage of cell survival was quantified. Two separate experiments were performed testing two different HSA concentrations: the usual high concentration of 1 mg/mL and a much lower concentration of 0.05 mg/mL (**Figure31a** and **b** respectively). ICOVIR15 and ICOVIR15-ABD showed very similar cytotoxic profile in the absence of albumin in both experiments, and the ABD insertion did not seem to hinder the replication and propagation of the virus in this case. This suggests that although the production of ICOVIR15-ABD is lower, it might be enough to ensure an efficient replication of the virus. Similar to what happened with the infectivity (see section 2.2.3.), albumin at a high concentration (1 mg/mL) interfered in the cytotoxicity of both viruses (**Figure 31a**). However, ICOVIR15 only suffered a 2-fold loss of cytotoxicity compared to a 6-fold loss of ICOVIR15-ABD. When albumin was present at a much lower concentration (0.05 mg/ml) the cytotoxicity of the control virus was unaffected, whereas that of the ABD-modified virus was only reduced 2.5-fold (**Figure 31b**), suggesting that the decrease of cytotoxicity is dependent on albumin concentration. In any case, it is reasonable to consider the loss of cytotoxicity to be a consequence of the loss of infectivity caused by albumin binding.

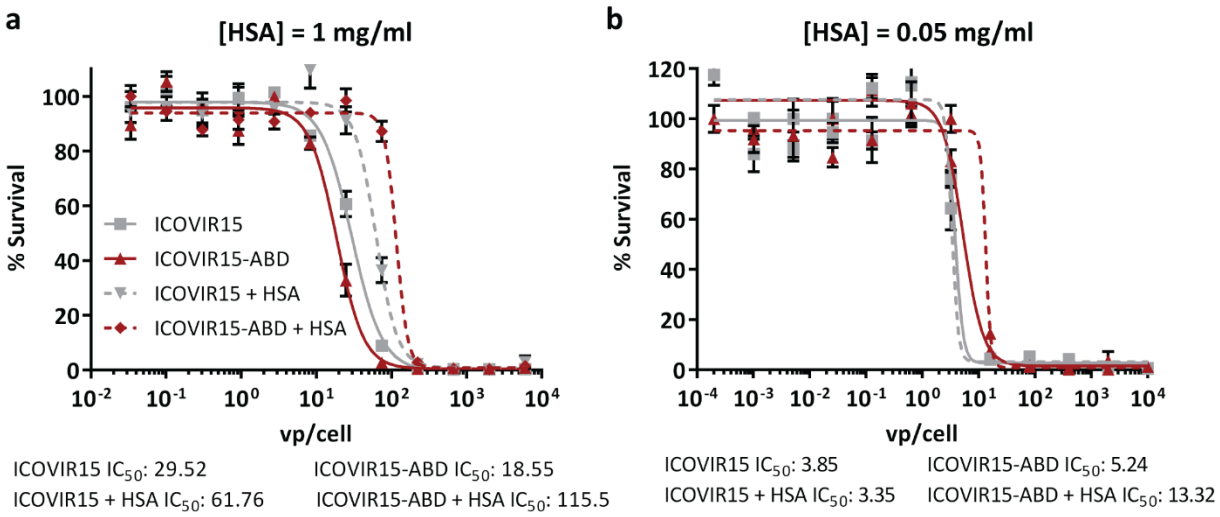

Figure 31. *In vitro* cytotoxicity of ICOVIR15-ABD in absence and presence of HSA at high and low concentrations. A549 cells were infected with serial dilutions of ICOVIR15 or ICOVIR15-ABD in the absence or presence of HSA at (a) 1 mg/ml, or (b) 0.05 mg/ml. At day 5-7 post-infection, cell viability was measured by BCA protein assay. Dose-response curves are shown along with the IC_{50} values for each virus and condition. Mean values ± SD are plotted.

2.3.3. Blood persistence after systemic administration

The ABD has been successfully used to increase the plasma half-life of therapeutic proteins, but never tested in the context of a virus. Although our main objective was to protect the virus against NAbs, we also tested whether albumin binding increased the blood persistence of the adenovirus. The blood persistence of ICOVIR15 and ICOVIR15-ABD was compared by direct competition after intravenous injection of a mixture of both viruses ($2.5x10^{10}$ vp each) in nude mice. Blood samples were collected at different time points. The genomes of the viruses in serum were detected by PCR of the HVR1, and were distinguished by the size of the PCR product (199 bp for ICOVIR15, and 361 bp for ICOVIR15-ABD due to the ABD insertion). The difference in blood persistence was analyzed comparing the relative intensity of the bands. Equally intense bands were obtained in the pre-injection control and 5 min after the injection (**Figure 32**). From then on, a shift on the intensity of the bands can be seen, as the band corresponding to ICOVIR15-ABD becomes more intense than the ICOVIR15 one. One hour after the injection, the extended circulation of ICOVIR15-ABD was clearly evident, but at 4 h after injection the level of both viruses dropped notably.

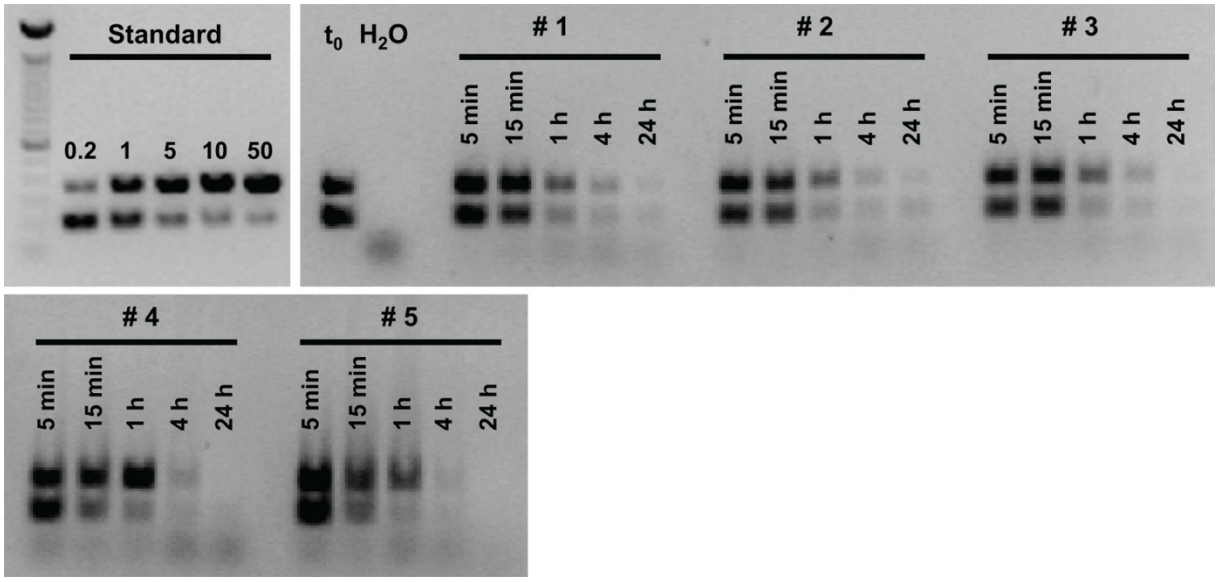

Figure 32. Competitive blood persistence of ICOVIR15 and ICOVIR15-ABD after intravenous administration. Serum samples of nude mice were collected at the indicated time points after intravenous administration of a mixture containing ICOVIR15 and ICOVIR15-ABD ($2.5x10^{10}$ vp each, n = 5 mice). PCR amplification of the HVR1 was performed and samples were analyzed by electrophoresis. The upper band corresponds to ICOVIR15-ABD and the lower band to ICOVIR15, as the ABD insertion increases the size of the HVR1 from 299 to 361 bp. The gel shows a standard with several ratios of ICOVIR15-ABD:ICOVIR15 genomes (0.2, 1, 5, 10, and 50), a pre-injection control (t_0), a water negative control of the PCR (H_2O), and the PCR of the sera of 5 different mice (#1 to #5).

2.3.4. Biodistribution profile after systemic administration

To check if such an increase in viremia enhanced tumor transduction, the biodistribution of the ABD-modified adenovirus was analyzed. Subcutaneous tumors of Sk-mel28 melanoma cell line were implanted in nude mice and when they reached an appropriate tumor volume, mice were intravenously injected with PBS or $5x10^{10}$ vp of reporter vectors AdGLRGD or AdGLRGD-ABD. Three days after vector injection mice were killed and organs were collected for *in vivo* bioluminescence imaging (IVIS). Despite the advantage observed after 1 h in blood persistence due to ABD insertion, there were no differences in transduction between the vectors in all the organs analyzed (**Figure 33**). Only a non-significant 1.6-fold loss of liver and tumor transduction was observed with AdGLRGD-ABD. Likely, the viremia increase of the modified virus compensated its lower infectivity in the presence of albumin (**Figure 23**), resulting in a final tumor transduction similar to the non-modified virus.

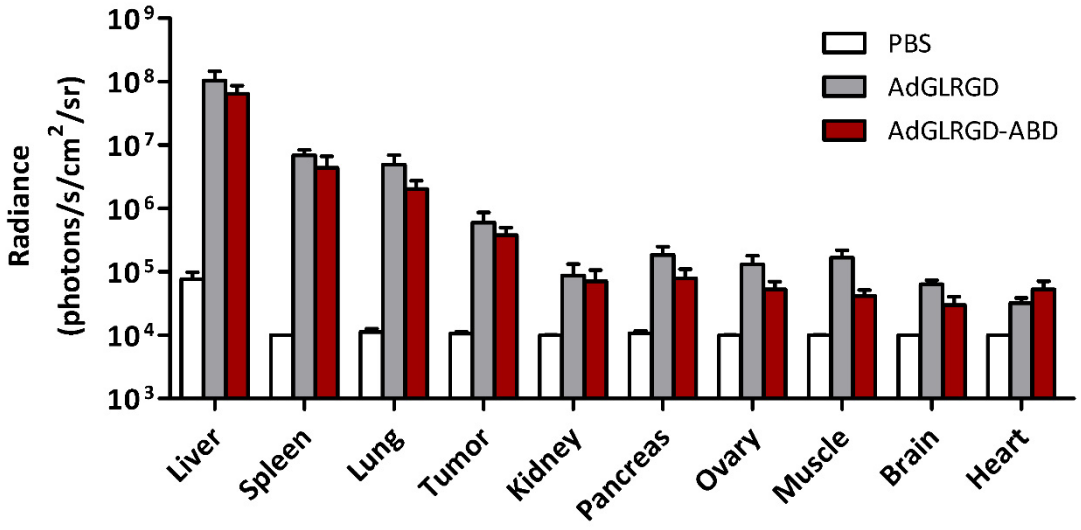

Figure 33. Biodistribution profile of AdGLRGD-ABD in nude mice after intravenous administration. Nude mice bearing Sk-mel28 melanoma tumors were systemically injected with PBS, or $5x10^{10}$ vp of AdGLRGD, or AdGLRGD-ABD. Three days after virus administration mice were sacrificed. Comparative luciferase expression in different organs was measured by *in vivo* imaging system (IVIS) (n = 5 mice/group). Mean + SEM.

2.3.5. Toxicity profile after systemic administration

The toxicity of ICOVIR15 was previously studied by our group, showing a very low toxicity profile compared to the Adwt virus (Rojas et al., 2010). Intravenous injection of ICOVIR15 causes a small loss of body weight around day 3-4, that is quickly rescued to normal levels. In a similar way, it causes a small increase of liver enzymes (AST and ALT) that is also rapidly recovered.

To determine the effect of albumin binding in the toxicity of ICOVIR15, Balb/C immunocompetent mice were injected with PBS or $5x10^{10}$ vp of ICOVIR15 or ICOVIR15-ABD via tail vein. Body weight was monitored until day 4 when animals were sacrificed to analyze the serum levels of liver enzymes (aspartate aminotransferase (AST), and alanine aminotransferase (ALT)), and other serum markers such as creatinine, lipase, and albumin.

Significant body weight loss was detected at day 3 post-injection with both viral treatments (**Figure 34a**). At this time, ICOVIR15-treated animals had lost almost a 6% of body weight whereas mice treated with ICOVIR15-ABD had lost only a 2.5% (the differences between the viruses were not significant). At day 4 post-injection, animals treated with ICOVIR15-ABD had completely recovered the body weight to the same levels of PBS-treated

mice. Although mice treated with ICOVIR15 had started to recover, the body weight loss at this time was still of 4%.

The injection of both oncolytic adenoviruses provoked an increase in the levels of liver transaminases AST and ALT at day 4 post-injection. ICOVIR15 raised the levels of AST 7-fold compared to a 3-fold increase caused by ICOVIR15-ABD, although the differences between the viruses were not statistically significant. A significant difference was observed in the levels of ALT as ICOVIR15 caused a 19-fold increase compared to a 7-fold caused by ICOVIR15-ABD (**Figure 34b**). Lipase, creatinine, and albumin serum levels were not altered by the injection of the oncolytic viruses (**Figure 34c-e**). In general terms, the ABD insertion reduced even more the low toxicity profile of oncolytic adenovirus ICOVIR15.

2.3.6. Antitumor efficacy after systemic administration

Next, the antitumor efficacy of ICOVIR15-ABD was tested in the model of naïve nude mice bearing melanoma Sk-mel28 subcutaneous tumors. With this aim, mice were treated with a single intravenous administration of PBS, or $5x10^{10}$ vp of oncolytic viruses ICOVIR15 or ICOVIR15-ABD, and the tumor volume was monitored. Both viruses were able to significantly reduce the tumor growth compared to the PBS-treated group (**Figure 35**). At the end of the experiment, ICOVIR15-ABD induced a 2-fold reduction in tumor volume, compared to a 1.4-fold induced by ICOVIR15. Although ICOVIR15-ABD showed a tendency towards higher antitumor efficacy, the difference between the oncolytic viruses was not statistically significant.

Altogether, the results obtained in this chapter indicated that the ABD insertion does not have an important impact on the oncolytic properties in the absence of neutralizing antibodies. Whereas *in vitro* the ABD-modified virus seems attenuated in the presence of albumin, its performance *in vivo* is very similar to that of the parental virus. However, the conditions studied in this section are always in the absence of NAbs, and such conditions do not reflect what is expected in the clinic, where a high percentage of human population has high levels of anti-Ad5 NAbs.

2.4. CHARACTERIZATION OF THE ABD INSERTION IN THE PRESENCE OF NEUTRALIZING ANTIBODIES

The following sections will assess the effects of the ABD modification on the adenovirus bioactivity both *in vitro* and *in vivo* in the presence of anti-Ad5 NAbs. *In vitro* experiments were

performed using commercially available NAbs, as well as anti-Ad5 pre-immune sera from both mouse and human origin. *In vivo* studies were performed using immunocompetent mice previously immunized with Ad5 or immunodeficient mice infused with pre-immune mouse serum.

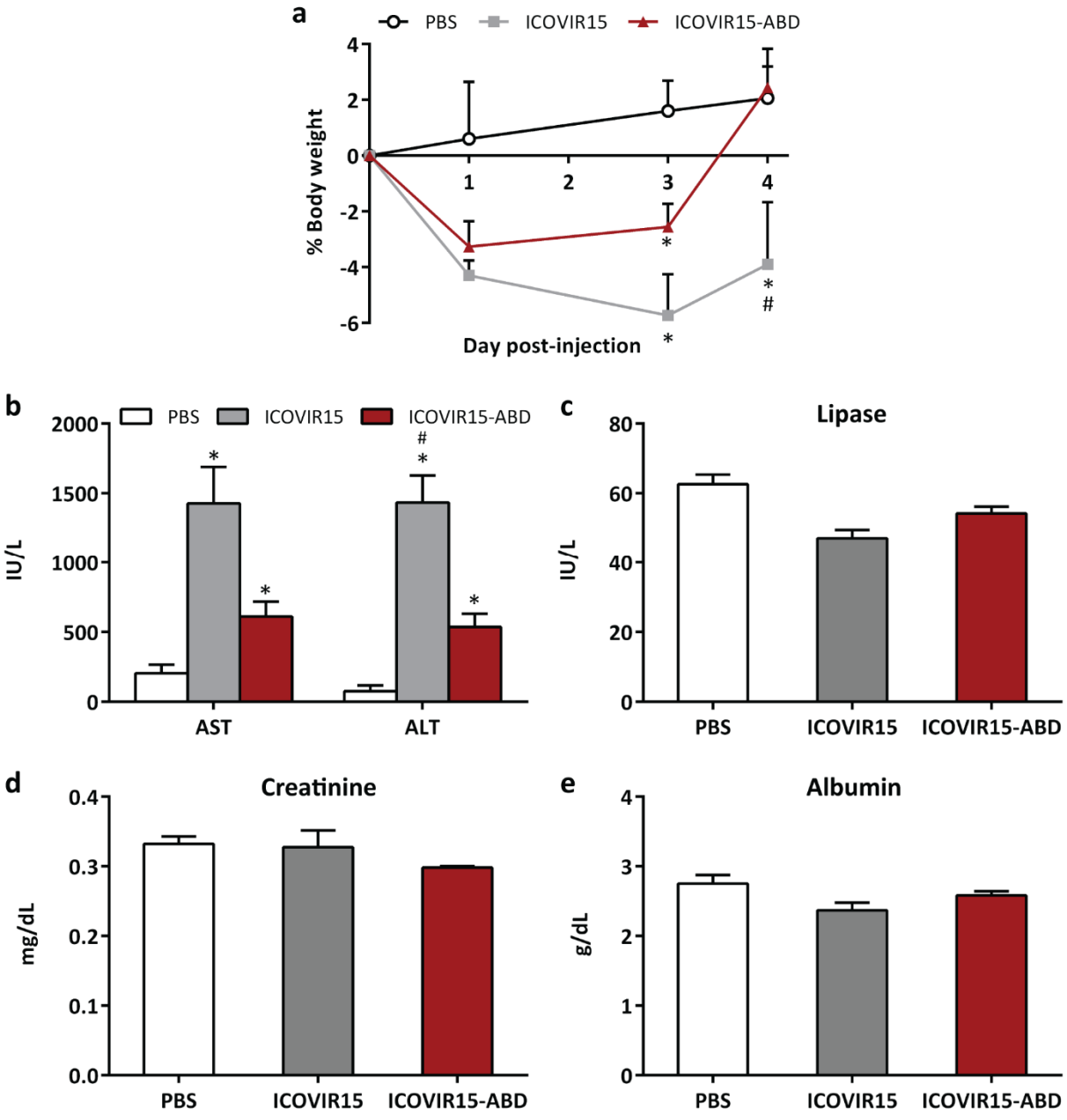

Figure 34. Toxicity after the intravenous administration of ICOVIR15-ABD in immunocompetent mice. (a) Body weight variation of Balb/C mice injected intravenously with PBS, or $5x10^{10}$ vp of ICOVIR15 or ICOVIR15-ABD (n = 6-7 mice). At day 4 post-injection mice were sacrificed to analyze the serum levels of (b) liver transaminases, (c) lipase, (d) creatinine, and (e) albumin (n = 4-5 mice). *, significant ($p<0.05$) by two-tailed unpaired Student's t-test compared with PBS. #, significant ($p<0.05$) by two-tailed unpaired Student's t-test compared with ICOVIR15-ABD.

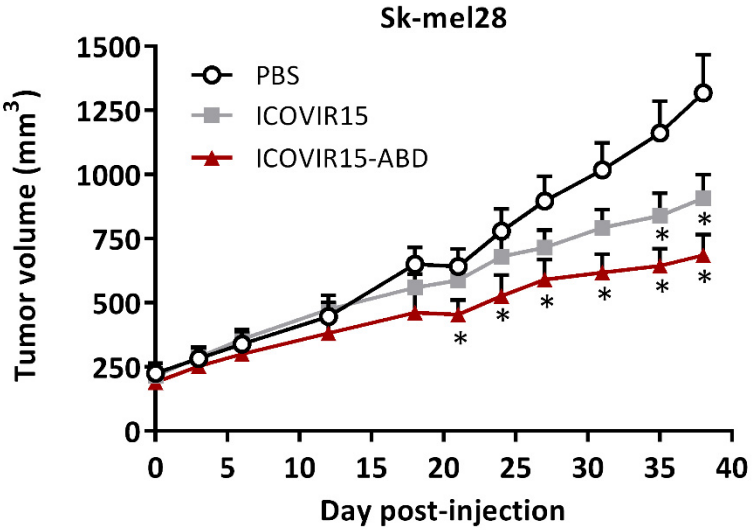

Figure 35. Antitumor efficacy of ICOVIR15-ABD in nude mice after intravenous administration. Nude mice bearing subcutaneous Sk-mel28 melanoma tumors were treated with a single intravenous injection of PBS, ICOVIR15, or ICOVIR15-ABD at a dose of $5x10^{10}$ vp per mouse (n = 10-12 tumors/group). Mean values of tumor volume + SEM are shown. *, significant ($p<0.05$) by two-tailed unpaired Student's t-test compared with PBS.

2.4.1. *In vitro* evasion of neutralizing antibodies

2.4.1.1. Effect of HSA concentration on virus transduction and neutralization

As previously explained, the physiological concentration of HSA (50 mg/ml) is too high to be used for *in vitro* assays, and a concentration of 1 mg/mL was used instead in most of the studies. To understand the impact of HSA concentration on the ABD-modified adenovirus, the transduction of the vectors was analyzed in the presence and absence of NAbs, using four different concentrations of HSA (0.01, 0.1, 1, and 10 mg/mL).

As previously observed in **Figure 23**, albumin negatively interferes in the infectivity of both adenovirus vectors when NAbs are absent. In this case, albumin reduced the transduction of the vectors in a dose-dependent manner in 293 and A549 cells, again affecting much more the ABD-modified virus (**Figure 36**). Unexpectedly, the transduction loss due to albumin binding was notably lower in 293 cells than in A549 cells (e.g. at 1 mg/ml AdGLRGD-ABD suffered a 3.4-fold loss in 293 cells compared to a 24-fold loss in A549 cells). Remarkably, the concentration of 10 mg/ml caused a very high inhibition in the transduction of both vectors. At this albumin concentration, AdGLRGD suffered a 5- and 12-fold loss of transduction, and the loss of AdGLRGD-ABD was 27- and 91-fold, in 293 and A549 cells respectively.

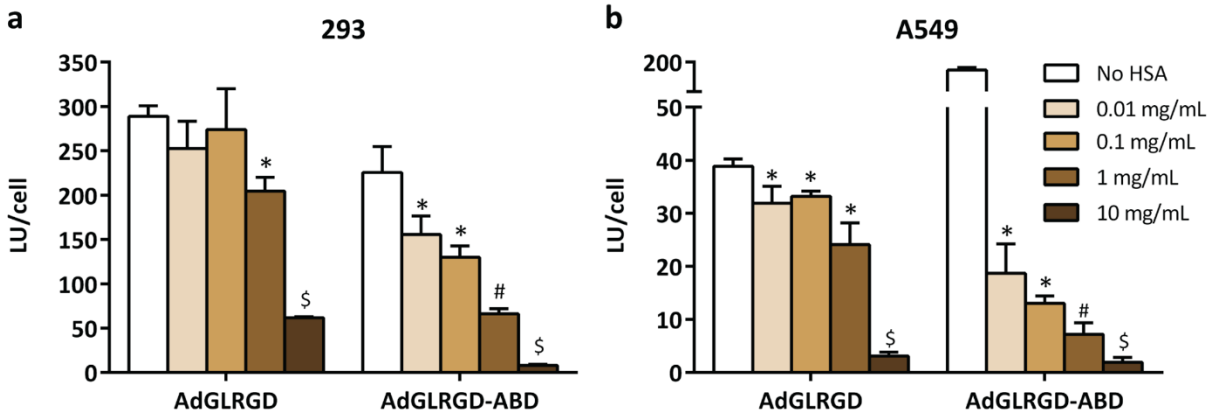

Figure 36. Infectivity of adenovirus vectors in the presence of different albumin concentrations. (a) HEK293 cells or (b) A549 cells were infected with 100 vp/cell and 800 vp/cell respectively of the adenovirus vectors in normal medium or in medium containing the indicated HSA concentrations. At 36 hours post-infection, cell transduction was analyzed by luciferase expression. Mean + SD is shown. *, significant ($p<0.05$) by two-tailed unpaired Student's t-test compared with no HSA. #, significant ($p<0.05$) by two-tailed unpaired Student's t-test compared with no HSA, 0.01 mg/ml, and 0.1 mg/ml. $, significant ($p<0.05$) by two-tailed unpaired Student's t-test compared with all groups.

The same study was conducted in the presence of NAbs in A549 cells. In particular, the commercial neutralizing antibody Ab6982 was used (previously described in section 2.2.5.) at a single dilution of 1/36. This represents a highly concentrated amount of NAbs, which should neutralize the majority of the virus used in this assay. Results are shown in percentage of transduction normalized versus a 100% transduction control without NAbs (**Figure 37a**), and in absolute light unit values per cell (**Figure 37b**). As relative protection and absolute transduction are different parameters, these could differ. Accordingly, AdGLRGD was highly neutralized regardless of albumin concentration, showing very low transduction levels and a maxim percentage of transduction of 0.3%. By contrast, the percentage of transduction of AdGLRGD-ABD was increased by the presence of albumin also in a dose-dependent manner, reaching the highest level of protection with an albumin concentration of 10 mg/mL (**Figure 37a**). However, if results are analyzed by the total light units, the advantage provided by the albumin concentration of 10 mg/mL is lost. While albumin concentrations of 0.01, 0.1, and 1 mg/mL increased the transduction of the ABD-modified vector, a concentration of 10 mg/mL caused the same level of transduction as the absence of albumin condition (**Figure 37b**). Despite this albumin concentration provides the highest level of protection, it also significantly reduces adenovirus transduction, as previously observed in **Figure 36**. Therefore, the value of the 100% transduction control is very low compared to the other albumin concentrations, and when normalizing the light units versus this control a high value of protection is obtained. This

means that at this albumin concentration, the adenovirus transduction is much lower but it is more protected from antibody neutralization. This discrepancy in the representation of the data does not occur with the three lower concentrations, in which more albumin confers more transduction and protection. In any case, the transduction of AdGLRGD-ABD in the presence of Ab6982 was always higher than that of AdGLRGD independently of albumin concentration. Even in the absence of albumin AdGLRGD-ABD showed higher transduction and protection than the non-modified vector, suggesting that the ABD modification of the HVR1 precluded binding of some NAbs, likely directed against the wt HVR1. Nevertheless, the working concentration of albumin in the following *in vitro* studies was maintained at 1 mg/ml. These results suggest that physiological albumin concentrations might severely inactivate the ABD-modified adenovirus. However, physiological conditions are reflected in the *in vivo* studies where the adenovirus is injected systemically in mice. In this context, biodistribution (**Figure 33**) and antitumor efficacy studies (**Figure 35**) did not show an inactivation of the ABD-modified virus.

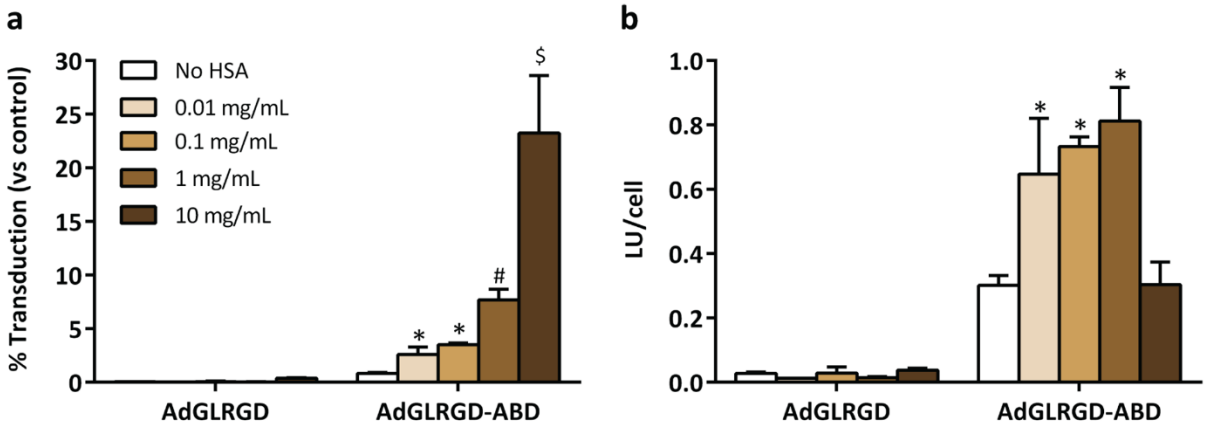

Figure 37. Escape of Ab6982 neutralization in the presence of different albumin concentrations. Adenovirus vectors, in medium containing the indicated HSA concentrations, were incubated with Ab6982 at a single dilution of 1/32. After 1 hour incubation, the viruses were used to infect A549 cells. Luciferase expression was analyzed 24 hours after the infection. A control without Ab6982 was included to obtain the 100 % infection value. (a) Results are represented as % transduction versus the 100 % infection control. Mean values + SD are depicted. *, significant ($p<0.05$) by two-tailed unpaired Student's t-test compared with no HSA. #, significant ($p<0.05$) by two-tailed unpaired Student's t-test compared with no HSA, 0.01 mg/ml, and 0.1 mg/ml. $, significant ($p<0.05$) by two-tailed unpaired Student's t-test compared with all groups. (b) Results are represented as total light units per cell. Mean values + SD are depicted. *, significant ($p<0.05$) by two-tailed unpaired Student's t-test compared with no HSA and 10 mg/ml.

2.4.1.2. In vitro neutralization by Ab6982

The ability of the ABD-modified vector to efficiently transduce target cells in the presence of Ab6982 when coated with albumin has already been demonstrated in section 2.2.5., and in this last section using a single antibody dilution. However, a more exhaustive study was performed not only in terms of cell transduction but also of viral replication in tumor cells.

To confirm the evasion results previously obtained, the ability of the vectors to transduce target cells in the presence of Ab6982 was analyzed. AdGLRGD and AdGLRGD-ABD in absence and presence of HSA were incubated with serial dilutions of Ab6982 and used to infect 293 and A549 cells. Very similar results were obtained in both cell lines (**Figure 38a and b**). We observed again that AdGLRGD-ABD was less neutralized than AdGLRGD even in the absence of albumin. Importanly, a clear increase on the transduction efficiency of the ABD-modified vector was observed when albumin was present in the medium. As expected, the non-modified vector AdGLRGD was highly neutralized regardless of albumin presence.

The capacity of the viruses to escape neutralization was not only assessed by their transduction efficiency but also by their cytotoxicity in presence of Ab6982. For this purpose, the oncolytic adenoviruses ICOVIR15 or ICOVIR15-ABD in presence or absence of HSA were incubated with serial dilutions of Ab6982, and used to infect A549 cells. Cell survival was analyzed 5 days after infection. In absence of HSA both viruses showed similar capacity to kill tumor cells (**Figure 39**), and only a small increase of cytotoxicity was observed with ICOVIR15-ABD probably due to the certain evasion of NAbs observed in transduction (**Figure 38a and b**). Importantly, HSA shifted the cytotoxicity curve of ICOVIR15-ABD towards higher NAbs concentrations, whereas it did not protect ICOVIR15 from neutralization.

2.4.1.3. In vitro neutralization by anti-Ad5 pre-immune mouse serum

To better understand the potential of the ABD-adenovirus to escape neutralization *in vivo*, the same neutralization tests were performed with serum from mice immunized with Ad5. To generate the neutralizing serum, C57BL/6 immunocompetent mice were primed intraperitoneally with $3x10^{10}$ vp of Ad5wt, and boosted intravenously seven days later with the same dose. Seven days after boosting, mice were killed and the blood was collected to obtain the serum.

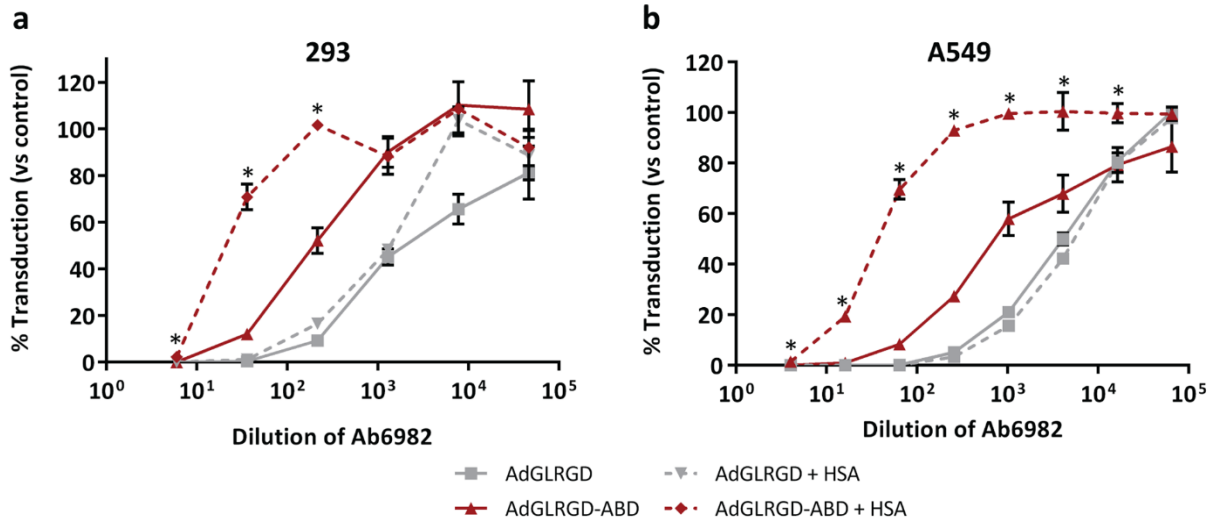

Figure 38. *In vitro* transduction of AdGLRGD-ABD in presence of Ab6982. Adenovirus vectors, in the presence or absence of HSA, were incubated with serial dilutions of the polyclonal neutralizing antibody Ab6982. After 1 hour incubation, the viruses were used to infect (a) HEK293 cells or (b) A549 cells at 10 vp/cell. Luciferase expression was analyzed 24 hours after the infection. A control without Ab6982 was included to obtain the 100 % infection value. Results are represented as % transduction versus the 100 % infection control. Mean values ± SD. *, significant ($p<0.05$) by two-tailed unpaired Student's t-test compared with all groups.

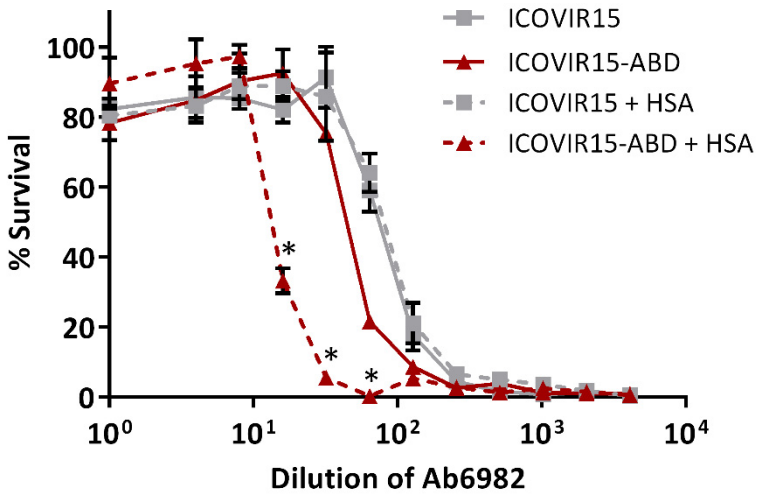

Figure 39. Cytotoxicity of ICOVIR15-ABD in presence of Ab6982. Oncolytic adenoviruses ICOVIR15 or ICOVIR15-ABD, in presence or absence of HSA, were incubated with serial dilutions of Ab6982 for 1 hour, and then used to infect A549 cells. Cell survival was measured at day 5 post-infection by BCA staining. Mean values ± SD are shown. *, significant ($p<0.05$) by two-tailed unpaired Student's t-test compared with all groups.

Since mouse serum contains a high concentration of albumin, the absence of albumin condition could not be analyzed in these studies. On the other hand, HSA was added to the medium at a concentration of 1 mg/mL in order to maintain a minimum albumin concentration throughout the dilutions. The evasion of the NAbs present in the serum was first analyzed in terms of cell transduction in A549 cells. A clear advantage was observed again with AdGLRGD-ABD, showing high levels of transduction even at low serum dilutions, where the non-modified vector was completely neutralized (**Figure 40a**). The neutralization escape in the mouse serum was also tested in terms of cytotoxicity in A549 cells, where ICOVIR15-ABD was able to kill the tumor cells more efficiently than ICOVIR15 (**Figure 40b**), demonstrating a higher bioactivity in the presence of NAbs.

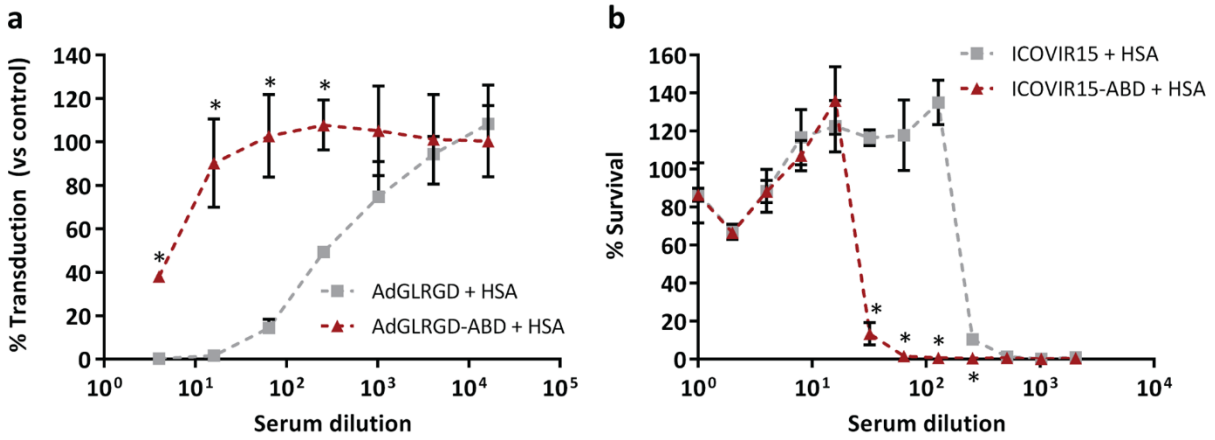

Figure 40. ***In vitro*** **evasion of anti-Ad5 neutralizing mouse serum.** (a) Transduction analysis after incubation with anti-Ad5 neutralizing mouse serum. AdGLRGD or AdGLRGD-ABD in the presence of HSA were incubated with serial dilutions of the serum for 1 hour, and then used to infect A549 cells at 10 vp/cell. Luciferase expression was analyzed 24 hours after infection. A control without serum was included to obtain the 100 % infection value. Results are represented as % transduction versus the 100 % infection control. Mean ± SD. *, significant ($p<0.05$) by two-tailed unpaired Student's t-test compared with AdGLRGD-ABD + HSA. (b) Cytotoxicity analysis after incubation with anti-Ad5 neutralizing mouse serum. ICOVIR15 or ICOVIR15-ABD in the presence of HSA were incubated with serial dilutions of the serum for 1 hour, and then used to infect A549 cells. Cell survival was measured at day 5 post-infection by BCA staining. Mean values ± SD. *, significant ($p<0.05$) by two-tailed unpaired Student's t-test compared with ICOVIR15 + HSA.

2.4.1.4. In vitro neutralization by anti-Ad5 pre-immune human sera

To test whether the ABD-modified adenovirus could also evade NAbs developed in humans, sera from six human donors (previously tested by our group for anti-Ad5

seropositivity) were used to test the neutralization escape of the viruses by transduction analysis in 293 cells. A clear neutralization escape of the ABD-vector was observed in three of the six sera analyzed (#1, #2, and #6), whereas no advantage versus the non-modified vector was detected in the other three sera (#3, #4, and #5) (**Figure 41a**). This is observed when representing the data as % transduction versus the 100% transduction control as explained in section 2.2.5. However, if the data is not normalized, we observe that in general terms AdGLRGD-ABD shows higher transduction levels than AdGLRGD at low serum dilutions, when the NAbs concentration are higher (**Figure 41b**), which are the conditions that better mimic the intravenous administration of the virus. When the sera were highly diluted, the advantage of the ABD-modified virus was lost, as previously observed in presence of albumin and absence of neutralizing antibodies (**Figure 23**).

2.4.2. Blood persistence in pre-immune mice after systemic administration

Not having observed an improvement in tumor transduction nor a significant benefit in antitumor efficacy in naïve mice, we next studied the behavior of the ABD-adenoviruses in pre-immune mouse models. First, the blood persistence was analyzed in both naïve and pre-immune immunocompetent mice. To generate anti-Ad5 NAbs, C57BL/6 mice were immunized with an intraperitoneal injection of PBS or $3x10^{10}$ vp of Ad5wt (naïve or pre-immune groups), and seven days later mice were intravenously injected with $3x10^{10}$ vp of AdGLRGD or AdGLRGD-ABD. Serum samples were collected from the tail vein at the indicated time points to detect adenovirus genomes by real-time PCR, and transducing units by anti-hexon staining method.

In naïve mice, the clearance curve shows an advantage of the ABD-modified virus in terms of viral particles (significant differences at 15 min and 1 h post-injection) but not of transducing units (**Figure 42** left panels). This result matches with the increased blood persistence at 1 h after injection in nude mice (**Figure 32**), which did not translate in an increased organ transduction (**Figure 33**). However, in pre-immune mice the advantage of the ABD-modified virus was evident not only in circulating viral particles (significant differences at 30 min post-injection) but also in transducing units (**Figure 42** right panels). Although the clearance curve of transducing units in pre-immune mice shows higher levels of AdGLRGD-ABD versus AdGLRGD, the differences were not statistically significant at any time point.

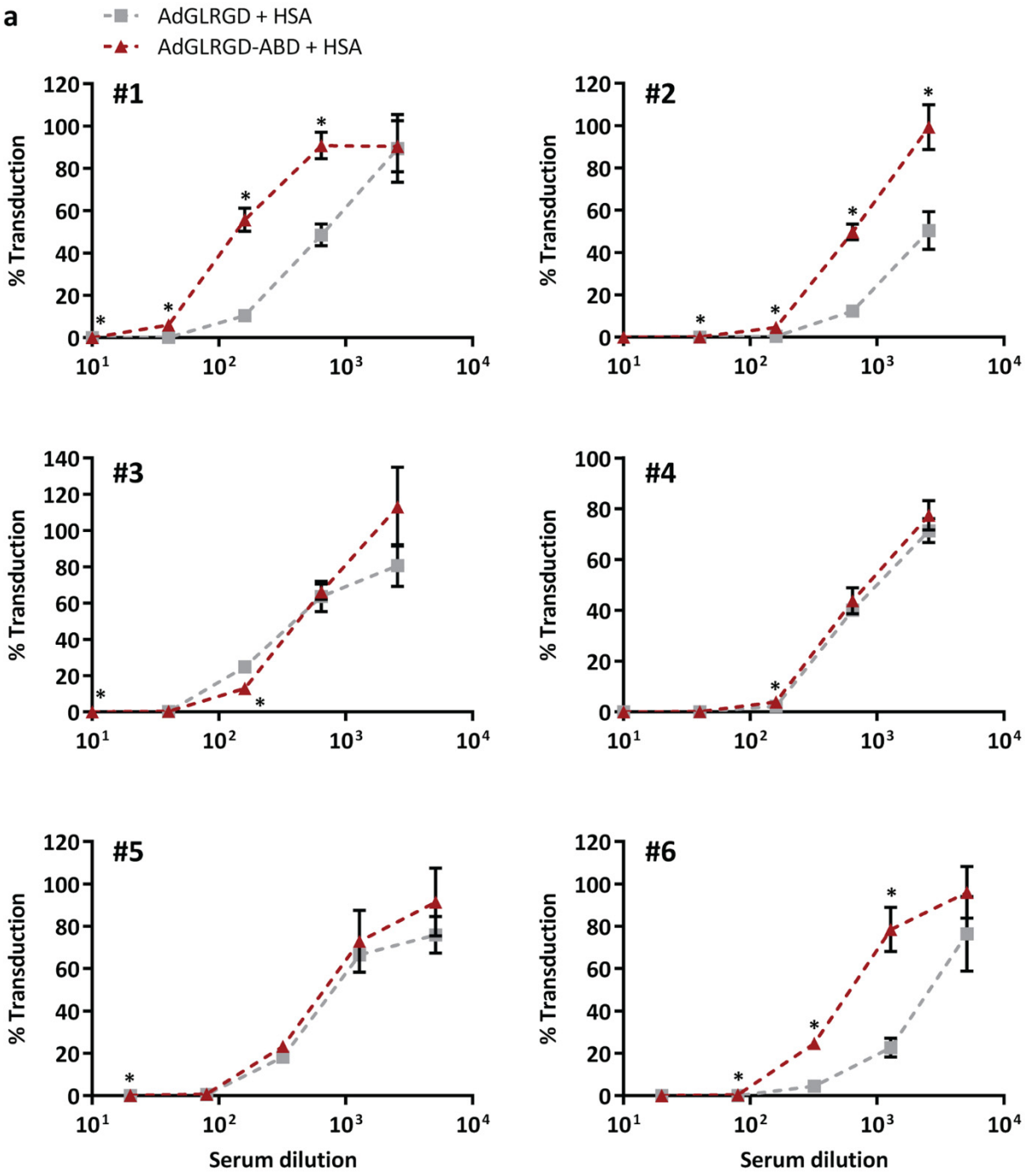
a
AdGLRGD + HSA
AdGLRGD-ABD + HSA
#1
#2
#3
#4
#5
#6
% Transduction
Serum dilution

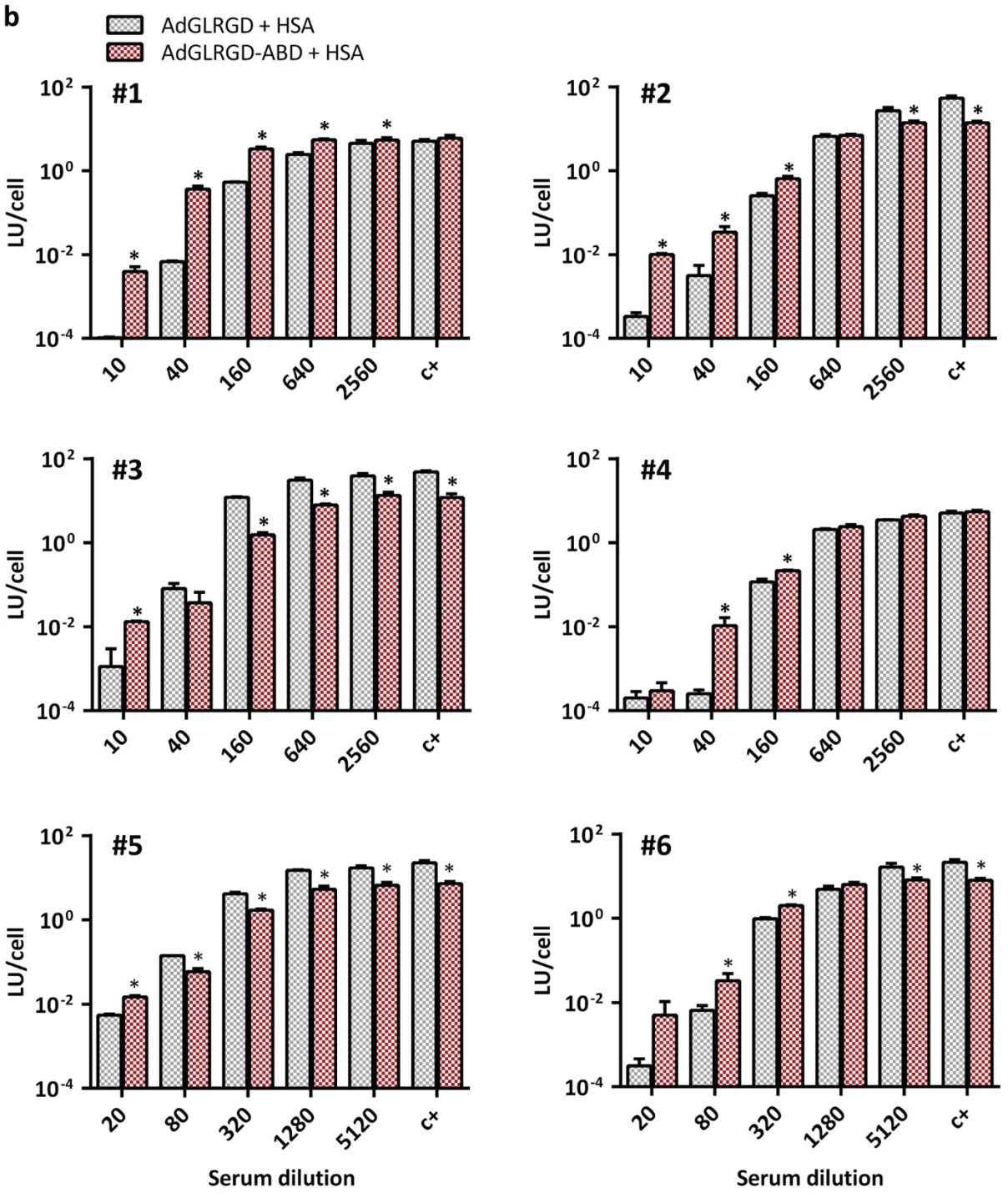

Figure 41. *In vitro* neutralization analysis after incubation with human sera. AdGLRGD or AdGLRGD-ABD in presence of HSA were incubated with serial dilutions of human sera from six anonymous donors (#1-6). After 1 hour incubation, the vectors were used to infect HEK293 cells at 10 vp/cell. Luciferase expression was analyzed 24 hours after infection. A control without serum was included to obtain the 100 % infection value. Results are represented as (a) % transduction versus the 100 % infection control or (b) total light units per cell. The value of the positive transduction control without serum is shown (c+). Mean values + SD are depicted. *, significant ($p<0.05$) by two-tailed unpaired Student's t-test compared with AdGLRGD + HSA.

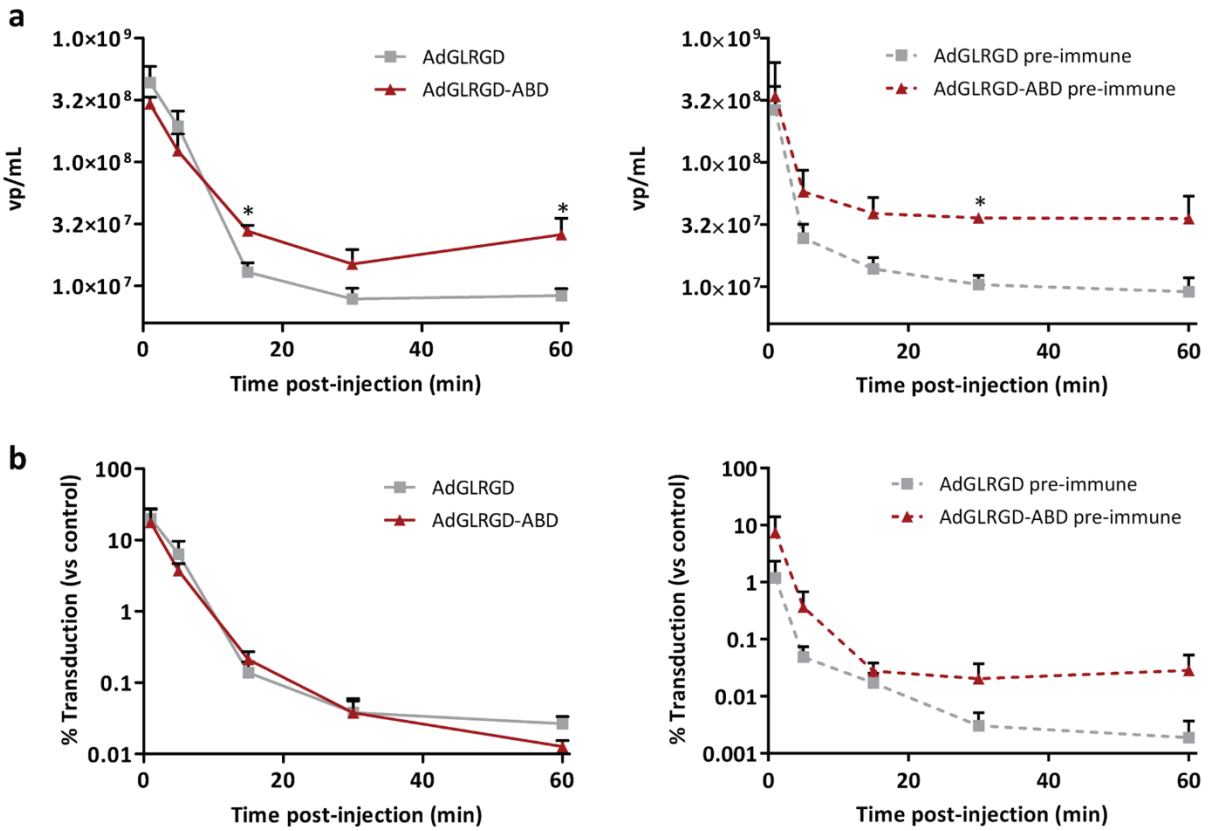

Figure 42. Blood persistence of AdGLRGD and AdGLRGD-ABD after intravenous administration in naïve and pre-immune mice. C57BL/6 immunocompetent mice were immunized with an intraperitoneal injection of $3x10^{10}$ vp of Ad5wt or PBS. Seven days later mice were intravenously injected with AdGLRGD or AdGLRGD-ABD ($3x10^{10}$ vp, n=5 mice), and serum samples were collected from the tail vein 1 min, 5 min, 15 min, 30 min, and 60 min after injection. (a) Adenovirus genome quantification was performed by real-time PCR in serum samples of naïve (left) and pre-immune mice (right). (b) Adenovirus transducing units titration in serum samples of naïve (left) and pre-immune (right) mice was performed by infection of HEK293 cells followed by antihexon staining. The titers were normalized to the transduction value of each virus in naïve mouse serum (100% transduction control). *, significant ($p<0.05$) by two-tailed unpaired Student's t-test compared to AdGLRGD.

2.4.3. Organ transduction in pre-immune mice after systemic administration

Next, the effect of anti-Ad5 NAbs on adenovirus organ transduction after intravenous administration was analyzed. C57BL/6 mice bearing subcutaneous B16-CAR melanoma tumors were immunized with an intraperitoneal injection of PBS or $3x10^{10}$ vp of Ad5wt (naïve or pre-immune groups), and seven days later mice received a single intravenous dose of PBS, or $3x10^{10}$ vp of AdGLRGD or AdGLRGD-ABD.

A blood sample was taken from the tail vein 1 h post-injection to analyze the amount of virus in blood, which was confirmed to be significantly higher (2.3-fold) in both naïve and pre-

immune mice injected with the ABD-modified vector (**Figure 43**), compared to those injected with the control vector. This further supports the results showed in **Figures 32** and **42**.

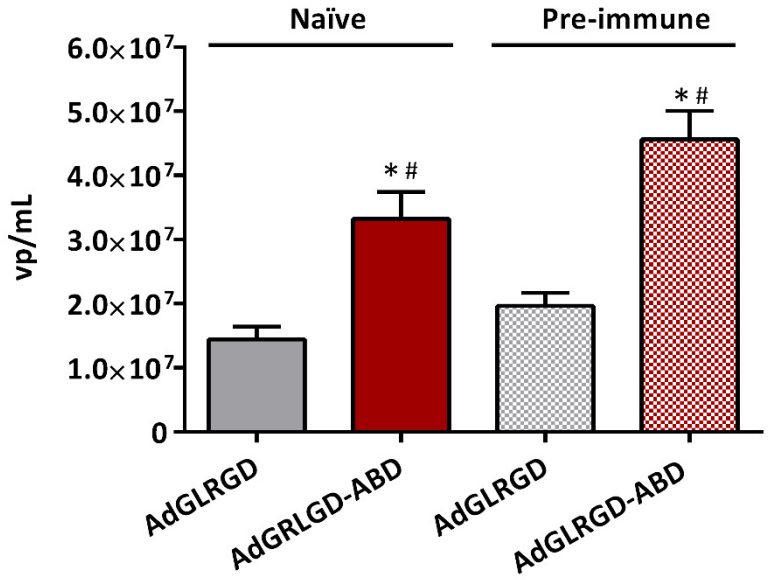

Figure 43. Viral load in blood 1 hour after injection in naïve and pre-immune mice. C57BL/6 immunocompetent mice previously immunized or not with Ad5wt were intravenously injected with AdGLRGD or AdGLRGD-ABD ($3x10^{10}$ vp, n=4-6 mice). Serum samples were collected 1 hour after injection to quantify adenovirus genomes by real-time PCR. *, significant ($p<0.05$) by two-tailed unpaired Student's t-test compared to AdGLRGD in naïve mice. #, significant ($p<0.05$) by two-tailed unpaired Student's t-test compared with AdGLRGD in pre-immune mice.

Three days after vector injection mice were killed and the luciferase expression in livers and tumors was analyzed by *in vivo* imaging system (IVIS). In naïve animals, AdGLRGD-ABD showed a 9- and 7-fold non-significant loss of liver and tumor transduction respectively compared to the non-modified vector (**Figure 44**). Importantly, when animals were pre-immunized with Ad5wt, the parental AdGLRGD vector suffered a complete neutralization as the transduction of liver and tumors was completely abolished. On the contrary, AdGLRGD-ABD only suffered a 3.9- and 1.5-fold non-significant loss of liver and tumor transduction respectively, indicating an efficient protection from anti-Ad5 NAbs *in vivo*.

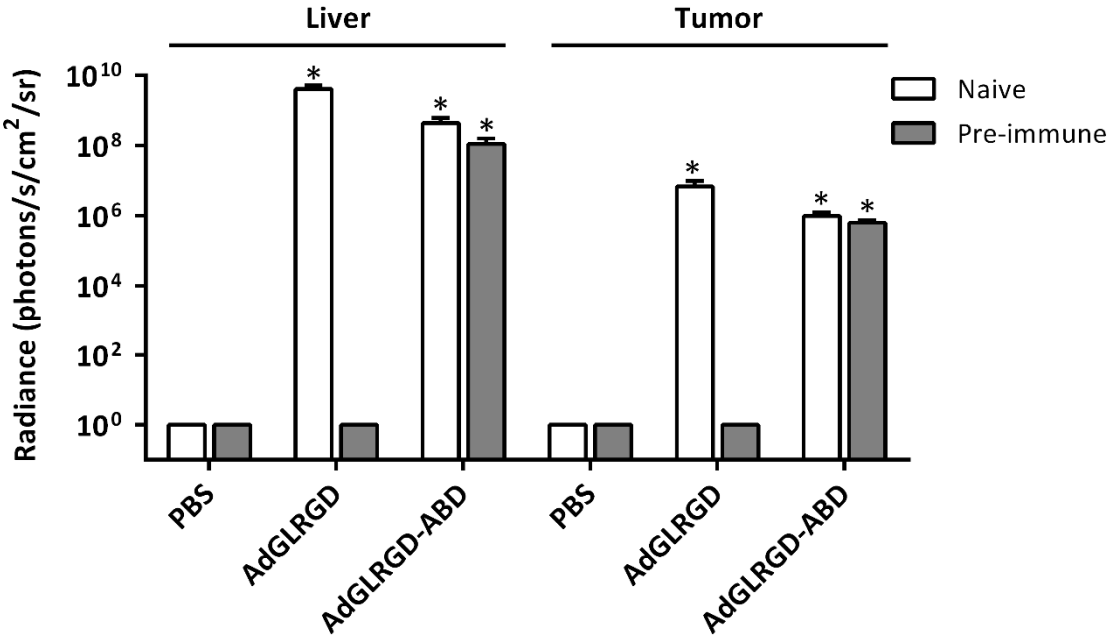

Figure 44. Liver and tumor transduction in naïve and pre-immune mice after systemic administration. C57BL/6 immunocompetent mice bearing subcutaneous B16-CAR melanoma tumors were immunized with an intraperitoneal injection of $3x10^{10}$ vp of Ad5wt or PBS, and seven days later mice were intravenously injected with AdGLRGD or AdGLRGD-ABD ($3x10^{10}$ vp). Three days after virus administration mice were killed and luciferase activity in liver and tumors was analyzed by *in vivo* imaging system (IVIS) (livers n = 3-6, tumors n = 6-12). Mean + SEM is shown. *, significant ($p<0.05$) by two-tailed unpaired Student's t-test compared with AdGLRGD pre-immune.

2.4.4. Generation of an anti-Ad5 pre-immune status in immunodeficient mice to test the antitumor efficacy

After observing the efficient tumor transduction of the ABD-modified adenovirus in pre-immune mice, the next step was to evaluate the antitumor efficacy of ICOVIR15-ABD in mice with anti-Ad5 NAbs. However, since the human adenovirus does not replicate in mouse cells, an immunodeficient mouse model with engrafted human tumors is required to test the antitumor activity. The strategy used to generate an anti-Ad5 pre-immune status in nude mice was the passive transfer of neutralizing serum from C57BL/6 mice.

2.4.4.1. Generation of anti-Ad5 immune sera

C57BL/6 were primed intraperitoneally with $3x10^{10}$ vp of Ad5wt, and boosted intravenously seven days later with the same dose of the same virus. Seven days later mice were killed, the blood was collected by intracardiac puncture, and the serum of each mouse

was pooled. To analyze the variability in the generation of NAbs, we compared the neutralizing activity of four batches of pooled serum obtained at different dates during this thesis. The AdGL vector (a GFP/luciferase expressing vector with a wt capsid) was incubated with serial 1/2 dilutions of the sera, and then used to infect 293 cells. The transduction is compared to a control without serum (0% neutralization control) to obtain the percentage of neutralization at each serum dilution. The titer of each serum corresponds to the dilution in which a 50% of adenovirus neutralization was obtained. Although the four sera displayed high neutralizing activity, variability was observed in the titer of the sera (serum #0315: 1280-2560, serum #0615: >5120, serum #1015: 2560, and serum #0416: 5120) (**Figure 45**). Of note, serum #0615 displayed a titer more than a 2-fold higher than serum #0416. This variability in the neutralizing activity was taken into consideration when transferring the sera to nude mice.

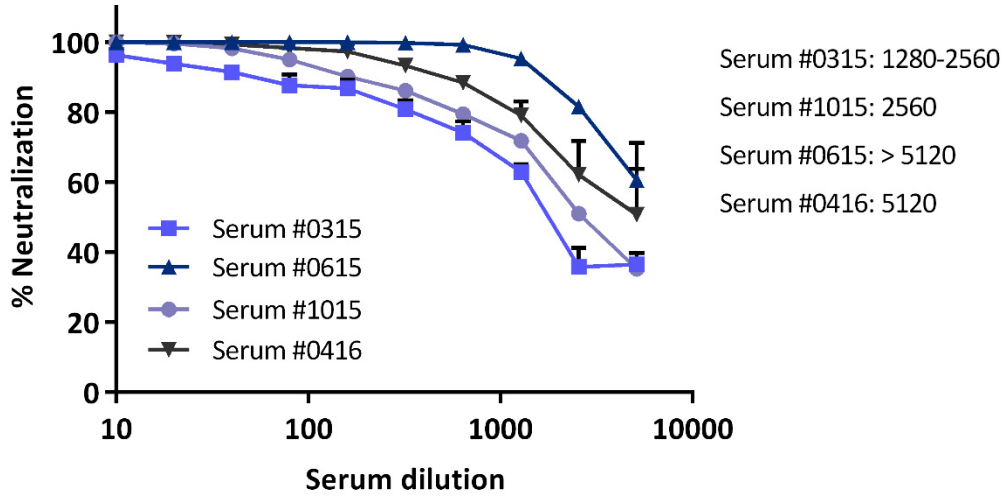

Figure 45. Neutralizing activity of anti-Ad5 mouse sera. Neutralizing sera were obtained by immunization of C57BL/6 immunocompetent mice with Ad5wt using a prime and boost regimen. Serum titration was performed by incubating AdGL with serial 1/2 dilutions of the serum and analyzing the transduction in HEK293 cells using an MOI of 0.25 TU/cell. A control without serum was included to obtain the 0% neutralization value. The serum titer corresponds to the dilution required to neutralize the 50% of the virus. Four different serum batches were compared. Titration curves are shown along with serum titers. Mean + SD.

2.4.4.2. Passive immunization of nude mice: preliminary test of organ transduction and antitumor efficacy to evaluate neutralization

The serum transfer to nude mice was performed via intraperitoneal route 24 hours prior to virus injection, as previously described (Tsai et al., 2004). In a first test, nude mice bearing A549 subcutaneous tumors were transferred with PBS (mock), 5µL, or 50 µL of the serum #0315 (titer of 1280-2560) diluted in 200 µL of PBS. The next day mice were intravenously injected with $4.5x10^{10}$ vp of AdGL. Three days after vector injection mice were killed and livers and tumors were collected for *in vivo* bioluminescence imaging (IVIS). As expected, the sham passively immunized mouse with PBS displayed very high luciferase signal in the liver and, to a lesser extent, in tumors (**Figure 46**). Passive immunization with 5 µL of serum reduced the transduction of tumors, but high levels of luciferase signal were still detected in the liver. In contrast, administration of 50 µL of serum caused a very important drop in the luciferase signal of liver and tumors, indicating an efficient neutralization of the virus.

Having demonstrated the ability of passively immunized nude mice to neutralize the Ad5, the antitumor activity of the oncolytic adenoviruses was tested in this mouse model. Nude mice bearing A549 subcutaneous tumors were sham-immunized with PBS, or passively immunized with 50 µL of the serum #0315 intraperitoneally (naïve or pre-immune groups). The next day mice were injected with PBS or $4.5x10^{10}$ vp of ICOVIR15, or ICOVIR15-ABD via tail vein. To our surprise, the oncolytic activity of ICOVIR15 was not hindered by the passive immunization of mice (**Figure 47**). The experiment was stopped at day 21 post-injection, as tumors of naïve and pre-immune mice treated with ICOVIR15 were growing at the same speed. This result suggests that the virus was not completely neutralized. We hypothesized that despite not having observed any sign of transduction at day 3, a certain amount of virus might still be reaching the tumor, being able to replicate and control tumor growth. We proceeded to test this hypothesis using a reporter oncolytic virus.

2.4.4.3. Passive immunization of nude mice: replication analysis with a reporter oncolytic adenovirus

To be able to visually detect replication foci several days after virus administration, a replicative reporter virus is required. In this work we constructed ICOVIR15-Luc, a reporter oncolytic adenovirus generated by insertion of the luciferase gene in the genome of ICOVIR15 after the fiber. To drive the expression under the major late promoter (MLP) as a late expression cassette, the luciferase transgene included the splicing acceptor from the IIIa

adenoviral protein, and a polyadenylation sequence (**Figure 48a**). In this manner, luciferase expression is linked to the replication of the virus and not just to virus transduction, as it occurs with the regular CMV-Luciferase cassette in AdGL and its variations. The *in vitro* characterization of ICOVIR15-Luc was performed by analyzing the luciferase expression kinetics and the cytotoxicity of the virus.

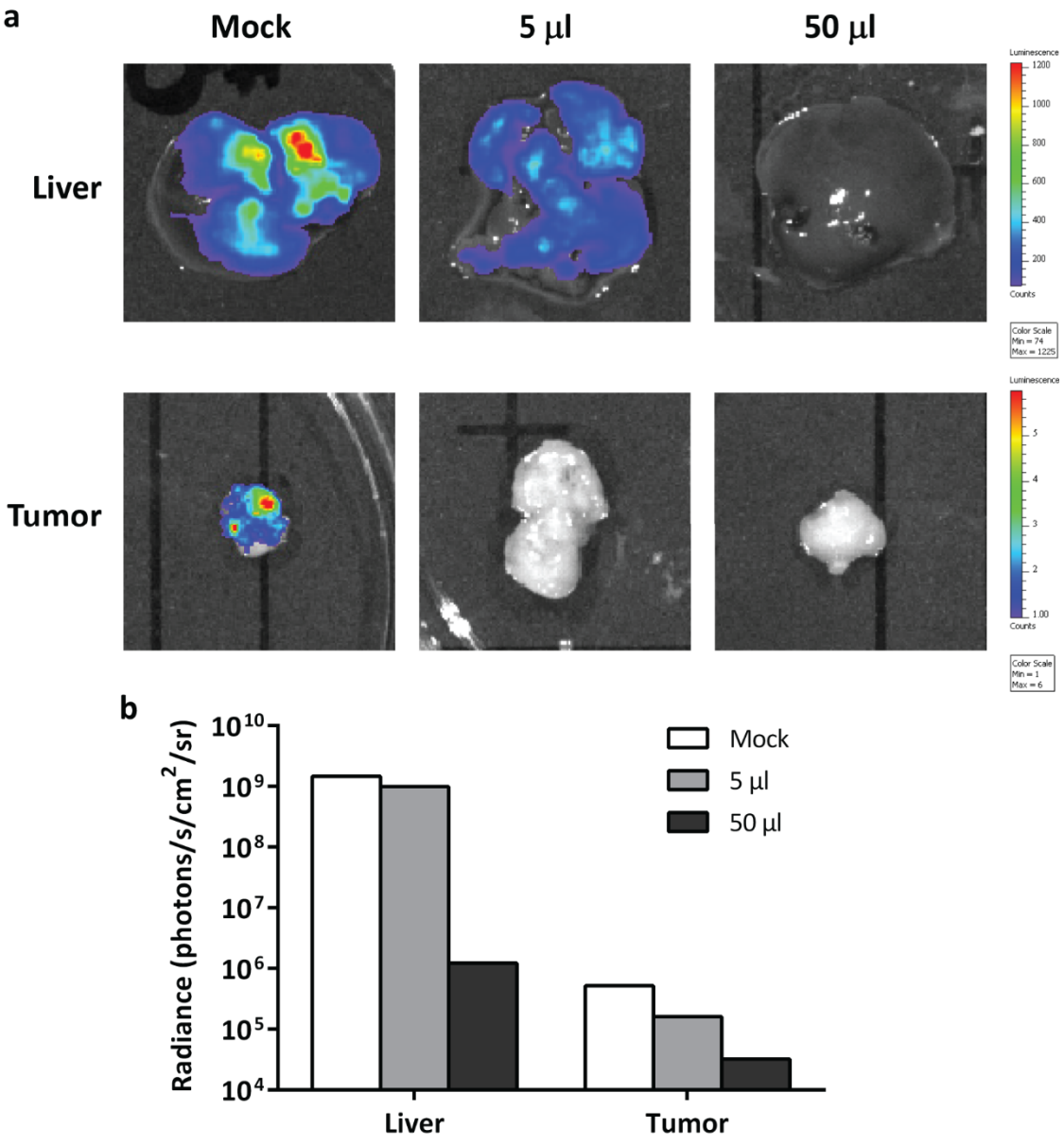

Figure 46. Preliminary analysis of liver and tumor transduction after passive immunization of nude mice. Nude mice bearing subcutaneous A549 tumors were injected intraperitoneally with PBS (mock), 5 µL, or 50 µL of anti-Ad5 neutralizing mouse serum (serum #0315) diluted in 200 µL of PBS. The next day mice received an intravenous injection of $4.5x10^{10}$ vp of AdGL (n = 1 mouse per condition). (a) Livers and tumors were imaged for luciferase expression at day three after vector injection. An overlay of the white image and the luciferase signal is shown. (b) Quantification of luciferase expression in livers and tumors.

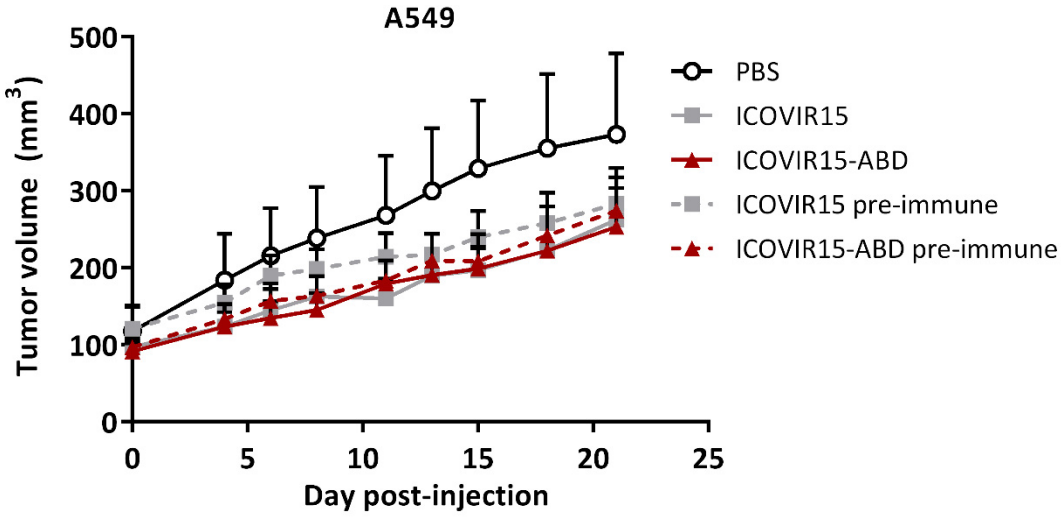

Figure 47. Preliminary analysis of antitumor efficacy after passive immunization of nude mice. Nude mice bearing subcutaneous A549 tumors were passively immunized with an intraperitoneal injection of PBS (naïve), or 50 µL of anti-Ad5 neutralizing mouse serum (serum #0315). The next day mice were treated with a single intravenous injection of PBS or $5x10^{10}$ vp of ICOVIR15, or ICOVIR15-ABD. Mean values of tumor volume + SEM are shown (n = 10-11 tumors/group).

The luciferase expression kinetics of ICOVIR15-Luc were compared to those of AdGLRGD in human A549 and canine Dk-cre cells (**Figure 48b**). The delayed luciferase expression of ICOVIR15-Luc compared to AdGLRGD in A549 cells indicates that the expression occurs in the late phase of the viral cycle, associated with the replication of the virus. In contrast, since the human adenovirus cannot replicate in canine cells, the expression of luciferase in Dk-cre cells is significantly reduced compared to A549 cells, demonstrating a replication-dependent expression. Regarding the cytotoxicity, ICOVIR15-Luc showed a 7.8-fold loss compared to ICOVIR15 (**Figure 48c**), suggesting that the either the size of the genome or the expression of the transgene negatively affects the virus life cycle. Despite this cytotoxicity loss, ICOVIR15-Luc represents a useful tool to monitor the viral replication by *in vivo* imaging.

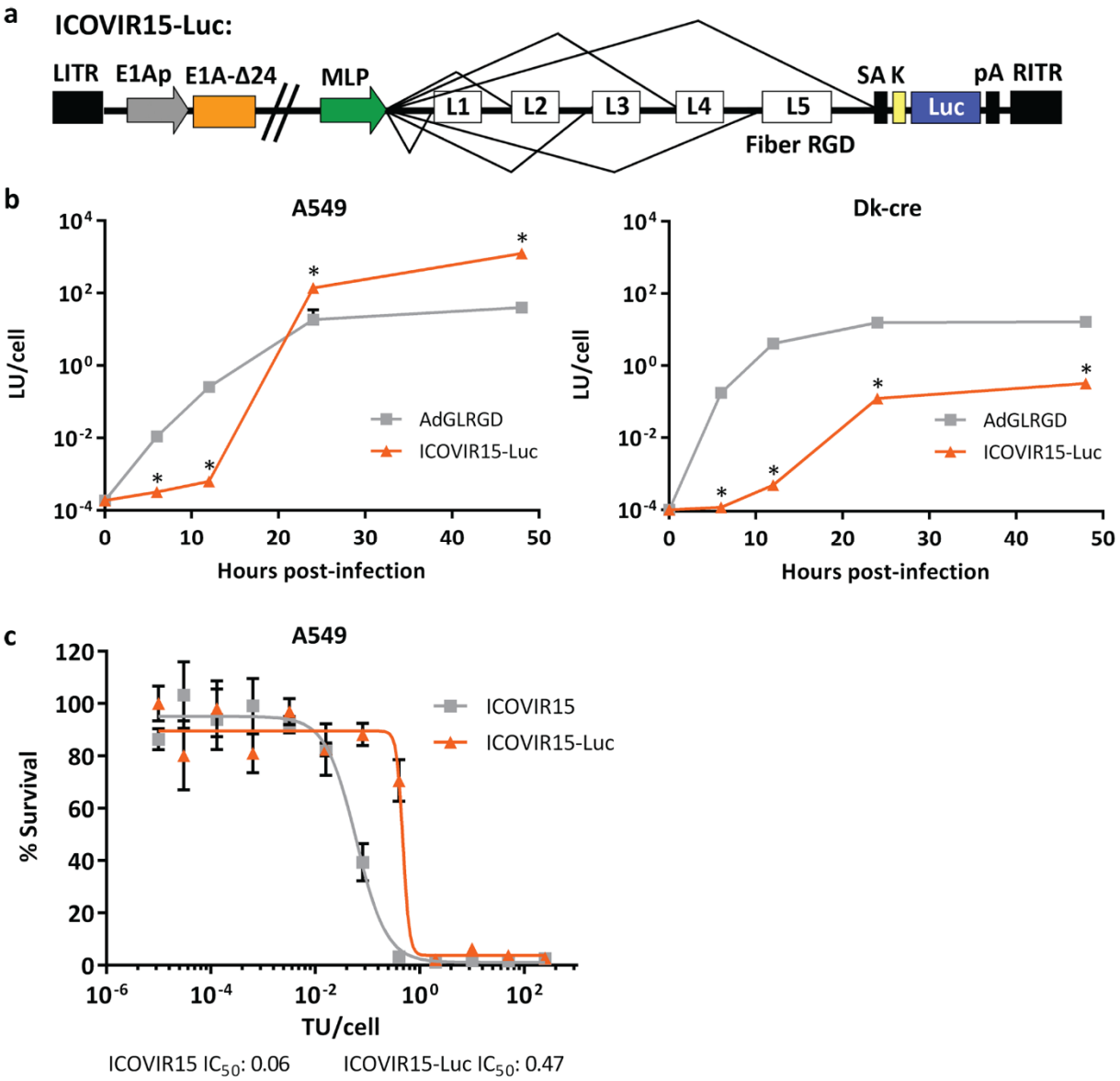

Figure 48. Construction and *in vitro* characterization of ICOVIR15-Luc. (a) Schematic representation of the genome of ICOVIR15-Luc. The luciferase transgene (Luc) was cloned after the fiber gene in the genome of ICOVIR15. To drive the expression under the control of the major late promoter (MLP), a splicing acceptor (SA) and a polyadenylation sequence (pA) were cloned before and after the transgene respectively. A Kozak sequence (K) was also included before the Luc gene to increase the translation efficiency. (b) Luciferase expression kinetics. A549 cells (left) or Dk-cre cells (right) were infected with AdGLRGD or ICOVIR15-Luc at an MOI of 25 TU/cell and 10 TU/cell, respectively. At the indicated time points, cells were lysed and the luciferase activity in the protein extract was measured with a luminometer. Mean values + SD are depicted. *, significant ($p<0.05$) by two-tailed unpaired Student's t-test compared with AdGLRGD. (c) Cytotoxicity. A549 cells were infected with a broad range of MOIs with ICOVIR15 or ICOVIR15-Luc. At day 6 post-infection, cell viability was measured by BCA staining. Dose-response curves are shown along with the IC_{50} values for each virus. Mean values ± SD are plotted.

In a second passive immunization test, nude mice bearing subcutaneous A549 tumors were injected intraperitoneally with 150 µL of PBS or serum #0615 (titer >5120) (naïve or pre-immune groups). Since in the first test the neutralization of the virus was not complete, a higher volume of a more neutralizing serum was used in this case. In addition, the viral dose was reduced to $4x10^{10}$ vp. The next day after immunization, naïve and passively immunized mice were injected with $4x10^{10}$ vp of ICOVIR15-Luc, and a group injected with PBS was also included as negative control. Luciferase expression in mice was monitored and quantified in liver and tumors using IVIS imaging (**Figure 49** and **Figure 50**). At day 3 post-injection, naïve mice showed a strong luciferase signal in the liver and a much lower signal in tumors. Even though ICOVIR15-Luc cannot replicate in normal tissues, a certain level of expression in the absence of replication is expected (as observed in **Figure 48b**), and since most of the injected dose is retained by the liver, a strong signal is generated in this organ. Accordingly, the absence of replication in the liver causes the signal to rapidly drop over time. On the contrary, luciferase signal in the tumor increases notably due to active viral replication, confirming the replication-dependent luciferase expression of ICOVIR15-Luc. Same as the PBS-treated group, pre-immune mice transferred with the neutralizing serum did not show any luciferase signal in the liver nor the tumors throughout the study, suggesting an efficient neutralization of the virus. However, if the luminescence scale is lowered to levels where the signal in naïve mice is highly saturated, we observe a focus of replication in a tumor of a pre-immune mouse that appears at day 12 post-injection, and that increases over time (**Figure 49b**). **Figure 50** shows the quantification of the luciferase signal throughout the study in liver (**Figure 50a**) and tumors (**Figure 50b**), showing positive signal in tumors of pre-immune mice at day 12 that increases until day 24 when mice were sacrificed. Individual plotting of tumors indicated that adenoviral replication occurred in at least two out of four tumors of pre-immune mice (**Figure 50c**). This result indicates that once again, not all the adenovirus dose was neutralized in some mice, and that a very high amount of NAbs needs to be transferred to neutralize such a high viral dose. Nonetheless, the differences in virus replication between naïve and pre-immune mice were noteworthy, and this level of neutralization was thought to be sufficient to inhibit the antitumor efficacy of an oncolytic adenovirus.

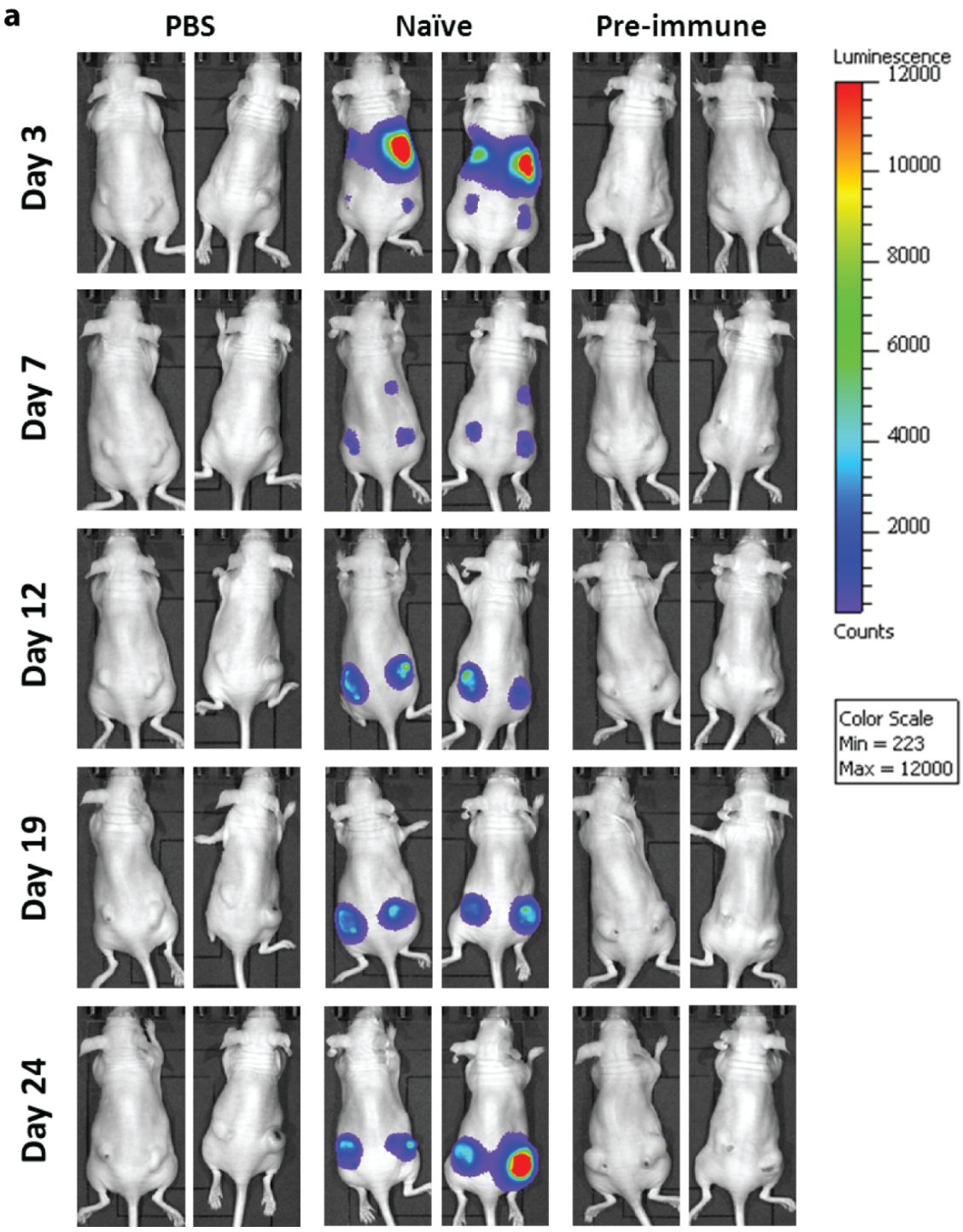
a
PBS
Naïve
Pre-immune
Day 3
Day 7
Day 12
Day 19
Day 24
Luminescence
12000
10000
8000
6000
4000
2000
Counts
Color Scale
Min = 223
Max = 12000

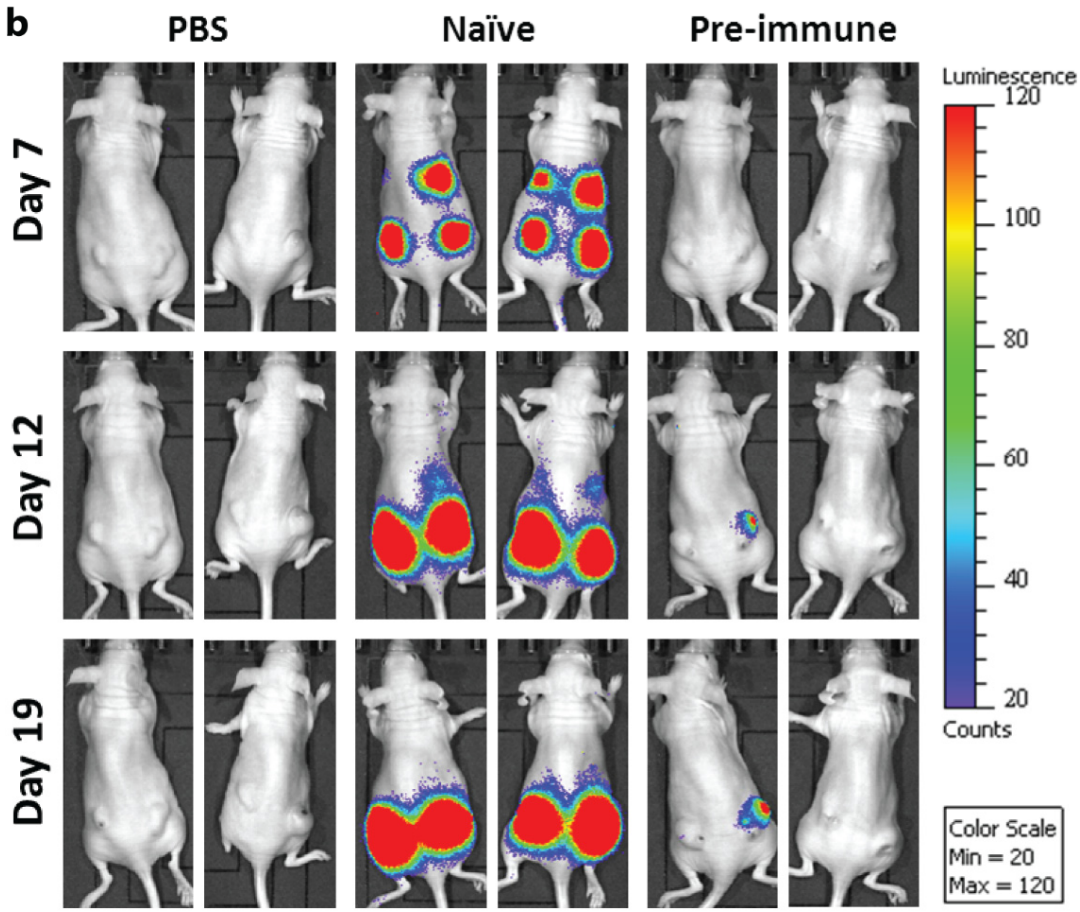

Figure 49. *In vivo* imaging of ICOVIR15-Luc replication in naïve or passively immunized nude mice. Nude mice bearing subcutaneous A549 tumors were injected intraperitoneally with 150 µL of PBS, or anti-Ad5 neutralizing mouse serum (serum #0615). The next day mice received an intravenous injection of PBS, or $4x10^{10}$ vp of ICOVIR15-Luc (n = 2 mice/group). Mice were imaged for luciferase expression at the indicated days after virus injection using (a) the default luminescence color scale (min = 223, max = 12000), or (b) a much lower luminescence color scale (min = 20, max = 120). White light images overlaid with luciferase signal are shown.

2.4.4.4. Passive immunization of nude mice: antitumor efficacy

To test the antitumor activity with the new conditions optimized in the previous section, nude mice bearing subcutaneous A549 tumors were passively immunized with PBS or serum #0615 (titer >5120). The volume of the serum transferred was further increased to 200 µl to achieve higher levels of neutralization. The next day mice received a single intravenous injection of PBS or $4x10^{10}$ vp of ICOVIR15, or ICOVIR15-ABD. No differences were observed in antitumor efficacy between the oncolytic viruses in naïve mice. Both viruses were able to significantly reduce the tumor growth compared to the PBS-treated group, and at the end of the study, ICOVIR15 and ICOVIR15-ABD induced a 2-fold and 1.7-fold reduction in tumor volume respectively (**Figure 51a**). Importantly, in pre-immune mice the non-modified

ICOVIR15 was completely inefficacious, but the oncolytic activity of ICOVIR15-ABD was preserved. At the end of the study, ICOVIR15-ABD induced a 1.9-fold reduction of tumor volume compared to the PBS-treated group and a 2.4-fold reduction compared to the ICOVIR15-treated group. The same experiment was conducted in mice bearing Sk-mel28 melanoma tumors. The stock of serum #0615 was spent in the previous study and to transfer equivalent levels of NAbs, mice were injected with 400 µl of serum #1015 (titer of 2560). The outcome was very similar to that in A549 tumors. Both ICOVIR15 and ICOVIR15-ABD induced a similar antitumor effect in naïve animals, showing a 1.6 and a 1.8-fold reduction of tumor volume respectively. In pre-immune mice, we observed again no impairment in the antitumor activity of ICOVIR15-ABD in presence of neutralizing antibodies, which caused a 1.6-fold reduction of tumor volume compared to ICOVIR15, which totally lost its antitumor effect (**Figure 51b**).

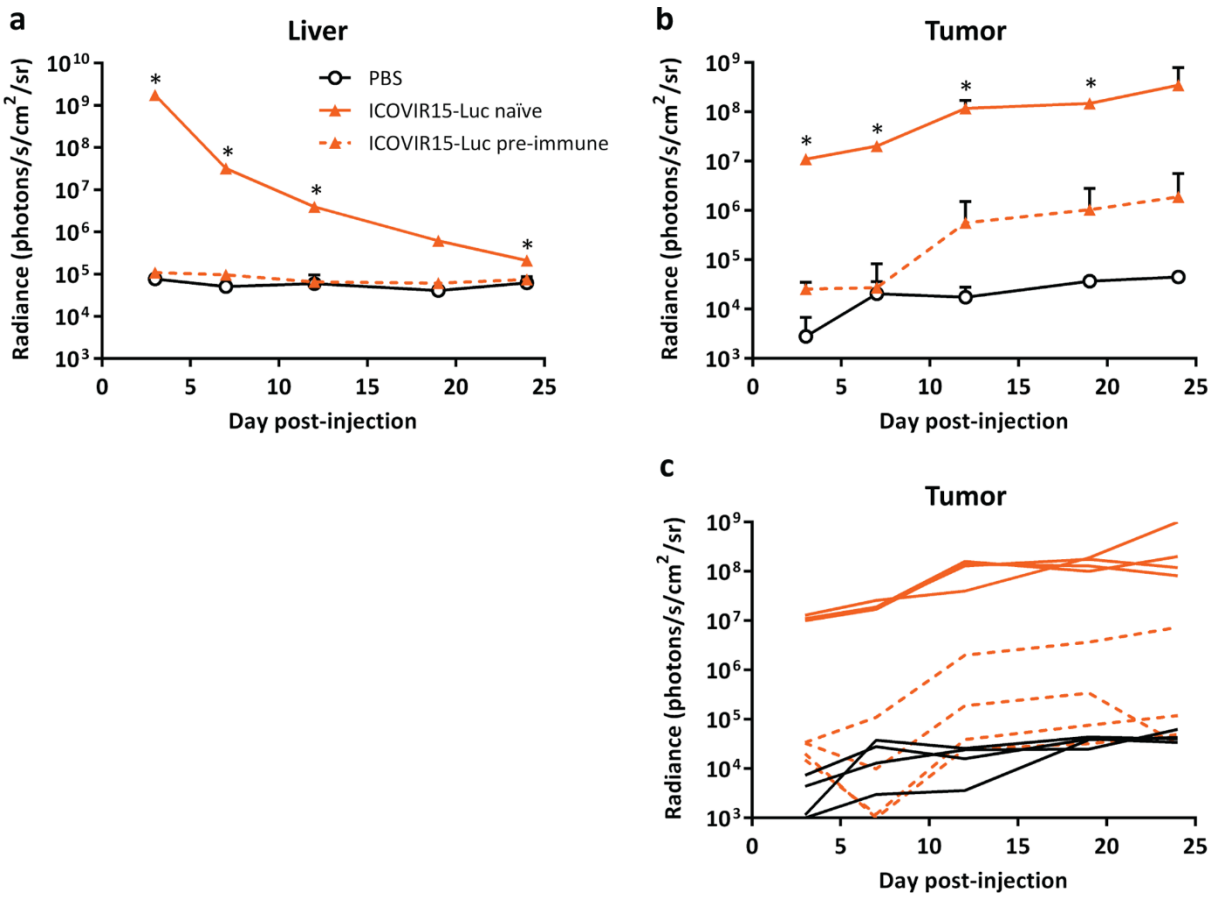

Figure 50. Quantification of luciferase expression in naïve or passively immunized nude mice intravenously injected with ICOVIR15-Luc. Nude mice bearing subcutaneous A549 tumors were injected intraperitoneally with 150 µL of PBS or anti-Ad5 neutralizing mouse serum (serum #0615). The next day mice received an intravenous injection of PBS or $4x10^{10}$ vp of ICOVIR15-Luc (n = 2 mice/group). Quantification of luciferase signal in (a) liver and (b) tumors. Mean values + SD are depicted. *, significant ($p<0.05$) by two-tailed unpaired Student's t-test compared with PBS and ICOVIR15-Luc naïve. (c) Quantification of the luciferase expression of individual tumors.

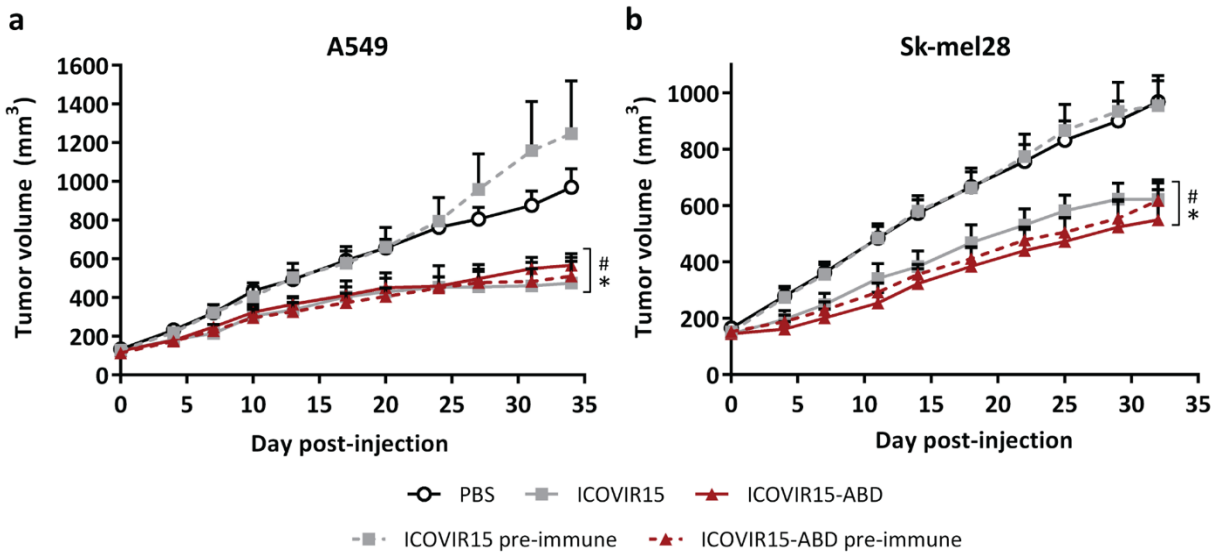

Figure 51. Antitumor efficacy in naïve and passively immunized nude mice. Nude mice bearing subcutaneous xenografts of (a) A549 (lung adenocarcinoma) or (b) Sk-mel28 (melanoma) tumors were injected intraperitoneally with PBS, or anti-Ad5 neutralizing mouse serum (200 µL of serum #0615 for mice bearing A549 tumors, and 400 µL of serum #1015 for mice bearing Sk-mel28 tumors). The day after, mice were treated with a single intravenous injection of PBS or $4x10^{10}$ vp of ICOVIR15 or ICOVIR15-ABD. Mean values of tumor volume + SEM are plotted (n = 10-13 tumors/group). *, significant ($p<0.05$) by two-tailed unpaired Student's t-test compared with PBS (A549 tumors: ICOVIR15 from day 7, ICOVIR15-ABD from day 13, ICOVIR15-ABD from day 10; Sk-mel28 tumors: ICOVIR15 from day 7, ICOVIR15-ABD and ICOVIR15-ABD pre-immune from day 4). #, significant ($p<0.05$) by two-tailed unpaired Student's t-test compared with ICOVIR15 pre-immune (A549 tumors: ICOVIR15 from day 27, ICOVIR15-ABD and ICOVIR15-ABD pre-immune from day 24; Sk-mel28 tumors: ICOVIR15 from day 14, ICOVIR15-ABD and ICOVIR15-ABD pre-immune from day 4).

Besides controlling tumor growth, oncolytic adenovirus treatment was also able to increase mice survival. As shown in **Figure 52**, treatment with ICOVIR15 significantly increased the survival of naïve mice compared to the PBS-treated group in both tumor models, but could not increase the survival of pre-immune mice. ICOVIR15-ABD also increased the survival in naïve mice compared to PBS treatment. In addition, the treatment with ICOVIR15-ABD could also significantly increase the survival of pre-immune mice compared to the PBS and ICOVIR15-treated groups. Overall, these results validate the pre-immune immunodeficient mouse model, and demonstrate again the efficient neutralization escape of the ABD-modified adenovirus.

At the end of the study, mice were sacrificed and tumors were collected for Ad detection. A549 tumors were used for Ad genome detection by quantitative real-time PCR and immunohistochemical staining of E1A viral protein. Intriguingly, the amount of adenovirus detected in tumors did not correlate with the tumor volume at the end of the experiment.

Quantification of Ad genomes in A549 tumors revealed no differences between naïve and pre-immune animals treated with ICOVIR15, which in general contained high amounts of virus genomes in their tumors (**Figure 53**). However, certain heterogeneity is observed and some tumors contained lower viral loads, especially in pre-immune mice. In addition, we could not detect ICOVIR15-ABD genomes in pre-immune mice, and a very low amount in naïve mice, neither group being statistically significant versus the PBS. This result was confirmed by the immune staining of E1A viral protein in paraffin sections of the tumors. Abundant replication foci were observed in tumors of naïve mice treated with ICOVIR15 (**Figure 54**). Pre-immune mice treated with the same virus showed variability as some tumors showed many E1A-stained areas whereas no virus was detected in others. ICOVIR15-ABD could not be detected by E1A staining in tumors of neither naïve nor pre-immune mice.

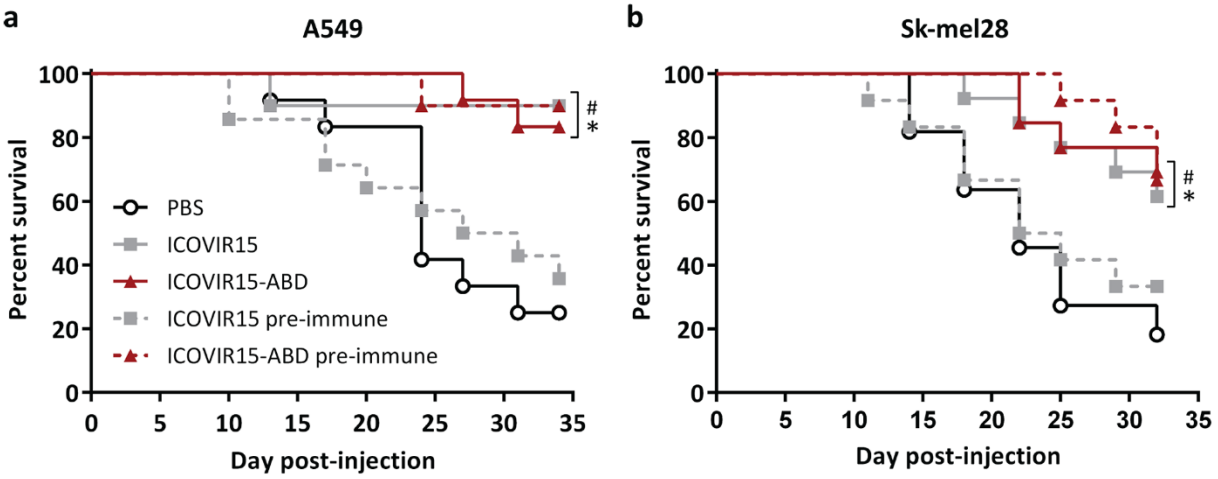

Figure 52. Kaplan-Meier survival curves upon systemic administration of oncolytic adenoviruses in naïve and passively immunized nude mice. Nude mice bearing subcutaneous xenografts of (a) A549 (lung adenocarcinoma) or (b) Sk-mel28 (melanoma) tumors were injected intraperitoneally with PBS or anti-Ad5 neutralizing mouse serum (200 µL of serum #0615 for mice bearing A549 tumors, and 400 µL of serum #1015 for mice bearing Sk-mel28 tumors). The day after, mice were treated with a single intravenous injection with PBS, or $4x10^{10}$ vp of ICOVIR15 or ICOVIR15-ABD. Kaplan-Meier curves are plotted (n = 10-13 tumors/group). End-point was established at 750 mm^3 of tumor volume. *, significant ($p<0.05$) by log-rank test compared with PBS. #, significant ($p<0.05$) by log-rank test compared with ICOVIR15 pre-immune.

Detection of E1A by immunohistochemistry was also performed in Sk-mel28 tumors with a very similar result. Strong E1A staining was observed in naïve mice treated with ICOVIR15 (**Figure 55**). Variability was observed again with in pre-immune mice, showing many replication areas in some tumors whereas very few were detected in others. ICOVIR15-ABD

was barely detected in tumors of naïve mice whereas tumors of pre-immune mice showed some small stained areas.

Figure 53. Adenovirus detection in A549 tumors by real-time PCR. Nude mice bearing subcutaneous xenografts of A549 (lung adenocarcinoma) tumors were injected intraperitoneally with 200 µL of PBS, or anti-Ad5 neutralizing mouse serum (serum #0615). The next day mice were treated with a single intravenous injection with PBS or $4x10^{10}$ vp of ICOVIR15 or ICOVIR15-ABD. At day 34 after virus injection, mice were killed and tumors were collected. Adenovirus genome quantification was performed by real-time PCR of DNA samples extracted from frozen tumors. Mean values are represented by horizontal lines within scatterplots. *, significant ($p<0.05$) by two-tailed unpaired Student's t-test compared with PBS. #, significant ($p<0.05$) by two-tailed unpaired Student's t-test compared with ICOVIR15-ABD. $, significant ($p<0.05$) by two-tailed unpaired Student's t-test compared with ICOVIR15-ABD pre-immune.

To understand this lack of correlation between the amount of virus in tumors and the antitumor efficacy, the same experiment was conducted to detect the adenovirus at a much earlier time point, when fewer rounds of replication had occurred. Nude mice bearing A549 tumors were passively immunized with 300 µL of serum #0416 (titer of 5120), to achieve the same levels of neutralization of the last experiments. The next day mice were treated systemically with PBS or $4x10^{10}$ vp of ICOVIR15, or ICOVIR15-ABD. Mice were sacrificed at day 11 post-injection and adenovirus genomes were detected by real-time PCR, since it is a more quantitative method than immunohistochemistry. In this case, all tumors of naïve mice treated with ICOVIR15 contained high levels of adenovirus genomes, which were significantly higher than in tumors of pre-immune mice (**Figure 56**). Unlike in naïve mice, the amount of ICOVIR15 genomes in pre-immune mice at day 11 was significantly lower than at day 34. In fact, there were no significant differences between the PBS and the ICOVIR15 pre-immune

groups. In contrast, ICOVIR15-ABD genomes could be detected in tumors of both naïve and pre-immune mice at higher levels than ICOVIR15 in pre-immune mice. Nevertheless, the levels of ICOVIR15-ABD in naïve and pre-immune mice were lower compared to those of ICOVIR15 in naïve mice.

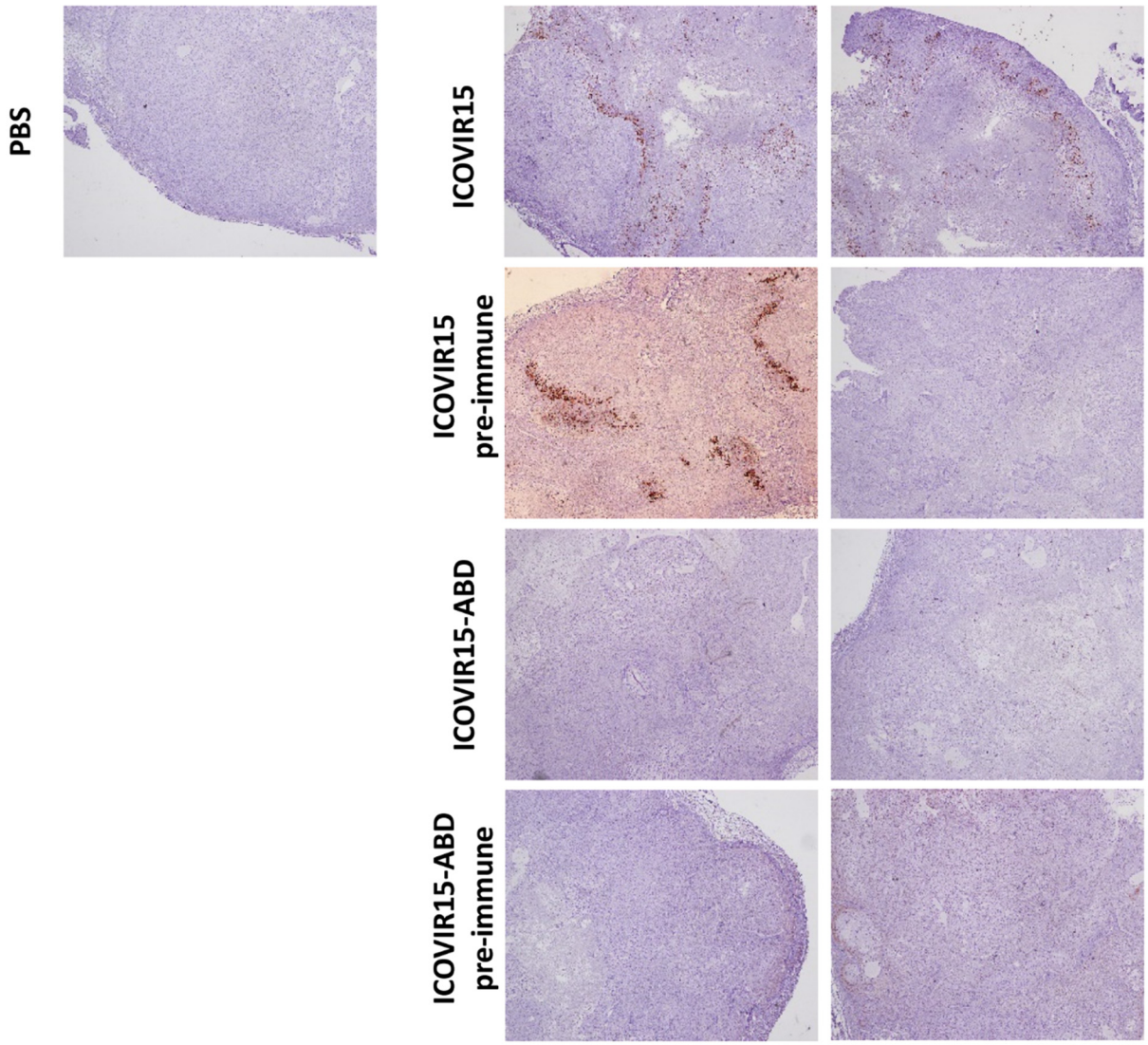

Figure 54. Adenovirus detection in A549 tumors by immunohistochemistry. Nude mice bearing subcutaneous xenografts of A549 (lung adenocarcinoma) tumors were injected intraperitoneally with 200 µL of PBS or anti-Ad5 neutralizing mouse serum (serum #0615). The next day mice were treated with a single intravenous injection with PBS or $4x10^{10}$ vp of ICOVIR15, or ICOVIR15-ABD. At day 34 after virus injection, mice were killed and tumors were collected. Immunohistochemistry of E1A viral protein was performed in paraffin embedded tumor sections. Original magnification, 4X.

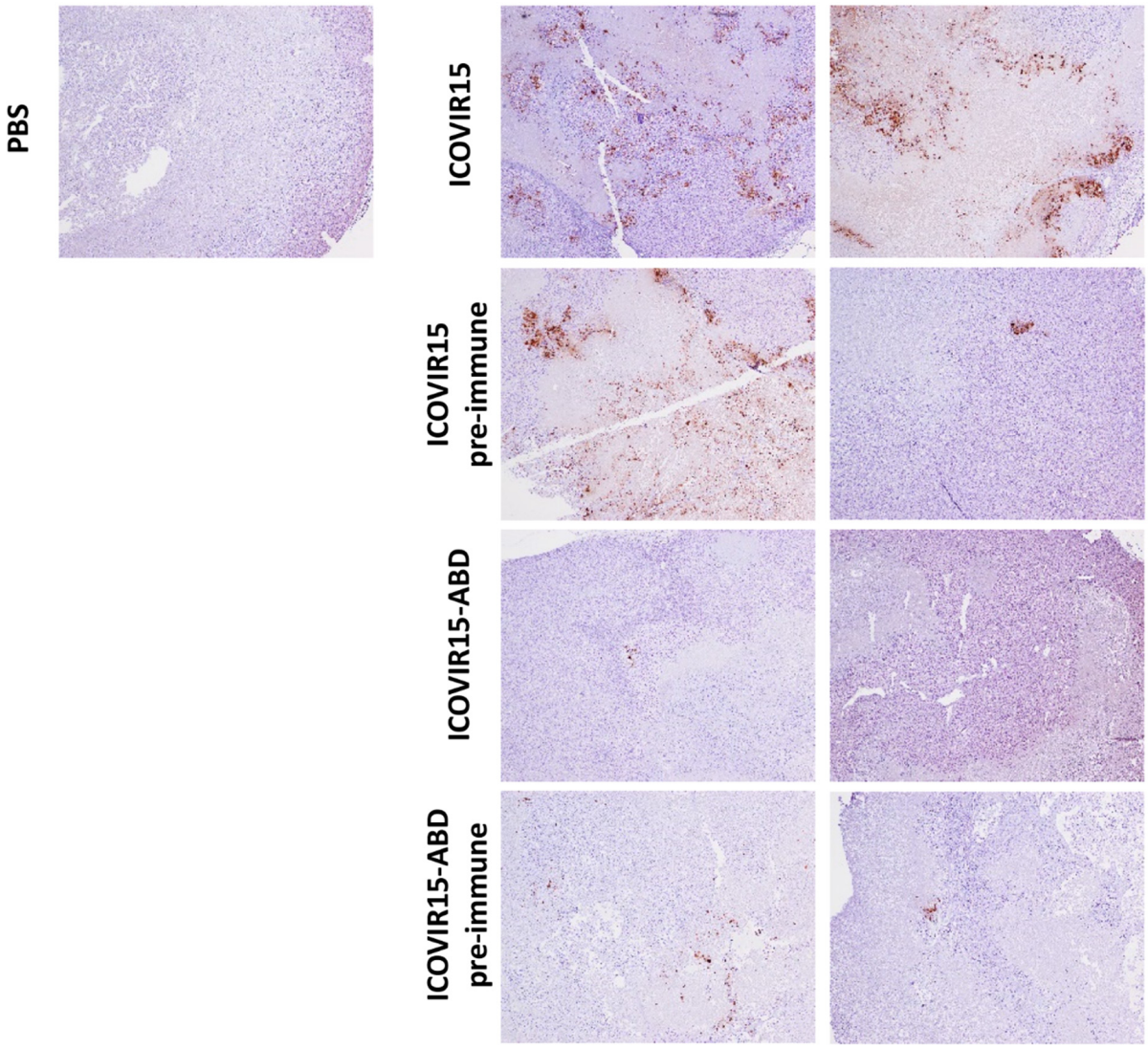

Figure 55. Adenovirus detection in Sk-mel28 tumors by immunohistochemistry. Nude mice bearing subcutaneous xenografts of Sk-mel28 (melanoma) tumors were injected intraperitoneally with 400 µL of PBS, or anti-Ad5 neutralizing mouse serum (serum #1015). The next day mice were treated with a single intravenous injection with PBS or $4x10^{10}$ vp of ICOVIR15, or ICOVIR15-ABD. At day 32 after virus injection, mice were killed and tumors were collected. Immunohistochemistry of E1A viral protein was performed in paraffin embedded tumor sections. Original magnification, 4X.

These differences in the amount of adenovirus genomes at day 11 and day 34 suggest a quicker clearance of the ABD-modified virus from tumors, probably related to the lower production and replication of this virus combined with the stromal barriers present in tumors (**Figure 57**). In addition, it can be observed that the neutralization of ICOVIR15 was not complete (as previously observed with ICOVIR15-Luc, see **Figure 49b**) and the small amount

of virus that reaches tumors can eventually replicate, albeit is incapable of controlling tumor growth. This matter will be addressed in depth in the Discussion section.

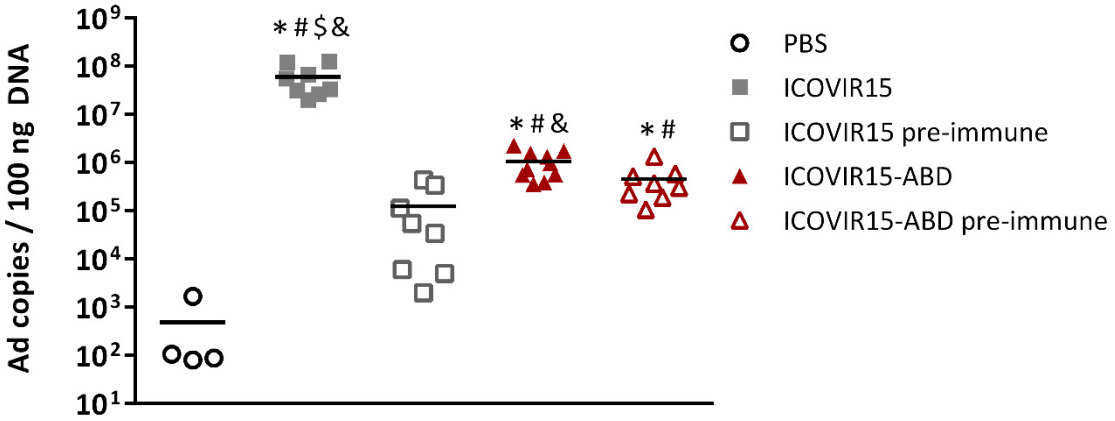

Figure 56. Early detection of adenovirus in A549 tumors by real-time PCR. Nude mice bearing subcutaneous xenografts of A549 (lung adenocarcinoma) tumors were injected intraperitoneally with 300 µL of PBS, or anti-Ad5 neutralizing mouse serum (serum #0416). The next day mice were treated with a single intravenous injection with PBS or $4x10^{10}$ vp of ICOVIR15, or ICOVIR15-ABD. At day 11 after virus injection, mice were killed and tumors were collected. Adenovirus genome quantification was performed by real-time PCR of DNA samples extracted from frozen tumors (n = 4-8 tumors/group). Mean values are represented by horizontal lines within scatterplots. *, significant ($p<0.05$) by two-tailed unpaired Student's t-test compared with PBS. #, significant ($p<0.05$) by two-tailed unpaired Student's t-test compared with ICOVIR15 pre-immune. $, significant ($p<0.05$) by two-tailed unpaired Student's t-test compared with ICOVIR15-ABD. &, significant ($p<0.05$) by two-tailed unpaired Student's t-test compared with ICOVIR15-ABD pre-immune.

2.4.5. Immune response against proteins expressed from the viral genome in pre-immune mice

Recombinant adenoviruses are also used as vaccine platforms, which also face the problem of pre-existing NAbs. Neutralization of the vector impairs transgene expression and therefore, no immune response can be mounted against the desired antigen. We hypothesized that the ABD insertion could also be useful in the field of adenovirus-based vaccines. To demonstrate this, we analyzed the CTL immune response generated against a protein expressed from the virus genome in naïve and anti-Ad5 pre-immune mice. E1b was chosen as a model protein, emulating the antigen against which we want to generate immunity. C57BL/6 mice were immunized with an intraperitoneal injection of $3x10^{10}$ vp of AdGL. Immunization with this vector allows the generation of anti-Ad5 NAbs, and being an E1-

deleted vector it avoids generating immunity against E1b, which would interfere in the experiment outcome. Seven days after immunization mice were injected intravenously with $3x10^{10}$ vp of the oncolytic adenoviruses ICOVIR15 or ICOVIR15-ABD, both containing E1b. Mice were sacrificed seven days after, and specific immune responses against $E1b_{192}$ viral epitope were assessed by ELISPOT. As expected, mice treated with ICOVIR15 could not generate a very high immune response against E1b due to the neutralization of the virus by NAbs (**Figure 58**). In contrast, the anti-E1b immune response in mice treated with ICOVIR15-ABD was significantly higher (5.5-fold), indicating that pre-existing anti-adenovirus immunity cannot prevent the immunogenicity of a transgene encoded in an ABD-modified virus. This experiment included an additional group that will be explained in the readministration section (see **Figure 61**).

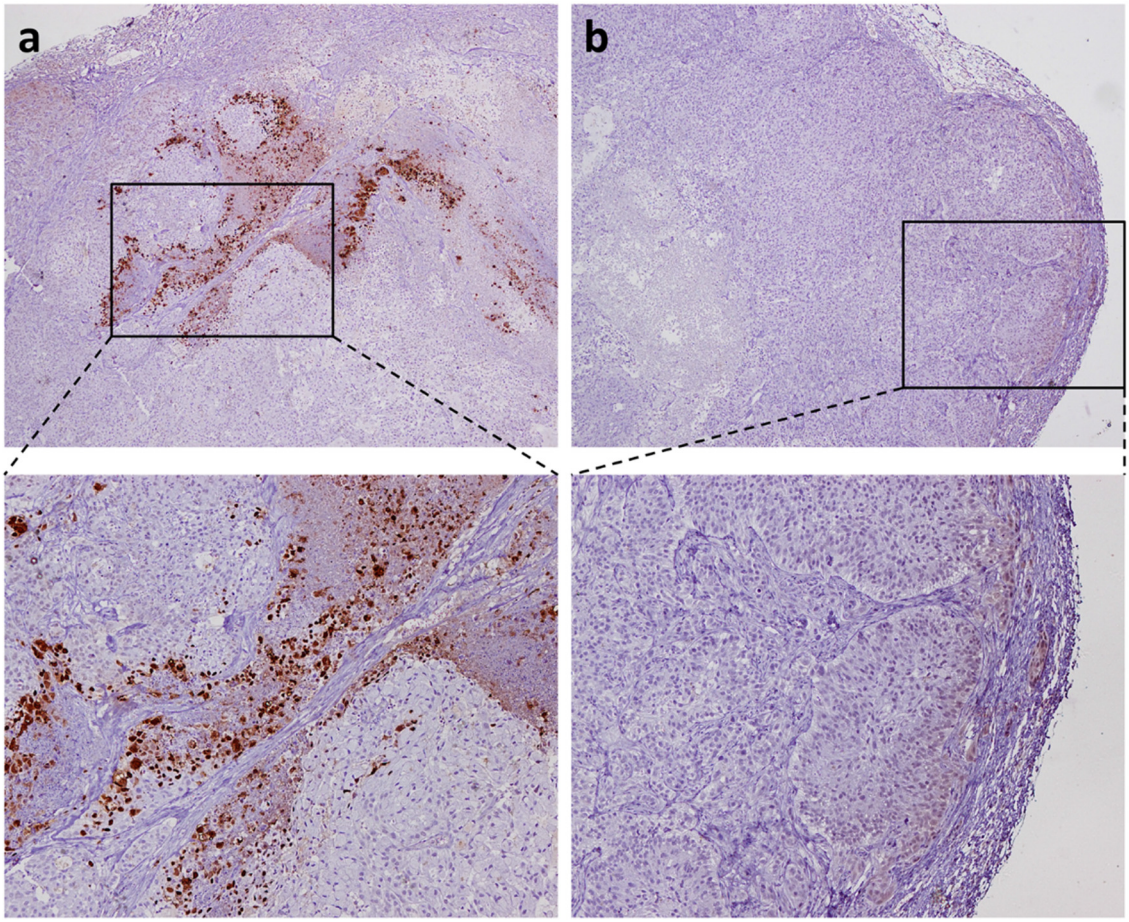

Figure 57. Stroma barriers present in A549 subcutaneous tumors. Immunohistochemistry of E1A viral protein in A549 tumors treated with (a) ICOVIR15 or (b) ICOVIR15-ABD at day 34 after virus injection. Lower panels show magnifications where stromal barriers formed by fibroblast can be observed. Upper panels magnification, 4X. Lower panels magnification, 10X.

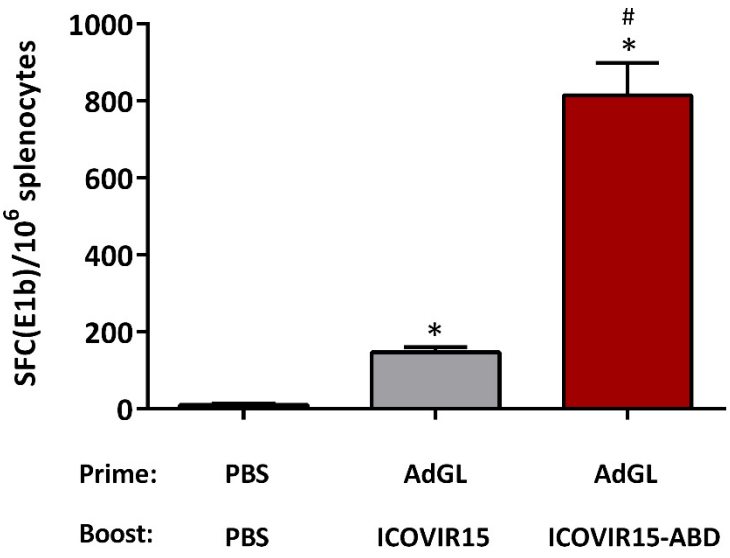

Figure 58. Immune response against E1b protein expressed from the viral genome in pre-immune mice. C57BL/6 mice were immunized with an intraperitoneal injection of the E1-deleted vector AdGL ($3x10^{10}$ vp), and seven days later were injected intravenously with ICOVIR15 or ICOVIR15-ABD ($3x10^{10}$ vp). Seven days after, animals were euthanized and splenocytes were isolated. Specific responses against $E1b_{192}$ peptide were analyzed by anti-IFN-γ ELISpot technique. Mean + SEM is plotted (n = 3 mice/group). *, significant ($p<0.05$) by two-tailed unpaired Student's t-test compared with PBS. #, significant ($p<0.05$) by two-tailed unpaired Student's t-test compared with AdGL + ICOVIR15.

2.5. READMINISTRATION STUDY OF AN ABD-MODIFIED ADENOVIRUS

Pre-existing immunity represents a major obstacle for adenovirus-based therapies. As we have observed, pre-existing anti-Ad5 NAbs can inhibit the bioactivity of the vector, severely compromising the efficacy of the treatment. In addition, another major problem is the readministration of the vector. Even if the patient has no pre-existing immunity, the first administration of the virus will generate NAbs and memory cells that will efficiently inactivate a second viral dose. We have already demonstrated the ability of an ABD-modified adenovirus type 5 to successfully evade pre-existing NAbs due to albumin shielding. The next question was whether this virus can escape neutralization from NAbs generated against its own capsid. In this section, we present a preliminary study where the feasibility of readministration of an ABD-modified adenovirus is analyzed.

2.5.1. Generation of neutralizing antibodies against an ABD-modified capsid

To study the NAbs generated against an adenovirus bearing the ABD insertion in the HVR1 of the hexon, C57BL/6 immunocompetent mice were immunized with AdGLRGD-ABD using a prime and boost regimen as previously explained (see section 2.4.1.3). Two different serum batches obtained at different dates were analyzed. These sera were tittered in HEK293 cells against the AdGLRGD-ABD vector in the absence of albumin (**Figure 59**). The specific titer of the serum #0415 could not be determined due to its high neutralizing activity, and at the highest dilution (5120) the 86% of the virus was neutralized. For this reason, the serum #0515 was tittered using a much higher starting dilution. However, the neutralizing activity of this serum was even higher, being able to neutralize the 71% of the virus at a dilution of 51,200. These analyses reveal that mice immunized with an ABD-modified adenovirus develop a high neutralizing response against this virus.

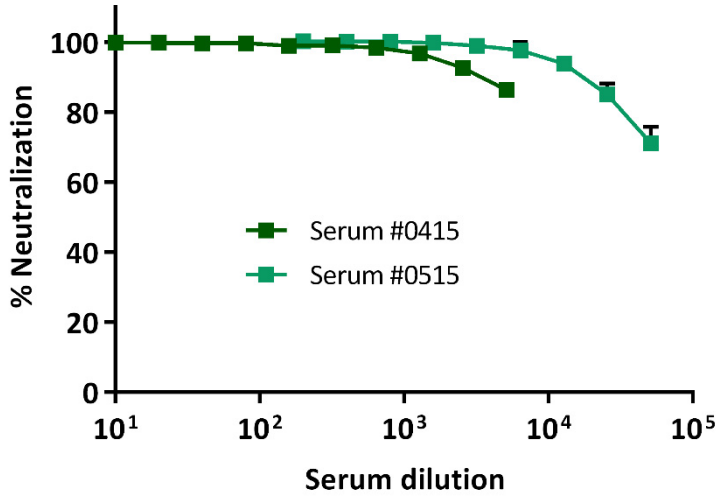

Figure 59. Neutralizing activity of anti-ABD-modified adenovirus serum. Neutralizing sera were obtained by immunization of C57BL/6 immunocompetent mice with AdGLRGD-ABD using a prime and boost regimen. Serum titration was performed by incubating AdGLRGD-ABD with serial 1/2 dilutions of the serum and analyzing the transduction in HEK293 cells using an MOI of 0.25 TU/cell. A control without serum was included to obtain the 0% neutralization value. Two different serum batches were compared. Titration curves are shown. Mean + SD.

2.5.2. *In vitro* evasion of neutralizing antibodies against an ABD-modified capsid

We next evaluated if albumin can protect the ABD adenovirus from NAbs generated against its own capsid. AdGLRGD and AdGLRGD-ABD, in absence or presence of HSA, were

incubated with serial dilutions of serum and used to transduce 293 cells. The absence of HSA condition was not tested in previous experiments where serum was used, due to the high mouse albumin content in serum. However, this albumin content will be reduced with each dilution. For this reason, we included the absence of HSA condition in this case to try to observe a difference in protection. Surprisingly, the neutralizing activity of this serum against the parental vector AdGLRGD was significantly lower compared to AdGLRGD-ABD (**Figure 60**). This suggests either that the majority of the NAbs in this serum are targeted against the ABD, or that those NAbs against the ABD have a very high neutralizing activity. Nevertheless, the transduction of AdGLRGD-ABD was remarkably enhanced in the conditions where HSA was present and the albumin of the serum had been highly diluted. This demonstrates that albumin can also protect the ABD-modified adenovirus from the NAbs generated against its own capsid. However, the high neutralizing activity of these NAbs might still represent a problem for the readministration of the virus. In order to elucidate this, we proceeded to test a readministration schedule *in vivo.*

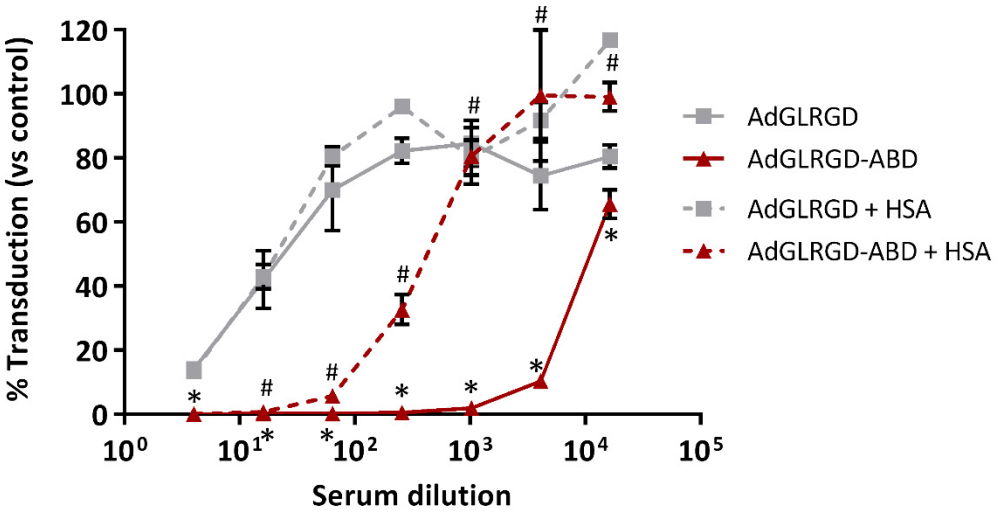

Figure 60. ***In vitro*** **evasion of anti-ABD-modified adenovirus neutralizing mouse serum.** Transduction analysis after incubation with anti-ABD-modified adenovirus neutralizing mouse serum. AdGLRGD or AdGLRGD-ABD, in the presence or absence of HSA, were incubated with serial dilutions of the serum for 1 hour, and then used to infect HEK293 cells at 10 vp/cell. Luciferase expression was analyzed 24 hours after infection. A control without serum was included to obtain the 100 % infection value. Results are represented as % transduction versus the 100 % infection control. Mean ± SD. *, significant ($p<0.05$) by two-tailed unpaired Student's t-test compared with AdGLRGD and AdGLRGD + HSA. #, significant ($p<0.05$) by two-tailed unpaired Student's t-test compared with AdGLRGD-ABD.

2.5.3. *In vivo* liver transduction after adenovirus readministration

To test the feasibility of the readministration *in vivo*, the liver was used as a reporter organ for the transduction of the vectors after generating NAbs against their own capsid in immunocompetent mice. C57BL/6 mice received an intravenous injection of $3x10^{10}$ vp of ICOVIR15 or ICOVIR15-ABD, and seven days later another intravenous injection of $3x10^{10}$ vp of AdGLRGD or AdGLRGD-ABD, respectively. The luciferase expression in the liver was analyzed three days later by *in vivo* imaging system (IVIS). Neither vector displayed detectable luciferase signal in the liver (data now shown), indicating that both viruses were efficiently neutralized by the NAbs generated in the first injection. However, our previous results of passive immunization of nude mice showed that luciferase expression at day 3 post-injection is not a reliable method to detect adenovirus neutralization. Albeit most of the virus is probably neutralized in this case, small levels of liver transduction might be lost using this readout.

2.5.4. Immune response against proteins expressed from the adenovirus genome after readministration

The feasibility of the readministration was also tested by detecting the immune response generated against E1b protein, after generating NAbs against a non-ABD- and an ABD-modified adenovirus in immunocompetent mice, as previously performed in section 2.4.5. In the experiment presented in that section, another group was included to test the readministration of the ABD-modified virus. The same results with this additional group is now presented in **Figure 61**. C57BL/6 mice were immunized with an intraperitoneal injection of $3x10^{10}$ vp of the E1-deleted vectors AdGL or AdGL-ABD, to avoid generating immunity against E1b. Seven days later, mice immunized with AdGL were injected intravenously with $3x10^{10}$ vp of ICOVIR15 or ICOVIR15-ABD, and mice immunized with AdGL-ABD were injected only with $3x10^{10}$ vp of ICOVIR15-ABD. Seven days after mice were sacrificed and quantitation of CTL immune responses against $E1b_{192}$ viral epitope was performed by ELISPOT (**Figure 61**). As expected, the anti-E1b immune response after the injection of ICOVIR15-ABD was significantly lower in mice pre-injected with AdGL-ABD than in those pre-injected with AdGL (2.4-fold), indicating that the ABD-modified adenovirus can evade much more efficiently the NAbs generated against the wt capsid than those generated against the ABD capsid. Importantly, we also observed that the immune response generated against ICOVIR15-ABD in mice pre-injected with AdGL-ABD was 2.3-fold higher than that generated against ICOVIR15 in mice pre-injected with AdGL, although this difference was not statistically significant.

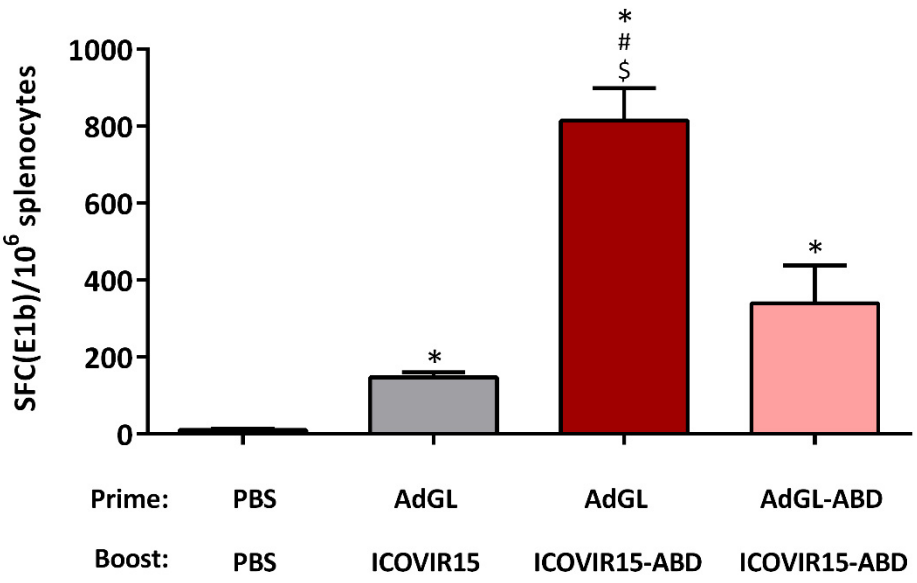

Figure 61. Immune response against E1b protein expressed from the viral genome after readministration. C57BL/6 mice were immunized with an intraperitoneal injection of the E1-deleted vectors AdGL or AdGL-ABD ($3x10^{10}$ vp). Seven days later mice immunized with AdGL were injected intravenously with ICOVIR15 or ICOVIR15-ABD ($3x10^{10}$ vp), and mice immunized with AdGL-ABD were injected intravenously with ICOVIR15-ABD ($3x10^{10}$ vp). Seven days after, animals were euthanized and splenocytes were isolated. Specific responses against $E1b_{192}$ peptide were analyzed by anti-IFN-γ ELISpot technique. Mean + SEM is plotted (n = 3 mice/group). *, significant ($p<0.05$) by two-tailed unpaired Student's t-test compared with PBS. #, significant ($p<0.05$) by two-tailed unpaired Student's t-test compared with AdGL + ICOVIR15. $, significant ($p<0.05$) by two-tailed unpaired Student's t-test compared with AdGL-ABD + ICOVIR15-ABD.

At the end of the study, mice were killed, and the serum of those mice pre-injected with AdGL and then treated with ICOVIR15-ABD was collected and pooled for *in vitro* neutralization studies. This situation mimics the ability of the virus to evade the NAbs of a subject with anti-Ad5 pre-immunity that had been treated with an ABD-modified adenovirus, which would be the more realistic situation of readministration (due to the high prevalence of anti-Ad5 NAbs in humans). AdGLRGD and AdGLRGD-ABD, in absence or presence of HSA, were incubated with serial dilutions of the serum and used to transduce 293 cells. In contrast to the serum of a mouse only immunized with an ABD-modified adenovirus, the neutralizing activity of this serum versus the AdGLRGD was very high (titer of 12,800) (**Figure 62**), even higher than the other sera previously generated immunizing with the Ad5wt (see **Figure 45**). In the absence of albumin, the AdGLRGD-ABD was more neutralized than the non-modified vector, demonstrating again the high neutralizing activity of the NAbs directed against the ABD.

However, it is worthy of note the transduction increase of the ABD-modified vector in the presence of HSA, showing higher transduction efficiencies than the non-modified vector.

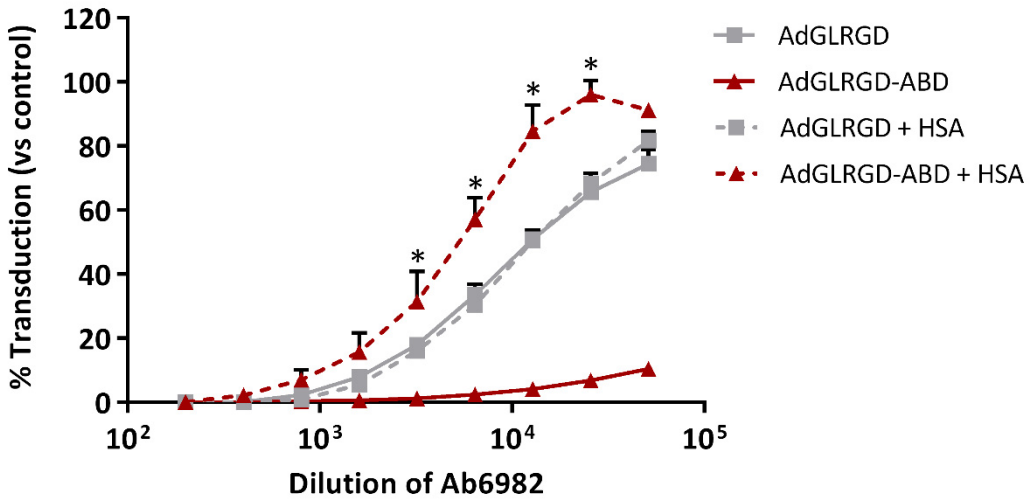

Figure 62. *In vitro* evasion of a serum of a mouse primed with AdGL and boosted with ICOVIR15-ABD. AdGLRGD or AdGLRGD-ABD, in the presence or absence of HSA, were incubated with serial dilutions of the serum of a mouse primed with AdGL and boosted with ICOVIR15-ABD. After 1 hour incubation, vectors were used to transduce HEK293 cells at 10 vp/cell. Luciferase expression was analyzed 24 hours after infection. A control without serum was included to obtain the 100 % infection value. Results are represented as % transduction versus the 100 % infection control. Mean ± SD. *, significant ($p<0.05$) by two-tailed unpaired Student's t-test compared with all groups.

Overall, these results indicate that there is a partial escape from the NAbs generated against the ABD capsid. Despite the protection is not as efficient as it is against anti-Ad5 pre-existing NAbs, the ABD-modified adenovirus still presents an advantage in terms of readministration compared to a non-modified adenovirus. In any case, these results were preliminary and a more thorough study including antitumor activity after readministration is required to draw solid conclusion on this subject.

2.6. COMBINATION OF THE ABD INSERTION WITH THE REPLACEMENT OF THE FIBER SHAFT HSG-BINDING MOTIF WITH RGD

2.6.1. Construction of the oncolytic adenovirus ICOVIR15K-ABD

The heparan sulfate glycosaminoglycan (HSG)-binding motif KKTK in the shaft of the fiber plays an important role in the hepatic tropism of the type 5 adenovirus (Bayo-Puxan et al.,

2006; Smith et al., 2003). Our group has previously published the replacement of this KKTK domain with an RGDK motif (Bayo-Puxan et al., 2009). In the context of an adenoviral vector expressing luciferase, this mutation reduced liver transduction and increased tumor transduction compared with a non-modified vector after intravenous administration. Thus, this modification offers simultaneously liver detargeting and tumor targeting properties. In the context of the oncolytic adenovirus ICOVIR15, the RGDK mutation increased the bioavailability and the antitumor efficacy, compared with its counterpart presenting the HI-loop RGD-modified fiber (Rojas et al., 2012). For this reason, ICOVIR15K became the standard oncolytic platform in our group where new modifications are usually tested. Nevertheless, the location of the RGD in the fiber shaft of ICOVIR15K is very close to the penton base, and albumin binding to neighboring hexons might compromise the exposure of the motif and therefore the interaction with cell receptors. For this reason, the ABD insertion was first tested in the ICOVIR15 platform, where the RGD would be well exposed (**Figure 63)**. In this section, we studied the compatibility of the ABD insertion with the RGDK mutation. The ABD was inserted in the HVR1 of the hexon of ICOVIR15K by homologous recombination in bacteria, and the plasmid was transfected into HEK293 cells for virus generation. ICOVIR15K-ABD was successfully rescued, amplified, and purified for *in vitro* and *in vivo* studies.

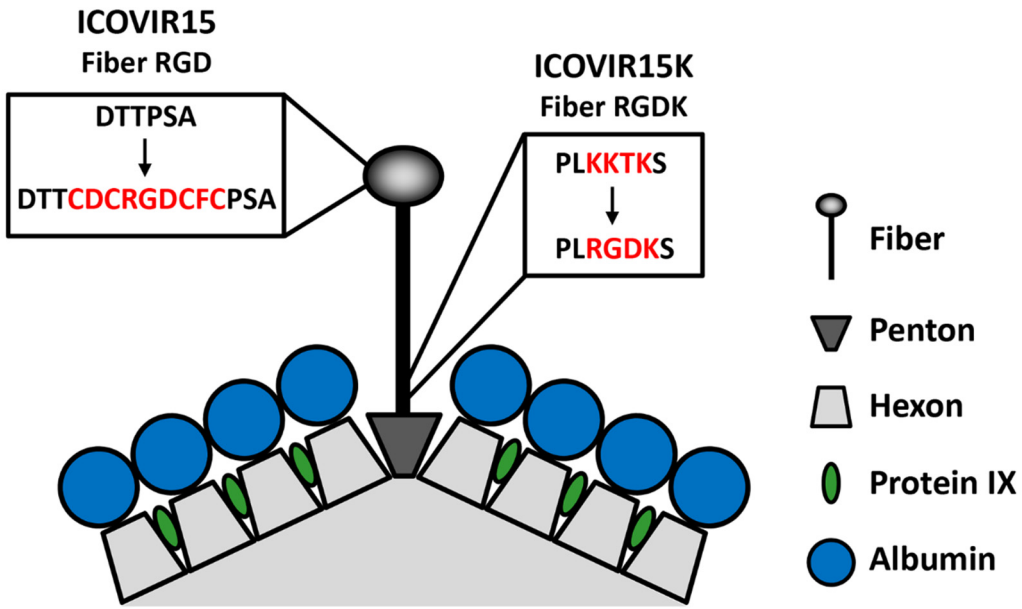

Figure 63. Schematic representation of fiber RGD and fiber RGDK in an ABD-modified capsid. RGD fiber, contained in ICOVIR15 and ICOVIR15-ABD, incorporates the motif CDCRGDCFC (RGD-4C) in the HI-loop of the knob domain of the fiber. In the viruses containing the RGDK fiber, namely ICOVIR15K and ICOVIR15K-ABD, this insertion is deleted and the RGD is incorporated replacing the KKTK of the shaft of the fiber. In the latter location, the RGD exposure might be compromised by the binding of albumin to neighboring hexons.

2.6.2. Cytotoxicity of ICOVIR15K-ABD in the presence and absence of HSA

It was previously observed that in the absence of NAbs albumin binding not only caused a reduction in cell transduction, but as a consequence, the cytotoxicity of the virus was also diminished. For this reason, we first analyzed the effect of albumin binding on the cytotoxicity of ICOVIR15K-ABD compared to that of ICOVIR15-ABD. A549 cells were infected with different MOIs, in normal or in HSA-containing medium, and 6 days later the percentage of cell survival was quantified. In the absence of albumin, both oncolytic viruses showed a very similar cytotoxic activity (**Figure 64**). As previously observed (**see Figure 31**), albumin binding caused a reduction in the cytotoxicity of both ABD-modified adenoviruses. However, the cytotoxicity of ICOVIR15K-ABD was much more diminished by albumin binding than that of ICOVIR15-ABD, suffering a 26-fold versus a 7-fold reduction respectively. This notable decrease in the replication capacity of the RGDK-modified virus suggests an interference of albumin in the interaction between the RGD and cell integrins, likely causing a reduction in cell transduction and consequently, in the cytotoxicity of the virus.

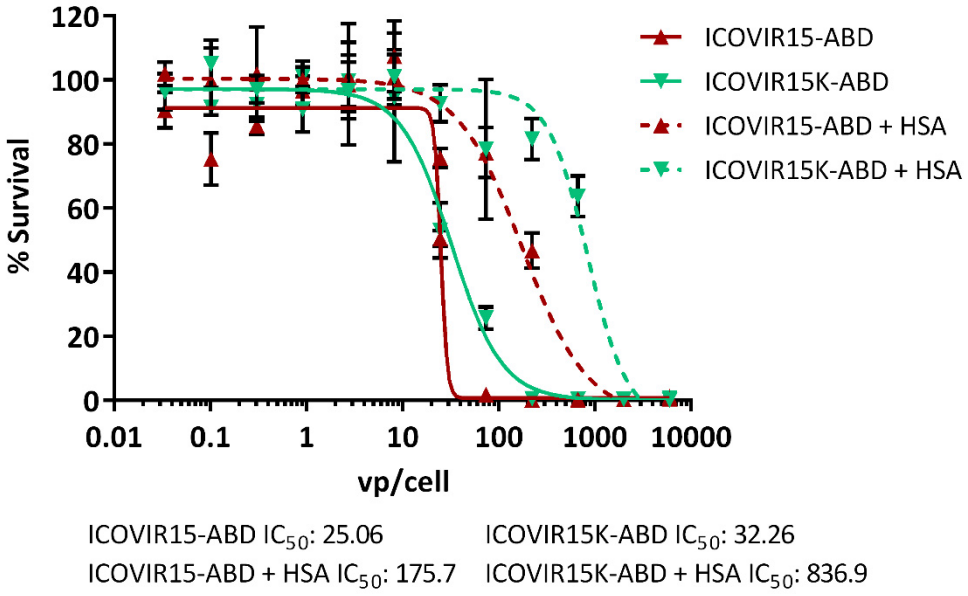

Figure 64. Comparative cytotoxicity of ICOVIR15K-ABD and ICOVIR15-ABD in the presence or absence of HSA. A549 cells were infected with serial dilutions of ICOVIR15 or ICOVIR15-ABD in the absence or presence of HSA at 1 mg/mL. At day 6 post-infection, cell viability was measured by BCA staining (n = 3). Dose-response curves are shown along with the IC_{50} values for each virus and condition. Mean values ± SD are plotted.

2.6.3. *In vitro* evasion of neutralizing antibodies by ICOVIR15K-ABD

The ability of the ABD to protect the virus from neutralization was also analyzed in the RGDK-modified capsid. The oncolytic adenoviruses, in the presence or absence of albumin, were incubated with serial dilutions of Ab6982, and then used to transduce 293 cells. Since no reporter vector was generated with this capsid, the number of transduced cells was determined by anti-hexon staining method 36 hours after infection. The evasion of ICOVIR15K-ABD was compared to that of ICOVIR15-ABD, and the parental RGDK virus lacking the ABD (ICOVIR15K) was also included as control. As shown in **Figure 65**, the non-ABD virus ICOVIR15K was highly neutralized at all the dilutions tested compared to both viruses containing ABD, which efficiently evaded the NAbs. In addition, there were no differences in the evasion of neutralization between ICOVIR15-ABD and ICOVIR15K-ABD, indicating that the ABD can also efficiently protect an RGDK-modified capsid.

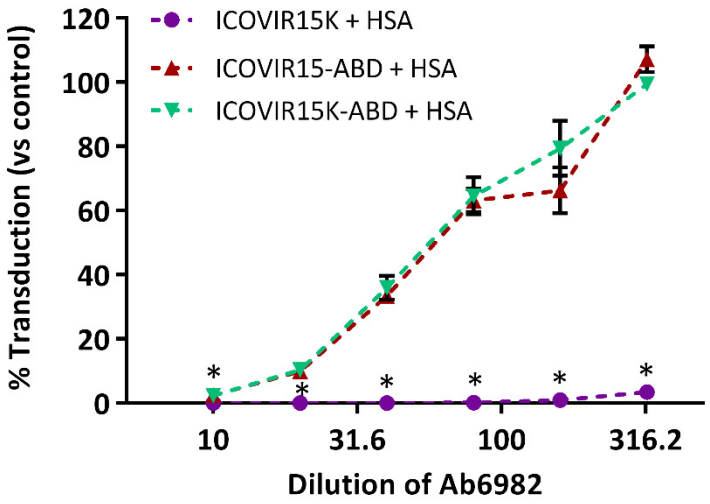

Figure 65. *In vitro* transduction of ICOVIR15K-ABD in presence of Ab6982. Oncolytic adenoviruses ICOVIR15K, ICOVIR15-ABD, and ICOVIR15K-ABD, were incubated with serial dilutions of the polyclonal neutralizing antibody Ab6982 in the presence of HSA. After 1 hour incubation, the viruses were used to infect HEK293 cells at 10 vp/cell. Cell transduction was analyzed at 36 hours post-infection by anti-hexon staining method. A control without Ab6982 was included to obtain the 100 % infection value. Results are represented as % transduction versus the 100 % infection control. Mean values ± SD. *, significant ($p<0.05$) by two-tailed unpaired Student's t-test compared with all groups.

2.6.4. Antitumor activity of ICOVIR15K-ABD in pre-immune mice after systemic administration

The RGDK mutation represented a significant improvement in the antitumor efficacy of ICOVIR15 after the systemic administration (Rojas et al., 2012). However, this might not be the case in ABD-modified adenoviruses due to the hypothetic interference of albumin with the interaction of the RGD motif with cell receptors. To analyze such effect, we compared the antitumor efficacy of ICOVIR15-ABD and ICOVIR15K-ABD in mice bearing subcutaneous NP-18 pancreatic cancer tumors, a tumor model where ICOVIR15K showed a significant advantage over ICOVIR15 (Rojas et al., 2012). In addition, mice were passively immunized to also test the ability of ICOVIR15K-ABD to overcome pre-existing immunity *in vivo*. To achieve similar levels of neutralization as in previous studies, mice were injected intraperitoneally with 300 µL of serum #0416 (titer of 5120). The next day mice received an intravenous injection of PBS or $4x10^{10}$ vp of ICOVIR15-ABD, or ICOVIR15K-ABD. Both oncolytic viruses were able to significantly reduce the tumor growth compared to the PBS-treated group, indicating an efficient escape of NAbs *in vivo* (**Figure 66a**). However, no significant differences were observed in the antitumor efficacy of the viruses. Furthermore, the analysis of survival curves showed the same result: both viral treatments had a significant effect in prolonging survival with respect to PBS group, but no differences were observed between the oncolytic viruses (**Figure 66b**). These results indicate that the advantage provided by the RGDK fiber is lost in an ABD-modified adenovirus. The cytotoxicity loss due to albumin binding was probably compensated with the increased bioavailability provided by the RGDK, resulting in an antitumor efficacy similar to ICOVIR15-ABD. The experiments performed in this thesis did not clearly reveal the best location of the RGD in an ABD-modified capsid. More studies are required to evaluate which is the best modified fiber to combine with the ABD insertion for a future clinical candidate.

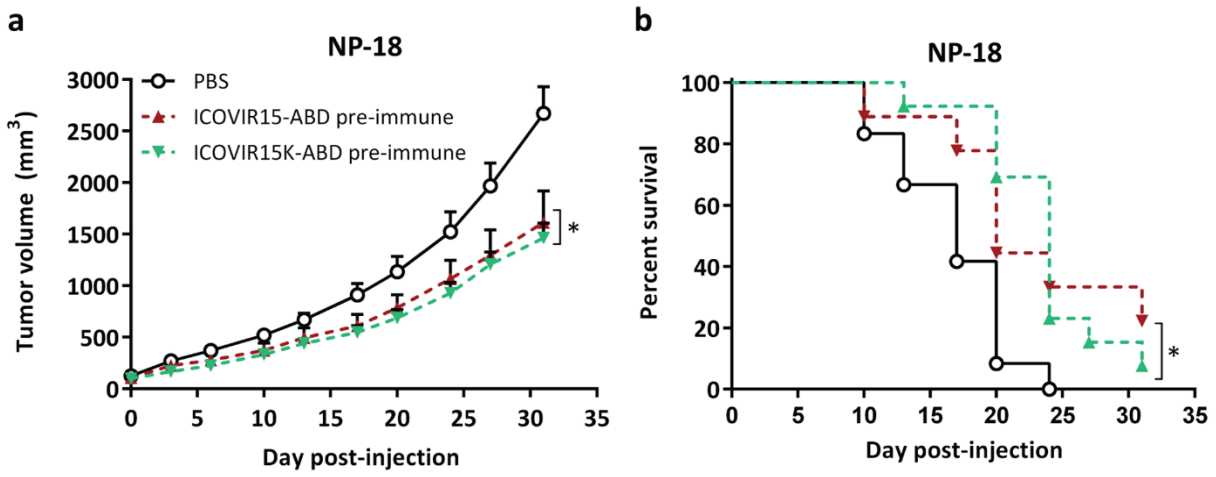

Figure 66. Antitumor activity and survival upon systemic administration of ICOVIR15K-ABD in pre-immune mice. Nude mice bearing subcutaneous xenografts of NP-18 (pancreatic carcinoma) tumors were injected intraperitoneally with 300 µL of PBS or anti-Ad5 neutralizing mouse serum (serum #0416). The day after, mice were treated with a single intravenous injection of PBS or $4x10^{10}$ vp of ICOVIR15-ABD, or ICOVIR15K-ABD. (a) Mean values of tumor volume + SEM are plotted (n = 9-13 tumors/group). *, significant ($p<0.05$) by two-tailed unpaired Student's t-test compared with PBS at end-point. (b) Kaplan-Meier curves are plotted. End-point was established at 750 mm^3 of tumor volume. *, significant ($p<0.05$) by log-rank test compared with PBS.

DISCUSSION

Cancer virotherapy has shown promising clinical results in the last few years. Oncolytic viruses not only can kill cancer cells directly by lysis, but their replication within tumors can also elicit effective antitumor immune responses. Successful clinical outcomes are often attributed to this antitumor immunity. However, to generate such immune reactions the oncolytic virus needs to reach the tumor site where it will replicate, causing tumor cell lysis and the release of tumor antigens. For this reason, classic virocentric traits such as efficient arrival to tumors, good intratumoral spread, and oncolytic potency are still of key importance (Russell et al., 2012).

The human adenovirus serotype 5 (Ad5) is not only used as an oncolytic agent, but also as a gene therapy vector, and as a vaccine platform. Generally speaking, the intravenous injection is usually the preferred administration route, as it allows reaching multiple organs or disseminated lesions. However, the human bloodstream is a highly hostile environment for Ad5, where it will encounter multiple barriers that will contribute to its elimination. In this thesis, we have studied the interaction of Ad5 with two blood components, erythrocytes and neutralizing antibodies (NAbs). In the first chapter, we analyzed the interaction of Ad5 with human erythrocytes via the coxsackie and adenovirus receptor (CAR), and its effect on virus bioactivity. In the second chapter, we developed a strategy to protect adenovirus from NAbs using serum albumin as a shield.

1. ADENOVIRUS CAR-MEDIATED INTERACTION WITH HUMAN ERYTHROCYTES DOES NOT PRECLUDE SYSTEMIC TRANSDUCTION

The *ex vivo* interaction between adenoviruses and erythrocytes has been known for 50 years, although the molecular and structural basis of this interaction has been a longstanding enigma. Hemagglutination assays, usually performed for the serotyping of human adenoviruses, demonstrated that Ad5 interacts with human and rat erythrocytes but not with those of mouse (Cichon et al., 2003). Nicol *et al.* demonstrated the importance of the fiber knob in this interaction, since CAR-ablated adenoviruses or non-CAR-binding serotypes were unable to agglutinate rat or human red blood cells (Nicol et al., 2004). In addition, another study showed that binding to human blood cells was not mediated by viral RGD motifs (Lyons et al., 2006). It was not until 2009 when two groups described that human erythrocytes express the primary Ad5 receptor, the coxsackie and adenovirus receptor (CAR) (Carlisle et al., 2009; Seiradake et al., 2009). CAR was first identified in 1997, and has been widely studied

since then. Among other functions, CAR acts as a mediator of cell adhesion, mostly in the junctional complexes of epithelial cells in many tissues (Freimuth et al., 2008). The presence of CAR on mature human erythrocytes was unexpected, and inconsistent with previous reports (Lyons et al., 2006).

According to the studies performed by Carlisle *et al*. and Seiradake *et al.* (Carlisle et al., 2009; Seiradake et al., 2009), the CAR-mediated interaction between adenovirus and human erythrocytes has major consequences for intravenous Ad5 therapeutics. Erythrocytes act as "circulating viral traps", sequestering the virus and inhibiting systemic infection and gene transfer to target cells. This defense mechanism against Ad5 and its inhibition of adenovirus bioactivity are well accepted on the field, as reflected in several reviews (Alonso-Padilla et al., 2016; Coughlan et al., 2010; Khare et al., 2011b). Thus, there is now great skepticism towards the ability of CAR-tropic adenoviruses to reach specific organs or tumors upon systemic administration, independently of neutralizing antibody status. Some authors have claimed the necessity to develop CAR-independent retargeting strategies, such as the use of non-CAR-binding fibers or serotypes, or the physical coating of adenovirus particles to avoid erythrocyte sequestration (Carlisle et al., 2009; Coughlan et al., 2010; Seiradake et al., 2009). However, Carlisle *et al.* also demonstrated that the erythrocyte-bound adenovirus particle cannot be internalized due to the absence of integrins on erythrocyte membrane. Evidence of adenovirus reaching tumors after systemic administration in clinical trials has been reported before (Nemunaitis et al., 2001). Additionally, in a clinical trial with oncolytic adenovirus ICOVIR-5 (NCT01864759) injected endovenously in metastatic melanoma patients, we have detected the presence of the virus in tumor biopsies of patients treated with $1x10^{12}$ and $1x10^{13}$ vp (unpublished data). Due to the inability of erythrocytes to internalize the adenovirus particles, and to the results in clinical trials demonstrating tumor infection after systemic administration, we hypothesized that this CAR-mediated interaction is probably reversible, allowing the release of the virus and the subsequent transduction of target cells. This possibility has already been suggested, albeit not experimentally demonstrated (Lyons et al., 2006).

In the first chapter of this thesis, we studied the CAR-mediated interaction between Ad5 and human erythrocytes, and how this interaction affected the ability of the virus to infect cells and transduce organs. We first demonstrated the role of CAR on this interaction by a competition assay (**Figure 14**). Our results confirm the *ex vivo* binding experiments performed by other authors (Carlisle et al., 2009; Cichon et al., 2003; Lyons et al., 2006), and the ability

of human erythrocytes to pull down Ad5 particles after centrifugation. We used three different Ad:erythrocyte ratios to study the binding (**Figure 13**). When a high ratio was used (100 Ad particles per erythrocyte), no adenovirus pull-down was observed. The ratio of 0.04 (which corresponds to 25 erythrocytes per Ad particle) represents a clinically relevant condition, as it would correspond to an intravenous dose of $1x10^{12}$ viral particles in 5 L of blood. Carlisle *et al.* showed that in these same conditions, the 90% of the viral dose was erythrocyte-bound, and accordingly, we found the 88% of the viral dose in the erythrocyte pellet. A further 10% reduction in the relative amount of Ad particles (Ad:erythrocyte ratio of 0.036, that is 27.7 erythrocytes per Ad particle) resulted in an almost complete pull-down, with the 99.6% of the viral dose in the erythrocyte fraction.

Albeit these results show an efficient pull-down of Ad particles by erythrocytes, some considerations are worth discussing. First, finding the 90% of the viral input in the erythrocyte fraction may not imply that the 90% of the virus particles are bound to erythrocytes. The physiological concentration of erythrocytes in human blood is so high that after centrifugation the cell pellet usually takes up half the volume of the tube, and therefore, half of the viral dose would be found in this fraction by random distribution. This fact is not considered by other authors, which directly correlate the virus presence in erythrocyte fraction with binding. For this reason, we calculated the fold-clearance of Ad particles in the supernatant, which we believe is a more real measure to calculate the Ad pull-down. In addition, considering the MOIs used in the pull-down studies we observed that the erythrocyte capacity to bind Ad5 via CAR is relatively low (28 erythrocytes would be required to efficiently pull-down one Ad5 particles), which is in accordance with the studies that showed low levels of CAR expression in human erythrocytes (Carlisle et al., 2009; Seiradake et al., 2009). From a clinical point of view, intravenous administration of $1x10^{12}$ vp would result in an 88% of erythrocyte-bound Ad particles. Conditions reflecting other clinically relevant but higher doses such as $1x10^{13}$ vp were not tested, but would likely result in a high percentage of non-bound Ad particles.

The common belief is that erythrocyte binding prevents the adenovirus infection of target cells. However, due to the inability of erythrocytes to internalize Ad5, the interaction could be reversible and therefore, not neutralizing. In recent reports, *in vitro* studies in the presence of human erythrocytes described a strong inhibition of Ad5 infectivity of A549 cell monolayers (Carlisle et al., 2009; Lyons et al., 2006). In contrast, previous studies of adenovirus titration in human blood claimed that the erythrocyte-bound adenovirus particles were still infective (Cichon et al., 2003). According to Lyons *et al.* these discrepancies lie in the concentration of

erythrocytes, and concentrations lower than $1.7x10^7$ erythrocytes/mL no longer inhibit the infection. However, we incubated Ad5 with physiological concentrations of human erythrocytes ($5x10^9$/mL) and used the erythrocyte-bound particles to infect A549 cells, resulting in a final concentration of $1.5x10^8$ erythrocytes/mL in the well. In these conditions, we observed the same cell transduction regardless of previous incubation with human erythrocytes (**Figure 15**). A possible explanation for these discrepancies is the washout step of the Ad-erythrocyte complex from the tumor cells performed by Lyons *et al.* and by Carlisle *et al.* In those studies the Ad-erythrocyte complex was removed 90 min after adding it to tumor cells, probably resulting in the removal of bound but not internalized Ad particles, and causing a significant drop of cell transduction. In contrast, we left the Ad-erythrocyte complex in contact with tumor cells for 48 hours. Assuming a reversible binding to CAR, this allowed the virus to detach from CAR on erythrocytes and attach to CAR on tumor cells. In line with this observation, no washout step of adenovirus was mentioned by Cichon *et al.,* who had also described that erythrocyte-bound particles were still infective. Hence, these results indicate that although Ad5 efficiently binds to erythrocytes via CAR, this binding is reversible and in the long term it does not inhibit the infection of tumor cells.

Seiradake *et al.* analyzed the expression of CAR on erythrocytes of different mammal species. CAR expression was also found in rat erythrocytes, whereas surprisingly, erythrocytes of other mammalian species such as mouse, dog, rabbit, or non-human primates do not express CAR on their surface (Carlisle et al., 2009; Seiradake et al., 2009). These findings agree with the previous studies with Ad5 that showed no hemagglutination of mice and rabbit erythrocytes, and positive hemagglutination with those of rats and humans (Cichon et al., 2003). These differences in the expression of CAR have raised important questions about the use of several models to predict the clinical behavior of systemically administered Ad5. According to some authors, mouse and non-human primates poorly mimic the environment that Ad5 will encounter in the human bloodstream, whereas rats provide a better model regarding systemic Ad5 biodistribution (Carlisle et al., 2009; Seiradake et al., 2009). However, Seiradake *et al.* also demonstrated that the levels of CAR in rat erythrocytes were remarkably higher than in human erythrocytes. We believe this difference in the levels of CAR could also cause differences in adenovirus systemic biodistribution.

The *in vivo* impact of erythrocyte binding after systemic injection of Ad5 in mice was analyzed by Seiradake *et al.* and Carlisle *et al.*, reaching to the conclusion that the virus can neither extravasate nor transduce target organs due to erythrocyte sequestration. In these

studies, two different mouse models were used to test the effect of erythrocyte binding *in vivo*. Carlisle *et al.* used NOD/SCID mice transplanted with washed human erythrocytes by systemic injection. An extended circulation of Ad5 was observed in those animals that received human erythrocytes, and the virus was predominantly associated to circulating blood cells. In contrast, animals without human erythrocytes showed a much quicker clearance, with the majority of the virus detected in the plasma. Despite this increase in blood persistence, mice that received human erythrocytes showed 100-fold less adenovirus genomes in tumors compared to those without human erythrocytes, indicating that human erythrocytes inhibit adenovirus extravasation.

In this thesis, we have also tested the erythrocyte transplantation approach, but in nude mice instead of NOD/SCID. To understand the relevance of this model, we first analyzed the persistence of the transferred human erythrocytes into the recipient nude mice. Erythrocytes were labeled with CFSE and detected in the mouse blood by flow cytometry, observing a very rapid clearance of human erythrocytes from mouse circulation (**Figure 16**). This method for measuring human erythrocyte clearance from mouse circulation has been performed before in NOD/SCID mice, also showing a low persistence (Hu et al., 2011). Hu *et al.* demonstrated that this rejection of human erythrocytes in immunodeficient mice is macrophage-mediated. NOD-SCID mouse macrophages showed high phagocytic activity towards human erythrocytes, and the depletion of macrophages significantly increased the erythrocyte persistence. Nevertheless, the very low blood persistence of Ad5 should also be considered when evaluating this model. In fact, we compared the erythrocyte clearance with our historical data of Ad5 persistence in nude mice (Gimenez-Alejandre et al., 2008), and observed a remarkably slower clearance of human erythrocytes (**Figure 16**). Although we did not measure the blood persistence of adenovirus when co-injected with erythrocytes, we believe it is likely that erythrocyte binding extends the plasma half-life of the virus as previously reported (Carlisle et al., 2009). Since adenovirus particles are cleared from circulation quicker than human erythrocytes, we believe this model should be sensitive enough to detect an alteration of Ad5 biodistribution caused by erythrocyte binding. Accordingly, an efficient adenovirus sequestration was reported by Carlisle *et al.* in this model despite the rapid erythrocyte clearance described by Hu *et al*. Contrary to Carlisle *et al*., we observed the same presence of Ad5 genomes and the same tumor and liver transduction in mouse with or without human erythrocytes three days after virus injection (**Figure 17**). Different mouse strains (nude vs NOD/SCID), but in particular the delayed times of our analysis (72 hours compared to 24 hours) could explain these differences. Likely, due to the reversibility of the CAR-mediated

binding, Ad particles are eventually released from human erythrocytes and are able to extravasate and transduce the liver and the tumors. This effect might be reduced when analyzing Ad genome presence at such an early time point as 24 hours.

A high MOI of 62.5 Ad particles per erythrocyte was used in our *in vivo* study in which the transduction capacity of Ad5 in presence of human erythrocytes was analyzed. The limitations of the mouse model forced us to use this proportion. First of all, Kupffer cells produce a viral dose threshold effect. Low doses of virus are efficiently taken up by these liver macrophages preventing transgene expression, whereas high doses saturate these cells and are able to productively transduce hepatocytes. Doses of 1-3x10^{10} vp yield barely detectable transgene expression in nude mice (Tao et al., 2001), and therefore a dose of 5x10^{10} vp per mouse was used. This adenovirus dose along with the maximum intravenously injectable volume of a solution with physiological concentration of erythrocytes, results in an MOI of 62.5. Likely, a significant amount of adenovirus particles would not be erythrocyte-bound in these conditions. However, considering the quick clearance of adenovirus compared to erythrocytes, we believe these conditions should be valid to reflect a possible inhibition of transduction caused by erythrocyte binding. Accordingly, inhibition of adenovirus extravasation was described by Carlisle *et al.* also using a relatively high MOI *in vivo* (20 Ad particles per erythrocyte). In this published report, SCID mice were used , and a lower viral dose was possible due to the fact that the threshold dose for Ad5-mediated gene expression in the liver of SCID mice is significantly lower than in nude mice (Engler et al., 2004). In our case, a higher virus dose was required.

Another mouse model used to test the effect of erythrocyte binding via CAR *in vivo* is the GATA1-CAR transgenic mouse, which expresses human CAR on erythrocytes (Asher et al., 2005). Carlisle *et al.* reported an 875-fold loss of liver transduction in this mouse model compared to isogenic control mice 24 hours after vector administration (Carlisle et al., 2009). In contrast, Seiradake *et al.* showed only a 25-fold decrease in liver viral load at 72 hours post virus injection in the same mouse model. These data suggest that with time the detrimental effect of erythrocytes on liver infection is reduced. Even though adenovirus extravasation was still diminished in this case at 72 hours, the differences in CAR expression between human and GATA1-CAR erythrocytes are noteworthy. GATA1-CAR erythrocytes showed significantly higher levels of CAR compared to human erythrocytes (Seiradake et al., 2009). In fact, when compared to other CAR-expressing cells (HEK293, rat erythrocytes, and GATA1-CAR erythrocytes), human erythrocytes showed the lowest levels of CAR expression. We believe

this difference in the levels of CAR likely account for the discrepancies of our results and the reported in these mice, as a higher CAR expression probably leads to a stronger and more permanent binding of the Ad particle.

In conclusion, our results indicate that the interaction between human erythrocytes and Ad5 via CAR is reversible. Since the virus particle cannot be internalized, it is eventually released to infect other CAR-expressing cells. Nevertheless, Carlisle *et al.* also described that Ad5 can interact with human erythrocytes via complement receptor 1 (CR1). This is an indirect interaction which requires the previous opsonization of the adenovirus particle with antibodies (either anti-Ad5 neutralizing antibodies or low-affinity natural IgMs) and subsequent complement fixation. CR1-bound Ad5 is then targeted for rapid clearance by deposition in hepatic and splenic macrophages. *In vitro* this interaction was described to occur by incubating Ad5 with human erythrocytes in both human and mouse plasma. However, when we injected Ad5 with human erythrocytes intravenously in nude mice (where interactions via CAR and CR1 could occur) no reduction of extravasation or transduction was observed (**Figure 17**). Although we acknowledge the CR1-mediated interaction probably inactivates adenovirus, we do not believe erythrocytes are the main concern in this situation. Even if CR1 was absent in erythrocytes the virus would still be inactivated directly by neutralizing antibodies, or subsequently eliminated by phagocytes via Fc receptor or CR1. These interactions could be avoided using shielding strategies such as the ABD modification described in the second chapter of this thesis. In any case, our work was focused on the interaction with erythrocytes via CAR, which according to our results is not a neutralizing interaction. Thus, we believe human erythrocytes are not a major threat to systemic Ad5 therapeutics whereas other blood components such as neutralizing antibodies deserve greater attention.

2. ALBUMIN-BINDING ADENOVIRUSES CIRCUMVENT PRE-EXISTING NEUTRALIZING ANTIBODIES

Among the different barriers Ad5 finds in the human bloodstream, neutralizing antibodies (NAbs) represent a major obstacle for efficacy. NAbs directed against capsid proteins not only inhibit cell transduction directly by blocking specific adenovirus motifs, but also opsonize and target the virus for elimination (Uusi-Kerttula et al., 2015). In addition, Ad5 is a very common pathogen and most of the human population has been exposed to the virus by natural

infection. Although the levels of NAbs vary geographically in humans, the general prevalence of anti-Ad5 NAbs is very high, reaching >90% in some locations (Barouch et al., 2011; Mast et al., 2010). This compromises the potential clinical efficacy of Ad5-based therapies, not only of oncolytic viruses but also of gene therapy vectors and vaccines. Studies by Chen *et al.* already suggested the screening for pre-existent anti-Ad NAbs in each patient, prior to intravascular adenovirus therapy (Chen et al., 2000b). This is currently being applied in the clinical trial by intravenous administration of VCN01 oncolytic adenovirus (NCT02045602), which considers high levels of circulating NAbs in patients as an exclusion criterion. In this second chapter, we developed a modification on the adenovirus capsid, consisting in the insertion of an albumin-binding domain. We hypothesized that upon injection of such adenovirus in the bloodstream, albumin would shield the viral capsid protecting the virus from NAbs (**Figure 67**).

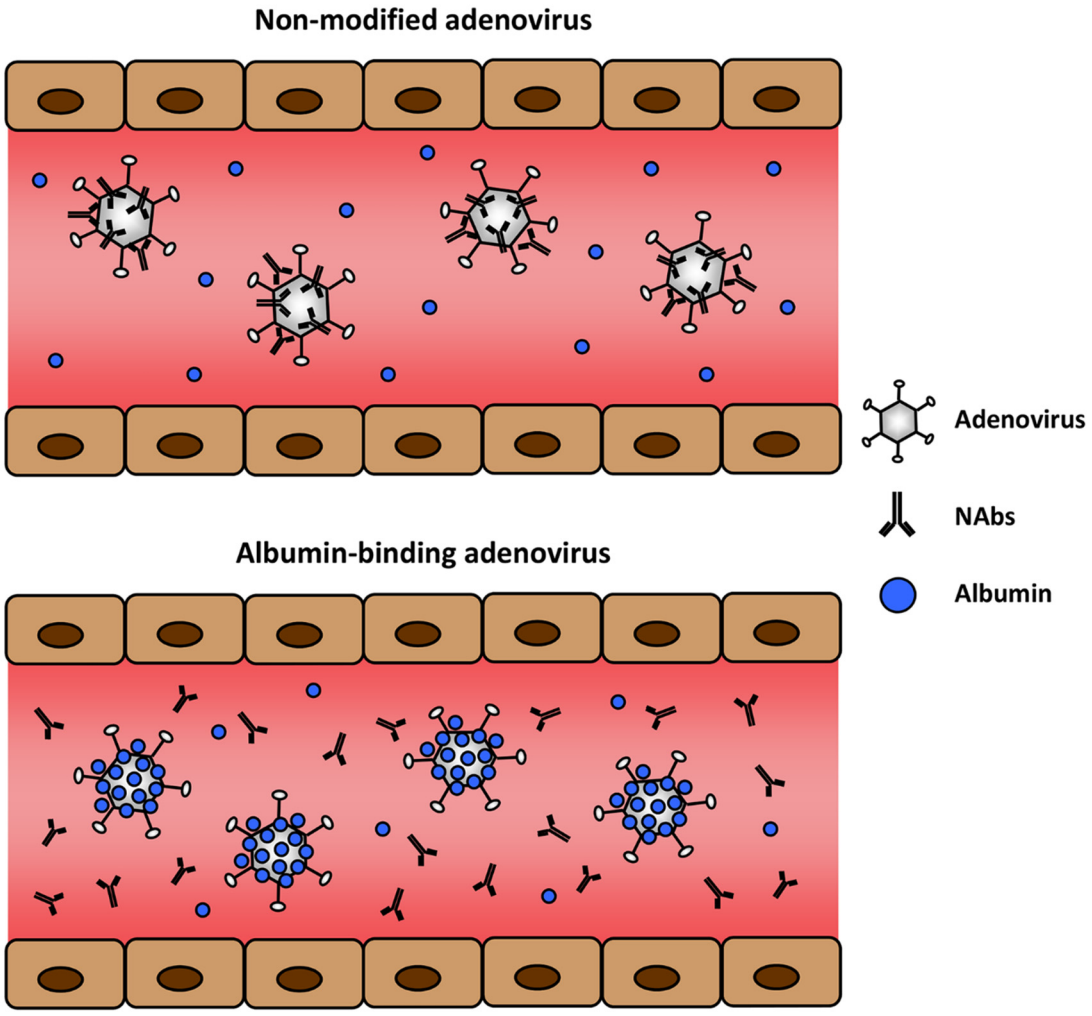

Figure 67. Albumin protection conferred by insertion of an albumin-binding moiety on adenovirus capsid. Compared to a non-modified adenovirus (above), the albumin-binding adenovirus is coated with albumin present in blood, shielding the virus from neutralizing antibodies (below).

Among the different strategies to achieve albumin binding we used the genetic insertion of small peptidic albumin-binding motifs, which in our opinion offers multiple advantages over other alternatives. Being a genetic insertion, it allows the preservation of the modification in the viral progeny unlike chemical shielding of the virus capsid or liposome encapsulation, which will be lost after the first round of viral replication. Moreover, these conjugation processes will add batch-to-batch heterogeneity in the virus composition, raising important issues regarding scale-up and regulatory approval for clinical applications. In this regard, the high affinity of the domain and the high physiological albumin concentration allow a good protection just by directly injecting the modified virus in the bloodstream, avoiding any *ex vivo* conjugation step with albumin. The direct genetic fusion of whole proteins in adenovirus capsid has also been proposed (Hedley et al., 2006). Hedley *et al*. tested the insertion of alpha-1-antitrypsin (A1A) and human albumin (HSA) in pIX to shield the virus from NAbs. A1A could not provide sufficient coverage to protect the virus, whereas HSA fusion was shown incompatible with virus production (Hedley et al., 2009). Generally, the insertion of small peptides is more desirable compared to big proteins in order to avoid viability issues. However, two of the three small motifs used in this thesis resulted in non-viable virus, although a different insertion point was used. Furthermore, the reversible non-covalent binding provided by this strategy is also a key issue. Irreversible fusions such as insertion of proteins can likely compromise the interaction of adenovirus motifs with cellular receptors, or with other cellular components important for capsid transportation such as dynein.

The use of non-prevalent human serotypes, non-human serotypes, or the substitution of Ad5 HVRs with those of non-prevalent serotypes has also been explored, especially in the fields of gene therapy and vaccination (Bruder et al., 2012; Holterman et al., 2004; Lopez-Gordo et al., 2014; Roberts et al., 2006; Vogels et al., 2003). In general, alternative serotypes usually underperform Ad5 vectors (Lemckert et al., 2005; Shiver and Emini, 2004), and imply GMP production challenges as well. Substitution of Ad5 HVRs with those of rare serotype Ad48 in an Ad-based vaccine against simian immunodeficiency virus, resulted in efficient escape of anti-Ad5 NAbs (Roberts et al., 2006). Nevertheless, Ad5 HVR1 plays a key role in recruiting dynein for proper capsid transport to nucleus, and when substituted by HVR1 of Ad48 capsid trafficking was severely affected (Scherer and Vallee, 2015). In addition, albeit showing efficient escape of anti-Ad5 NAbs, it is likely that a humoral response against these serotypes will eventually occur. With our approach we hypothesized that albumin could also protect from NAbs generated against the modified virus. Although protection against such antibodies

is not as efficient as against anti-Ad5wt antibodies, there is a certain evidence of escape, suggesting the possibility of readministration. This matter will be further discussed below.

The hexon protein was selected for the insertion of the albumin-binding motifs mainly because it is the most abundant protein of the adenovirus capsid. As the viral capsid is composed by 240 trimeric hexons, the albumin-binding motif will be repeated 720 times on the virion surface, allowing the binding of more albumin molecules than any other capsid protein. Therefore, the hexon is the best location to ensure an efficient capsid shielding. Accordingly, Hedley *et al.* inserted the streptococcal Albumin-binding domain (ABD) in the pIX of adenovirus capsid but such insertion failed to protect the virus from NAbs (Hedley et al., 2009). As the main protein of the capsid, the proper folding of the hexon is indispensable for the assembly and functionality of virus particles. The majority of hexon modifications have been performed in the hypervariable regions (HVRs) of the protein (Alba et al., 2009; Khare et al., 2011a; Matthews, 2011; Roberts et al., 2006). These regions are poorly conserved loops without a defined structure, which usually allow the insertion of foreign sequences without altering the structure of the protein. Importantly, the HVR loops are solvent-exposed (Rux and Burnett, 2000), an indispensable trait for the proper interaction between the virus and albumin in the bloodstream. In addition, albumin would be directly blocking the HVRs of the hexon which are the main target of anti-Ad NAbs (Bradley et al., 2012b; Roberts et al., 2006). Although NAbs directed against the fiber protein have also been described, these are subdominant and not very efficient on their own (Bradley et al., 2012a; Gall et al., 1996). Certainly, we demonstrate a very efficient neutralization escape just by modifying the hexon, despite the fiber protein is probably unprotected by albumin. Altogether, these characteristics pointed the HVRs of the hexon as the best location for the insertion.

On the other hand, albeit HVRs are more flexible and permissive, their modification can also be complex and cause deleterious effects on the virus. The HVR5 is in general the most flexible with respect to incorporation of foreign sequences (Gil-Hoyos, 2014; Matthews, 2011) and, since our group also had previous experience in successfully modifying the HVR1, these two locations were selected for the incorporation of the albumin-binding motifs. Many groups have published the replacement of the HVR loop for the desired peptide or antigen (Gil-Hoyos, 2014; Kalyuzhniy et al., 2008; Lucas et al., 2015; Vigant et al., 2008). However, the replacement of both HVR1 and HVR5 loops for the albumin-binding motifs resulted in non-viable viruses. For this reason, we decided to change the strategy and insert the foreign motifs in the middle of the loops without deleting any residue from the wt HVRs. Even using this conservative

insertion strategy, viruses with the SA-21 and RB5 peptides were non-viable and only the viruses containing the ABD insertions were successfully generated. These results were completely unexpected. The peptides were initially selected due to their short sequence and their lack of secondary structure, and even though their effects have not been as extensively studied as the ABD, we believed they would be better accommodated in the HVRs. Previous experience of modification of HVRs in our group suggested that the tolerance to modification is not only related with the length of the inserted motif but also with its sequence, and probably with the effect that the introduced amino acids have on the conformation of the protein (Gil-Hoyos, 2014). The results of this work agree with this view.

The functionality of the ABD was maintained after its insertion in both HVR1 and HVR5. We demonstrate albumin binding of the modified adenoviruses by ELISA (**Figure 21**), adapting a previously published protocol where also an ABD was used (Konig and Skerra, 1998). Our results add up with the previously published data on the species specificity of the ABD, being able to bind to human and mouse serum albumin, but not to bovine (Falkenberg et al., 1992; Nygren et al., 1990). The inability to bind BSA could represent an advantage in the production process of these viruses when bovine serum is employed to supplement the media. Our results indicate that the affinity of the ABD for albumin was notably higher in the HVR1 than in the HVR5. This was reflected in the ELISA where a significantly higher signal was obtained with both HSA and MSA with the H1-ABD virus, even though the same amount of both viruses was used (**Figure 21**). Also, the deleterious effect on cell transduction caused by albumin binding (which will be further discussed below) was significantly smaller with the H5-ABD virus (**Figure 23**), suggesting a weaker binding to albumin. Transduction studies in presence of FX and HSA revealed that both viruses could bind FX in the absence of albumin (observed by an increase of transduction mediated by FX). However, when both FX and HSA were present in the medium, only the H5-ABD vector could maintain the increased transduction levels provided by FX binding, whereas the H1-ABD vector suffered the transduction loss caused by HSA binding (**Figure 24**). These results suggest that in the competition between FX and HSA to bind to the viral capsid, FX had higher affinity for the H5-ABD virus whereas HSA had higher affinity for the H1-ABD virus. In a similar way, the same competition effect was observed in the transduction studies with HSA and NAbs. In the absence of HSA both vectors were similarly neutralized by NAbs. However, HSA could only efficiently protect the H1-ABD vector from antibody neutralization, whereas the H5-ABD vector was highly neutralized by NAbs even in the presence of HSA (**Figure 25**). Overall, these comparative studies suggest that the affinity of HSA for the ABD in the HVR5 is low compared to the HVR1, and can be easily displaced from

the viral capsid by other molecules with higher affinity such as FX or NAbs. Due to the inability of the H5-ABD virus to evade NAbs, this virus was discarded and the project was continued only with the H1-ABD virus.

The viruses with the ABD in the HVR1 (the non-replicative vector AdGLRGD-ABD and the oncolytic ICOVIR15-ABD) were characterized in depth. In the absence of NAbs and albumin, the insertion did not have a big impact on the virus life cycle. The transduction was very much the same as the parental vector in most of the cell lines analyzed (**Figure 23**). A certain deleterious effect was observed regarding the viral production, which was reduced up to 6-fold and 3-fold in 293 and A549 cells, respectively (**Figure 30**). Since no albumin was included in these assays, this loss is likely related to a certain affectation of the hexon structure due to the insertion of the domain. Even though the production in a single-round replication experiment was reduced, cytotoxicity studies with several rounds of replication did not show any cytotoxicity loss (**Figure 31**). This might indicate that the amount of virus produced is in excess and despite the production is lower, it does not affect the capacity of the virus to kill tumor cells.

On the other hand, conditions without NAbs but with albumin showed a clear impact on the virus life cycle. Albumin binding caused a reduction in the infectivity of the viruses in all cell lines tested (**Figure 23**), in a dose-dependent manner (**Figure 36**). High albumin concentrations close to physiological conditions caused an important inhibition of cell transduction, not only of the ABD-modified vector but also of the parental vector (although the modified vector was more affected). However, such negative effects with high albumin concentrations were not reflected *in vivo* with real physiological conditions, as observed with the transduction of the organs (**Figure 33**). A possible explanation for this transduction loss would be that albumin could be blocking the interaction of viral domains with cell receptors. While the fiber is supposedly not affected by albumin, the penton base will probably be blocked by an albumin molecule bound to a neighboring hexon. Albeit the viruses used in this work contain an RGD-modified fiber, the interaction of cell integrins with the RGD of the penton base might still be necessary to achieve a proper internalization. However, a most likely hypothesis is that albumin might be interfering with the capsid transport to the nucleus. As recently described, HVR1 plays a key role in dynein recruitment for capsid transportation (Scherer and Vallee, 2015) and therefore, albumin could be blocking dynein binding to hexon. In this situation, the reversibility nature of the binding represents an important advantage as dynein could eventually displace albumin, allowing the progression of the viral cycle. This

reduced infectivity affects the subsequent rounds of replication, causing a reduction in the cytotoxicity of the virus, also in a dose-dependent manner (**Figure 31**). Nonetheless, these experimental conditions in the presence of albumin but absence of NAbs do not reflect the clinical problem that represents the high prevalence of pre-existing immunity against Ad5.

In vitro studies in the presence of anti-Ad5 NAbs showed a strong inhibition of the bioactivity of the non-modified virus, in terms of cell transduction and cytotoxicity. In contrast, the HSA-shielded ABD-modified adenoviruses showed enhanced bioactivity in the presence of NAbs compared to the parental virus. While in the absence of albumin both viruses showed very low levels of transduction, in the presence of albumin only the ABD-modified virus showed a remarkable increase in the transduction efficiency, demonstrating an albumin-mediated protection against NAbs (**Figure25** and **Figure 38**). This albumin-mediated protection was also dose-dependent, and increased with higher albumin concentrations (**Figure 37**). The evasion of neutralization observed in terms of cell transduction with the reporter vector also translated in enhanced cytotoxicity of the oncolytic virus, showing higher capacity to kill cancer cells in presence of albumin and NAbs (**Figure 39**). Such protection was not only observed against commercial Ab6982 but also against NAbs generated in immunocompetent mice by immunization with Ad5wt (**Figure 40**). Human sera from six donors were also tested for neutralization escape of the ABD-modified vectors. A clear protection was observed only in three of the sera, whereas no apparent differences between viruses were observed in the other three (**Figure 41a**). A possible explanation would be the differential contribution of anti-fiber NAbs in the neutralization of the virus. In this direction, contradictory conclusions have been published: while some studies stated that anti-fiber NAbs play a more important role when the response is generated by natural infection than by vaccination with a recombinant adenovirus (Cheng et al., 2010; Yu et al., 2013), another study shows that NAb responses to hexon are dominant regardless of the route of exposure (Bradley et al., 2012a). Nonetheless, the lack of protection observed in three sera was only apparent, as these neutralization curves do not reflect the differences between viruses that occur at low dilutions of the serum. The ABD-modified vector displayed higher transduction levels at low serum dilutions, in almost all sera analyzed (**Figure 41b**). However, since these values are very low compared to the 100% transduction control, the differences are not visible in the neutralization curves. Although the advantage is restricted to low serum dilutions, these are the most relevant conditions as the virus will face undiluted serum after the systemic administration, and the conditions where the serum is highly diluted do not mimic the real *in*

vivo situation. Therefore, our results also indicate an escape of anti-Ad5 NAbs raised by humans.

We demonstrated as well that the ABD-modified virus could bind not only to purified albumins, but also to the albumin present in serum both from human and mouse origin (**Figure 27**). This fact is relevant as it allows the virus to bind to circulating serum albumin after the systemic administration, rather than incubating the virus *ex vivo* with purified albumin prior to the injection. Also, this result was important to confirm that the virus would bind to albumin *in vivo* in our mouse models.

Albumin binding has shown to increase the blood persistence of small drugs (Larsen et al., 2016), but has never been tested in the context of a whole virus. Here we show a reduced blood clearance of the ABD-modified adenovirus in terms of circulating viral particles (genomes in serum). This was detected in nude mice qualitatively by competition with the non-modified virus (**Figure 32**), and in C57BL/6 mice by direct genome quantification (**Figure 42a**). Natural immunoglobulins and complement system have been described to influence Ad5 pharmacokinetics, by enhancing clearance by Kupffer cells and by docking the viral particles to Fc receptors in monocytes and neutrophils (Alonso-Padilla et al., 2016; Khare et al., 2013; Xu et al., 2008). Preventing such interactions by albumin protection could likely contribute to an increased blood persistence. The albumin-mediated increase in the blood persistence of small drugs has been usually attributed to albumin recycling through neonatal Fc receptor (FcRn) (Andersen et al., 2011; Sleep et al., 2013). However, this mechanism seems less plausible in this case given the large size of the virus particle and the interaction of the virus capsid with cellular receptors.

Oncolytic adenoviruses derived from ICOVIR15 present low toxicity profiles after the systemic administration due to their inability to replicate in normal tissue, and their strong transcriptional control of E1A protein (Guedan et al., 2010; Rodriguez-Garcia et al., 2015; Rojas et al., 2010, 2012). Here we analyzed whether the insertion of the ABD caused any change in the toxicity profile of ICOVIR15. A reduction and a faster recovery of the body weight loss were observed as well as a reduction in the increase of transaminases levels (**Figure 34**). A possible explanation for this lower toxicity could be a lower transduction of the liver. Even though the differences between vectors were not statistically significant, the values of liver transduction of AdGLRGD-ABD were lower especially in C57BL/6 mice. Other toxicity markers such as lipase or creatinine were not altered, and importantly, the concentration of albumin in the serum was not reduced by the treatment with the albumin-binding adenovirus. The reduced toxicity

of the ABD-modified virus could allow for the use of higher viral doses to increase the antitumor effect, although this objective was not pursued in this thesis. The toxicity study was only performed in naïve mice and the effect of NAbs on adenovirus toxicity was not analyzed in this work. Various reports demonstrated that pre-existing NAbs inhibit the toxicity caused by an intravenously administered oncolytic adenovirus in both mouse and hamster models (Chen et al., 2000b; Dhar et al., 2009). In this regard, we would expect a similar toxicity of ICOVIR15-ABD in naïve and pre-immune mice, due to the ability of this virus to escape neutralization by antibodies. From a toxicity point of view, some authors claim pre-existing immunity can be beneficial, as it blocks vector spillover from the injection site to other tissues such as the liver (Chen et al., 2000b; Dhar et al., 2009). While this might be true for therapies that require a localized injection, it does not apply when the systemic injection is necessary to reach disseminated metastases. Furthermore, this blockade of virus spillover would be less relevant in our setting since our oncolytic adenoviruses show a low toxicity profile even after the intravenous injection of high doses, due to the modifications that make them selective for cancer cells.

The reduction of transduction observed *in vitro* due to albumin binding in the absence of NAbs was not observed *in vivo*. Experiments in nude mice with no pre-existing immunity revealed no significant reduction in the organ transduction of the ABD-modified vector compared to the parental virus (**Figure 33**). *In vitro* studies with a high albumin concentration (10 mg/mL) also showed a strong inhibition of the transduction, but this was not observed *in vivo* neither, where the physiological albumin concentration in mice is even higher (35 mg/mL). These differences reflect the complexity of an *in vivo* system where longer persistence in blood or other interactions seem to compensate for the loss of infectivity. The organ transduction in nude mice matches with the blood persistence in naïve C57BL/6 mice, where we observed an increase of circulating virus particles with the ABD-modified viruses, but not of circulating transducing units (**Figure 42** left panels). The expected outcome of an enhanced blood persistence of virus particles would be an enhanced tumor transduction. However, the improved blood persistence was probably compensated with the reduced transduction observed *in vitro*, and the tumor transduction was not significantly altered in naïve mice (**Figure 33** and **Figure 44** naïve groups). As a consequence of these compensatory effects, the ABD-modified oncolytic adenovirus did not show any significant disadvantage nor advantage regarding antitumor efficacy in mice when NAbs are not present to block the virus (**Figure 35** and **Figure 51** naïve groups).

Apparently, the albumin coating of the viral capsid did not have a great impact in mice with no pre-existing humoral immunity. Neither the organ transduction nor the antitumor activity were significantly altered by the insertion of the ABD. One could believe the ABD modification causes no significant effect. However, we believe the unaltered results are the consequence of multiple factors that likely compensate each other. As discussed above, the albumin-mediated reduction of cell transduction was probably compensated by the increased blood persistence, resulting in the same tumor transduction as the parental vector. In addition, the binding of the virus to FX is another important parameter to consider. FX was described to mediate liver transduction *in vivo* by bridging adenovirus hexon with HSGs in hepatocytes (Kalyuzhniy et al., 2008; Waddington et al., 2008). Ad5 vectors modified not to bind FX showed a significantly reduced liver transduction (Alba et al., 2009, 2010; Kalyuzhniy et al., 2008; Vigant et al., 2008; Waddington et al., 2008). Our *in vitro* results suggest that in the presence of albumin, FX cannot bind to the virus with the ABD in the HVR1 (**Figure 24**). Nevertheless, albeit a certain reduction in liver transduction can be observed (especially in C57BL/6 mice) (**Figure 33** and **Figure 44**), this difference was never statistically significant. Additionally and contrary to previous reports (Doronin et al., 2012), it was recently described that FX binding protects Ad5 from the attack by the classical complement pathway (Xu et al., 2013). In fact, it was shown that the enhanced liver transduction of Ad5 promoted by FX is due to its ability to protect the virus rather than bridging the virus to the hepatocyte. Our results seem to agree with this theory. In our case, albumin is likely playing the protective role of FX against natural IgMs and complement, and therefore, the ABD-modified vector showed no significant reduction in liver transduction even though the virus cannot bind FX. Furthermore, albumin shows an additional protective capacity compared to FX, which is the protection against NAbs. The very high concentration of albumin in serum compared to that of FX might be a key factor for this additional protection. For these reasons, we believe albumin binding is causing important changes in the interaction of Ad5 with blood components and cell receptors, although no significant changes can be appreciated in naïve mice.

Pre-immune mouse models showed the dramatic effect of NAbs on adenovirus bioactivity *in vivo*. Whereas in naïve mice the non-modified vector displayed high levels of liver and tumor transduction, this transduction was completely inhibited in mice previously immunized with Ad5. On the other hand, the protection provided by albumin proved to be remarkably effective *in vivo*. In pre-immune mice, the ABD-modified vector was able to maintain the same high levels of liver and tumor transduction as in naïve mice (**Figure 44**). Again, the transduction

results agree with the blood persistence, as in pre-immune C57BL/6 mice we observed not only an increased number of circulating genomes but also of circulating transducing units of the vector bearing the ABD (**Figure 42** right panels). In our opinion, these are very relevant results as this new modification allows a very efficient transduction *in vivo* even with pre-existing humoral immunity, a highly probable clinical situation.

The model to study the impact of pre-existing humoral immunity on the antitumor efficacy of oncolytic adenoviruses was challenging. Human adenoviruses replicate very poorly in mouse cells (Jogler et al., 2006), and therefore an immunodeficient mouse grafted with human tumors is required. However, the lack of CD4 helper T cells in nude mice prevents the proper generation of antibody responses. Passive immunization with neutralizing serum or purified neutralizing antibodies represents a feasible option (Chen et al., 2000b; Dhar et al., 2009; Tsai et al., 2004). To validate the model we analyzed the ability of the passively immunized mice to block cell transduction and virus replication. For this last purpose we generated ICOVIR15-Luc, a reporter oncolytic adenovirus that expresses luciferase under the control of the MLP, and therefore, this expression is associated to the replication of the virus (**Figure 48**). The space optimization on the genome of ICOVIR15 has allowed the insertion of foreign transgenes without affecting the virus replication (Guedan et al., 2010, 2012; Rojas et al., 2010). However, contrary to these previous reports we observed a 7.8-fold loss of cytotoxicity due to the luciferase insertion. Since larger transgenes have been successfully inserted into ICOVIR15 genome (Guedan et al., 2012), we believe this loss could be related to the specific sequence of the transgene rather than to its size. Despite this cytotoxicity loss, ICOVIR15-Luc proved to be a useful tool to monitor the viral replication within tumors *in vivo*, and to validate the passive immunization approach. The significant inhibition of luciferase expression foci in tumors indicated that most of the administered virus dose was neutralized by the transferred serum (**Figure 49**). We also observed that analysis of transduction at day 3 post-injection by luciferase expression cannot detect the arrival of small amounts of virus that can eventually replicate (**Figure 46**).

Although the detrimental effect of NAbs on the transduction of adenovirus vectors is accepted, there is certain controversy regarding the effect of NAbs on the antitumor activity of oncolytic adenoviruses. Chen *et al.* transferred purified rabbit anti-Ad NAbs to a xenografted mouse model, and observed the antitumor activity of the intravenously administered oncolytic adenovirus was prevented in a dose-dependent manner (Chen et al., 2000b). However, a subsequent study by Tsai *et al.* showed that the transference of human

serum could not decrease the antitumor efficacy of the intravenously injected virus, also in a xenografted mouse model (Tsai et al., 2004). In this last case, the use of human serum into a mouse environment raise some concerns regarding the incompatibility of the human Fc-portion with mouse cells, as previously reviewed (Zaiss et al., 2009). In this work, we used neutralizing mouse serum to preserve Fc-dependent effector functions. Our results also suggest a dose-dependent inhibition of the antitumor efficacy of the oncolytic adenovirus. Transference of small volumes of serum did not show differences in the antitumor activity compared to naïve mice (**Figure 47**). However, when higher serum volumes were used and the viral dose was slightly reduced, we observed a complete inhibition of the antitumor activity of ICOVIR15 in two independent experiments (**Figure 51**), demonstrating that NAbs can efficiently block oncolytic adenovirus activity.

The antitumor efficacy studies in passively immunized mice corroborated the efficient protection provided by albumin shielding *in vivo*, in two different human tumor xenograft models (A549 lung adenocarcinoma, and Sk-mel28 melanoma). Control virus ICOVIR15 displayed a significant reduction of tumor growth in naïve mice, but completely lost its antitumor activity in passively immunized mice, indicating an efficient neutralization of the virus. In contrast, ICOVIR15-ABD efficiently controlled the tumor growth in both naïve and pre-immune mice, not showing any signs of inactivation due to NAbs (**Figure 51**). Additionally, survival of naïve and pre-immune mice was increased with ICOVIR15-ABD treatment, whereas ICOVIR15 could only increase the survival of naïve mice (**Figure 52**). To our knowledge, this is the first report of an intravenously administered oncolytic adenovirus able to generate an antitumor effect in presence of NAbs *in vivo*. These results are especially relevant, suggesting the possible treatment of seropositive human patients with an oncolytic adenovirus by systemic injection.

Despite passive immunization is useful to test the impact of pre-existing NAbs on antitumor efficacy, some limitations of this model should be noted. Circulating pre-existing NAbs block the systemically administered virus, impeding its arrival to tumors. However, this approach does not contemplate the effect of neither NAbs generated *de novo* against the virus, nor other important components of the immune system such as pre-existing or newly generated cytotoxic T cells. Other possibilities were considered such as the immunocompetent Syrian hamster model (Thomas et al., 2006). Our group demonstrated the binding of the ABD to hamster albumin (Martí Farreras, personal communication) as it was previously described (Falkenberg et al., 1992). Although this model allows evaluating the role

of a fully functional immune system, the low replication of the human adenovirus in hamster cell lines is a major drawback. Viral production in hamster cells was described to be 10 to 100-fold lower than in the A549 human cell line (Wold and Toth, 2012). This observation was reproduced in our laboratory and the adenocarcinoma hamster cell line HP-1 (the most productive cell line in our hands) showed a 36-fold less productivity than A549 cells (Rodriguez-García, 2015). Despite we have observed a clear antitumor effect after the intratumor administration many times in this model, antitumor efficacy after intravenous injection has seldom been observed (Rodriguez-García, 2015). Furthermore, this marginal antitumor effect after the systemic administration was observed with our most potent oncolytic adenovirus ICOVIR-17K (currently named VCN-01), notably superior to the ICOVIR15 used in this work. For these reasons, we considered that differences in antitumor activity between naïve and pre-immune hamsters treated intravenously with ICOVIR15 or ICOVIR15-ABD would hardly be observed in the hamster model.

Adenovirus detection at the end of the antitumor efficacy experiments revealed no correlation between the adenovirus content in tumors and the antitumor activity observed with each virus. To explain this lack of correlation, we developed a hypothesis shown in **Figure 68**, considering the transduction results at day 3 (**Figure 44**), the virus detection at day 11 (**Figure 56**) and at the end of the experiments (**Figure 53**, **Figure 54**, and **Figure 55**). The transduction results demonstrated that ICOVIR15-ABD could efficiently reach tumors in naïve and pre-immune mice, whereas ICOVIR15 could only reach tumors in naïve mice. However, as observed in the passive immunization tests, not all the adenovirus dose is neutralized. A small amount of ICOVIR15 can reach tumors in pre-immune mice, but it is insufficient to control tumor growth and generate an antitumor effect. Nevertheless, as observed with ICOVIR15-Luc, this virus can replicate and increase the amount of adenovirus genomes in tumors. As a result, a high number of adenovirus genomes are detected at the end of the experiment, albeit the treatment is inefficacious. Regarding the viruses that displayed significant antitumor efficacy (ICOVIR15 in naïve mice, and ICOVIR15-ABD in naïve and pre-immune mice), the high levels of virus that reached tumors can replicate since the first days of treatment, and as tumors are still small, they can efficiently control tumor growth. Although ICOVIR15-ABD generates less virus genomes (due to the lowest production and replication observed *in vitro*), virus genomes are generated in excess and accumulate in the nucleus, and the virus can lyse tumor cells. However, as the viruses destroy cancer cells, they find barriers within tumors that limit their spread and that contribute to their elimination. Immunohistochemistry of both A549 (**Figure 57**) and Sk-mel28 tumors (data not shown) revealed the presence of abundant

fibroblast barriers, which do not allow the efficient spread of the virus (**Figure 57a**), and that can completely surround tumor cells creating compartments within the tumors (**Figure 57b**). When ICOVIR15-ABD finds these barriers, its lower production and replication could result in a quicker clearance of this virus compared to ICOVIR15. Genome detection at day 11 post-injection revealed the levels of ICOVIR15-ABD (both in naïve and in pre-immune mice) were diminishing compared to those of ICOVIR15 in naïve mice, whereas the levels of ICOVIR15 in pre-immune mice were already increasing (**Figure 56**). ICOVIR15 will also find such barriers, but it will probably take longer for the genomes to disappear from tumors due to the higher production and replication of this virus. The fact that at day 11 all tumors of naïve mice treated with ICOVIR15 presented high amounts of genomes, whereas at day 34 some tumors presented notably lower genome contents (**Figure 53**), suggest that ICOVIR15 will also be eventually eliminated from tumors. **Figure 68** shows the hypothetical adenovirus content in tumors of each group over time. The AUC (area under the curve) of each treatment at earlier stages will determine the antitumor efficacy at later stages. There is a time lag between the presence of virus in tumors (AUC) and the antitumor efficacy in terms of reduced tumor size, and therefore, it is important that the high content of virus occurs before tumors reach a volume close to the maximum allowed tumor size. Other work in our group has confirmed the lack of correlation between the antitumor efficacy and adenovirus genome content in tumors (Rafael Moreno, personal communication).

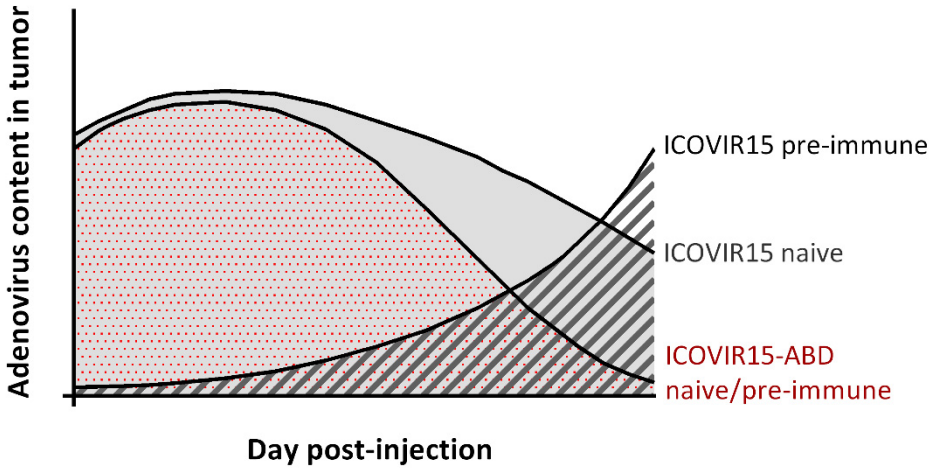

Figure 68. Adenovirus content in tumors over time. The hypothetic evolution of the content of the different oncolytic adenoviruses in tumors is plotted over time, considering the transduction results at day 3, and the virus detection in tumors at day 11 and at the end of the experiments. The AUC (area under the curve) at earlier stages will determine the antitumor efficacy displayed by each virus at later stages.

Despite the lower replication rates and quicker elimination of the ABD-modified virus are not desirable, we need to consider the flaws of the immunodeficient mouse model. The inability of nude mice to generate an immune response against the virus allows for this long persistence, observing high amounts of the non-modified virus at such late days as 32 and 34 after virus injection. However, this long persistence of the virus in tumors would be hindered in an immunocompetent model, or in a human patient. From a clinical point of view, an efficient tumor arrival and virus replication in the first days of treatment is critical to disrupt the immunotolerant state of tumors, and trigger an efficient antitumor immune response. In addition, tumor debulking caused by this active viral replication will facilitate the elimination of tumors. However, the eventual generation of an anti-viral immune response will probably eliminate the virus from tumors at more advanced days. For these reasons, we strongly believe the virus replication and antitumor activity observed in the first days of treatment is more relevant than the one observed in the late days in the immunodeficient mouse model.

The advantage of the ABD modification regarding evasion of NAbs has been demonstrated in terms of organ transduction and oncolysis, proving its usefulness in the fields of gene therapy vectors and oncolytic viruses. In addition, adenoviruses are also extensively used as vaccine platforms against multiple infectious diseases (malaria, influenza, HIV, Ebola, etc.) and cancer (Barouch, 2010; Majhen et al., 2014; Schuldt and Amalfitano, 2012; Tatsis and Ertl, 2004), which also face the problem of pre-existing humoral immunity. In contrast to the immunogenicity of capsid proteins, the immunogenicity of transgenes in adenovirus vectors depends on their expression and it can be blocked by NAbs (Bruder et al., 2012; Roberts et al., 2006; Zak et al., 2012). In this work, we used the E1b viral protein emulating a hypothetical antigen encoded in the adenovirus genome, to test the CTL immune response generated against E1b in immunocompetent mice previously immunized with Ad5. Indeed, we show a low anti-E1b immune response in mice treated with ICOVIR15, due to the neutralization of the virus by NAbs. In contrast, significantly higher anti-E1b immune responses were detected in pre-immune mice treated with ICOVIR15-ABD (**Figure 58**). These results demonstrate the potential utility of the ABD-insertion also in the field of adenovirus-based vaccines.

In addition to pre-existing humoral immunity, the virus-specific NAbs generated *de novo* after the first administration will hinder repeated administrations of the virus. So far, skeletal muscle was one of the few tissues where repeated adenovirus administration was successfully demonstrated, likely due to a lower concentration of NAbs in the muscle than in the serum (Chen et al., 2000a). In this thesis, we also tested whether the ABD insertion could protect the

virus against the NAbs generated against its own capsid and therefore, allow for readministration of the virus. Previous studies have reported the immunogenicity of the big albumin-binding region of the streptococcal protein G (BB), containing the specific ABD we used (Libon et al., 1999; Sjolander et al., 1993, 1997). In these works, BB was used to increase the immunogenicity of weakly immunogenic peptides. Higher antibody responses against a respiratory syncytial virus (RSV) protein (Libon et al., 1999) or a *Plasmodium falciparum* malaria antigen (Sjolander et al., 1997) were observed if these were fused to BB. This effect is not observed in our results, since sera of mice treated with an ABD-modified virus did not show higher neutralizing activities against Ad5 than sera from non-modified virus-treated mice, indicating that the ABD does not increase the immunogenicity of the rest of the capsid. Interestingly, these studies reported the generation of specific antibodies against the BB region in C57BL/6 mice. Accordingly, our immunization studies demonstrated that serum from C57BL/6 mice immunized with an ABD-virus had higher neutralizing activity against the ABD-virus than against the non-modified virus, suggesting that specific NAbs against the ABD were also generated. Furthermore, the low neutralizing activity of sera from ABD-virus-treated mice against the non-modified virus also suggest that the antibody response against the capsid proteins is reduced in favor to the response against the ABD, opposite to what is reported in these studies. We also observed apparent higher titers of NAbs in sera against the ABD virus compared to sera against the parental virus (tittered with the respective viruses used to immunize). This could be associated with higher amounts of NAbs against the ABD, or to a higher neutralizing activity of such NAbs, given that the affinity of the modified HVR1 to dynein could have been reduced.

Despite these sera against the ABD-modified virus displayed a high neutralizing activity, albumin binding to the virus capsid demonstrated a notable protection (**Figure 60**). However, whether this level of protection will be enough to obtain a therapeutic effect after a second administration remains unclear. While liver transduction analysis with IVIS indicated that both viruses were neutralized after a second administration (although as previously discussed, this readout method cannot detect small levels of transduction), ELISPOT studies suggested a higher response against E1b with the ABD-modified vector than with the control vector, in mice previously immunized with their respective capsid (**Figure 61**). In addition, since the prevalence of anti-Ad5 NAbs is very high in humans, a more realistic situation would be immunizing first with Ad5wt (emulating the pre-existing immunity), and then with an ABD-modified virus (emulating the first administration). *In vitro* neutralization studies using serum of mice immunized with this pattern demonstrated an advantage of the ABD vector versus the

control vector in terms of cell transduction (**Figure 62**). Our group is further investigating the feasibility of readministration since no final conclusive results were obtained in this thesis. In any case, although the protection observed after repeated administration is not as efficient as it is against pre-existing Ad5 immunity in mice, this should be tested in the clinic as the response against the ABD in humans is not known.

The combination of the ABD insertion with other previously published modifications is of interest due to its probably synergistic effects. Hyaluronidase expression or KKTK to RGDK replacement in the fiber shaft have successfully improved the oncolytic activity of ICOVIR15 (Guedan et al., 2010; Rojas et al., 2012). VCN01, an ICOVIR15-based adenovirus harboring both of these modifications is currently being tested in two phase I clinical trials (NCT02045602 and NCT02045589). In this work, we have tested the compatibility of the RGDK fiber and the ABD insertion. At the beginning of the project, we chose ICOVIR15 (RGD in the HI-loop of the fiber knob) instead of ICOVIR15K (RGD in the fiber shaft) to test the ABD insertion, due to the possible hiding of the RGD in the shaft by albumin binding (**Figure 63**). Cytotoxicity studies in the absence of NAbs seem to support this hypothesis, as in the presence of albumin ICOVIR15K-ABD suffers a 5-fold loss of cytotoxicity compared to ICOVIR15-ABD (**Figure 64**). In contrast, neutralization studies in the presence of NAbs and albumin demonstrated an equally effective protection of both viruses (**Figure 65**), and suggested no impairment of cell transduction due to the RGD location in the shaft. However, to obtain a more reliable result this assay should be performed by quantifying the luciferase expression of reporter vectors (rather than counting GFP positive cells), which could not be constructed in this thesis due to time constraints.

Antitumor efficacy of ICOVIR15K-ABD was assessed in nude mice with NP-18 tumors, a model where ICOVIR15K had shown a significant improvement compared to ICOVIR15 (Rojas et al., 2012). Nonetheless, when these viruses were bearing the ABD insertion, the advantage of the RGDK fiber was lost, and no differences between viruses were observed in terms of antitumor effect (**Figure 66a**) or in increasing mice survival (**Figure 66b**). Again, we believe multiple factors are contributing to the antitumor efficacy outcome, rather than the combination of ABD and RGDK fiber causes no effect at all. If albumin is really hindering the exposure of the RGD in the fiber shaft, this loss could be compensated with the increased bioavailability provided by the RGDK fiber, resulting in a similar antitumor effect in this model. Blood persistence experiments and more antitumor efficacy studies should be performed to obtain conclusive results, especially in tumor models where the RGDK fiber does not provide

a big advantage. An alternative would be the combination of the ABD with the iRGD fiber. The insertion of the iRGD tumor penetrating peptide in the C terminus of the fiber significantly increased the intratumoral dissemination and antitumor activity of ICOVIR15K (Puig-Saus et al., 2014). Currently, the combination of the ABD with other modifications such as hyaluronidase expression and the iRGD fiber is being tested in our group.

In conclusion, in this thesis we have analyzed the impact of two blood components on the bioactivity of the intravenously administered Ad5. We first show that the interaction of Ad5 with human erythrocytes via CAR does not inactivate the virus, supporting the use of CAR-tropic adenoviruses as systemic therapies. In contrast, NAbs can significantly inhibit the therapeutic effect of adenovirus-based drugs. In this regard, we have designed a modification consisting in the insertion of an albumin-binding domain (ABD), which promotes albumin to shield the adenovirus capsid and protect it from neutralization by antibodies after the systemic administration. This modification proved to be remarkably effective protecting the virus against pre-existing anti-Ad5 NAbs, which is highly relevant from a clinical point of view due to the high prevalence of immunity against Ad5 in humans. The feasibility of readministration as well as the combination of the ABD with other modifications that improve the efficacy of the oncolytic adenovirus is currently being tested in our group to develop a possible new clinical candidate.

CONCLUSIONS

1. Human erythrocytes bind Ad5 via CAR and efficiently pull-down the virus at a ratio of 28 erythrocytes per Ad particle.

2. Ad5 binding to human erythrocytes via CAR does not inhibit *in vitro* cell transduction, nor *in vivo* extravasation and organ transduction after the systemic administration in immunodeficient mice, suggesting that the interaction is reversible.

3. The substitution of HVRs loops by the albumin-binding moieties always results in non-viable viruses, whereas only the insertion of the ABD in the middle of the loops generates viable viruses.

4. The functionality of the ABD is preserved after its insertion in the viral capsid (HVR1 and HVR5), being able to bind both human and mouse serum albumin, but it is only able to protect the virus from NAbs when inserted in the HVR1.

5. Albumin binding causes a slight reduction in cell transduction and cytotoxicity in the absence of NAbs *in vitro*, in a dose-dependent manner.

6. ABD-modified adenoviruses have increased blood persistence after systemic administration, but maintain the same levels of organ transduction and antitumor efficacy in immunodeficient naïve mice.

7. The ABD-modified oncolytic adenovirus shows a reduced toxicity profile after the systemic administration in immunocompetent naïve mice.

8. In the presence of NAbs, albumin protects the ABD-modified virus from neutralization *in vitro*, in terms of cell transduction and cytotoxicity in a dose dependent manner.

9. *In vivo*, the protection provided by albumin against NAbs preserves the ABD-modified virus capability to transduce target organs, induce antitumor activity or generate immune responses to expressed proteins in pre-immune mouse models.

10. The immunogenicity of the ABD results in the generation of highly neutralizing antibodies against the inserted domain. However, the partial protection provided by albumin against these NAbs suggests the possibility of virus readministration.

11. The combination of the ABD insertion and the RGDK fiber reduced the cytotoxicity *in vitro* in absence of NAbs, but maintained the same *in vitro* protection and antitumor efficacy *in vivo* in pre-immune mice.

REFERENCES

A

Alba, R., Bradshaw, A.C., Parker, A.L., Bhella, D., Waddington, S.N., Nicklin, S.A., van Rooijen, N., Custers, J., Goudsmit, J., Barouch, D.H., et al. (2009). Identification of coagulation factor (F)X binding sites on the adenovirus serotype 5 hexon: effect of mutagenesis on FX interactions and gene transfer. Blood *114*, 965–971.

Alba, R., Bradshaw, A.C., Coughlan, L., Denby, L., McDonald, R.A., Waddington, S.N., Buckley, S.M.K., Greig, J.A., Parker, A.L., Miller, A.M., et al. (2010). Biodistribution and retargeting of FX-binding ablated adenovirus serotype 5 vectors. Blood *116*, 2656–2664.

Alemany, R., and Cascallo, M. (2009). Oncolytic viruses from the perspective of the immune system. Futur. Microbiol *4*, 527–536.

Alemany, R., Suzuki, K., and Curiel, D.T. (2000). Blood clearance rates of adenovirus type 5 in mice. J Gen Virol *81*, 2605–2609.

Alonso-Padilla, J., Papp, T., Kajan, G.L., Benko, M., Havenga, M., Lemckert, A., Harrach, B., and Baker, A.H. (2016). Development of Novel Adenoviral Vectors to Overcome Challenges Observed With HAdV-5-based Constructs. Mol Ther *24*, 6–16.

Andersen, J.T., Pehrson, R., Tolmachev, V., Daba, M.B., Abrahmsen, L., and Ekblad, C. (2011). Extending half-life by indirect targeting of the neonatal Fc receptor (FcRn) using a minimal albumin binding domain. J Biol Chem *286*, 5234–5241.

Asher, D.R., Cerny, A.M., and Finberg, R.W. (2005). The erythrocyte viral trap: transgenic expression of viral receptor on erythrocytes attenuates coxsackievirus B infection. Proc Natl Acad Sci U S A *102*, 12897–12902.

B

Barouch, D.H. (2010). Novel adenovirus vector-based vaccines for HIV-1. Curr Opin HIV AIDS *5*, 386–390.

Barouch, D.H., Kik, S. V, Weverling, G.J., Dilan, R., King, S.L., Maxfield, L.F., Clark, S., Ng'ang'a, D., Brandariz, K.L., Abbink, P., et al. (2011). International seroepidemiology of adenovirus serotypes 5, 26, 35, and 48 in pediatric and adult populations. Vaccine *29*, 5203–5209.

Bartlett, D.L., Liu, Z., Sathaiah, M., Ravindranathan, R., Guo, Z., He, Y., and Guo, Z.S. (2013). Oncolytic viruses as therapeutic cancer vaccines. Mol Cancer *12*, 103.

Bauerschmitz, G.J., Lam, J.T., Kanerva, A., Suzuki, K., Nettelbeck, D.M., Dmitriev, I., Krasnykh, V., Mikheeva, G. V, Barnes, M.N., Alvarez, R.D., et al. (2002). Treatment of ovarian cancer with a tropism modified oncolytic adenovirus. Cancer Res *62*, 1266–1270.

Bayo-Puxan, N., Cascallo, M., Gros, A., Huch, M., Fillat, C., and Alemany, R. (2006). Role of the putative heparan sulfate glycosaminoglycan-binding site of the adenovirus type 5 fiber shaft on liver detargeting and knob-mediated retargeting. J Gen Virol *87*, 2487–2495.

Bayo-Puxan, N., Gimenez-Alejandre, M., Lavilla-Alonso, S., Gros, A., Cascallo, M., Hemminki, A., and Alemany, R. (2009). Replacement of adenovirus type 5 fiber shaft heparan sulfate proteoglycan-binding domain with RGD for improved tumor infectivity and targeting. Hum Gene Ther *20*, 1214–1221.

Birnboim, H.C., and Doly, J. (1979). A rapid alkaline extraction procedure for screening recombinant plasmid DNA. Nucleic Acids Res *7*, 1513–1523.

Bischoff, J.R., Kirn, D.H., Williams, A., Heise, C., Horn, S., Muna, M., Ng, L., Nye, J.A., Sampson-Johannes, A., Fattaey, A., et al. (1996). An adenovirus mutant that replicates selectively in p53-deficient human tumor cells. Science (80-.). *274*, 373–376.

Bolling, C., Graefe, T., Lubbing, C., Jankevicius, F., Uktveris, S., Cesas, A., Meyer-Moldenhauer, W.H., Starkmann, H., Weigel, M., Burk, K., et al. (2006). Phase II study of MTX-HSA in combination with cisplatin as first line treatment in patients with advanced or metastatic transitional cell carcinoma. Invest New Drugs *24*, 521–527.

Bradley, R.R., Lynch, D.M., Iampietro, M.J., Borducchi, E.N., and Barouch, D.H. (2012a). Adenovirus serotype 5 neutralizing antibodies target both hexon and fiber following vaccination and natural infection. J Virol *86*, 625–629.

Bradley, R.R., Maxfield, L.F., Lynch, D.M., Iampietro, M.J., Borducchi, E.N., and Barouch, D.H. (2012b). Adenovirus serotype 5-specific neutralizing antibodies target multiple hexon hypervariable regions. J Virol *86*, 1267–1272.

Breitbach, C.J., Burke, J., Jonker, D., Stephenson, J., Haas, A.R., Chow, L.Q., Nieva, J., Hwang, T.H., Moon, A., Patt, R., et al. (2011). Intravenous delivery of a multi-mechanistic cancer-targeted oncolytic poxvirus in humans. Nature *477*, 99–102.

Bruder, J.T., Semenova, E., Chen, P., Limbach, K., Patterson, N.B., Stefaniak, M.E., Konovalova, S., Thomas, C., Hamilton, M., King, C.R., et al. (2012). Modification of Ad5 hexon hypervariable regions circumvents pre-existing Ad5 neutralizing antibodies and induces protective immune responses. PLoS One *7*, e33920.

Bush, M.A., Matthews, J.E., De Boever, E.H., Dobbins, R.L., Hodge, R.J., Walker, S.E., Holland, M.C., Gutierrez, M., and Stewart, M.W. (2009). Safety, tolerability, pharmacodynamics and pharmacokinetics of albiglutide, a long-acting glucagon-like peptide-1 mimetic, in healthy subjects. Diabetes Obes Metab *11*, 498–505.

Byrnes, A.P. (2016). 15 – Antibodies against Adenoviruses. In Adenoviral Vectors for Gene Therapy, pp. 367–390.

C

Carlisle, R.C., Di, Y., Cerny, A.M., Sonnen, A.F., Sim, R.B., Green, N.K., Subr, V., Ulbrich, K., Gilbert, R.J., Fisher, K.D., et al. (2009). Human erythrocytes bind and inactivate type 5 adenovirus by presenting Coxsackie virus-adenovirus receptor and complement receptor 1. Blood *113*, 1909–1918.

Cascallo, M., Alonso, M.M., Rojas, J.J., Perez-Gimenez, A., Fueyo, J., and Alemany, R. (2007). Systemic toxicity-efficacy profile of ICOVIR-5, a potent and selective oncolytic adenovirus based on the pRB pathway. Mol Ther *15*, 1607–1615.

Chaudhury, C., Mehnaz, S., Robinson, J.M., Hayton, W.L., Pearl, D.K., Roopenian, D.C., and Anderson, C.L. (2003). The major histocompatibility complex-related Fc receptor for IgG (FcRn) binds albumin and prolongs its lifespan. J Exp Med *197*, 315–322.

Chawla, S.P., Chua, V.S., Hendifar, A.F., Quon, D. V, Soman, N., Sankhala, K.K., Wieland, D.S., and Levitt, D.J. (2015). A phase 1B/2 study of aldoxorubicin in patients with soft tissue sarcoma. Cancer *121*, 570–579.

Chen, C.Y., Senac, J.S., Weaver, E.A., May, S.M., Jelinek, D.F., Greipp, P., Witzig, T., and Barry, M.A. (2011). Species D adenoviruses as oncolytics against B-cell cancers. Clin Cancer Res *17*, 6712–6722.

Chen, P., Kovesdi, I., and Bruder, J.T. (2000a). Effective repeat administration with adenovirus vectors to the muscle. Gene Ther *7*, 587–595.

Chen, Y., Yu, D.C., Charlton, D., and Henderson, D.R. (2000b). Pre-existent adenovirus antibody inhibits systemic toxicity and antitumor activity of CN706 in the nude mouse LNCaP xenograft model: implications and proposals for human therapy. Hum Gene Ther *11*, 1553–1567.

Cheng, C., Gall, J.G., Nason, M., King, C.R., Koup, R.A., Roederer, M., McElrath, M.J., Morgan, C.A., Churchyard, G., Baden, L.R., et al. (2010). Differential specificity and immunogenicity of adenovirus type 5 neutralizing antibodies elicited by natural infection or immunization. J Virol *84*, 630–638.

Choi, J.W., Lee, J.S., Kim, S.W., and Yun, C.O. (2012). Evolution of oncolytic adenovirus for cancer treatment. Adv. Drug Deliv. Rev. *64*, 720–729.

Cichon, G., Boeckh-Herwig, S., Kuemin, D., Hoffmann, C., Schmidt, H.H., Wehnes, E., Haensch, W., Schneider, U., Eckhardt, U., Burger, R., et al. (2003). Titer determination of Ad5 in blood: a cautionary note. Gene Ther *10*, 1012–1017.

Cody, J.J., and Douglas, J.T. (2009). Armed replicating adenoviruses for cancer virotherapy. Cancer Gene Ther *16*, 473–488.

Colloca, S., Barnes, E., Folgori, A., Ammendola, V., Capone, S., Cirillo, A., Siani, L., Naddeo, M., Grazioli, F., Esposito, M.L., et al. (2012). Vaccine vectors derived from a large collection of simian adenoviruses induce potent cellular immunity across multiple species. Sci Transl Med *4*, 115ra2.

Cotter, M.J., Zaiss, A.K., and Muruve, D.A. (2005). Neutrophils interact with adenovirus vectors via Fc receptors and complement receptor 1. J. Virol. *79*, 14622–14631.

Coughlan, L., Alba, R., Parker, A.L., Bradshaw, A.C., McNeish, I.A., Nicklin, S.A., and Baker, A.H. (2010). Tropism-modification strategies for targeted gene delivery using adenoviral vectors. Viruses *2*, 2290–2355.

Crawford-Miksza, L., and Schnurr, D.P. (1996). Analysis of 15 adenovirus hexon proteins reveals the location and structure of seven hypervariable regions containing serotype-specific residues. J Virol *70*, 1836–1844.

Cripe, T.P., Dunphy, E.J., Holub, A.D., Saini, A., Vasi, N.H., Mahller, Y.Y., Collins, M.H., Snyder, J.D., Krasnykh, V., Curiel, D.T., et al. (2001). Fiber knob modifications overcome low, heterogeneous expression of the coxsackievirus-adenovirus receptor that limits adenovirus gene transfer and oncolysis for human rhabdomyosarcoma cells. Cancer Res *61*, 2953–2960.

Croyle, M.A., Chirmule, N., Zhang, Y., and Wilson, J.M. (2001). “Stealth” adenoviruses blunt cell-mediated and humoral immune responses against the virus and allow for significant gene expression upon readministration in the lung. J. Virol. *75*, 4792–4801.

D

De la Rosa-Trevin, J.M., Oton, J., Marabini, R., Zaldivar, A., Vargas, J., Carazo, J.M., and Sorzano, C.O. (2013). Xmipp 3.0: an improved software suite for image processing in electron microscopy. J Struct Biol *184*, 321–328.

Dennis, M.S., Zhang, M., Meng, Y.G., Kadkhodayan, M., Kirchhofer, D., Combs, D., and Damico, L.A. (2002). Albumin binding as a general strategy for improving the pharmacokinetics of proteins. J Biol Chem *277*, 35035–35043.

De Pace, N. (1912). Sulla scomparsa di un enorme cancro vegetante del collo dell'utero senza cura chirurgica. Ginecologia *9*, 82-89.

Desai, N., Trieu, V., Yao, Z., Louie, L., Ci, S., Yang, A., Tao, C., De, T., Beals, B., Dykes, D., et al. (2006). Increased antitumor activity, intratumor paclitaxel concentrations, and endothelial cell transport of cremophor-free, albumin-bound paclitaxel, ABI-007, compared with cremophor-based paclitaxel. Clin Cancer Res *12*, 1317–1324.

Desai, N., Trieu, V., Damascelli, B., and Soon-Shiong, P. (2009). SPARC Expression Correlates with Tumor Response to Albumin-Bound Paclitaxel in Head and Neck Cancer Patients. Transl Oncol *2*, 59–64.

Dhar, D., Spencer, J.F., Toth, K., and Wold, W.S. (2009). Pre-existing immunity and passive immunity to adenovirus 5 prevents toxicity caused by an oncolytic adenovirus vector in the Syrian hamster model. Mol Ther *17*, 1724–1732.

Di, Y., Seymour, L., and Fisher, K. (2014). Activity of a group B oncolytic adenovirus (ColoAd1) in whole human blood. Gene Ther *21*, 440–443.

Dmitriev, I., Krasnykh, V., Miller, C.R., Wang, M., Kashentseva, E., Mikheeva, G., Belousova, N., and Curiel, D.T. (1998). An adenovirus vector with genetically modified fibers demonstrates expanded tropism via utilization of a coxsackievirus and adenovirus receptor-independent cell entry mechanism. J Virol *72*, 9706–9713.

Dock, G. (1904). The Influence of Complicating Diseases Upon Leukaemia. Am J Med Sci *127*, 563-592.

Dornhorst, A., Luddeke, H.J., Sreenan, S., Koenen, C., Hansen, J.B., Tsur, A., and Landstedt-Hallin, L. (2007). Safety and efficacy of insulin detemir in clinical practice: 14-week follow-up data from type 1 and type 2 diabetes patients in the PREDICTIVE European cohort. Int J Clin Pr. *61*, 523–528.

Doronin, K., Flatt, J.W., Di Paolo, N.C., Khare, R., Kalyuzhniy, O., Acchione, M., Sumida, J.P., Ohto, U., Shimizu, T., Akashi-Takamura, S., et al. (2012). Coagulation factor X activates innate immunity to human species C adenovirus. Science (80-.). *338*, 795–798.

Draper, S.J., Biswas, S., Spencer, A.J., Remarque, E.J., Capone, S., Naddeo, M., Dicks, M.D.J., Faber, B.W., de Cassan, S.C., Folgori, A., et al. (2010). Enhancing blood-stage malaria subunit vaccine immunogenicity in rhesus macaques by combining adenovirus, poxvirus, and protein-in-adjuvant vaccines. J. Immunol. *185*, 7583–7595.

E

Engler, H., Machemer, T., Philopena, J., Wen, S.F., Quijano, E., Ramachandra, M., Tsai, V., and Ralston, R. (2004). Acute hepatotoxicity of oncolytic adenoviruses in mouse models is associated with expression of wild-type E1a and induction of TNF-alpha. Virology *328*, 52–61.

Eto, Y., Gao, J.Q., Sekiguchi, F., Kurachi, S., Katayama, K., Maeda, M., Kawasaki, K., Mizuguchi, H., Hayakawa, T., Tsutsumi, Y., et al. (2005). PEGylated adenovirus vectors containing RGD peptides on the tip of PEG show high transduction efficiency and antibody evasion ability. J. Gene Med. *7*, 604–612.

F

Falkenberg, C., Bjorck, L., and Akerstrom, B. (1992). Localization of the binding site for streptococcal protein G on human serum albumin. Identification of a 5.5-kilodalton protein G binding albumin fragment. Biochemistry *31*, 1451–1457.

Fisher, K.D., and Seymour, L.W. (2010). HPMA copolymers for masking and retargeting of therapeutic viruses. Adv. Drug Deliv. Rev. *62*, 240–245.

Freimuth, P., Philipson, L., and Carson, S.D. (2008). The coxsackievirus and adenovirus receptor. In Group B Coxsackieviruses, (Springer), pp. 67–87.

Fueyo, J., Gomez-Manzano, C., Alemany, R., Lee, P.S., McDonnell, T.J., Mitlianga, P., Shi, Y.X., Levin, V.A., Yung, W.K., and Kyritsis, A.P. (2000). A mutant oncolytic adenovirus targeting the Rb pathway produces anti-glioma effect in vivo. Oncogene *19*, 2–12.

G

Gall, J., Kass-Eisler, A., Leinwand, L., and Falck-Pedersen, E. (1996). Adenovirus type 5 and 7 capsid chimera: fiber replacement alters receptor tropism without affecting primary immune neutralization epitopes. J Virol *70*, 2116–2123.

Gall, J.G., Crystal, R.G., and Falck-Pedersen, E. (1998). Construction and characterization of hexon-chimeric adenoviruses: specification of adenovirus serotype. J. Virol. *72*, 10260–10264.

Ganesan, L.P., Mohanty, S., Kim, J., Clark, K.R., Robinson, J.M., and Anderson, C.L. (2011). Rapid and efficient clearance of blood-borne virus by liver sinusoidal endothelium. PLoS Pathog *7*, e1002281.

Garber, K. (2006). China approves world's first oncolytic virus therapy for cancer treatment. J Natl Cancer Inst *98*, 298–300.

Gil-Hoyos, R. (2014). Modificación genética de la inmunodominancia epitópica del adenovirus para potenciar la respuesta inmune contra epítopos no virales. (Doctoral thesis). Universitat de Barcelona.

Gimenez-Alejandre, M., Cascallo, M., Bayo-Puxan, N., and Alemany, R. (2008). Coagulation factors determine tumor transduction in vivo. Hum Gene Ther *19*, 1415–1419.

Gong, J., Sachdev, E., Mita, A.C., and Mita, M.M. (2016). Clinical development of reovirus for cancer therapy: An oncolytic virus with immune-mediated antitumor activity. World J Methodol *6*, 25–42.

Graeser, R., Esser, N., Unger, H., Fichtner, I., Zhu, A., Unger, C., and Kratz, F. (2010). INNO-206, the (6-maleimidocaproyl hydrazone derivative of doxorubicin), shows superior antitumor efficacy compared to doxorubicin in different tumor xenograft models and in an orthotopic pancreas carcinoma model. Invest New Drugs *28*, 14–19.

Graham, F.L., Smiley, J., Russell, W.C., and Nairn, R. (1977). Characteristics of a human cell line transformed by DNA from human adenovirus type 5. J Gen Virol *36*, 59–74.

Green, N.K., Herbert, C.W., Hale, S.J., Hale, A.B., Mautner, V., Harkins, R., Hermiston, T., Ulbrich, K., Fisher, K.D., and Seymour, L.W. (2004). Extended plasma circulation time and decreased toxicity of polymer-coated adenovirus. Gene Ther. *11*, 1256–1263.

Green, N.K., Morrison, J., Hale, S., Briggs, S.S., Stevenson, M., Subr, V., Ulbrich, K., Chandler, L., Mautner, V., Seymour, L.W., et al. (2008). Retargeting polymer-coated adenovirus to the FGF receptor

allows productive infection and mediates efficacy in a peritoneal model of human ovarian cancer. J. Gene Med. *10*, 280–289.

Grill, J., Van Beusechem, V.W., Van Der Valk, P., Dirven, C.M., Leonhart, A., Pherai, D.S., Haisma, H.J., Pinedo, H.M., Curiel, D.T., and Gerritsen, W.R. (2001). Combined targeting of adenoviruses to integrins and epidermal growth factor receptors increases gene transfer into primary glioma cells and spheroids. Clin Cancer Res *7*, 641–650.

Guedan, S., Rojas, J.J., Gros, A., Mercade, E., Cascallo, M., and Alemany, R. (2010). Hyaluronidase expression by an oncolytic adenovirus enhances its intratumoral spread and suppresses tumor growth. Mol Ther *18*, 1275–1283.

Guedan, S., Grases, D., Rojas, J.J., Gros, A., Vilardell, F., Vile, R., Mercade, E., Cascallo, M., and Alemany, R. (2012). GALV expression enhances the therapeutic efficacy of an oncolytic adenovirus by inducing cell fusion and enhancing virus distribution. Gene Ther *19*, 1048–1057.

Guimet, D., and Hearing, P. (2016). 3 – Adenovirus Replication. In Adenoviral Vectors for Gene Therapy, pp. 59–84.

Guo, R., Guo, W., Cao, L., Liu, H., Liu, J., Xu, H., Huang, W., Wang, F., and Hong, Z. (2016). Fusion of an albumin-binding domain extends the half-life of immunotoxins. Int. J. Pharm. *511*, 538–549.

Gupalo, E., Buriachkovskaia, L., and Othman, M. (2011). Human platelets express CAR with localization at the sites of intercellular interaction. Virol. J. *8*, 456.

H

Habib, N., Salama, H., Abd El Latif Abu Median, A., Isac Anis, I., Abd Al Aziz, R.A., Sarraf, C., Mitry, R., Havlik, R., Seth, P., Hartwigsen, J., et al. (2002). Clinical trial of E1B-deleted adenovirus (dl1520) gene therapy for hepatocellular carcinoma. Cancer Gene Ther *9*, 254–259.

Haisma, H.J., Kamps, J.A., Kamps, G.K., Plantinga, J.A., Rots, M.G., and Bellu, A.R. (2008). Polyinosinic acid enhances delivery of adenovirus vectors in vivo by preventing sequestration in liver macrophages. J Gen Virol *89*, 1097–1105.

Haisma, H.J., Boesjes, M., Beerens, A.M., van der Strate, B.W.A., Curiel, D.T., Plüddemann, A., Gordon, S., and Bellu, A.R. (2009). Scavenger Receptor A: A New Route for Adenovirus 5. Mol. Pharm. *6*, 366–374.

Hall, K., Blair Zajdel, M.E., and Blair, G.E. (2010). Unity and diversity in the human adenoviruses: exploiting alternative entry pathways for gene therapy. Biochem. J. *431*, 321–336.

Hamid, O., Varterasian, M.L., Wadler, S., Hecht, J.R., Benson 3rd, A., Galanis, E., Uprichard, M., Omer, C., Bycott, P., Hackman, R.C., et al. (2003). Phase II trial of intravenous CI-1042 in patients with metastatic colorectal cancer. J Clin Oncol *21*, 1498–1504.

Hartman, Z.C., Appledorn, D.M., and Amalfitano, A. (2008). Adenovirus vector induced innate immune responses: impact upon efficacy and toxicity in gene therapy and vaccine applications. Virus Res *132*, 1–14.

Hedley, S.J., Chen, J., Mountz, J.D., Li, J., Curiel, D.T., Korokhov, N., and Kovesdi, I. (2006). Targeted and shielded adenovectors for cancer therapy. Cancer Immunol Immunother *55*, 1412–1419.

Hedley, S.J., Krendelshchikov, A., Kim, M.-H., Chen, J., Hsu, H.-C., Mountz, J.D., Curiel, D.T., and Kovesdi,

I. (2009). Assessment of genetic shielding for adenovirus vectors. Open Gene Ther. J. *2*, 1–11.

Heise, C., Hermiston, T., Johnson, L., Brooks, G., Sampson-Johannes, A., Williams, A., Hawkins, L., and Kirn, D. (2000). An adenovirus E1A mutant that demonstrates potent and selective systemic anti-tumoral efficacy. Nat Med *6*, 1134–1139.

Hemminki, O., Diaconu, I., Cerullo, V., Pesonen, S.K., Kanerva, A., Joensuu, T., Kairemo, K., Laasonen, L., Partanen, K., Kangasniemi, L., et al. (2012). Ad3-hTERT-E1A, a fully serotype 3 oncolytic adenovirus, in patients with chemotherapy refractory cancer. Mol. Ther. *20*, 1821–1830.

Heo, J., Reid, T., Ruo, L., Breitbach, C.J., Rose, S., Bloomston, M., Cho, M., Lim, H.Y., Chung, H.C., Kim, C.W., et al. (2013). Randomized dose-finding clinical trial of oncolytic immunotherapeutic vaccinia JX-594 in liver cancer. Nat Med *19*, 329–336.

Hofmann, C., Loser, P., Cichon, G., Arnold, W., Both, G.W., and Strauss, M. (1999). Ovine adenovirus vectors overcome preexisting humoral immunity against human adenoviruses in vivo. J Virol *73*, 6930–6936.

Holterman, L., Vogels, R., van der Vlugt, R., Sieuwerts, M., Grimbergen, J., Kaspers, J., Geelen, E., van der Helm, E., Lemckert, A., Gillissen, G., et al. (2004). Novel replication-incompetent vector derived from adenovirus type 11 (Ad11) for vaccination and gene therapy: low seroprevalence and non-cross-reactivity with Ad5. J Virol *78*, 13207–13215.

Hu, Z., Van Rooijen, N., and Yang, Y.G. (2011). Macrophages prevent human red blood cell reconstitution in immunodeficient mice. Blood *118*, 5938–5946.

J

Jogler, C., Hoffmann, D., Theegarten, D., Grunwald, T., Uberla, K., and Wildner, O. (2006). Replication properties of human adenovirus in vivo and in cultures of primary cells from different animal species. J Virol *80*, 3549–3558.

Johnson, L., Shen, A., Boyle, L., Kunich, J., Pandey, K., Lemmon, M., Hermiston, T., Giedlin, M., McCormick, F., and Fattaey, A. (2002). Selectively replicating adenoviruses targeting deregulated E2F activity are potent, systemic antitumor agents. Cancer Cell *1*, 325–337.

Jung, Y., Park, H.J., Kim, P.H., Lee, J., Hyung, W., Yang, J., Ko, H., Sohn, J.H., Kim, J.H., Huh, Y.M., et al. (2007). Retargeting of adenoviral gene delivery via Herceptin-PEG-adenovirus conjugates to breast cancer cells. J. Control. Release *123*, 164–171.

K

Kalyuzhniy, O., Di Paolo, N.C., Silvestry, M., Hofherr, S.E., Barry, M.A., Stewart, P.L., and Shayakhmetov, D.M. (2008). Adenovirus serotype 5 hexon is critical for virus infection of hepatocytes in vivo. Proc Natl Acad Sci U S A *105*, 5483–5488.

Kantoff, P.W., Higano, C.S., Shore, N.D., Berger, E.R., Small, E.J., Penson, D.F., Redfern, C.H., Ferrari, A.C., Dreicer, R., Sims, R.B., et al. (2010). Sipuleucel-T immunotherapy for castration-resistant prostate cancer. N Engl J Med *363*, 411–422.

Karapanagiotou, E.M., Roulstone, V., Twigger, K., Ball, M., Tanay, M., Nutting, C., Newbold, K., Gore, M.E., Larkin, J., Syrigos, K.N., et al. (2012). Phase I/II trial of carboplatin and paclitaxel chemotherapy

in combination with intravenous oncolytic reovirus in patients with advanced malignancies. Clin Cancer Res *18*, 2080–2089.

Karlseder, J., Rotheneder, H., and Wintersberger, E. (1996). Interaction of Sp1 with the growth- and cell cycle-regulated transcription factor E2F. Mol Cell Biol *16*, 1659–1667.

Kelly, E., and Russell, S.J. (2007). History of oncolytic viruses: genesis to genetic engineering. Mol Ther *15*, 651–659.

Khare, R., May, S.M., Vetrini, F., Weaver, E.A., Palmer, D., Rosewell, A., Grove, N., Ng, P., and Barry, M.A. (2011a). Generation of a Kupffer cell-evading adenovirus for systemic and liver-directed gene transfer. Mol Ther *19*, 1254–1262.

Khare, R., Chen, C.Y., Weaver, E.A., and Barry, M.A. (2011b). Advances and future challenges in adenoviral vector pharmacology and targeting. Curr Gene Ther *11*, 241–258.

Khare, R., Reddy, V.S., Nemerow, G.R., and Barry, M.A. (2012). Identification of adenovirus serotype 5 hexon regions that interact with scavenger receptors. J Virol *86*, 2293–2301.

Khare, R., Hillestad, M.L., Xu, Z., Byrnes, A.P., and Barry, M.A. (2013). Circulating antibodies and macrophages as modulators of adenovirus pharmacology. J Virol *87*, 3678–3686.

Kim, P.H., Sohn, J.H., Choi, J.W., Jung, Y., Kim, S.W., Haam, S., and Yun, C.O. (2011). Active targeting and safety profile of PEG-modified adenovirus conjugated with herceptin. Biomaterials *32*, 2314–2326.

Konig, T., and Skerra, A. (1998). Use of an albumin-binding domain for the selective immobilisation of recombinant capture antibody fragments on ELISA plates. J Immunol Methods *218*, 73–83.

Kontermann, R.E. (2009). Strategies to extend plasma half-lives of recombinant antibodies. BioDrugs *23*, 93–109.

Kontermann, R.E. (2011). Strategies for extended serum half-life of protein therapeutics. Curr Opin Biotechnol *22*, 868–876.

Kratz, F. (2008). Albumin as a drug carrier: design of prodrugs, drug conjugates and nanoparticles. J Control Release *132*, 171–183.

Kratz, F. (2014). A clinical update of using albumin as a drug vehicle - a commentary. J Control Release *190*, 331–336.

Kraulis, P.J., Jonasson, P., Nygren, P.A., Uhlen, M., Jendeberg, L., Nilsson, B., and Kordel, J. (1996). The serum albumin-binding domain of streptococcal protein G is a three-helical bundle: a heteronuclear NMR study. FEBS Lett *378*, 190–194.

Kuhn, I., Harden, P., Bauzon, M., Chartier, C., Nye, J., Thorne, S., Reid, T., Ni, S., Lieber, A., Fisher, K., et al. (2008). Directed evolution generates a novel oncolytic virus for the treatment of colon cancer. PLoS One *3*, e2409.

L

Laborda, E., Puig-Saus, C., Rodriguez-García, A., Moreno, R., Cascalló, M., Pastor, J., and Alemany, R. (2014). A pRb-responsive, RGD-modified, and Hyaluronidase-armed Canine Oncolytic Adenovirus for Application in Veterinary Oncology. Mol. Ther. *22*, 986–998.

Larsen, M.T., Kuhlmann, M., Hvam, M.L., and Howard, K.A. (2016). Albumin-based drug delivery:

harnessing nature to cure disease. Mol Cell Ther *4*, 3.

Lemckert, A.A., Sumida, S.M., Holterman, L., Vogels, R., Truitt, D.M., Lynch, D.M., Nanda, A., Ewald, B.A., Gorgone, D.A., Lifton, M.A., et al. (2005). Immunogenicity of heterologous prime-boost regimens involving recombinant adenovirus serotype 11 (Ad11) and Ad35 vaccine vectors in the presence of anti-ad5 immunity. J Virol *79*, 9694–9701.

Lencer, W.I., and Blumberg, R.S. (2005). A passionate kiss, then run: exocytosis and recycling of IgG by FcRn. Trends Cell Biol *15*, 5–9.

Li, R., Yang, H., Jia, D., Nie, Q., Cai, H., Fan, Q., Wan, L., Li, L., and Lu, X. (2016). Fusion to an albumin-binding domain with a high affinity for albumin extends the circulatory half-life and enhances the in vivo antitumor effects of human TRAIL. J Control Release *228*, 96–106.

Li, Y., Pong, R.C., Bergelson, J.M., Hall, M.C., Sagalowsky, A.I., Tseng, C.P., Wang, Z., and Hsieh, J.T. (1999). Loss of adenoviral receptor expression in human bladder cancer cells: a potential impact on the efficacy of gene therapy. Cancer Res. *59*, 325–330.

Libon, C., Corvaia, N., Haeuw, J.F., Nguyen, T.N., Stahl, S., Bonnefoy, J.Y., and Andreoni, C. (1999). The serum albumin-binding region of streptococcal protein G (BB) potentiates the immunogenicity of the G130-230 RSV-A protein. Vaccine *17*, 406–414.

Lichty, B.D., Breitbach, C.J., Stojdl, D.F., and Bell, J.C. (2014). Going viral with cancer immunotherapy. Nat Rev Cancer *14*, 559–567.

Liu, Q., and Muruve, D.A. (2003). Molecular basis of the inflammatory response to adenovirus vectors. Gene Ther *10*, 935–940.

Liu, H., Jin, L., Koh, S.B., Atanasov, I., Schein, S., Wu, L., and Zhou, Z.H. (2010). Atomic structure of human adenovirus by cryo-EM reveals interactions among protein networks. Science (80-.). *329*, 1038–1043.

Lopez-Gordo, E., Podgorski II, Downes, N., and Alemany, R. (2014). Circumventing antivector immunity: potential use of nonhuman adenoviral vectors. Hum Gene Ther *25*, 285–300.

Lucas, T., Benihoud, K., Vigant, F., Schmidt, C.Q., Wortmann, A., Bachem, M.G., Simmet, T., and Kochanek, S. (2015). Hexon modification to improve the activity of oncolytic adenovirus vectors against neoplastic and stromal cells in pancreatic cancer. PLoS One *10*, e0117254.

Ludtke, S.J., Baldwin, P.R., and Chiu, W. (1999). EMAN: semiautomated software for high-resolution single-particle reconstructions. J Struct Biol *128*, 82–97.

Lyons, M., Onion, D., Green, N.K., Aslan, K., Rajaratnam, R., Bazan-Peregrino, M., Phipps, S., Hale, S., Mautner, V., Seymour, L.W., et al. (2006). Adenovirus type 5 interactions with human blood cells may compromise systemic delivery. Mol Ther *14*, 118–128.

M

Maeda, H., Wu, J., Sawa, T., Matsumura, Y., and Hori, K. (2000). Tumor vascular permeability and the EPR effect in macromolecular therapeutics: a review. J Control Release *65*, 271–284.

Majhen, D., Calderon, H., Chandra, N., Fajardo, C.A., Rajan, A., Alemany, R., and Custers, J. (2014). Adenovirus-based vaccines for fighting infectious diseases and cancer: progress in the field. Hum Gene Ther *25*, 301–317.

Manickan, E., Smith, J.S., Tian, J., Eggerman, T.L., Lozier, J.N., Muller, J., and Byrnes, A.P. (2006). Rapid Kupffer cell death after intravenous injection of adenovirus vectors. Mol Ther *13*, 108–117.

Martuza, R.L., Malick, A., Markert, J.M., Ruffner, K.L., and Coen, D.M. (1991). Experimental therapy of human glioma by means of a genetically engineered virus mutant. Science (80-.). *252*, 854–856.

Mast, T.C., Kierstead, L., Gupta, S.B., Nikas, A.A., Kallas, E.G., Novitsky, V., Mbewe, B., Pitisuttithum, P., Schechter, M., Vardas, E., et al. (2010). International epidemiology of human pre-existing adenovirus (Ad) type-5, type-6, type-26 and type-36 neutralizing antibodies: Correlates of high Ad5 titers and implications for potential HIV vaccine trials. Vaccine *28*, 950–957.

Matthews, Q.L. (2011). Capsid-incorporation of antigens into adenovirus capsid proteins for a vaccine approach. Mol Pharm *8*, 3–11.

McConnell, M.J., and Imperiale, M.J. (2004). Biology of adenovirus and its use as a vector for gene therapy. Hum Gene Ther *15*, 1022–1033.

McDonagh, C.F., Huhalov, A., Harms, B.D., Adams, S., Paragas, V., Oyama, S., Zhang, B., Luus, L., Overland, R., Nguyen, S., et al. (2012). Antitumor activity of a novel bispecific antibody that targets the ErbB2/ErbB3 oncogenic unit and inhibits heregulin-induced activation of ErbB3. Mol Cancer Ther *11*, 582–593.

N

Nagel, H., Maag, S., Tassis, A., Nestle, F.O., Greber, U.F., and Hemmi, S. (2003). The alphavbeta5 integrin of hematopoietic and nonhematopoietic cells is a transduction receptor of RGD-4C fiber-modified adenoviruses. Gene Ther *10*, 1643–1653.

Neil, I. (2007). Nab technology: a drug delivery platform utilizing endothelial gp60 receptor-based transport and tumor-derived SPARC for targeting. Drug Deliv Rep 37–41.

Nemerow, G.R., and Stewart, P.L. (1999). Role of alpha(v) integrins in adenovirus cell entry and gene delivery. Microbiol Mol Biol Rev *63*, 725–734.

Nemunaitis, J., Cunningham, C., Buchanan, A., Blackburn, A., Edelman, G., Maples, P., Netto, G., Tong, A., Randlev, B., Olson, S., et al. (2001). Intravenous infusion of a replication-selective adenovirus (ONYX-015) in cancer patients: safety, feasibility and biological activity. Gene Ther *8*, 746–759.

Nicol, C.G., Graham, D., Miller, W.H., White, S.J., Smith, T.A.G., Nicklin, S.A., Stevenson, S.C., and Baker, A.H. (2004). Effect of adenovirus serotype 5 fiber and penton modifications on in vivo tropism in rats. Mol. Ther. *10*, 344–354.

Nilvebrant, J., and Hober, S. (2013). The albumin-binding domain as a scaffold for protein engineering. Comput Struct Biotechnol J *6*, e201303009.

Nistal-Villan, E., Bunuales, M., Poutou, J., Gonzalez-Aparicio, M., Bravo-Perez, C., Quetglas, J.I., Carte, B., Gonzalez-Aseguinolaza, G., Prieto, J., Larrea, E., et al. (2015). Enhanced therapeutic effect using sequential administration of antigenically distinct oncolytic viruses expressing oncostatin M in a Syrian hamster orthotopic pancreatic cancer model. Mol. Cancer *14*, 210.

Nygren, P.A., Ljungquist, C., Tromborg, H., Nustad, K., and Uhlen, M. (1990). Species-dependent binding of serum albumins to the streptococcal receptor protein G. Eur J Biochem *193*, 143–148.

O

O'Riordan, C.R., Lachapelle, A., Delgado, C., Parkes, V., Wadsworth, S.C., Smith, A.E., and Francis, G.E. (1999). PEGylation of adenovirus with retention of infectivity and protection from neutralizing antibody in vitro and in vivo. Hum. Gene Ther. *10*, 1349–1358.

P

Pack, G.T. (1950). Note on the experimental use of rabies vaccine for melanomatosis. AMA Arch Derm Syphilol *62*, 694–695.

Papaioannou, N.E., Beniata, O. V, Vitsos, P., Tsitsilonis, O., and Samara, P. (2016). Harnessing the immune system to improve cancer therapy. Ann Transl Med *4*, 261.

Pardoll, D.M. (2012). The blockade of immune checkpoints in cancer immunotherapy. Nat Rev Cancer *12*, 252–264.

Park, B.H., Hwang, T., Liu, T.C., Sze, D.Y., Kim, J.S., Kwon, H.C., Oh, S.Y., Han, S.Y., Yoon, J.H., Hong, S.H., et al. (2008). Use of a targeted oncolytic poxvirus, JX-594, in patients with refractory primary or metastatic liver cancer: a phase I trial. Lancet Oncol *9*, 533–542.

Parker, A.L., Waddington, S.N., Nicol, C.G., Shayakhmetov, D.M., Buckley, S.M., Denby, L., Kemball-Cook, G., Ni, S., Lieber, A., McVey, J.H., et al. (2006). Multiple vitamin K-dependent coagulation zymogens promote adenovirus-mediated gene delivery to hepatocytes. Blood *108*, 2554–2561.

Parreno, M., Garriga, J., Limon, A., Albrecht, J.H., and Grana, X. (2001). E1A modulates phosphorylation of p130 and p107 by differentially regulating the activity of G1/S cyclin/CDK complexes. Oncogene *20*, 4793–4806.

Perreau, M., and Kremer, E.J. (2006). The conundrum between immunological memory to adenovirus and their use as vectors in clinical gene therapy. Mol Biotechnol *34*, 247–256.

Peters Jr, T. (1995). All about albumin: biochemistry, genetics, and medical applications (Academic press).

Pettersen, E.F., Goddard, T.D., Huang, C.C., Couch, G.S., Greenblatt, D.M., Meng, E.C., and Ferrin, T.E. (2004). UCSF Chimera--a visualization system for exploratory research and analysis. J Comput Chem *25*, 1605–1612.

Piccolo, P., Vetrini, F., Mithbaokar, P., Grove, N.C., Bertin, T., Palmer, D., Ng, P., and Brunetti-Pierri, N. (2013). SR-A and SREC-I are Kupffer and endothelial cell receptors for helper-dependent adenoviral vectors. Mol Ther *21*, 767–774.

Pratley, R.E., Nauck, M., Bailey, T., Montanya, E., Cuddihy, R., Filetti, S., Thomsen, A.B., Søndergaard, R.E., Davies, M., and 1860-LIRA-DPP-4 Study Group (2010). Liraglutide versus sitagliptin for patients with type 2 diabetes who did not have adequate glycaemic control with metformin: a 26-week, randomised, parallel-group, open-label trial. Lancet *375*, 1447–1456.

Puig-Saus, C., Rojas, L.A., Laborda, E., Figueras, A., Alba, R., Fillat, C., and Alemany, R. (2014). iRGD tumor-penetrating peptide-modified oncolytic adenovirus shows enhanced tumor transduction, intratumoral dissemination and antitumor efficacy. Gene Ther *21*, 767–774.

R

Reddy, P.S., Idamakanti, N., Chen, Y., Whale, T., Babiuk, L.A., Mehtali, M., and Tikoo, S.K. (1999). Replication-defective bovine adenovirus type 3 as an expression vector. J Virol *73*, 9137–9144.

Reid, T., Galanis, E., Abbruzzese, J., Sze, D., Wein, L.M., Andrews, J., Randlev, B., Heise, C., Uprichard, M., Hatfield, M., et al. (2002). Hepatic arterial infusion of a replication-selective oncolytic adenovirus (dl1520): phase II viral, immunologic, and clinical endpoints. Cancer Res *62*, 6070–6079.

Roberts, D.M., Nanda, A., Havenga, M.J., Abbink, P., Lynch, D.M., Ewald, B.A., Liu, J., Thorner, A.R., Swanson, P.E., Gorgone, D.A., et al. (2006). Hexon-chimaeric adenovirus serotype 5 vectors circumvent pre-existing anti-vector immunity. Nature *441*, 239–243.

Rodriguez-Garcia, A., Gimenez-Alejandre, M., Rojas, J.J., Moreno, R., Bazan-Peregrino, M., Cascallo, M., and Alemany, R. (2015). Safety and efficacy of VCN-01, an oncolytic adenovirus combining fiber HSG-binding domain replacement with RGD and hyaluronidase expression. Clin Cancer Res *21*, 1406–1418.

Rodriguez-García, A. (2015). Enhancing the Antitumor Activity of Oncolytic Adenoviruses by Combining Tumor Targeting with Hyaluronidase Expression Or by Increasing the Immunogenicity of Exogenous Epitopes. (Doctoral thesis). Universitat de Barcelona.

Rohou, A., and Grigorieff, N. (2015). CTFFIND4: Fast and accurate defocus estimation from electron micrographs. J Struct Biol *192*, 216–221.

Rojas, J.J., Cascallo, M., Guedan, S., Gros, A., Martinez-Quintanilla, J., Hemminki, A., and Alemany, R. (2009). A modified E2F-1 promoter improves the efficacy to toxicity ratio of oncolytic adenoviruses. Gene Ther *16*, 1441–1451.

Rojas, J.J., Guedan, S., Searle, P.F., Martinez-Quintanilla, J., Gil-Hoyos, R., Alcayaga-Miranda, F., Cascallo, M., and Alemany, R. (2010). Minimal RB-responsive E1A Promoter Modification to Attain Potency, Selectivity, and Transgene-arming Capacity in Oncolytic Adenoviruses. Mol Ther *18*, 1960–1971.

Rojas, J.J., Gimenez-Alejandre, M., Gil-Hoyos, R., Cascallo, M., and Alemany, R. (2012). Improved systemic antitumor therapy with oncolytic adenoviruses by replacing the fiber shaft HSG-binding domain with RGD. Gene Ther *19*, 453–457.

Rojas, J.J., Sampath, P., Hou, W., and Thorne, S.H. (2015). Defining Effective Combinations of Immune Checkpoint Blockade and Oncolytic Virotherapy. Clin. Cancer Res. *21*, 5543–5551.

Roopenian, D.C., and Akilesh, S. (2007). FcRn: the neonatal Fc receptor comes of age. Nat Rev Immunol *7*, 715–725.

Rowe, W.P., Huebner, R.J., Gilmore, L.K., Parrott, R.H., and Ward, T.G. (1953). Isolation of a cytopathogenic agent from human adenoids undergoing spontaneous degeneration in tissue culture. Proc Soc Exp Biol Med *84*, 570–573.

Roy, S., Shirley, P.S., McClelland, A., and Kaleko, M. (1998). Circumvention of immunity to the adenovirus major coat protein hexon. J. Virol. *72*, 6875–6879.

Roy, S., Clawson, D.S., Calcedo, R., Lebherz, C., Sanmiguel, J., Wu, D., and Wilson, J.M. (2005). Use of chimeric adenoviral vectors to assess capsid neutralization determinants. Virology *333*, 207–214.

Russell, W.C. (2009). Adenoviruses: update on structure and function. J Gen Virol *90*, 1–20.

Russell, S.J., Peng, K.W., and Bell, J.C. (2012). Oncolytic virotherapy. Nat Biotechnol *30*, 658–670.

Rustgi, V.K. (2009). Albinterferon alfa-2b, a novel fusion protein of human albumin and human interferon alfa-2b, for chronic hepatitis C. Curr Med Res Opin *25*, 991–1002.

Rux, J.J., and Burnett, R.M. (2000). Type-specific epitope locations revealed by X-ray crystallographic study of adenovirus type 5 hexon. Mol Ther *1*, 18–30.

S

Santagostino, E., Negrier, C., Klamroth, R., Tiede, A., Pabinger-Fasching, I., Voigt, C., Jacobs, I., and Morfini, M. (2012). Safety and pharmacokinetics of a novel recombinant fusion protein linking coagulation factor IX with albumin (rIX-FP) in hemophilia B patients. Blood *120*, 2405–2411.

Scherer, J., and Vallee, R.B. (2015). Conformational changes in the adenovirus hexon subunit responsible for regulating cytoplasmic dynein recruitment. J Virol *89*, 1013–1023.

Schlapschy, M., Theobald, I., Mack, H., Schottelius, M., Wester, H.J., and Skerra, A. (2007). Fusion of a recombinant antibody fragment with a homo-amino-acid polymer: effects on biophysical properties and prolonged plasma half-life. Protein Eng Des Sel *20*, 273–284.

Schnitzer, J.E. (1992). gp60 is an albumin-binding glycoprotein expressed by continuous endothelium involved in albumin transcytosis. Am J Physiol *262*, H246-54.

Schuldt, N.J., and Amalfitano, A. (2012). Malaria vaccines: focus on adenovirus based vectors. Vaccine *30*, 5191–5198.

Seiradake, E., Henaff, D., Wodrich, H., Billet, O., Perreau, M., Hippert, C., Mennechet, F., Schoehn, G., Lortat-Jacob, H., Dreja, H., et al. (2009). The cell adhesion molecule “CAR” and sialic acid on human erythrocytes influence adenovirus in vivo biodistribution. PLoS Pathog *5*, e1000277.

Senzer, N.N., Kaufman, H.L., Amatruda, T., Nemunaitis, M., Reid, T., Daniels, G., Gonzalez, R., Glaspy, J., Whitman, E., Harrington, K., et al. (2009). Phase II clinical trial of a granulocyte-macrophage colony-stimulating factor-encoding, second-generation oncolytic herpesvirus in patients with unresectable metastatic melanoma. J Clin Oncol *27*, 5763–5771.

Shayakhmetov, D.M., Gaggar, A., Ni, S., Li, Z.Y., and Lieber, A. (2005). Adenovirus binding to blood factors results in liver cell infection and hepatotoxicity. J Virol *79*, 7478–7491.

Shimizu, T., Ichihara, M., Yoshioka, Y., Ishida, T., Nakagawa, S., and Kiwada, H. (2012). Intravenous administration of polyethylene glycol-coated (PEGylated) proteins and PEGylated adenovirus elicits an anti-PEG immunoglobulin M response. Biol. Pharm. Bull. *35*, 1336–1342.

Shiver, J.W., and Emini, E.A. (2004). Recent advances in the development of HIV-1 vaccines using replication-incompetent adenovirus vectors. Annu Rev Med *55*, 355–372.

Sjolander, A., Stahl, S., and Perlmann, P. (1993). Bacterial Expression Systems Based on a Protein A and Protein G Designed for the Production of Immunogens: Applications to Plasmodium falciparum Malaria Antigens. Immunomethods *2*, 79–92.

Sjolander, A., Nygren, P.A., Stahl, S., Berzins, K., Uhlen, M., Perlmann, P., and Andersson, R. (1997). The serum albumin-binding region of streptococcal protein G: a bacterial fusion partner with carrier-related properties. J Immunol Methods *201*, 115–123.

Sleep, D., Cameron, J., and Evans, L.R. (2013). Albumin as a versatile platform for drug half-life extension. Biochim Biophys Acta *1830*, 5526–5534.

Small, E.J., Carducci, M.A., Burke, J.M., Rodriguez, R., Fong, L., van Ummersen, L., Yu, D.C., Aimi, J., Ando, D., Working, P., et al. (2006). A phase I trial of intravenous CG7870, a replication-selective, prostate-specific antigen-targeted oncolytic adenovirus, for the treatment of hormone-refractory, metastatic prostate cancer. Mol Ther *14*, 107–117.

Smith, J.S., Xu, Z., Tian, J., Stevenson, S.C., and Byrnes, A.P. (2008). Interaction of systemically delivered adenovirus vectors with Kupffer cells in mouse liver. Hum Gene Ther *19*, 547–554.

Smith, T.A., Idamakanti, N., Rollence, M.L., Marshall-Neff, J., Kim, J., Mulgrew, K., Nemerow, G.R., Kaleko, M., and Stevenson, S.C. (2003). Adenovirus serotype 5 fiber shaft influences in vivo gene transfer in mice. Hum Gene Ther *14*, 777–787.

Stanton, R.J., McSharry, B.P., Armstrong, M., Tomasec, P., and Wilkinson, G.W. (2008). Re-engineering adenovirus vector systems to enable high-throughput analyses of gene function. Biotechniques *45*, 659-662-668.

Steel, J.C., Cavanagh, H.M.A., Burton, M.A., and Kalle, W.H.J. (2004). Microsphere-liposome complexes protect adenoviral vectors from neutralising antibody without losses in transfection efficiency, in-vitro. J. Pharm. Pharmacol. *56*, 1371–1378.

Stone, D., Liu, Y., Li, Z.Y., Tuve, S., Strauss, R., and Lieber, A. (2007). Comparison of adenoviruses from species B, C, E, and F after intravenous delivery. Mol. Ther. *15*, 2146–2153.

Stork, R., Muller, D., and Kontermann, R.E. (2007). A novel tri-functional antibody fusion protein with improved pharmacokinetic properties generated by fusing a bispecific single-chain diabody with an albumin-binding domain from streptococcal protein G. Protein Eng Des Sel *20*, 569–576.

Stork, R., Campigna, E., Robert, B., Muller, D., and Kontermann, R.E. (2009). Biodistribution of a bispecific single-chain diabody and its half-life extended derivatives. J Biol Chem *284*, 25612–25619.

Sumida, S.M., Truitt, D.M., Lemckert, A.A., Vogels, R., Custers, J.H., Addo, M.M., Lockman, S., Peter, T., Peyerl, F.W., Kishko, M.G., et al. (2005). Neutralizing antibodies to adenovirus serotype 5 vaccine vectors are directed primarily against the adenovirus hexon protein. J Immunol *174*, 7179–7185.

Suzuki, K., Fueyo, J., Krasnykh, V., Reynolds, P.N., Curiel, D.T., and Alemany, R. (2001). A conditionally replicative adenovirus with enhanced infectivity shows improved oncolytic potency. Clin Cancer Res *7*, 120–126.

T

Tao, N., Gao, G.P., Parr, M., Johnston, J., Baradet, T., Wilson, J.M., Barsoum, J., and Fawell, S.E. (2001). Sequestration of adenoviral vector by Kupffer cells leads to a nonlinear dose response of transduction in liver. Mol Ther *3*, 28–35.

Tatsis, N., and Ertl, H.C. (2004). Adenoviruses as vaccine vectors. Mol Ther *10*, 616–629.

Tatsis, N., Tesema, L., Robinson, E.R., Giles-Davis, W., McCoy, K., Gao, G.P., Wilson, J.M., and Ertl, H.C. (2006). Chimpanzee-origin adenovirus vectors as vaccine carriers. Gene Ther *13*, 421–429.

Tauber, B., and Dobner, T. (2001). Adenovirus early E4 genes in viral oncogenesis. Oncogene *20*, 7847–7854.

Teigler, J.E., Iampietro, M.J., and Barouch, D.H. (2012). Vaccination with adenovirus serotypes 35, 26, and 48 elicits higher levels of innate cytokine responses than adenovirus serotype 5 in rhesus monkeys.

J Virol *86*, 9590–9598.

Thomas, M.A., Spencer, J.F., La Regina, M.C., Dhar, D., Tollefson, A.E., Toth, K., and Wold, W.S. (2006). Syrian hamster as a permissive immunocompetent animal model for the study of oncolytic adenovirus vectors. Cancer Res *66*, 1270–1276.

Thorner, A.R., Lemckert, A.A.C., Goudsmit, J., Lynch, D.M., Ewald, B.A., Denholtz, M., Havenga, M.J.E., and Barouch, D.H. (2006). Immunogenicity of heterologous recombinant adenovirus prime-boost vaccine regimens is enhanced by circumventing vector cross-reactivity. J. Virol. *80*, 12009–12016.

Tian, J., Xu, Z., Smith, J.S., Hofherr, S.E., Barry, M.A., and Byrnes, A.P. (2009). Adenovirus activates complement by distinctly different mechanisms in vitro and in vivo: indirect complement activation by virions in vivo. J. Virol. *83*, 5648–5658.

Tsai, V., Johnson, D.E., Rahman, A., Wen, S.F., LaFace, D., Philopena, J., Nery, J., Zepeda, M., Maneval, D.C., Demers, G.W., et al. (2004). Impact of human neutralizing antibodies on antitumor efficacy of an oncolytic adenovirus in a murine model. Clin Cancer Res *10*, 7199–7206.

Tsukuda, K., Wiewrodt, R., Molnar-Kimber, K., Jovanovic, V.P., and Amin, K.M. (2002). An E2F-responsive replication-selective adenovirus targeted to the defective cell cycle in cancer cells: potent antitumoral efficacy but no toxicity to normal cell. Cancer Res *62*, 3438–3447.

Tuboly, T., and Nagy, E. (2001). Construction and characterization of recombinant porcine adenovirus serotype 5 expressing the transmissible gastroenteritis virus spike gene. J Gen Virol *82*, 183–190.

U

Uchino, J., Curiel, D.T., and Ugai, H. (2014). Species D human adenovirus type 9 exhibits better virus-spread ability for antitumor efficacy among alternative serotypes. PLoS One *9*, e87342.

Unger, C., Haring, B., Medinger, M., Drevs, J., Steinbild, S., Kratz, F., and Mross, K. (2007). Phase I and pharmacokinetic study of the (6-maleimidocaproyl)hydrazone derivative of doxorubicin. Clin Cancer Res *13*, 4858–4866.

Ungerechts, G., Bossow, S., Leuchs, B., Holm, P.S., Rommelaere, J., Coffey, M., Coffin, R., Bell, J., and Nettelbeck, D.M. (2016). Moving oncolytic viruses into the clinic: clinical-grade production, purification, and characterization of diverse oncolytic viruses. Mol Ther Methods Clin Dev *3*, 16018.

Uusi-Kerttula, H., Hulin-Curtis, S., Davies, J., and Parker, A.L. (2015). Oncolytic Adenovirus: Strategies and Insights for Vector Design and Immuno-Oncolytic Applications. Viruses *7*, 6009–6042.

V

Verma, I.M., and Weitzman, M.D. (2005). Gene therapy: twenty-first century medicine. Annu Rev Biochem *74*, 711–738.

Vigant, F., Descamps, D., Jullienne, B., Esselin, S., Connault, E., Opolon, P., Tordjmann, T., Vigne, E., Perricaudet, M., and Benihoud, K. (2008). Substitution of hexon hypervariable region 5 of adenovirus serotype 5 abrogates blood factor binding and limits gene transfer to liver. Mol Ther *16*, 1474–1480.

Villalona-Calero, M.A., Lam, E., Otterson, G.A., Zhao, W., Timmons, M., Subramaniam, D., Hade, E.M., Gill, G.M., Coffey, M., Selvaggi, G., et al. (2016). Oncolytic reovirus in combination with chemotherapy

in metastatic or recurrent non-small cell lung cancer patients with KRAS-activated tumors. Cancer *122*, 875–883.

Villanueva, A., Garcia, C., Paules, A.B., Vicente, M., Megias, M., Reyes, G., de Villalonga, P., Agell, N., Lluis, F., Bachs, O., et al. (1998). Disruption of the antiproliferative TGF-beta signaling pathways in human pancreatic cancer cells. Oncogene *17*, 1969–1978.

Vogels, R., Zuijdgeest, D., van Rijnsoever, R., Hartkoorn, E., Damen, I., de Bethune, M.P., Kostense, S., Penders, G., Helmus, N., Koudstaal, W., et al. (2003). Replication-deficient human adenovirus type 35 vectors for gene transfer and vaccination: efficient human cell infection and bypass of preexisting adenovirus immunity. J Virol *77*, 8263–8271.

Von Hoff, D.D., Ramanathan, R.K., Borad, M.J., Laheru, D.A., Smith, L.S., Wood, T.E., Korn, R.L., Desai, N., Trieu, V., Iglesias, J.L., et al. (2011). Gemcitabine plus nab-paclitaxel is an active regimen in patients with advanced pancreatic cancer: a phase I/II trial. J Clin Oncol *29*, 4548–4554.

W

Waddington, S.N., McVey, J.H., Bhella, D., Parker, A.L., Barker, K., Atoda, H., Pink, R., Buckley, S.M., Greig, J.A., Denby, L., et al. (2008). Adenovirus serotype 5 hexon mediates liver gene transfer. Cell *132*, 397–409.

Wein, L.M., Wu, J.T., and Kirn, D.H. (2003). Validation and analysis of a mathematical model of a replication-competent oncolytic virus for cancer treatment: implications for virus design and delivery. Cancer Res *63*, 1317–1324.

Wesseling, J.G., Bosma, P.J., Krasnykh, V., Kashentseva, E.A., Blackwell, J.L., Reynolds, P.N., Li, H., Parameshwar, M., Vickers, S.M., Jaffee, E.M., et al. (2001). Improved gene transfer efficiency to primary and established human pancreatic carcinoma target cells via epidermal growth factor receptor and integrin-targeted adenoviral vectors. Gene Ther *8*, 969–976.

Wohlfart, C. (1988). Neutralization of adenoviruses: kinetics, stoichiometry, and mechanisms. J Virol *62*, 2321–2328.

Wohlfart, C.E., Svensson, U.K., and Everitt, E. (1985). Interaction between HeLa cells and adenovirus type 2 virions neutralized by different antisera. J Virol *56*, 896–903.

Wold, W.S., and Toth, K. (2012). Chapter three--Syrian hamster as an animal model to study oncolytic adenoviruses and to evaluate the efficacy of antiviral compounds. Adv Cancer Res *115*, 69–92.

Woller, N., Gurlevik, E., Ureche, C.I., Schumacher, A., and Kuhnel, F. (2014). Oncolytic viruses as anticancer vaccines. Front Oncol *4*, 188.

Wortmann, A., Vohringer, S., Engler, T., Corjon, S., Schirmbeck, R., Reimann, J., Kochanek, S., and Kreppel, F. (2008). Fully detargeted polyethylene glycol-coated adenovirus vectors are potent genetic vaccines and escape from pre-existing anti-adenovirus antibodies. Mol Ther *16*, 154–162.

Wu, H., Dmitriev, I., Kashentseva, E., Seki, T., Wang, M., and Curiel, D.T. (2002). Construction and characterization of adenovirus serotype 5 packaged by serotype 3 hexon. J. Virol. *76*, 12775–12782.

Wunder, T., Schumacher, U., and Friedrich, R.E. (2012). Coxsackie adenovirus receptor expression in carcinomas of the head and neck. Anticancer Res. *32*, 1057–1062.

X

Xie, D., Yao, C., Wang, L., Min, W., Xu, J., Xiao, J., Huang, M., Chen, B., Liu, B., Li, X., et al. (2010). An albumin-conjugated peptide exhibits potent anti-HIV activity and long in vivo half-life. Antimicrob Agents Chemother *54*, 191–196.

Xu, Z., Tian, J., Smith, J.S., and Byrnes, A.P. (2008). Clearance of adenovirus by Kupffer cells is mediated by scavenger receptors, natural antibodies, and complement. J Virol *82*, 11705–11713.

Xu, Z., Qiu, Q., Tian, J., Smith, J.S., Conenello, G.M., Morita, T., and Byrnes, A.P. (2013). Coagulation factor X shields adenovirus type 5 from attack by natural antibodies and complement. Nat Med *19*, 452–457.

Y

Yotnda, P., Chen, D.H., Chiu, W., Piedra, P.A., Davis, A., Templeton, N.S., and Brenner, M.K. (2002). Bilamellar cationic liposomes protect adenovectors from preexisting humoral immune responses. Mol. Ther. *5*, 233–241.

Youil, R., Toner, T.J., Su, Q., Chen, M., Tang, A., Bett, A.J., and Casimiro, D. (2002). Hexon gene switch strategy for the generation of chimeric recombinant adenovirus. Hum. Gene Ther. *13*, 311–320.

Yu, B., Dong, J., Wang, C., Zhan, Y., Zhang, H., Wu, J., Kong, W., and Yu, X. (2013). Characteristics of neutralizing antibodies to adenovirus capsid proteins in human and animal sera. Virology *437*, 118–123.

Yu, D.C., Chen, Y., Seng, M., Dilley, J., and Henderson, D.R. (1999). The addition of adenovirus type 5 region E3 enables calydon virus 787 to eliminate distant prostate tumor xenografts. Cancer Res *59*, 4200–4203.

Z

Zahn, R., Gillisen, G., Roos, A., Koning, M., van der Helm, E., Spek, D., Weijtens, M., Grazia Pau, M., Radošević, K., Weverling, G.J., et al. (2012). Ad35 and ad26 vaccine vectors induce potent and cross-reactive antibody and T-cell responses to multiple filovirus species. PLoS One *7*, e44115.

Zaiss, A.K., Machado, H.B., and Herschman, H.R. (2009). The influence of innate and pre-existing immunity on adenovirus therapy. J Cell Biochem *108*, 778–790.

Zak, D.E., Andersen-Nissen, E., Peterson, E.R., Sato, A., Hamilton, M.K., Borgerding, J., Krishnamurty, A.T., Chang, J.T., Adams, D.J., Hensley, T.R., et al. (2012). Merck Ad5/HIV induces broad innate immune activation that predicts CD8(+) T-cell responses but is attenuated by preexisting Ad5 immunity. Proc Natl Acad Sci U S A *109*, E3503-12.

Zhang, Y., and Bergelson, J.M. (2005). Adenovirus receptors. J Virol *79*, 12125–12131.

ANNEX

Journal of Controlled Release 237 (2016) 78–88

Contents lists available at ScienceDirect

Journal of Controlled Release

journal homepage: www.elsevier.com/locate/jconrel

Albumin-binding adenoviruses circumvent pre-existing neutralizing antibodies upon systemic delivery

Luis Alfonso Rojas [a], Gabriela N. Condezo [b], Rafael Moreno Olié [a], Carlos Alberto Fajardo [a], Marcel Arias-Badia [a], Carmen San Martín [b], Ramon Alemany [a,*]

[a] Virotherapy and Gene therapy Group, ProCure Program, Instituto Catalan de Oncología-IDIBELL, L'Hospitalet de Llobregat 08908, Spain
[b] Department of Macromolecular Structure, Centro Nacional de Biotecnología (CNB-CSIC), Madrid 28049, Spain

ARTICLE INFO

Article history:
Received 21 March 2016
Received in revised form 30 June 2016
Accepted 2 July 2016
Available online 04 July 2016

Keywords:
Adenovirus
Albumin
Albumin-binding domain
Neutralizing antibodies

ABSTRACT

Recombinant adenoviruses are used as vaccines, gene therapy vectors, and oncolytic viruses. However, the efficacy of such therapies is limited by pre-existing neutralizing antibodies (NAbs), especially when the virus is administered systemically for a wider biodistribution or to reach multiple metastases. To protect adenovirus against NAbs we inserted an albumin-binding domain (ABD) in the main adenovirus capsid protein, the hexon. This domain binds serum albumin to shield the virus upon systemic administration. The ABD-modified adenoviruses bind human and mouse albumin and maintain the infectivity and replication capacity in presence of NAbs. In pre-immunized mice non-modified viruses are completely neutralized, whereas ABD-modified viruses preserve the ability to transduce target organs, induce oncolysis, or generate immune responses to expressed proteins. Our results indicate that albumin coating of the virus capsid represents an effective approach to evade pre-existing NAbs. This strategy has translational relevance in the use of adenovirus for gene therapy, cancer virotherapy, and vaccination.

1. Introduction

Oncolytic viruses have shown promising clinical results in the last few years. Several viruses are currently in phase II and III clinical trials [1], and the modified herpes simplex virus T-vec has recently been approved by the FDA and EMA for melanoma treatment by intratumoral administration. Nonetheless, in general terms pre-existing humoral immunity represents a major hurdle for efficacy, not only in cancer virotherapy but also in the fields of gene therapy vectors and vaccination [2,3], specially upon intravenous or systemic administration. The human adenovirus serotype 5 (Ad5) is the most commonly used for adenoviral virotherapy, however the prevalence of anti-Ad5 neutralizing antibodies (NAbs) is very high in the general population, reaching >90% in certain geographical locations [4,5]. Several studies have demonstrated that Ad5-specific NAbs are directed primarily against the hypervariable regions (HVRs) of hexon protein [6,7].

Multiple strategies have been explored to evade NAbs. Chemical conjugation of capsid with polymers such as polyethyleneglycol or N-(2-hydroxypropyl)methacrylamide shields the virus at the expense of virus infectivity [8,9]. Furthermore, a conjugated product increases the complexity of GMP production for clinical application. Use of non-prevalent human serotypes or simian serotypes usually underperform Ad5 vectors [10,11] and imply GMP production challenges as well. Replacement of Ad5 HVRs with those from non-prevalent serotypes has shown promising results in vaccination [12,13], but it has not been tested with oncolytic adenoviruses. In addition, Ad5 HVR1 recruits dynein for proper capsid transport to nucleus and when substituted by HVR1 of Ad48 capsid trafficking is affected [14].

The use of albumin as a drug carrier is a hot research field, recently leading to the approval of Abraxane® and Levemir® to treat cancer and diabetes, respectively [15]. Taking advantage of its long plasma half-life, non-covalent interaction with albumin has been shown to reduce the blood clearance of short-lived drugs [16–18]. Albumin acts also as a tumor-targeting carrier as it accumulates in solid tumors [15]. We aimed to use albumin binding as a protection mechanism against NAbs. To generate an albumin-binding adenovirus we have used the albumin-binding domain 3 (ABD) from the protein G of *Streptococcus* [19–21]. This domain was inserted in the HVR1 of adenovirus hexon, and flanked by two GSGS-linkers to confer flexibility. We generated both an oncolytic adenovirus (ICOVIR15-ABD) and an E1-deleted GFP-Luciferase vector (AdGLRGD-ABD) with ABD. We hypothesized that upon injection of the modified virus in the bloodstream albumin

* Corresponding author at: IDIBELL-Institut Català d'Oncologia, Av Gran Via de l'Hospitalet 199-203, L'Hospitalet de Llobregat 08907, Barcelona, Spain.
E-mail address: ralemany@iconcologia.net (R. Alemany).

http://dx.doi.org/10.1016/j.jconrel.2016.07.004
0168-3659/

would coat the viral capsid, increasing its plasma half-life and shielding it against circulating NAbs (Fig. 1A).

2. Results

2.1. ABD insertion promotes albumin binding

Parental oncolytic adenovirus ICOVIR15 has been described [22] and was used as a control. The albumin-binding domain 3 from the protein G of *Streptococcus* was inserted in the HVR1 of ICOVIR15 hexon, generating the oncolytic adenovirus ICOVIR15-ABD. The domain was flanked by GSGS-linkers and centered in HVR1 after the D150 amino acid without deleting any hexon sequence (Fig. 1B). The insertion was also introduced in the reporter non-replicative vector AdGLRGD, obtaining AdGLRGD-ABD.

To demonstrate the functionality of the ABD in adenovirus capsid, we tested the binding of ICOVIR15-ABD to purified human (HSA), mouse (MSA), and bovine serum albumin (BSA) by ELISA. Positive binding was observed when adding ICOVIR15-ABD to HSA- or MSA-coated wells (Fig. 2A). In agreement with the binding pattern of ABD to albumin of different species [23,24], the virus did not bind to BSA. As expected, the parental virus ICOVIR15 did not bind to any albumin. The ABD-modified virus was also able to bind to albumin in human and mouse serum in a dose-dependent manner (Fig. 2B), contrary to the non-modified virus which did not show any binding. Binding of ICOVIR15-ABD to HSA was confirmed by immunoelectron microscopy since positive albumin staining was only observed in ICOVIR15-ABD capsids (Fig. 2C). Cryo-electron microscopy studies showed additional electron density in the vicinity of the HVR1 of ICOVIR15-ABD, compatible with the presence of bound albumin (Fig. 2D–E).

To understand how the ABD insertion affected the viability of the virus we studied the virus life cycle in absence of NAbs. We observed a minor loss of ICOVIR15-ABD production yields (2–3 times) compared to the non-modified ICOVIR15 (Fig. 3A) in A549 cells (e.g. 4900 TU/cell ICOVIR15 vs 1500 TU/cell ICOVIR15-ABD at 72 h post-infection, $p = 0.00083$). Infectivity and cytotoxicity were analyzed in presence and absence of HSA. No differences in infectivity were observed among vectors in a panel of tumor cell lines in the absence of albumin. However, albumin caused a 2-fold loss of transduction in the non-modified vector in most of the cell lines, and an even a higher impairment for the ABD-vector (20-fold in A549, 10-fold in NP-9 and Sk-mel28, 6-fold in B16, and 3-fold in B16-CAR, Fig. 3B). No differences in cytotoxicity were observed among viruses in absence of HSA. With HSA in the medium, parental virus ICOVIR15 suffered a 2-fold loss of cytotoxicity, compared to a 6-fold loss for ICOVIR15-ABD (Fig. 3C). In general terms, these results indicate an attenuation of the ABD-modified virus in presence of albumin.

2.2. Albumin binding protects adenovirus from neutralizing antibodies in vitro

Having demonstrated the binding of ICOVIR15-ABD to HSA, we tested if this binding could protect the virus from NAbs in vitro. AdGLRGD or AdGLRGD-ABD in absence or presence of HSA, were incubated with serial dilutions of the commercial neutralizing antibody Ab6982 (rabbit polyclonal against Ad5), and then used to transduce A549 cells. Even in absence of human albumin the modified AdGLRGD-ABD was less neutralized than the non-modified vector (Fig. 4A), suggesting that the ABD modification of the HVR1 precluded binding of some NAbs, likely directed against the wt HVR1. In presence of albumin, the transduction efficiency of AdGLRGD-ABD was remarkably enhanced (e.g. 8% of transduction of AdGLRGD-ABD vs 70% of transduction of AdGLRGD-ABD + HSA at 1/64 dilution of Ab6982, $p = 0.000011$), indicating that albumin was able to protect the virus from NAbs. Addition of HSA did not alter the transduction of the non-modified vector AdGLRGD, which was efficiently neutralized.

In addition, the capacity of viruses to kill cancer cells in presence of NAbs was also evaluated. For this purpose, ICOVIR15 or ICOVIR15-ABD in absence or presence of HSA were incubated with serial dilutions of Ab6982, and used to infect A549 cells. Cell survival was analyzed 5 days after infection. In absence of HSA both viruses showed similar capacity to kill tumor cells (Fig. 4B), and only a small increase of cytotoxicity was observed with ICOVIR15-ABD probably due to the certain evasion of NAbs observed in transduction (Fig. 4A). Importantly, HSA shifted the cytotoxicity curve of ICOVIR15-ABD towards higher NAbs concentrations (e.g. 75% of cell survival of ICOVIR15-ABD vs 8% of cell survival of ICOVIR15-ABD + HSA at 1/32 dilution of Ab6982, $p = 0.000015$), whereas it did not protect ICOVIR15 from neutralization.

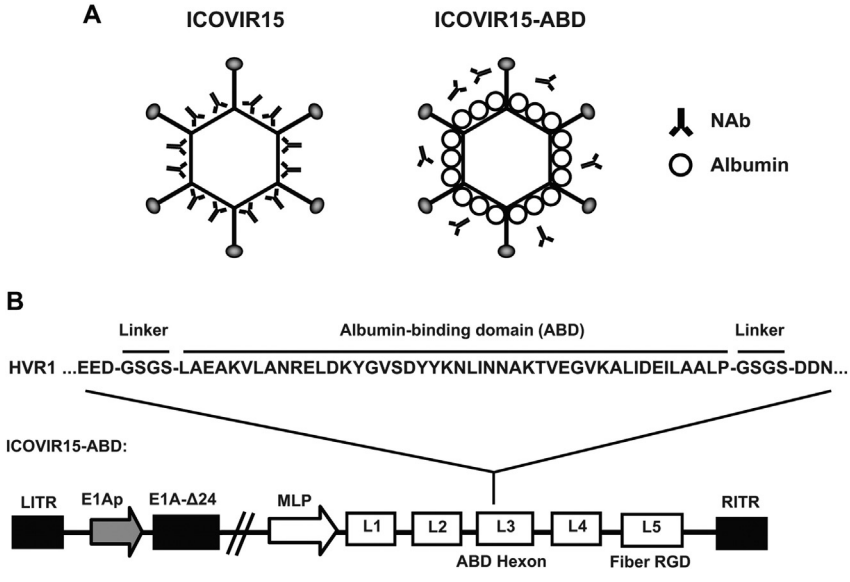

Fig. 1. Design of an oncolytic adenovirus containing an albumin-binding domain (ABD) inserted in the hexon. A, Albumin-protection conferred by ABD insertion. Compared to a non-modified adenovirus ICOVIR15 (left), the ABD-modified virus ICOVIR15-ABD (right) is coated with albumin present in blood, shielding the virus from neutralizing antibodies (NAbs). B, schematic diagram of ABD insertion in ICOVIR15-ABD genome. The ABD 3 from streptococcal protein G is flanked by two GSGS linkers and inserted in the middle of the HVR1 of hexon of ICOVIR15 obtaining ICOVIR15-ABD. LITR/RITR, left and right inverted terminal repeats; MLP, major late promoter; E1Ap, modified E1A promoter; E1A-Δ24, mutant version of E1A protein with deletion of aminoacids 121–129; L1 to L5, late genes; Fiber RGD, modified fiber by insertion of the RGD peptide at the HI-loop.

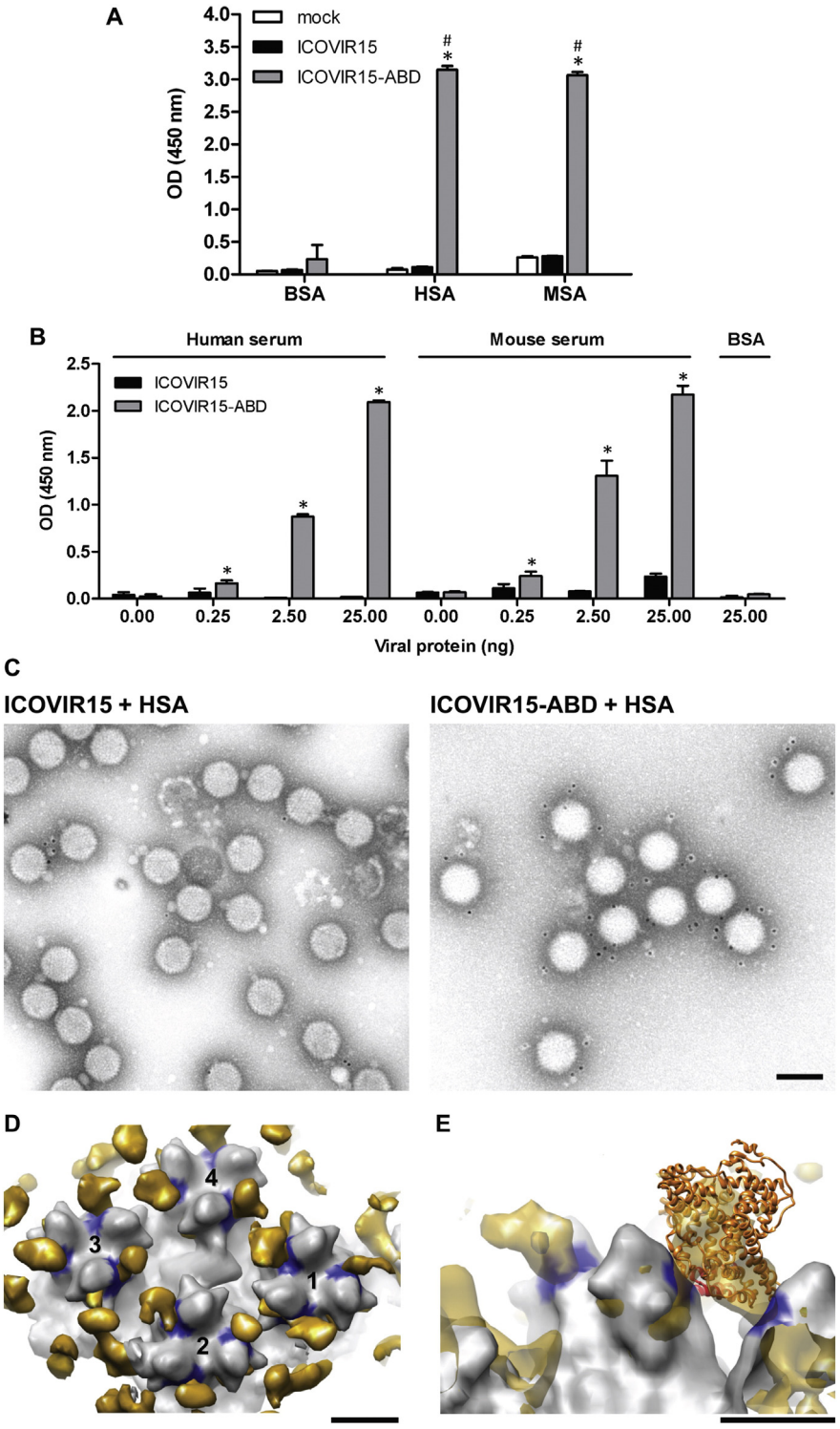

Fig. 2. Adenovirus with ABD insertion binds to human and mouse serum albumin. A, adenovirus binding to BSA-, HSA-, and MSA-coated wells was detected by ELISA with antihexon antibody and peroxidase-labeled secondary antibody by colorimetric analysis. A mock group with no virus was included as negative control. Mean + SD is plotted. *, significant ($p < 0.05$) by two-tailed unpaired Student's *t*-test compared to mock group. #, significant ($p < 0.05$) by two-tailed unpaired Student's *t*-test compared to ICOVIR15 group. OD, optic density. B, adenovirus binding to albumin in human or mouse-serum was also detected by ELISA. Different amounts of viral protein were used. BSA-coated wells were used as negative control. Mean + SD is plotted. *, significant ($p < 0.05$) by two-tailed unpaired Student's *t*-test compared to ICOVIR15 group. C, immuno-EM of ICOVIR15 (left) and ICOVIR15-ABD (right) after incubation with HSA, labeled with mouse anti-HSA and 10 nm gold conjugated goat anti-mouse. Black dots indicate positive HSA staining. Scale bar, 100 nm. D, cryo-EM difference mapping showing the location of bound HSA in the ICOVIR15-ABD capsid. View from outside the capsid. The four hexon trimers in the capsid asymmetric unit (numbered 1–4) are shown in gray. In each hexon, the location of the HVR1 flanking residues is indicated in blue. The difference density between Ad5 and the ICOVIR-ABD-HSA complex, shown in gold, is present near the HVR1 location in all hexons. E, side view, close up detail showing the crystallographic structure of a bacterial albumin binding domain (red ribbon) and bound HSA (orange ribbon) fitted to the difference density located between two hexon trimers. Scale bars, 50 Å in (D) and (E). (For interpretation of the references to color in this figure legend, the reader is referred to the web version of this article.)

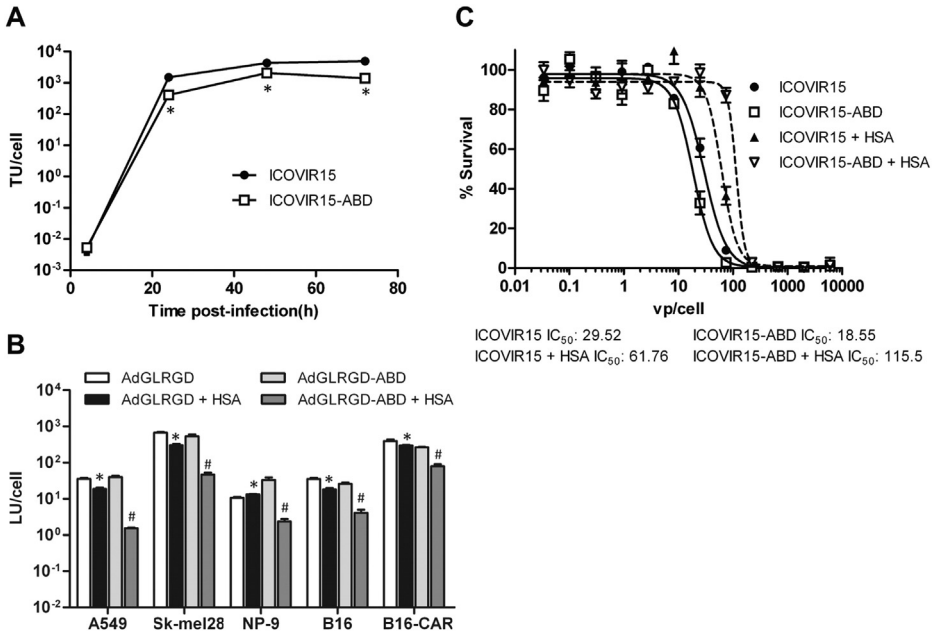

Fig. 3. In vitro characterization of ABD-modified adenoviruses in absence of NAbs. A, viral production of ICOVIR15-ABD. A549 cells were infected with ICOVIR15 or ICOVIR15-ABD and at indicated time points, cell extracts were harvested and titrated. *, significant ($p < 0.05$) by two-tailed unpaired Student's *t*-test compared to ICOVIR15. B, transduction assay in presence and absence of HSA in tumor cells. A panel of tumor cell lines was infected with the indicated luciferase-expressing vectors. At 36 h post-infection cell transduction was analyzed by luciferase expression. *, significant ($p < 0.05$) by two-tailed unpaired Student's *t*-test compared to AdGLRGD group. #, significant ($p < 0.05$) by two-tailed unpaired Student's *t*-test compared to AdGLRGD-ABD group. C, comparative cytotoxicity of ICOVIR15-ABD. A549 cells were infected with serial dilutions of the indicated viruses in presence and absence of HSA. Cell survival was measured at day 5 post-infection. IC_{50} values are shown. Mean values ± SD are plotted. TU, transducing units; LU, light units; vp, viral particles.

Evasion of NAbs was also assessed with serum from Ad5-immunized C57BL6 mice. The absence of albumin condition could not be analyzed in this case because mouse serum contains albumin. A clear advantage was observed again with the ABD-modified adenoviruses in terms of cell transduction (Fig. 4C) and cytotoxicity (Fig. 4D) compared to the non-modified viruses, which were effectively neutralized by the serum of immunized mice (e.g. AdGLRGD 1.7% of transduction vs AdGLRGD-ABD 90% of transduction at 1/16 dilution of serum, $p = 0.0016$; AdGLRGD 117% of cell survival vs AdGLRGD-ABD 1.62% of cell survival at 1/32 dilution of serum, $p = 0.000015$). Similarly, human sera from six donors were used to test neutralization escape of the ABD-vector. In general terms, AdGLRGD-ABD showed higher

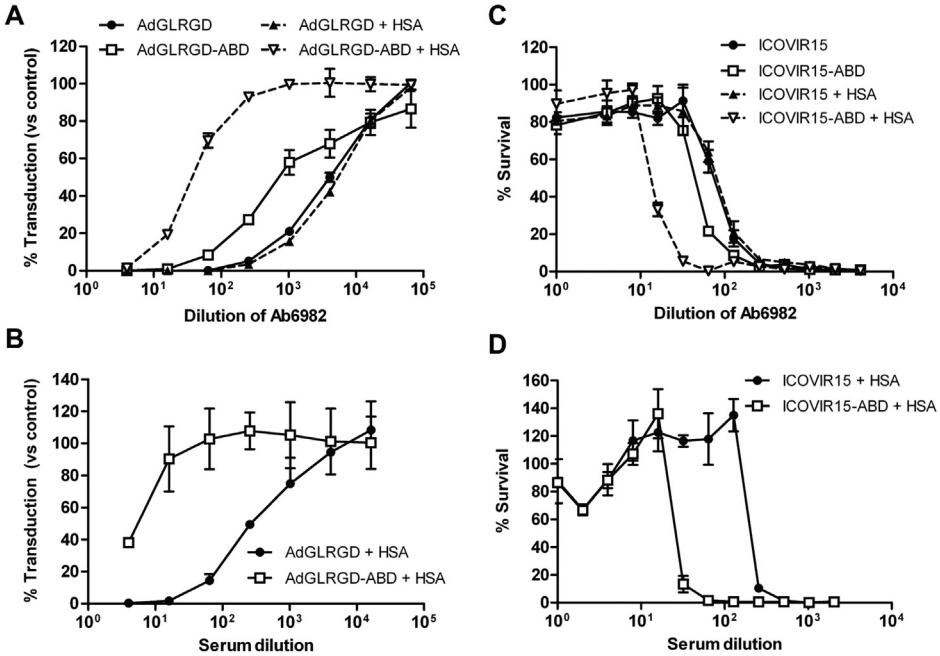

Fig. 4. Albumin binding protects adenovirus from neutralizing antibodies in vitro. Transduction analysis after incubation with polyclonal neutralizing antibody Ab6982 (A) or anti-Ad5 neutralizing mice serum (B). AdGLRGD or AdGLRGD-ABD ± HSA were incubated with serial dilutions of the neutralizing agent and then used to infect A549 cells. Luciferase expression was analyzed 24 h after infection. A control without neutralizing agent was included to obtain the 100% infection value. Cytotoxicity analysis after incubation with Ab6982 (C) or anti-Ad5 neutralizing mice serum (D). ICOVIR15 or ICOVIR15-ABD ± HSA were incubated with serial dilutions of the neutralizing agent and then used to infect A549 cells. Cell survival was measured at day 5 post-infection. Mean values ± SD are depicted.

transduction levels than AdGLRGD at low serum dilutions, which are the conditions that better mimic the intravenous administration of the virus (Fig. S1). When the sera were highly diluted the advantage of the ABD-modified virus was lost, as previously observed in presence of albumin and absence of neutralizing antibodies (Fig. 3B).

2.3. Blood persistence and biodistribution profile of ABD-modified adenovirus after systemic administration in naïve mice

The ABD has been successfully used to increase the plasma half-life of therapeutic proteins, but never tested in the context of a virus. We compared the blood persistence of ICOVIR15-ABD and ICOVIR15 by direct competition after intravenous injection of a mixture of both viruses (2.5×10^{10}vp each) in nude mice. The genomes of the viruses in serum were detected by PCR of the HVR1, and were distinguished by the size of the PCR product (199 bp for ICOVIR15 and 361 bp for ICOVIR15-ABD). The difference in blood persistence was analyzed comparing the relative intensity of the bands. Equally intense bands were obtained in the pre-injection control and 5 min after the injection (Fig. 5A). From then on, a shift on the intensity of the bands can be seen as the band corresponding to ICOVIR15-ABD becomes more intense than the ICOVIR15 one. One hour after the injection the extended circulation of ICOVIR15-ABD was clearly evident, but at 4 h after injection the level of both viruses dropped notably.

To check if such an increase in viremia enhanced tumor transduction, we analyzed the biodistribution of the ABD-modified adenovirus. Nude mice bearing Sk-mel28 melanoma tumors were intravenously injected with PBS, or 5×10^{10}vp of AdGLRGD, or AdGLRGD-ABD. Three days after vector injection mice were sacrificed and organs were collected for in vivo bioluminescent imaging (IVIS). Despite the advantage observed in blood persistence due to ABD insertion, there were no differences in transduction among vectors in all the organs analyzed (Fig. 5B). Only a 1.6-fold loss (non-significant) of liver and tumor transduction was observed with AdGLRGD-ABD. Likely, the viremia increase of the modified virus compensated its lower infectivity in presence of albumin and absence of NAbs (Fig. 3B), resulting in a final tumor transduction similar to the non-modified virus.

2.4. Blood persistence and organ transduction of ABD-modified adenovirus in pre-immune mice after systemic administration

Not having observed higher tumor transduction in naïve mice, we studied the behavior of the ABD-adenoviruses in pre-immune mouse models. Immunocompetent C57BL6 mice were immunized with an intraperitoneal injection of PBS or 3×10^{10}vp of Ad5wt (naïve or pre-immune groups) to generate anti-Ad5 NAbs, and seven days later mice were injected with 3×10^{10}vp of AdGLRGD or AdGLRGD-ABD. Serum samples were collected at different time points to detect adenovirus genomes and transducing units (Fig. S2). In naïve mice the clearance curve shows an advantage of the ABD-modified virus in terms of viral particles (e.g. 2×10^{7}vp/ml of AdGLRGD-ABD vs 8×10^{6}vp/ml of AdGLRGD at 60 min, $p = 0.042$) but not of transducing units (Fig. S2 left panels). This result adds up with the increased blood persistence at 1 h after injection in nude mice (Fig. 5A) which did not translate in an increased organ transduction (Fig. 5B). However, in pre-immune mice the advantage of the ABD-modified virus was evident not only in circulating viral

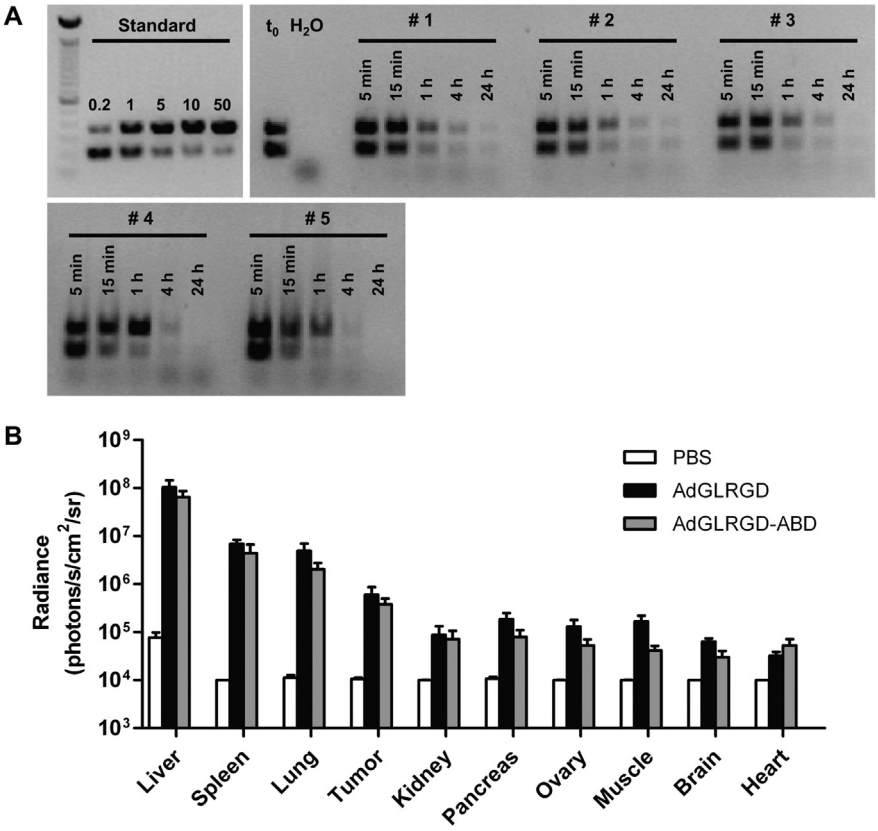

Fig. 5. Blood persistence, and biodistribution profile of ABD-modified adenovirus in naïve mice. A, blood persistence of ICOVIR15-ABD. Serum samples of nude mice were collected at the indicated time points after intravenous administration of a mixture containing ICOVIR15 and ICOVIR15-ABD (2.5×10^{10}vp each, n = 5 mice). PCR amplification of the HVR1 was performed and samples were analyzed by electrophoresis. The upper band corresponds to ICOVIR15-ABD and the lower band to ICOVIR15 as the ABD insertion increases the size of the HVR1 from 299 to 361 bp. The gel shows a standard with several ratios of ICOVIR15-ABD: ICOVIR15 genomes (0.2, 1, 5, 10, and 50), a pre-injection control (t_0), a water negative control of the PCR (H_2O), and the PCR of the serum samples (#1 to #5). B, biodistribution profile of AdGLRGD-ABD. Nude mice bearing Sk-mel28 melanoma tumors were systemically injected with PBS, or 5×10^{10} viral particles of AdGLRGD, or AdGLRGD-ABD. Three days after virus administration mice were sacrificed. Comparative luciferase expression in different organs was measured by bioluminescence imaging (IVIS) (n = 5 mice). Mean + SEM. sr, steradian.

particles but also in transducing units (Fig. S2 right panels). To analyze the impact of pre-immunization in organ transduction C57BL6 mice bearing B16-CAR melanoma tumors were immunized with PBS or Ad5wt as just described. Seven days later, mice received a single intravenous dose of PBS, AdGLRGD, or AdGLRGD-ABD at 3×10^{10}vp per mouse. Three days after vector injection mice were sacrificed and liver and tumors were harvested for in vivo bioluminescent imaging (IVIS). In naïve animals, AdGLRGD-ABD showed a 9- and 7-fold non-significant loss of liver and tumor transduction respectively (Fig. 6A). Importantly, when animals were pre-immunized the non-modified AdGLRGD vector suffered a complete neutralization as the transduction of liver and tumors was completely abolished. On the contrary, AdGLRGD-ABD only suffered a 3.9- and 1.5-fold non-significant loss of liver and tumor transduction respectively, indicating a protection from anti-Ad5 NAbs.

2.5. Oncolytic ABD-modified adenovirus maintains its antitumor activity in pre-immune mice after systemic administration

ICOVIR15-ABD efficacy after systemic administration was compared with that of ICOVIR15 in naïve or anti-Ad5 pre-immune mice. To generate a pre-immune status in nude mice, we passively immunized them by an intraperitoneal injection of neutralizing serum from C57BL6 mice. The next day, naïve or passively immunized nude mice bearing A549 or Sk-mel28 tumors were injected intravenously with PBS or 4×10^{10}vp of ICOVIR15 or ICOVIR15-ABD and the tumor volume was monitored. In naïve A549-bearing mice no differences were observed in antitumor efficacy among the viruses (Fig. 6B left). Both viruses were able to significantly reduce the tumor growth compared to the PBS-treated group, and at the end of the study ICOVIR15 and ICOVIR15-ABD induced a 2-fold ($p = 0.0072$) and 1.7-fold ($p = 0.0019$) reduction in tumor volume respectively. In contrast, in pre-immune mice the non-modified ICOVIR15 was completely inefficacious, but the oncolytic activity of ICOVIR15-ABD was preserved. At the end of the study, ICOVIR15-ABD induced a 1.9-fold reduction in tumor volume compared to the PBS-treated group (511 vs 970 mm^3, $p = 0.0011$) and a 2.4-fold reduction compared to the ICOVIR15-treated group (511 vs 1247 mm^3, $p = 0.02$). A similar result was observed in Sk-mel28-bearing mice (Fig. 6B right), where both viruses showed similar antitumor activity in naïve animals (ICOVIR15 1.6-fold reduction, $p = 0.0015$; ICOVIR15-ABD 1.8-fold reduction, $p = 0.004$). In pre-immune mice we observed again no impairment of ICOVIR15-ABD, which caused a 1.6-fold reduction of tumor volume compared to ICOVIR15 which totally lost its antitumor effect (618 vs 954 mm^3, $p = 0.016$). In both tumor models ICOVIR15-ABD was able to

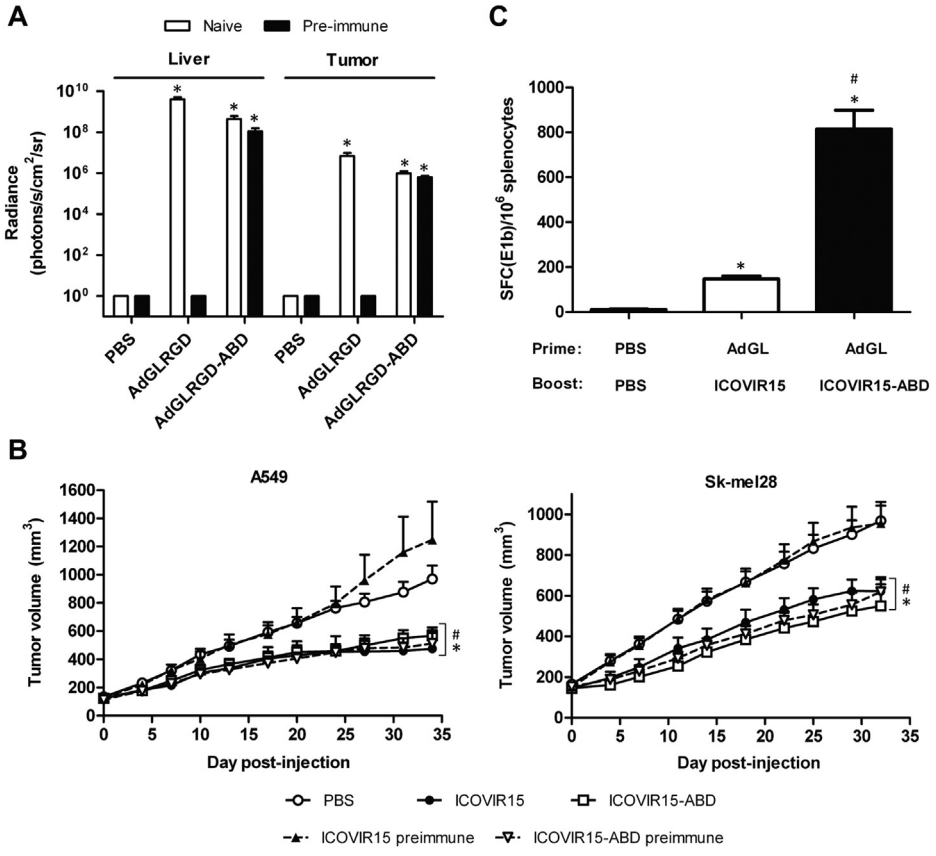

Fig. 6. ABD-modified adenoviruses evade NAbs after systemic administration in pre-immune mice. A, liver and tumor transduction. C57BL/6 mice bearing subcutaneous B16-CAR melanoma tumors were immunized with an intraperitoneal injection of Ad5wt (3×10^{10}vp) or vehicle, and 7 days later were injected intravenously with AdGLRGD or AdGLRGD-ABD (3×10^{10}vp). Three days later luciferase activity in liver and tumor was analyzed by bioluminescence imaging (IVIS) (livers: n = 3 PBS, n = 6 AdGLRGD-ABD naïve, n = 5 rest of groups; n for tumors is twice that of livers for each group). Mean + SEM is shown. *, significant ($p < 0.05$) by two-tailed unpaired Student's *t*-test compared to AdGLRGD pre-immune. B, antitumor activity. Nude mice bearing subcutaneous A549 (lung carcinoma) or Sk-mel28 (melanoma) tumors were injected intraperitoneally with PBS (naïve groups) or anti-Ad5 neutralizing mice serum (pre-immune groups). The next day, mice were injected with an intravenous dose of PBS, ICOVIR15, or ICOVIR15-ABD (4×10^{10}vp) (A549 tumors: n = 10 ICOVIR15 and ICOVIR15-ABD pre-immune, n = 12 PBS, ICOVIR15 pre-immune, and ICOVIR15-ABD; Sk-mel28 tumors: n = 11 PBS, n = 12 ICOVIR15 pre-immune and ICOVIR15-ABD pre-immune, n = 13 ICOVIR15 and ICOVIR15-ABD). Mean values + SEM. *, significant ($p < 0.05$) by two-tailed unpaired Student's *t*-test compared to PBS. #, significant ($p < 0.05$) by two-tailed unpaired Student's *t*-test compared to ICOVIR15 pre-immune. C, Immune responses against E1b protein expressed from the viral genome. C57BL/6 mice were immunized with an intraperitoneal injection of the E1-deleted vector AdGL (3×10^{10}vp) and seven days later were injected intravenously with ICOVIR15 or ICOVIR15-ABD (3×10^{10}vp). Seven days after, animals were euthanized and specific responses against $E1b_{192}$ peptide were analyzed by ELISPOT (n = 3 mice). Mean + SEM. *, significant ($p < 0.05$) by two-tailed unpaired Student's *t*-test compared to PBS. #, significant ($p < 0.05$) by two-tailed unpaired Student's *t*-test compared to ICOVIR15.

significantly increase the survival of naïve and pre-immune animals, whereas ICOVIR15 could only increase the survival of naïve mice (Fig. S3).

2.6. ABD-modified adenovirus can generate immune responses against expressed genes in pre-immune mice

Recombinant adenoviruses are also used as vaccine platforms which also face the problem of pre-existing NAbs. Neutralization of the vector impairs transgene expression and therefore no immune response can be mounted against the desired antigen. To analyze the potential of the ABD insertion in the field of vaccination, we measured CTL immune responses against the E1b protein expressed from the viral genome. To generate anti-Ad5 NAbs, C57BL/6 mice were immunized with an intraperitoneal injection of 3×10^{10}vp of the E1-deleted AdGL vector (lacking E1b). Seven days later mice were treated with an intravenous injection of 3×10^{10}vp of ICOVIR15 or ICOVIR15-ABD, both containing E1b. Mice were sacrificed seven days after and specific immune responses against $E1b_{192}$ viral epitope were assessed by ELISPOT. Specific anti-E1b response showed to be significantly higher (5.5-fold, 814 vs 147 SFC/10^6 splenocytes, $p = 0.0015$) in pre-immune animals treated with ICOVIR15-ABD than in those treated with ICOVIR15 (Fig. 6C). This indicates that pre-existing anti-adenovirus immunity cannot prevent the immunogenicity of a viral gene or a transgene encoded in an ABD-modified virus.

3. Discussion

The antitumor immune response raised by oncolytic viruses is thought to be a critical mechanism to obtain therapeutic responses [25]. To generate such a response, the oncolytic virus needs to reach the tumor site where it will replicate, causing tumor cell lysis. Nevertheless, a high prevalence of anti-viral NAbs is a major barrier to reach tumors systemically. NAbs directed against capsid proteins not only block cell transduction but opsonize and target the virus for elimination [2], severely hindering its therapeutic efficacy. Currently, an ongoing clinical trial by intravenous administration of VCN01 oncolytic adenovirus (NCT02045602) considers high levels of circulating NAbs in patients as an exclusion criterion.

Albumin is a promising drug carrier. It is the most abundant plasma protein (35–50 g/L human serum) with an extraordinary long half-life (19 days in humans) [17,26], which make it an ideal candidate for this purpose. Binding to albumin, either by direct fusion or using albumin-binding moieties, has shown to improve the plasma half-life of short-lived drugs from minutes to several hours [18,21,27]. Several albumin-bound molecules have been tested in clinical trials, some of which have already been approved [15,18]. Furthermore, albumin has also been used for tumor targeting, as it causes accumulation in solid tumors. The interplay of two albumin-binding proteins, gp60 and SPARC, facilitates the uptake and retention of albumin in the tumor interstitium [15]. Indeed, studies have revealed a significant benefit in overall survival in patients with high SPARC levels when treated with the combination of Abraxane® and gemcitabine [28,29].

In the present work, we used the albumin-binding strategy as a method to reduce the blood clearance of adenovirus and protect it from NAbs. Among the various approaches used to achieve albumin binding, we used the albumin-binding domain (ABD) from the Streptococcal protein G [19–21,30]. This genetic insertion confers a reversible non-covalent binding that will be maintained in viral progeny, unlike other strategies such as conjugation. The domain was inserted in the HVR1 of the hexon protein, which is the most abundant protein of the capsid. HVRs are exposed loops which would facilitate the interaction between albumin and the domain. Additionally, albumin would be directly blocking the HVRs of hexon which are the main target of anti-Ad NAbs. There are also NAbs directed against the fiber, but these are subdominant and not very efficient on their own [6,31]. Certainly, we demonstrate that adenoviruses with ABD inserted in the HVR1 successfully evade neutralization. The specific insertion in the viral capsid was not straightforward. We also inserted the ABD in the HVR5 and such a virus bound human and mouse albumin less efficiently and it could not evade NAbs (data not shown).

The functionality of the ABD was preserved after its insertion in the viral capsid. We demonstrate albumin binding of the modified adenovirus by ELISA, adapting a previously published protocol where also an ABD was used [32]. Our results add up with the previously published data on the species specificity of the ABD, being able to bind to human and mouse albumin, but not to bovine [23,24]. The inability to bind BSA could represent an advantage in the production process of these viruses as bovine serum is usually employed to supplement the media.

In vitro studies in absence of NAbs showed that the infectivity of the ABD-adenovirus was decreased in presence of HSA. A possible explanation would be that albumin could be blocking the interaction of viral domains with cell receptors. While the fiber is supposedly not affected by albumin, the penton base will probably be blocked by an albumin molecule bound to a neighboring hexon. Albeit the viruses used in this work contain an RGD-modified fiber, the interaction of cell integrins with the RGD of the penton base might still be necessary to achieve a proper internalization. However, a most likely hypothesis is that albumin might be interfering with the capsid transport to the nucleus. As recently described, HVR1 plays a key role in dynein recruitment for capsid transportation [14], so albumin could be blocking dynein binding to hexon. An interesting trait is that albumin is not covalently bound to hexon, so the binding is reversible and dynein could eventually displace albumin. Nonetheless, NAbs-free conditions do not reflect what is expected in the clinic, where a high percentage of human population has high levels of anti-Ad5 NAbs. Accordingly, ABD-modified adenoviruses showed enhanced in vitro bioactivity in presence of NAbs compared to a non-modified adenovirus, which was highly neutralized. Effective shielding was also observed with serum from pre-immune immunocompetent mice and from human donors. The evasion of neutralization observed in terms of cell transduction also translated in enhanced oncolysis.

Albumin binding has shown to increase the blood persistence of small drugs, but has never been tested in the context of a virus. Here we show a reduced blood clearance of the ABD-modified adenovirus. Natural immunoglobulins and complement system have been described to influence Ad5 pharmacokinetics, by enhancing clearance by Kupffer cells and by docking the viral particles to Fc receptors in monocytes and neutrophils [33–35]. Preventing such interactions by albumin protection likely contributed to an increased blood persistence. Albumin recycling through neonatal Fc receptor (FcRn) could also contribute to increase viremia. However, this mechanism seems less plausible given the large size of the virus and the interaction of the virus capsid with cellular receptors.

The expected outcome of such enhanced blood persistence would be an enhanced tumor transduction, but this was not observed. The improved blood persistence was probably compensated with the reduced transduction observed in vitro, and the tumor transduction was not significantly altered in naïve mice. Pre-immune mouse models showed the dramatic effect of NAbs on adenovirus bioactivity in vivo. Transduction of liver and tumors was completely inhibited with the parental virus. On the other hand, the protection provided by albumin proved to be remarkably effective in vivo, as no significant reduction in organ transduction was observed with the ABD-adenovirus.

Since human adenoviruses do not replicate in mouse cells, the model to study the impact of humoral immunity on oncolytic adenoviruses was challenging. Passive immunization with neutralizing serum or purified neutralizing antibodies represents a feasible option [36,37]. However, a previous study by Tsai et al. showed that the serum did not decrease the antitumor efficacy of an intravenously administered oncolytic adenovirus in a xenograft model [37]. Nonetheless, human serum was employed in those experiments and, as previously reviewed

[38], the human Fc-portion might be incompatible with mouse cells. In our work, we used neutralizing mice serum, to preserve Fc-dependent effector functions. Indeed, passive immunization completely inhibited the antitumor effect of control virus ICOVIR15, demonstrating that NAbs can efficiently block oncolytic adenovirus activity. Of note, ICOVIR15-ABD showed the same antitumor activity in naïve and pre-immune mice, demonstrating again a very effective albumin-mediated protection.

ABD insertion could be combined with other previously published modifications. Hyaluronidase expression or KKTK to RGDK replacement in the fiber shaft have successfully improved the oncolytic activity of ICOVIR15 [39–41]. VCN01, an ICOVIR15-based adenovirus harboring both these modifications is currently being tested in two phase I clinical trials (NCT02045602 and NCT02045589). The compatibility of the ABD with these modifications would be of interest. The potential of ABD modification to allow for repeated administrations of the virus, which may be required for therapy, is also an area great interest for future studies.

Adenovirus-based vaccines also face the problem of pre-existing humoral immunity. In contrast to the immunogenicity of capsid proteins, the immunogenicity of transgenes in adenovirus vectors depends on their expression and it can be blocked by NAbs [12,13]. Here we demonstrate how an ABD-modified adenovirus is also able to generate significantly higher immune responses against expressed genes than the parental virus in pre-immune mice.

4. Conclusions

ABD insertion in the hexon HVR1 of adenovirus capsid mediates binding to both human and mouse albumin. Upon systemic administration of the virus, albumin is able to shield the capsid from NAbs. In adenovirus pre-immune mice, where a non-modified virus is completely neutralized, ABD insertion protected the virus allowing same organ transduction and oncolysis as in naïve mice. These results demonstrate that protection of viral capsid with albumin using an albumin-binding domain is a useful strategy to overcome pre-existing NAbs.

5. Materials and methods

5.1. Cell lines

HEK293 (human embryonic kidney), A549 (human lung adenocarcinoma), Sk-mel28 (human melanoma), and B16 (murine melanoma) cells were obtained from the American Type Culture Collection (ATCC, Manassas, VA). B16-CAR (murine melanoma) cell line was obtained from Dr. NM Greenberg (Baylor College of Medicine, Houston, TX). NP-9 (pancreatic adenocarcinoma) cell line was established in our laboratory [42]. All tumor cell lines were maintained with Dulbecco's Modified Eagle's Medium supplemented with 5% fetal bovine serum at 37 °C, 5% CO_2. B16-CAR cells were maintained with 0.5 mg/ml hygromycin (Invivogene, San Diego, CA, USA). All cell lines were routinely tested for mycoplasma.

5.2. Recombinant adenoviruses

ICOVIR15 oncolytic adenovirus has been previously described [22]. All genetic modifications were performed following a recombineering protocol adapted from Stanton et al. [43] based on homologous recombination in bacteria using a positive-negative selection with the rpsL-Neo cassette. AdGL is an E1-deleted first generation vector expressing the EGFP-Luciferase fusion protein cassette from pEGFPLuc (Clontech, Mountain View, CA, USA). To generate AdGLRGD, the RGD (Arg-Gly-Asp) domain was inserted in the HI-loop of the fiber. ICOVIR15 was propagated in A549 cells and the replication-deficient AdGL and AdGLRGD were propagated in HEK293 cells. ICOVIR15-ABD and AdGLRGD-ABD were constructed by inserting the albumin-binding domain (ABD) flanked by two GSGS-linkers in the hyper-variable region 1 (HVR1) of the adenovirus hexon after the D150 aminoacid. ICOVIR15-ABD and AdGLRGD-ABD were generated by transfection of the plasmids with calcium phosphate standard protocol in HEK293 cells. ICOVIR15-ABD and AdGLRGD-ABD were plaque-purified and further amplified in A549 and HEK293 cells respectively. Viruses were purified using cesium chloride double-gradients.

5.3. Elisa

Detection of binding to human serum albumin (HSA) and mouse serum albumin (MSA) was performed following an ELISA protocol adapted from Konig and Skerra [32]. Briefly, the 96-well plate was coated with BSA, HSA, or MSA (2 mg/ml, Sigma, St. Louis, MO), and then blocked with BSA. Viruses or buffer alone (mock) were added (25 ng of viral protein) and detection was performed with antihexon antibody from 2Hx-2 hybridoma supernatant (1/5 dilution, ATCC, Manassas, VA) and polyclonal goat antimouse HRP (1/500 dilution, Life Technologies, Carlsbad, CA, USA). Wells were stained with 3,3′,5,5′-Tetramethylbenzidine (Thermo Fisher, Waltham, MA, USA). The reaction was stopped with sulfuric acid 2 N and the absorbance was measured at 450 nm. Alternatively, detection of albumin binding was also performed in serum. Wells were coated with human or mouse serum (1/25 dilution), and after blocking, different amount of viruses were added (0, 0.25, 2.5, and 25 ng of viral protein). Detection was performed as described above.

5.4. Immunoelectron microscopy

Samples of ICOVIR15 and ICOVIR15-ABD were adsorbed for 2 min onto glow-discharged, collodion/carbon coated nickel grids. Unspecific binding was blocked with TBG (30 mMTris-HCl pH 8, 150 mMNaCl, 0.1% BSA and 1% gelatin) for 10 min. Grids were then incubated for 30 min with a 1:1 dilution of stock (2 mg/ml in 20 mMTris-HCl pH 7.8, 150 mMNaCl) HSA in TBG, washed in TBG (3 × 3 min), and incubated for 15 min on a drop of mouse anti-HSA (Sigma, St. Louis, MO) diluted 1:500 in TBG. After four 2 min rinses with 0.1% gelatin in PBS and 5 min incubation in TBG, grids were incubated for 15 min in goat anti-mouse IgG-gold conjugate (British Biocell International EM.GAF10) diluted 1:40 in TBG. Finally, grids were washed in 0.1% gelatin in PBS (5 × 2 min), milliQ water (3 × 2 min), and stained with 2% uranyl acetate (30 s). Grids were examined in a JEOL 1230 electron microscope.

5.5. Cryo-electron microscopy

75 μl of ICOVIR15-ABD (8×10^{11}vp/ml) were mixed with 0.75 μl of stock HSA and incubated for 30 min at room temperature to obtain an ICOVIR-ABD-HSA complex for cryo-EM imaging. Glycerol and free HSA were removed, and the virus concentrated by adding 2.3 volumes of 20 mMTris pH 7.8, NaCl 25 mM and spinning at 4 °C in a 100,000 MWCO Amicon Ultra centrifugal filter (Millipore, Billerica, MA, USA). Final virus concentration was 2.4×10^{12}vp/ml. Samples were applied to glow discharged Quantifoil R2/4300 mesh Cu/Rh grids, vitrified in liquid ethane using a Leica CPC plunger, mounted in a Gatan 626 cryostage and examined in a FEI Tecnai G2 FEG microscope operating at 200 kV. Low dose cryo-EM images were acquired using a 4 K × 4 K Eagle CCD camera, with a magnification of ×50000 and a defocus range of 0.5–4 μm, with a nominal sampling rate of 2.16 Å/px in the sample.

5.6. Three-dimensional reconstruction and difference mapping

Image processing and three-dimensional reconstruction were performed using the software Xmipp. The contrast transfer function (CTF) parameters of 177 micrographs were determined using CTFFIND4 [44]. An initial set of 1181 particles manually selected was extracted into 516 × 516 pixel boxes, with one pixel corresponding to 2.16 Å in

the sample, normalized, and reduced to 256 × 256 box size (4.35 Å/px) for computational efficiency. Orientation search and 3D reconstruction were carried out using projection matching in Xmipp. The initial model for the first refinement iteration was a map calculated from the high resolution cryo-EM model of human adenovirus type 5 (HAdV-C5) [45] using the program pdb2mrc [46] and low-pass filtered to 60 Å resolution. A total of 1121 particles were included in the final 3D map at 19.6 Å resolution, estimated by Fourier shell correlation with the threshold set at 0.5. Icosahedral symmetry was imposed throughout refinement. A difference map showing the HVR1, ABD and HSA density was calculated by subtracting the HAdV-C5 model from the ICOVIR15-ABD-HSA map after filtering both to the same resolution (19.6 Å), normalizing, and refining the scale of the experimental map. Scale refinement, subtraction and figure creation were carried out with UCSF Chimera [47].

5.7. Virus production, transduction, and cytotoxicity

Viral production in A549 (800vp/cell) cell extracts was performed as described [22]. For transduction assays, SK-mel28 (10,000 cells/well), NP-9 (15,000 cells/well), A549, B16, and B16-CAR (30,000 cells/well) were seeded in 96-well plates. The following day, cells were infected in normal medium or in HSA-containing medium (1 mg/ml) with 100vp/cell for A549, 400vp/cell for B16, 1200vp/cell for B16-CAR, and 600vp/cell for SK-mel28 and NP-9. At 36 h post-infection medium was removed and cells were lysed adding 50 μl of Cell Lysis reagent (Promega, Madison, Wi) and frozen-thawed once. Lysates were centrifuged at 13,000 g for 5 min at 4 °C and the luciferase activity of the supernatant was measured using Luciferase Assay Reagent (Promega) in a luminometer (Berthold Junior, Berthold GmbH&Co, KG, Germany). Cytotoxicity in A549 cells was performed as described [48], in normal or HSA-containing medium (1 mg/ml). IC_{50} values were determined from dose-response curves by standard nonlinear regression (GraphPad Prism 5; GraphPad Inc., La Jolla, CA).

5.8. Mice immunization and sera collection

In vivo studies were performed at the ICO-IDIBELL facility (Barcelona, Spain) AAALAC unit 1155, and approved by IDIBELL's Ethical Committee for Animal Experimentation. Viral solutions were always administered (intraperitoneally and intravenously) in 200 μl of PBS per animal. Seven-week-old C57BL6 female mice were immunized with an intraperitoneal injection of Ad5wt (3×10^{10}vp). For boosting, 3×10^{10}vp of the same virus were injected intravenously 7 days after immunization. Mice were sacrificed 7 days after and blood samples were collected by intracardiac puncture and allowed to clot. After centrifugation (8000 rpm, 5 min), serum samples were pooled and subjected to heat-treatment (56 °C, 30 min).

5.9. In vitro antibody-mediated neutralization assays

For the infectivity analysis, serial dilutions of the antibody Ab6982 (Abcam, Cambridge, UK) or serum were performed in medium ± HSA (1 mg/ml) containing AdGLRGD or AdGLRGD-ABD in 96-well plates. After one hour incubation at room temperature, 30,000 A549 cells/well were added to obtain a multiplicity of infection of 10vp/cell. Twenty-four hours after the infection, luciferase activity was analyzed as described in "in vitro transduction assay". For the analysis of cytotoxicity, Ab6982 or serum were serially diluted in medium ± HSA containing ICOVIR15 or ICOVIR15-ABD. One hour after incubation at room temperature, 30,000 A549 cells/well were added to obtain a multiplicity of infection of 100vp/cell. At day 5 post-infection cell viability was analyzed as described [48].

5.10. In vivo blood clearance

Seven-week-old Athymic *nu/nu* female mice were injected intravenously with a mixture of ICOVIR15 and ICOVIR15-ABD (ratio 1:1) with a total dose of 5×10^{10}vp. At 5 min, 15 min, 1 h, 4 h, and 24 h post-administration, blood samples were collected from the tail vein. The serum fraction was separated and digested with proteinase K and SDS for 45 min at 54 °C and later for 10 min at 90 °C to release the viral DNA. A PCR of the samples was performed using hexon HVR1-flanking oligonucleotides Ad19121F 5′-CTGGACATGGCTTCCACGTA-3′ and Ad19300R 5-'GCTCGTCTACTTCGTCTTCG-3', and analyzed by electrophoresis on a 1% agarose gel. A standard with several ratios of ICOVIR15-ABD:ICOVIR15 genomes (0.2, 1, 5, 10, and 50), the pre-injection 1:1 mixture, and water were included as PCR controls.

5.11. In vivo transduction analysis

Melanoma tumors were established implanting 1×10^7 Sk-mel28, or 1×10^6 B16-CAR cells subcutaneously into both flanks of seven-week-old female Athymic *nu/nu*, or C57BL6 mice respectively. When B16-CAR tumors reached 100 mm^3 animals were randomized. C57BL6 mice were immunized intraperitoneally with PBS (naïve) or with 2×10^{10}vp of Ad5wt (pre-immune). Seven days after, animals were injected intravenously with PBS, AdGLRGD, or AdGLRGD-ABD (3×10^{10}vp). When Sk-mel28 tumors reached 150 mm^3 animals were randomized, and injected intravenously with PBS, AdGLRGD or AdGLRGD-ABD (5×10^{10}vp). Three days after vector administration mice received an intraperitoneal injection of 250 μl of D-Luciferin (15 mg/ml; Biosynth, Staad, Switzerland) and were sacrificed to harvest the organs for bioluminescent imaging. Organs were imaged on the IVIS Lumina XR (Caliper Life Sciences, Hopkinton, MA) and the Living Image v4.0 software was used to quantify the emission of light.

5.12. In vivo antitumoural efficacy

Subcutaneous tumors were established by injection of 1×10^7 Sk-mel28, or 5×10^6 A549 cells into the flanks of seven-week-old female Athymic *nu/nu* mice. When tumors reached 150 mm^3 (tumors not progressing were excluded from the study), mice were randomized and passively immunized with an intraperitoneal injection of 200 μl of PBS (naïve) or anti-Ad5 neutralizing mice serum (pre-immune). One day after, mice were treated intravenously with PBS, ICOVIR15, or ICOVIR15-ABD (4×10^{10}vp). Tumor size and mice status were monitored thrice per week. Tumor volume was measured with a digital caliper and defined by the equation $V(mm^3) = \pi/6 \times W^2 \times L$, where W and L are the width and the length of the tumor, respectively.

5.13. Immune responses against E1b protein

Seven-week-old C57BL6 mice were immunized intraperitoneally with the E1-deleted AdGL vector (3×10^{10}vp). Seven days later mice received an intravenous administration of ICOVIR15 or ICOVIR15-ABD (3×10^{10}vp). Mice were sacrificed and spleens were collected 7 days after virus injection. CTL-specific responses against $E1b_{192}$ epitope were evaluated by IFN-γ ELISPOT as described [49].

5.14. Statistical analysis

Two-tailed Student's *t*-test was used to evaluate the statistical significance between groups, except for the comparison of survival curves where a log-rank test was used.

Acknowledgements

L. A. Rojas was supported by an IDIBELL grant. C. San Martín was supported by BFU2013-41249-P grant. R. Alemany was supported by

BIO2011-30299-C02-01 and BIO2014-57716-C2-1-R grants from the "Ministerio de Economía y Competitividad" of Spain, EU contract 29002 FP7-PEOPLE-2011-ITN, and 2014SGR364 research grant from the 'Generalitat de Catalunya'. C. San Martín and R. Alemany belong to the cooperative network BIO2015-68990-REDT. The authors declare no conflict of interest exists.

Appendix A. Supplementary data

Supplementary data to this article can be found online at http://dx.doi.org/10.1016/j.jconrel.2016.07.004.

References

[1] H.L. Kaufman, F.J. Kohlhapp, A. Zloza, Oncolytic viruses: a new class of immunotherapy drugs, Nat. Rev. Drug Discov. 14 (9) (2015) 642–662.
[2] H. Uusi-Kerttula, S. Hulin-Curtis, J. Davies, A.L. Parker, Oncolytic adenovirus: strategies and insights for vector design and immuno-oncolytic applications, Viruses 7 (11) (2015) 6009–6042.
[3] D.E. Zak, E. Andersen-Nissen, E.R. Peterson, A. Sato, M.K. Hamilton, J. Borgerding, A.T. Krishnamurty, J.T. Chang, D.J. Adams, T.R. Hensley, A.I. Salter, C.A. Morgan, A.C. Duerr, S.C. De Rosa, A. Aderem, M.J. McElrath, Merck Ad5/HIV induces broad innate immune activation that predicts CD8(+) T-cell responses but is attenuated by preexisting Ad5 immunity, Proc. Natl. Acad. Sci. U. S. A. 109 (50) (2012) E3503–E3512.
[4] D.H. Barouch, S.V. Kik, G.J. Weverling, R. Dilan, S.L. King, L.F. Maxfield, S. Clark, D. Ng'ang'a, K.L. Brandariz, P. Abbink, F. Sinangil, G. de Bruyn, G.E. Gray, S. Roux, L.G. Bekker, A. Dilraj, H. Kibuuka, M.L. Robb, N.L. Michael, O. Anzala, P.N. Amornkul, J. Gilmour, J. Hural, S.P. Buchbinder, M.S. Seaman, R. Dolin, L.R. Baden, A. Carville, K.G. Mansfield, M.G. Pau, J. Goudsmit, International seroepidemiology of adenovirus serotypes 5, 26, 35, and 48 in pediatric and adult populations, Vaccine 29 (32) (2011) 5203–5209.
[5] T.C. Mast, L. Kierstead, S.B. Gupta, A.A. Nikas, E.G. Kallas, V. Novitsky, B. Mbewe, P. Pitisuttithum, M. Schechter, E. Vardas, N.D. Wolfe, M. Aste-Amezaga, D.R. Casimiro, P. Coplan, W.L. Straus, J.W. Shiver, International epidemiology of human pre-existing adenovirus (Ad) type-5, type-6, type-26 and type-36 neutralizing antibodies: correlates of high Ad5 titers and implications for potential HIV vaccine trials, Vaccine 28 (4) (2010) 950–957.
[6] R.R. Bradley, D.M. Lynch, M.J. Iampietro, E.N. Borducchi, D.H. Barouch, Adenovirus serotype 5 neutralizing antibodies target both hexon and fiber following vaccination and natural infection, J. Virol. 86 (1) (2012) 625–629.
[7] S.M. Sumida, D.M. Truitt, A.A. Lemckert, R. Vogels, J.H. Custers, M.M. Addo, S. Lockman, T. Peter, F.W. Peyerl, M.G. Kishko, S.S. Jackson, D.A. Gorgone, M.A. Lifton, M. Essex, B.D. Walker, J. Goudsmit, M.J. Havenga, D.H. Barouch, Neutralizing antibodies to adenovirus serotype 5 vaccine vectors are directed primarily against the adenovirus hexon protein, J. Immunol. 174 (11) (2005) 7179–7185.
[8] L. Coughlan, R. Alba, A.L. Parker, A.C. Bradshaw, I.A. McNeish, S.A. Nicklin, A.H. Baker, Tropism-modification strategies for targeted gene delivery using adenoviral vectors, Viruses 2 (10) (2010) 2290–2355.
[9] J.M. Prill, V. Subr, N. Pasquarelli, T. Engler, A. Hoffmeister, S. Kochanek, K. Ulbrich, F. Kreppel, Traceless bioresponsive shielding of adenovirus hexon with HPMA copolymers maintains transduction capacity in vitro and in vivo, PLoS One 9 (1) (2014), e82716.
[10] A.A. Lemckert, S.M. Sumida, L. Holterman, R. Vogels, D.M. Truitt, D.M. Lynch, A. Nanda, B.A. Ewald, D.A. Gorgone, M.A. Lifton, J. Goudsmit, M.J. Havenga, D.H. Barouch, Immunogenicity of heterologous prime-boost regimens involving recombinant adenovirus serotype 11 (Ad11) and Ad35 vaccine vectors in the presence of anti-ad5 immunity, J. Virol. 79 (15) (2005) 9694–9701.
[11] J.W. Shiver, E.A. Emini, Recent advances in the development of HIV-1 vaccines using replication-incompetent adenovirus vectors, Annu. Rev. Med. 55 (2004) 355–372.
[12] J.T. Bruder, E. Semenova, P. Chen, K. Limbach, N.B. Patterson, M.E. Stefaniak, S. Konovalova, C. Thomas, M. Hamilton, C.R. King, T.L. Richie, D.L. Doolan, Modification of Ad5 hexon hypervariable regions circumvents pre-existing Ad5 neutralizing antibodies and induces protective immune responses, PLoS One 7 (4) (2012), e33920.
[13] D.M. Roberts, A. Nanda, M.J. Havenga, P. Abbink, D.M. Lynch, B.A. Ewald, J. Liu, A.R. Thorner, P.E. Swanson, D.A. Gorgone, M.A. Lifton, A.A. Lemckert, L. Holterman, B. Chen, A. Dilraj, A. Carville, K.G. Mansfield, J. Goudsmit, D.H. Barouch, Hexon-chimaeric adenovirus serotype 5 vectors circumvent pre-existing anti-vector immunity, Nature 441 (7090) (2006) 239–243.
[14] J. Scherer, R.B. Vallee, Conformational changes in the adenovirus hexon subunit responsible for regulating cytoplasmic dynein recruitment, J. Virol. 89 (2) (2015) 1013–1023.
[15] F. Kratz, A clinical update of using albumin as a drug vehicle — a commentary, J. Control. Release 190 (2014) 331–336.
[16] J.T. Andersen, R. Pehrson, V. Tolmachev, M.B. Daba, L. Abrahmsen, C. Ekblad, Extending half-life by indirect targeting of the neonatal Fc receptor (FcRn) using a minimal albumin binding domain, J. Biol. Chem. 286 (7) (2011) 5234–5241.
[17] M.S. Dennis, M. Zhang, Y.G. Meng, M. Kadkhodayan, D. Kirchhofer, D. Combs, L.A. Damico, Albumin binding as a general strategy for improving the pharmacokinetics of proteins, J. Biol. Chem. 277 (38) (2002) 35035–35043.
[18] D. Sleep, J. Cameron, L.R. Evans, Albumin as a versatile platform for drug half-life extension, Biochim. Biophys. Acta 1830 (12) (2013) 5526–5534.
[19] M.U. Johansson, I.M. Frick, H. Nilsson, P.J. Kraulis, S. Hober, P. Jonasson, M. Linhult, P.A. Nygren, M. Uhlen, L. Bjorck, T. Drakenberg, S. Forsen, M. Wikstrom, Structure, specificity, and mode of interaction for bacterial albumin-binding modules, J. Biol. Chem. 277 (10) (2002) 8114–8120.
[20] M. Linhult, H.K. Binz, M. Uhlen, S. Hober, Mutational analysis of the interaction between albumin-binding domain from streptococcal protein G and human serum albumin, Protein Sci. 11 (2) (2002) 206–213.
[21] R. Stork, D. Muller, R.E. Kontermann, A novel tri-functional antibody fusion protein with improved pharmacokinetic properties generated by fusing a bispecific single-chain diabody with an albumin-binding domain from streptococcal protein G, Protein Eng. Des. Sel. 20 (11) (2007) 569–576.
[22] J.J. Rojas, S. Guedan, P.F. Searle, J. Martinez-Quintanilla, R. Gil-Hoyos, F. Alcayaga-Miranda, M. Cascallo, R. Alemany, Minimal RB-responsive E1A promoter modification to attain potency, selectivity, and transgene-arming capacity in oncolytic adenoviruses, Mol. Ther. 18 (11) (2010) 1960–1971.
[23] C. Falkenberg, L. Bjorck, B. Akerstrom, Localization of the binding site for streptococcal protein G on human serum albumin. Identification of a 5.5-kilodalton protein G binding albumin fragment, Biochemistry 31 (5) (1992) 1451–1457.
[24] P.A. Nygren, C. Ljungquist, H. Tromborg, K. Nustad, M. Uhlen, Species-dependent binding of serum albumins to the streptococcal receptor protein G, Eur. J. Biochem. 193 (1) (1990) 143–148.
[25] N.B. Elsedawy, S.J. Russell, Oncolytic vaccines, Expert Rev. Vaccines 12 (10) (2013) 1155–1172.
[26] F. Kratz, Albumin as a drug carrier: design of prodrugs, drug conjugates and nanoparticles, J. Control. Release 132 (3) (2008) 171–183.
[27] L.J. Holt, A. Basran, K. Jones, J. Chorlton, L.S. Jespers, N.D. Brewis, I.M. Tomlinson, Anti-serum albumin domain antibodies for extending the half-lives of short lived drugs, Protein Eng. Des. Sel. 21 (5) (2008) 283–288.
[28] N. Desai, V. Trieu, B. Damascelli, P. Soon-Shiong, SPARC expression correlates with tumor response to albumin-bound paclitaxel in head and neck cancer patients, Transl. Oncol. 2 (2) (2009) 59–64.
[29] D.D. Von Hoff, R.K. Ramanathan, M.J. Borad, D.A. Laheru, L.S. Smith, T.E. Wood, R.L. Korn, N. Desai, V. Trieu, J.L. Iglesias, H. Zhang, P. Soon-Shiong, T. Shi, N.V. Rajeshkumar, A. Maitra, M. Hidalgo, Gemcitabine plus nab-paclitaxel is an active regimen in patients with advanced pancreatic cancer: a phase I/II trial, J. Clin. Oncol. 29 (34) (2011) 4548–4554.
[30] R.E. Kontermann, Strategies to extend plasma half-lives of recombinant antibodies, BioDrugs 23 (2) (2009) 93–109.
[31] J. Gall, A. Kass-Eisler, L. Leinwand, E. Falck-Pedersen, Adenovirus type 5 and 7 capsid chimera: fiber replacement alters receptor tropism without affecting primary immune neutralization epitopes, J. Virol. 70 (4) (1996) 2116–2123.
[32] T. Konig, A. Skerra, Use of an albumin-binding domain for the selective immobilisation of recombinant capture antibody fragments on ELISA plates, J. Immunol. Methods 218 (1–2) (1998) 73–83.
[33] J. Alonso-Padilla, T. Papp, G.L. Kajan, M. Benko, M. Havenga, A. Lemckert, B. Harrach, A.H. Baker, Development of novel adenoviral vectors to overcome challenges observed with HAdV-5-based constructs, Mol. Ther. 24 (1) (2016) 6–16.
[34] R. Khare, M.L. Hillestad, Z. Xu, A.P. Byrnes, M.A. Barry, Circulating antibodies and macrophages as modulators of adenovirus pharmacology, J. Virol. 87 (7) (2013) 3678–3686.
[35] Z. Xu, J. Tian, J.S. Smith, A.P. Byrnes, Clearance of adenovirus by Kupffer cells is mediated by scavenger receptors, natural antibodies, and complement, J. Virol. 82 (23) (2008) 11705–11713.
[36] Y. Chen, D.C. Yu, D. Charlton, D.R. Henderson, Pre-existent adenovirus antibody inhibits systemic toxicity and antitumor activity of CN706 in the nude mouse LNCaP xenograft model: implications and proposals for human therapy, Hum. Gene Ther. 11 (11) (2000) 1553–1567.
[37] V. Tsai, D.E. Johnson, A. Rahman, S.F. Wen, D. LaFace, J. Philopena, J. Nery, M. Zepeda, D.C. Maneval, G.W. Demers, R. Ralston, Impact of human neutralizing antibodies on antitumor efficacy of an oncolytic adenovirus in a murine model, Clin. Cancer Res. 10 (21) (2004) 7199–7206.
[38] A.K. Zaiss, H.B. Machado, H.R. Herschman, The influence of innate and pre-existing immunity on adenovirus therapy, J. Cell. Biochem. 108 (4) (2009) 778–790.
[39] S. Guedan, J.J. Rojas, A. Gros, E. Mercade, M. Cascallo, R. Alemany, Hyaluronidase expression by an oncolytic adenovirus enhances its intratumoral spread and suppresses tumor growth, Mol. Ther. 18 (7) (2010) 1275–1283.
[40] A. Rodriguez-Garcia, M. Gimenez-Alejandre, J.J. Rojas, R. Moreno, M. Bazan-Peregrino, M. Cascallo, R. Alemany, Safety and efficacy of VCN-01, an oncolytic adenovirus combining fiber HSG-binding domain replacement with RGD and hyaluronidase expression, Clin. Cancer Res. 21 (6) (2015) 1406–1418.
[41] J.J. Rojas, M. Gimenez-Alejandre, R. Gil-Hoyos, M. Cascallo, R. Alemany, Improved systemic antitumor therapy with oncolytic adenoviruses by replacing the fiber shaft HSG-binding domain with RGD, Gene Ther. 19 (4) (2012) 453–457.
[42] A. Villanueva, C. Garcia, A.B. Paules, M. Vicente, M. Megias, G. Reyes, P. de Villalonga, N. Agell, F. Lluis, O. Bachs, G. Capella, Disruption of the antiproliferative TGF-beta signaling pathways in human pancreatic cancer cells, Oncogene 17 (15) (1998) 1969–1978.
[43] R.J. Stanton, B.P. McSharry, M. Armstrong, P. Tomasec, G.W. Wilkinson, Re-engineering adenovirus vector systems to enable high-throughput analyses of gene function, Biotechniques 45 (6) (2008) 659–662 (664–658).
[44] A. Rohou, N. Grigorieff, CTFFIND4: fast and accurate defocus estimation from electron micrographs, J. Struct. Biol. 192 (2) (2015) 216–221.
[45] H. Liu, L. Jin, S.B. Koh, I. Atanasov, S. Schein, L. Wu, Z.H. Zhou, Atomic structure of human adenovirus by cryo-EM reveals interactions among protein networks, Science 329 (5995) (2010) 1038–1043.

[46] S.J. Ludtke, P.R. Baldwin, W. Chiu, EMAN: semiautomated software for high-resolution single-particle reconstructions, J. Struct. Biol. 128 (1) (1999) 82–97.
[47] E.F. Pettersen, T.D. Goddard, C.C. Huang, G.S. Couch, D.M. Greenblatt, E.C. Meng, T.E. Ferrin, UCSF Chimera—a visualization system for exploratory research and analysis, J. Comput. Chem. 25 (13) (2004) 1605–1612.
[48] C. Puig-Saus, L.A. Rojas, E. Laborda, A. Figueras, R. Alba, C. Fillat, R. Alemany, iRGD tumor-penetrating peptide-modified oncolytic adenovirus shows enhanced tumor transduction, intratumoral dissemination and antitumor efficacy, Gene Ther. 21 (8) (2014) 767–774.
[49] A. Rodriguez-Garcia, E. Svensson, R. Gil-Hoyos, C.A. Fajardo, L.A. Rojas, M. Arias-Badia, A.S. Loskog, R. Alemany, Insertion of exogenous epitopes in the E3-19K of oncolytic adenoviruses to enhance TAP-independent presentation and immunogenicity, Gene Ther. 22 (7) (2015) 596–601.

Cancer Gene Therapy (2016) 00, 1–4

www.nature.com/cgt

SHORT COMMUNICATION

Adenovirus coxsackie adenovirus receptor-mediated binding to human erythrocytes does not preclude systemic transduction

LA Rojas[1], R Moreno[1], H Calderón[2,3] and R Alemany[1]

There is great skepticism in the capability of adenovirus vectors and oncolytic adenoviruses to reach specific organs or tumors upon systemic administration. Besides antibodies, the presence of CAR (coxsackie and adenovirus receptor) in human erythrocytes has been postulated to sequester CAR-binding adenoviruses, commonly used in gene therapy and oncolytic applications. The use of non-CAR-binding fibers or serotypes has been postulated to solve this limitation. Given the lack of integrins in erythrocytes and therefore of internalization of the CAR-bound virus, we hypothesized that the interaction of adenovirus type 5 (Ad5) with CAR in human erythrocytes could be reversible. In this work, we have studied the effects of Ad5 interaction with human erythrocytes via CAR. Although erythrocyte binding was observed, it did not reduce viral transduction of tumor cells *in vitro* after long-term incubations. Transplantation of human erythrocytes into nude mice did not reduce Ad5 extravasation and transduction of liver and human xenograft tumors after systemic administration. These findings indicate that despite human erythrocytes are able to bind to Ad5, this binding is reversible and does not prevent extravasation and organ transduction after systemic delivery. Thus, the poor bioavailability of systemically delivered CAR-binding adenoviruses in humans is likely due to other factors such as liver sequestration or neutralizing antibodies.

Cancer Gene Therapy advance online publication, 21 October 2016; doi:10.1038/cgt.2016.50

INTRODUCTION

Adenoviruses are broadly used as gene therapy vectors as well as oncolytic agents for the treatment of cancer. More than 50 human adenovirus serotypes have been described,[1] but particularly adenovirus type 5 (Ad5) has been the most widely used for these applications. In the case of disseminated cancer or when multiple organs need to be transduced, a systemic delivery of the virus is required by injection into the bloodstream. However, clinical experience has shown that local delivery has usually outperformed intravenous administration, which has rarely demonstrated therapeutic effects.[2–5]

Ad5 encounters several important barriers when injected intravenously that may block transduction. Liver Kupffer cells and liver sinusoidal endothelial cells efficiently sequester circulating viral particles.[1] In addition, human blood represents a hostile environment for Ad5 because of multiple neutralizing interactions that reduce the bioavailability of the virus. Antibodies that occur naturally or develop upon infection directly block capsid infectivity or enhance its clearance by Fc receptors in phagocytes[6] and by complement receptor 1 in erythrocytes.[7] Independently of the presence of antibodies, human erythrocytes may also bind and inactivate Ad5 directly. Recent studies have demonstrated that unlike mouse erythrocytes, human erythrocytes express the primary adenovirus receptor, the Coxsackie and adenovirus receptor (CAR).[7,8] This CAR binding was shown to inhibit Ad5 infectivity, contrary to earlier reports of Ad5 titration in the presence of human blood.[9] However, the absence of integrins in erythrocytes precludes internalization of the erythrocyte-bound Ad5.[7] Therefore, we hypothesized that the interaction of Ad5 with CAR in human erythrocytes could be reversible, and upon long-term incubation periods, the virus could be available for infection. Our results support this hypothesis.

MATERIALS AND METHODS

Cell lines and viruses

Human lung adenocarcinoma A549 cells were obtained from the American Type Culture Collection (ATCC, Manassas, VA, USA) and maintained with Dulbecco's modified Eagle's medium supplemented with 5% fetal bovine serum at 37 °C with 5% CO_2. Cells were routinely tested for mycoplasma. AdGL is an Ad5-derived E1-deleted first-generation vector expressing the EGFP-luciferase fusion protein cassette from pEGFPLuc (Clontech, Mountain View, CA, USA). AdGL was propagated in human embryonic kidney 293 cells and purified using cesium chloride double gradients according to standard techniques.

Isolation of human erythrocytes

Human blood samples were obtained by venipuncture into lithium-heparinized tubes (Greiner Bio-One, Monroe, NC, USA) with donor consent and approval by the IDIBELL's Ethics Committee. After centrifugation (2000 *g* for 10 min), plasma and leukocyte layer were removed, and erythrocytes were washed with phosphate-buffered saline (PBS) four times. Erythrocytes were resuspended in PBS at the indicated concentrations.

[1]Virotherapy and Gene therapy Group, ProCure Program, Translational Research Laboratory, Instituto Catalan de Oncología-IDIBELL, Barcelona, Spain; [2]Psioxus Therapeutics, Oxford, UK and [3]Department of Oncology, University of Oxford, Oxford, UK. Correspondence: Dr R Alemany, Virotherapy and Gene Therapy Group, ProCure Program, Translational Research Laboratory, Instituto Catalan de Oncología-IDIBELL, Av Gran Via de l'Hospitalet 199-203, Via S/N Km2, 7, L'Hospitalet de Llobregat, Barcelona 08907, Spain. E-mail: ralemany@iconcologia.net
Received 1 July 2016; revised 22 September 2016; accepted 23 September 2016

Quantification of Ad5 binding to human erythrocytes

AdGL was incubated with human erythrocytes at the indicated concentrations for 30 min at 37 °C with constant agitation. After centrifugation (2000 *g* for 10 min), the supernatant was separated and the erythrocyte pellet resuspended in PBS. Supernatant and pellet samples were digested with proteinase K and sodium dodecyl sulfate for 45 min at 54 °C and later for 10 min at 90 °C to release the viral DNA. Genome copy levels were quantified by real-time PCR using the oligonucleotides (forward primer: 5'-CTTC GATGATGCCGCAGTG-3' and reverse primer: 5'-GGGCTCAGGTA CTCCGAGG-3') and a Taqman probe (5'-FAM-TTACATGCACATCT CGGGCCAGGAC-TAMRA-3'), which identify the hexon region. Genome copies were calculated using LightCycler v.4.05 software (Roche, Basel, Switzerland). For the CAR-blocking assay, a preincubation of human erythrocytes with anti-CAR antibody from RmcB hybridoma (ATCC, Manassas, VA, USA) was performed for 1 h at 4 °C, before the incubation with Ad5.

In vitro infectivity assay

In total, 1.8x10^8 vp (viral particles) of AdGL were incubated with 5×10^9 erythrocytes in 1 ml of PBS or in 1 ml of PBS without erythrocytes for 30 min at 37 °C with agitation. Samples were centrifuged, and the erythrocyte pellet was resuspended in 1 ml of PBS. A measure of 30 µl of the samples were used to infect A549 cells in 24-well plates (700 000 cells per well). Erythrocytes alone in A549 cells and erythrocytes with AdGL in the absence of A549 cells were used as negative controls. At 48 h after infection, the medium was removed and cells were lysed adding 200 µl of cell lysis reagent (Promega, Madison, WI, USA) and frozen-thawed once. Lysates were centrifuged at 13 000 *g* for 5 min at 4 °C, and the luciferase activity of the supernatant was measured using the Luciferase Assay Reagent (Promega) in a luminometer (Berthold Junior, Berthold GmbH & Co. KG, Bad Wildbad, Germany).

In vivo biodistribution studies

In vivo studies were performed at the ICO-IDIBELL facility (Barcelona, Spain) AAALAC unit 1155, and approved by IDIBELL's Ethical Committee for Animal Experimentation. Subcutaneous tumors were established by injection of 5×10^6 A549 cells into the flanks of 7-week-old male athymic *nu/nu* mice. When tumors reached 150 mm^3, mice were randomized and injected intravenously with 5×10^{10} vp of AdGL in 200 µl of PBS or with 5×10^{10} vp of AdGL previously incubated (30 min at 37 °C) with 8×10^8 human erythrocytes in 200 µl of PBS. Three days after vector administration, mice received an intraperitoneal injection of 250 µl of D-luciferin (15 mg ml^{-1}; Biosynth, Staad, Switzerland) and were killed to harvest liver and tumors for bioluminescent imaging. Organs were imaged on the IVIS Lumina XR (Caliper Life Sciences, Hopkinton, MA, USA), and the Living Image v.4.0 software (Caliper Life Sciences, Hopkinton, MA, USA) was used to quantify the emission of light. Organs were frozen for subsequent adenovirus genome detection by real-time PCR. Frozen tissues were ground to a fine powder in liquid nitrogen using a pestle and mortar, and DNA was purified following the QIAamp DNA Mini Kit (Qiagen, Valencia, CA, USA) protocol. Adenovirus genomes were quantified in DNA-purified samples by real-time PCR as described above.

Blood persistence of human erythrocytes after systemic administration in nude mice

Freshly isolated and washed human erythrocytes were incubated with carboxyfluorescein succinidyl ester (Sigma, St Louis, MO, USA) at a final concentration of 10 µM for 5 min protected from light. After washing, erythrocytes were brought to a concentration of 4×10^9 cells per ml in PBS. A total of 8×10^8 carboxyfluorescein succinidyl ester-labeled erythrocytes in 200 µl of PBS were intravenously injected in athymic *nu/nu* mice. Blood samples were collected from the tail vein at the indicated time points in EDTA-coated capillary tubes to avoid clotting. Carboxyfluorescein succinidyl ester-labeled human erythrocytes in blood samples were detected using Gallios Flow Cytometer (Beckman Coulter, Brea, CA, USA), and the FlowJo software (TreeStar, Ashland, OR, USA) was used for data analysis.

RESULTS AND DISCUSSION

Erythrocytes bind adenovirus 5 via CAR

AdGL is an Ad5-derived nonreplicative luciferase-expressing vector and was used throughout this study. Ad5 binding to human erythrocytes was first evaluated *in vitro* using different Ad: erythrocyte ratios. After incubation of erythrocytes and Ad5, the unbound and the cell-bound fractions were separated by centrifugation, and the Ad5 genomes were detected by real-time PCR (Figure 1a). The theoretical distribution of Ad5 particles in each fraction assuming no erythrocyte binding (considering the relative volume of the fractions in each condition) was used to calculate the fold clearance in the supernatant. In the first condition, we incubated 1×10^9 vp of AdGL with 1×10^7 erythrocytes in 1 ml of PBS (100 Ad particles per erythrocyte). After centrifugation, the supernatant represented the 99% of the total volume, whereas the cell pellet the 1%. Most of the Ad particles were found in the supernatant (98.5% free Ad vs 1.5% erythrocyte-bound), indicating that in this condition erythrocytes were not able to pull down efficiently the viral particles. A second condition was analyzed in which 2×10^8 vp of AdGL was incubated with 5×10^9 erythrocytes in 1 ml of PBS (0.04 Ad particles per erythrocyte). These are clinically relevant conditions (for 5 L of blood, it would correspond to an intravenous dose of 1×10^{12} vp) and as such have been analyzed previously.[7] Owing to the high erythrocyte concentration, the cell pellet occupied the 40% of the total volume. In this case, an 88% of the viral input was erythrocyte-bound, and only a 12% was found free in the supernatant, confirming the published results.[7] This corresponds to an eightfold clearance of the adenovirus content in the supernatant or liquid fraction, indicating that there was an efficient pulldown of Ad particles to the erythrocyte pellet. As only ~10% of the Ad input was found free, we next reduced the Ad dose by a further 10% to check if all the viral particles could be bound to erythrocytes in such conditions. Accordingly, 1.8×10^8 vp of AdGL was incubated with 5x10^9 erythrocytes in 1 ml of PBS (0.036 Ad particles per erythrocyte). Indeed, the 99.6% of the viral input was recovered in the erythrocyte fraction, corresponding to a 95-fold clearance of the adenovirus content in the liquid fraction. These data indicate that erythrocytes bind and pull down Ad5 particles, but taking into account the multiplicity of infections used, the erythrocyte capacity to bind adenovirus via CAR is limited as ~28 erythrocytes are needed to efficiently pull down one Ad5 particle. These results match with previous studies that show relatively low levels of CAR on human erythrocytes.[8] However, using physiological erythrocyte concentrations and a clinically relevant adenovirus dose (e.g. 1×10^{12} vp per patient), 88% of the viral input dose would bind to erythrocytes.

To prove that the interaction is CAR-mediated and not simply a nonspecific binding, we used an anti-CAR antibody to block the interaction. Adenovirus and human erythrocytes preincubated or not with anti-CAR antibody were incubated at an Ad:erythrocyte ratio of 0.04. In the absence of anti-CAR antibody, only a 4.2% of the viral input was found free, and considering that the supernatant represented the 55% of the total volume, this represents a 13-fold clearance of the viral content in this fraction (Figure 1b). In contrast, when human erythrocytes were pre-incubated with anti-CAR, the 33% of the viral dose was found free in the supernatant fraction, representing only a 1.6-fold clearance.

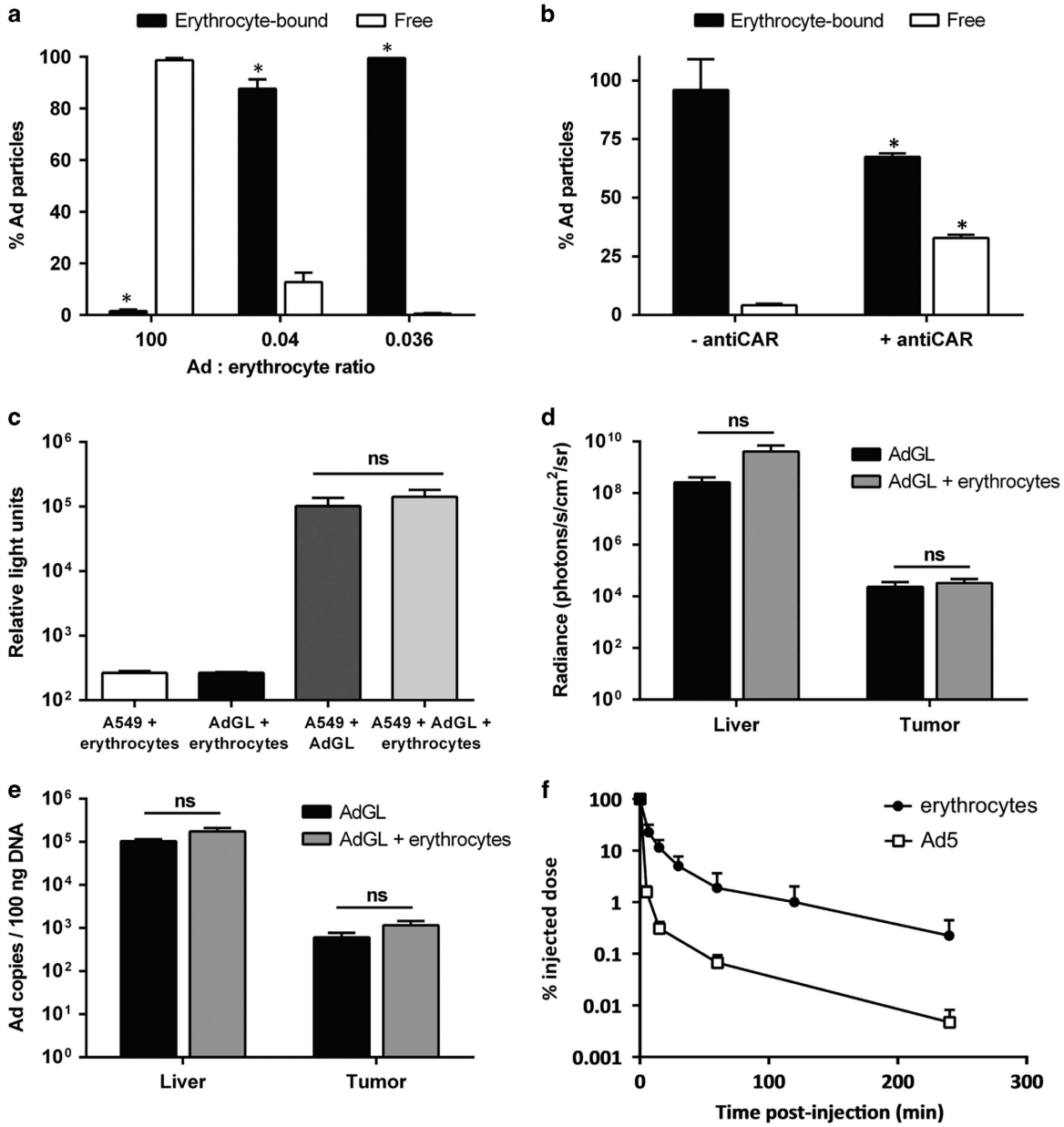

Figure 1. (**a**) Detection of adenovirus type 5 (Ad5) binding to human erythrocytes. Human erythrocytes were incubated with AdGL at the indicated proportions of virus particle per erythrocyte for 30 min at 37 °C. Samples were centrifuged to separate the liquid and cell fractions, and Ad5 detection was performed by quantitative real-time PCR. Data are represented as % of Ad particles recovered in each fraction ($n = 3$). Mean values ± s.d. *Significant ($P < 0.05$) by two-tailed unpaired Student's *t*-test compared with free Ad. (**b**) CAR (coxsackie and adenovirus receptor)-blocking assay to inhibit Ad5 binding. Human erythrocytes were preincubated or not with anti-CAR antibody (RmcB) and then incubated with AdGL. After centrifugation, Ad5 detection in the liquid and cell fractions was performed by quantitative real-time PCR. Data are represented as % of Ad particles recovered in each fraction ($n = 3$). Mean values ± s.d. *Significant ($P < 0.05$) by two-tailed unpaired Student's *t*-test compared with anti-CAR. (**c**) Ad5-mediated transduction of tumor cells in the absence or presence of human erythrocytes. AdGL was incubated with or without human erythrocytes (0.036 vp per cell), and after centrifugation, the cell fraction was used to infect A549 cells. At 48 h after infection, cell transduction was analyzed by luciferase expression. Erythrocytes alone in A549 cells and erythrocytes with AdGL in the absence of A549 cells were used as negative controls. NS, nonsignificant ($P < 0.05$) by two-tailed unpaired Student's *t*-test. (**d**) Systemic transduction of liver and tumor in the presence or absence of erythrocytes. Nude mice bearing subcutaneous A549 (human lung adenocarcinoma) tumors were injected intravenously with 5×10^{10} vp of AdGL previously incubated with or without 8×10^{8} human erythrocytes. After 3 days, liver and tumors were collected and luciferase activity was analyzed by bioluminescence imaging. Organs were frozen for subsequent Ad5 genome detection by real-time PCR. (**e**) Livers $n = 5$ and tumors $n = 8$–10. Mean ± s.e.m. is shown. NS, nonsignificant ($P < 0.05$) by two-tailed unpaired Student's *t*-test. sr, Steradian. (**f**) Blood persistence of human erythrocytes after intravenous injection in nude mice. Nude mice were intravenously injected with $8x10^{8}$ carboxyfluorescein succinidyl ester (CFSE)-labeled human erythrocytes. At the indicated time points, blood samples were collected and human erythrocytes were detected by flow cytometry ($n = 3$ mice). Results are plotted including our previous data of Ad5 persistence in nude mice.[11] Mean ± s.e.m. is shown.

CAR-mediated binding to human erythrocytes does not inhibit adenovirus bioactivity

To analyze whether erythrocyte binding inactivated Ad5 *in vitro*, we analyzed the infectivity of AdGL in A549 cells in the presence or absence of human erythrocytes. To achieve complete binding, the Ad:erythrocyte ratio used was 0.036. After incubation, the erythrocyte pellet was separated and used to infect A549 cells. The erythrocyte-bound Ad5 was kept in contact with the tumor cells for 48 h before luciferase expression was measured. Previous studies have shown a strong inhibition of Ad5 infection in A549 cells due to erythrocyte sequestration.[7,10] Nonetheless, we observed the same levels of transduction regardless of the presence of human erythrocytes (Figure 1c). A possible explanation for these discrepancies is the washout step of the Ad:erythrocyte complex from the tumor cells. Infection of A549 cells takes place by interaction with CAR as a primary receptor and with integrins as secondary or internalizing receptor. However, the lack of integrins in the erythrocyte membrane prevents adenovirus internalization.[7] Similarly, previous experiments, where the erythrocyte–Ad complex was removed 90 min after adding it to tumor cells, resulted in the removal of bound but not internalized Ad particles, causing a significant drop in cell transduction. In our experiments, the erythrocyte–Ad complex was left in contact with tumor cells for 48 h, and assuming a reversible binding to CAR, this allowed the virus to detach from CAR on erythrocytes and attach to CAR on tumor cells. In line with this observation, a previous study where erythrocytes were not removed during the incubation with target cells already reported that erythrocyte-bound adenoviruses were still infective.[9] Hence, these results indicate that although Ad5 efficiently binds to erythrocytes via CAR, this binding is reversible and in the long term it does not inhibit the infection of tumor cells.

Systemic delivery of Ad5-based vectors and oncolytic viruses is very attractive for gene therapy and cancer virotherapy. We next evaluated the impact of erythrocyte binding *in vivo* upon systemic administration of Ad5. Nude mice bearing A549 xenograft tumors were intravenously injected with AdGL alone or complexed with human erythrocytes. At 3 days after virus administration, mice were killed and livers and tumors were harvested for *in vivo* bioluminescent imaging (IVIS) and Ad genome detection by real-time PCR. Luciferase expression analysis showed no significant differences in liver ($P = 0.229$) and tumor transduction ($P = 0.609$) among AdGL alone versus AdGL+erythrocytes (Figure 1d). The adenovirus vector was able to transduce efficiently the liver and, to a lesser extent, the tumors regardless of previous incubation with human erythrocytes. Accordingly, no significant differences were found in the presence of adenovirus genomes in both conditions, for livers ($P = 0.208$) and tumors ($P = 0.270$) (Figure 1e), corroborating that human erythrocytes did not prevent extravasation or organ transduction. To understand the relevance of these results in the mouse model, we evaluated the persistence of the transferred human erythrocytes in the recipient nude mice (Figure 1f). Although human erythrocytes are cleared rapidly from mouse circulation, the kinetics of clearance compared with that of adenovirus is slow, and therefore the model should be sensitive to measure the effect of human erythrocytes in systemic transduction. This method has been used before and an extended Ad5 circulation but reduced presence (100-fold) of Ad genomes in livers of mice transfused with human erythrocytes were observed.[7] Different tumor models, mouse strains or times of analysis could cause differences. An extended blood persistence and reduced extravasation is likely associated with erythrocyte binding, but without virus internalization, and with a reversible binding Ad particles are eventually released from erythrocytes and can transduce target organs. Indeed, our results show that 72 h after injection the levels of genome accumulation and organ transduction were the same in mice with and without human erythrocytes. On the other hand, evidence of impaired liver transduction upon the presence of CAR-expressing erythrocytes *in vivo* has been also obtained in GATA1-CAR transgenic mice.[7,8] Compared with isogenic control mice, GATA1-CAR transgenic mice showed 875-fold lower liver transduction 24 h after vector administration.[7] A measure of genomes at 72 h in the same transgenic model showed a 25-fold decrease compared with that in the control mice.[8] These data suggest that with time the detrimental effect of erythrocytes on liver infection is reduced. The presence of much higher levels of CAR in GATA1-CAR erythrocytes compared with that in human erythrocytes likely accounts for the difference of our results and the reported in these mice.[7,8]

In summary, our results indicate that human erythrocytes bind Ad5 via CAR, but the viral particle is not internalized and is eventually released to infect other CAR-expressing cells. Of note, in an ongoing clinical trial with oncolytic adenovirus ICOVIR-5 (NCT01864759) injected endovenously in metastatic melanoma patients, we have detected the presence of the virus in tumor biopsies of patients treated with 1×10^{12} and 1×10^{13} vp (unpublished data). We therefore believe that human erythrocytes do not represent a major obstacle for systemic delivery of adenoviruses and consider that efforts should be focused on barriers such as liver sequestration and neutralizing antibodies.

CONFLICT OF INTEREST

The authors declare no conflict of interest.

ACKNOWLEDGEMENTS

LAR was supported by an IDIBELL grant. RA was supported by BIO2011-30299-C02-01 and BIO2014-57716-C2-1-R grants from the 'Ministerio de Economía y Competitividad' of Spain, EU contract 29002 FP7-PEOPLE-2011-ITN and 2014SGR364 research grant from the 'Generalitat de Catalunya'. Co-funded by the European Regional Development Fund, a way to Build Europe.

REFERENCES

1 Khare R, Chen CY, Weaver EA, Barry MA. Advances and future challenges in adenoviral vector pharmacology and targeting. *Curr Gene Ther* 2011; **11**: 241–258.
2 Khuri FR, Nemunaitis J, Ganly I, Arseneau J, Tannock IF, Romel L *et al.* A controlled trial of intratumoral ONYX-015, a selectively-replicating adenovirus, in combination with cisplatin and 5-fluorouracil in patients with recurrent head and neck cancer. *Nat Med* 2000; **6**: 879–885.
3 Nemunaitis J, Cunningham C, Buchanan A, Blackburn A, Edelman G, Maples P *et al.* Intravenous infusion of a replication-selective adenovirus (ONYX-015) in cancer patients: safety, feasibility and biological activity. *Gene Therapy* 2001; **8**: 746–759.
4 Small EJ, Carducci MA, Burke JM, Rodriguez R, Fong L, van Ummersen L *et al.* A phase I trial of intravenous CG7870, a replication-selective, prostate-specific antigen-targeted oncolytic adenovirus, for the treatment of hormone-refractory, metastatic prostate cancer. *Mol Ther* 2006; **14**: 107–117.
5 Nokisalmi P, Pesonen S, Escutenaire S, Sarkioja M, Raki M, Cerullo V *et al.* Oncolytic adenovirus ICOVIR-7 in patients with advanced and refractory solid tumors. *Clin Cancer Res* 2010; **16**: 3035–3043.
6 Alonso-Padilla J, Papp T, Kajan GL, Benko M, Havenga M, Lemckert A *et al.* Development of Novel adenoviral vectors to overcome challenges observed with HAdV-5-based constructs. *Mol Ther* 2016; **24**: 6–16.
7 Carlisle RC, Di Y, Cerny AM, Sonnen AF, Sim RB, Green NK *et al.* Human erythrocytes bind and inactivate type 5 adenovirus by presenting Coxsackie virus-adenovirus receptor and complement receptor 1. *Blood* 2009; **113**: 1909–1918.
8 Seiradake E, Henaff D, Wodrich H, Billet O, Perreau M, Hippert C *et al.* The cell adhesion molecule 'CAR' and sialic acid on human erythrocytes influence adenovirus *in vivo* biodistribution. *PLoS Pathog* 2009; **5**: e1000277.
9 Cichon G, Boeckh-Herwig S, Kuemin D, Hoffmann C, Schmidt HH, Wehnes E *et al.* Titer determination of Ad5 in blood: a cautionary note. *Gene Therapy* 2003; **10**: 1012–1017.
10 Lyons M, Onion D, Green NK, Aslan K, Rajaratnam R, Bazan-Peregrino M *et al.* Adenovirus type 5 interactions with human blood cells may compromise systemic delivery. *Mol Ther* 2006; **14**: 118–128.
11 Gimenez-Alejandre M, Cascallo M, Bayo-Puxan N, Alemany R. Coagulation factors determine tumor transduction *in vivo*. *Hum Gene Ther* 2008; **19**: 1415–1419.

(12) INTERNATIONAL APPLICATION PUBLISHED UNDER THE PATENT COOPERATION TREATY (PCT)

(19) World Intellectual Property Organization
International Bureau

(43) International Publication Date
5 November 2015 (05.11.2015)

WIPO | PCT

(10) International Publication Number
WO 2015/166082 A1

(51) International Patent Classification:
C12N 7/00 (2006.01) *C07K 14/075* (2006.01)

(21) International Application Number:
PCT/EP2015/059593

(22) International Filing Date:
30 April 2015 (30.04.2015)

(25) Filing Language: English

(26) Publication Language: English

(30) Priority Data:
14382162.7 30 April 2014 (30.04.2014) EP

(71) Applicants: **INSTITUT D'INVESTIGACIÓ BIOMÈDICA DE BELLVITGE (IDIBELL)** [ES/ES]; Hospital Duran i Reynals, 3ª planta, Gran Via de l´Hospitalet, 199, E-08908 Hospitalet de Llobregat-Barcelona (ES). **INSTITUT CATALÀ D'ONCOLOGIA (ICO)** [ES/ES]; Gran Via de L' Hospitalet, 199-203, E-08908 L' Hospitalet de Llobregat - Barcelona (ES).

(72) Inventors: **ALEMANY BONASTRE, Ramon**; Passatge del Cim 19, E-08860 Castelldefels-Barcelona (ES). **ROJAS EXPÓSITO, Luis Alfonso**; Urgell, 1-2, E-08207 Sabadell (ES).

(74) Agent: **VÁZQUEZ VÁZQUEZ, Irene**; ABG Patentes, S.L, Edificio Euromor, Avenida de Burgos 16D, E-28036 Madrid (ES).

(81) Designated States *(unless otherwise indicated, for every kind of national protection available)*: AE, AG, AL, AM, AO, AT, AU, AZ, BA, BB, BG, BH, BN, BR, BW, BY, BZ, CA, CH, CL, CN, CO, CR, CU, CZ, DE, DK, DM, DO, DZ, EC, EE, EG, ES, FI, GB, GD, GE, GH, GM, GT, HN, HR, HU, ID, IL, IN, IR, IS, JP, KE, KG, KN, KP, KR, KZ, LA, LC, LK, LR, LS, LU, LY, MA, MD, ME, MG, MK, MN, MW, MX, MY, MZ, NA, NG, NI, NO, NZ, OM, PA, PE, PG, PH, PL, PT, QA, RO, RS, RU, RW, SA, SC, SD, SE, SG, SK, SL, SM, ST, SV, SY, TH, TJ, TM, TN, TR, TT, TZ, UA, UG, US, UZ, VC, VN, ZA, ZM, ZW.

(84) Designated States *(unless otherwise indicated, for every kind of regional protection available)*: ARIPO (BW, GH, GM, KE, LR, LS, MW, MZ, NA, RW, SD, SL, ST, SZ, TZ, UG, ZM, ZW), Eurasian (AM, AZ, BY, KG, KZ, RU, TJ, TM), European (AL, AT, BE, BG, CH, CY, CZ, DE, DK, EE, ES, FI, FR, GB, GR, HR, HU, IE, IS, IT, LT, LU, LV, MC, MK, MT, NL, NO, PL, PT, RO, RS, SE, SI, SK, SM, TR), OAPI (BF, BJ, CF, CG, CI, CM, GA, GN, GQ, GW, KM, ML, MR, NE, SN, TD, TG).

Published:

— *with international search report (Art. 21(3))*

— *with sequence listing part of description (Rule 5.2(a))*

WO 2015/166082 A1

(54) Title: ADENOVIRUS COMPRISING AN ALBUMIN-BINDING MOIETY

(57) Abstract: The invention relates to a recombinant adenovirus comprising an albumin-binding moiety on the outer surface of the adenoviral hexon protein, pharmaceutical compositions containing it and its medical use. Particularly, the invention relates to an oncolytic adenovirus comprising a sequence encoding an albumin-binding moiety inserted in the hypervariable region 1 (HVR1) of the hexon protein coding sequence and its use in the prevention and/or treatment of cancer.